# HYDROGEOCHEMICAL CHARACTERISTICS OF THE BASEMENT AQUIFERS IN NAMAQUALAND

**Rian Ansel Titus**




**A thesis submitted in partial fulfillment of the requirements for the degree of Doctor Philosophiae in the Faculty of Science, Earth Sciences Department, University of the Western Cape, Republic of South Africa**

**March 2003**

**Promoter: Professor Y. Xu**

# ABSTRACT

At the onset of this research programme it became apparent that there is a dearth of research studies focusing on the groundwater resources of the region. As a result, a conceptual representation of the hydrogeological system (i.e. specific aquifer systems, groundwater flow regime, etc.) for the perceived problematic aquifer systems in the Namaqualand region did not exist. The research project contributes significantly to conceptual representation of the aquifer system, in particular a quantitative understanding of the regions' groundwater resources in terms of its hydrochemical development and the construction of a groundwater flow model at regional scale as well as at a local scale.

The groundwater resources for the Namaqualand region are developed predominantly in the basement rocks. The infiltration and flow of water is controlled by the prevailing complex fracture network and can vary in space and time. Such observations relate to structurally controlled flow systems and varying water chemistry amongst closely spaced fracture systems.

The primary objectives of the research project are:

- To provide a quantitative understanding of the region's resources in terms of quantity, and
- To investigate the cause(s) that result in the relatively 'poor' groundwater quality characteristic of the region.



The basement rocks of Namaqualand retained imprints of mostly the Proterozoic tectonic events, although much of the present landscape appears to have developed in the Cretaceous, following the break-up of Gondwanaland. The morphology of southern Africa is thus controlled by the underlying geology.

The warm and humid tropical climate of the Cretaceous period resulted in the development of deep, koalinised weathering mantles to depths of 50 m or more, especially on susceptible lithologies. Late Cretaceous and early Paleocene pedocrete cappings (i.e. duricrusts) comprising predominantly of silicrete and calcrete protected the deeply kaolinised saprolite from erosion processes in many localities.

However, early Miocene crustal uplift and subsequent erosion resulted in the removal of the deeply weathered mantles. In the western parts of southern Africa that was subjected to minimal Miocene uplift, scattered residuals or reduced thicknesses of the weathered mantles remained.

The proposed geometry for the aquifer system can be described as laterally extensive, linear, structurally controlled valley systems. Wide, open valleys may result from the

intersection of different sets of fracture systems. The saprock to saprolite transition zone constitutes the aquifer system. Infiltration of water occurs along vertical to sub-vertical fractures with lateral flow along horizontal to sub-horizontal fracture systems. The water chemistry varies considerably among closely spaced fracture systems. This model proposes a dominant vertical flow system (i.e. an infiltration phase) driven by local relief and an intermediate flow system driven by gradients along these laterally extensive valley systems.

The groundwater for Namaqualand is generally very similar in character with a dominant NaCl signature throughout the recorded EC ranges. The $Na^+$ and $Cl^-$ dominated groundwater for Namaqualand can be described as end-point waters. The initial NaCl character of the lower salinity groundwater in the mountainous regions is probably determined by the predominantly NaCl character of the precipitation in areas where direct rainfall recharge is dominant and to a limited extent the preferential dissolution and leaching of highly soluble Na/Cl salts to the subsurface. The Na/Cl character of the higher salinity groundwater in the lower lying regions of Namaqualand, is predominantly related to the preferential dissolution and periodic leaching of highly soluble evaporitic salts, particularly Na/Cl salts, to the subsurface.

$NaHCO_3$ type waters, due to the process of refreshening, is observed mainly in the higher lying, higher rainfall areas of Namaqualand. Similar $NaHCO_3$ type waters, in the lower lying regions of Namaqualand, is observed for relative young water intersected in highly conductive fracture zones. Most water sampled for the Namaqualand region is, however, too far down an evolutionary path to reflect $NaHCO_3$ type water.



Active weathering processes, with regard to various mineral phases, are evident throughout the EC range for the lower salinity groundwater. The dilute and relatively aggressive groundwater, associated with higher lying regions, controls the weathering (eg. acid-base reactions) of the mineral phases, while the significant head differences (related to differences in elevation for these mountainous areas) result in dynamic flow systems in which equilibrium is difficult to attain. Weathering products are also continuously removed in these highly transmissive systems. It may thus be inappropriate to apply a thermodynamic approach to characterise the waters in such systems.

A reduction in the weathering capacity, with regard to especially the aluminosilicate and probably the carbonate minerals, is suggested for the relatively deeper, higher salinity groundwater in the lower lying regions of Namaqualand. The reduction in the weathering capacity of the higher salinity groundwater can be related to the infiltration of evaporated waters or the leaching of evaporated salts, the increasing concentrations of dissolved constituents with residence time (i.e. the degree of saturation of the groundwater with various mineral phases), the incongruency relations of various minerals (including carbonates and aluminosilicate minerals), a reduction in the $CO^2_{(aq)}$ (in closed systems), the effects of cation exchange, the common-ion effect or even to the coating of primary minerals by residual clay minerals. The lower lying regions of Namaqualand are characterized by intermittent, periodic recharge events, lower hydraulic gradients within

the valley systems and varying hydraulic conductivity values within the saprock to saprolite aquifer zone.

The groundwater tends to react with both the primary mineral phases (i.e. carbonate and silicate minerals) and the reactive weathering products (i.e. crystallized aluminum oxide and hydroxide phases) or at least with an intermediate, meta-stable phase (i.e. amorphous aluminum oxide and hydroxide phases). It is clear, however, that the incongruent weathering processes of various aluminosilicate minerals cannot alone account for the groundwater compositions.

The groundwater chemistry is dependant on the point of sampling in either a dynamic or an evaporative and sluggish groundwater system. Stacked, multiple flow systems dominate that differ in terms of flow rates and the factors influencing the groundwater flow and chemistry including the recharge rate, hydraulic gradient and hydraulic conductivity. The rate of groundwater flow influences the reaction rates with primary and secondary mineral phases which in turn influence the resultant groundwater chemistry. Superimposing and probably masking the latter process is the direct infiltration of NaCl dominated precipitation and the preferential dissolution and leaching of the more soluble evaporitic salts during the infiltration process.

It is possible to spatially distinguish between dilute, shallow circulating and relatively young groundwater systems compared to more brackish, slower circulating and relatively older systems. The relatively dilute end-member is associated with dynamic, actively recharged groundwater systems with rapid through-flow rates occurring in the higher lying mountainous regions, or with infiltration through highly transmissive fracture zones within the lower lying valley systems. The more brackish end-member, associated with the valley systems or the lower lying regions, is characterized by a localized, predominantly vertical flow component (i.e. an infiltration phase associated with the repetitive processes of dissolution and leaching of evaporative salts) and possibly a lateral flow component (i.e. a lateral flow phase driven by reduced gradients within the valleys) that may approximate an intermediate flow system.

# DECLARATION

I declare that *Hydrochemical characteristics of the basement aquifers in Namaqualand* is my work, that it has not been submitted before for any degree or examination in any other university, and that all sources I have used or quoted have been indicated and acknowledged by complete references.

NAME: RIAN ANSEL TITUS DATE: MARCH 2003

SIGNED: .....

# ACKNOWLEDGEMENTS

I thank our LORD for the daily blessings.

My Family (Alice, Robin and Aria), and Extended Family Members for their much needed support and continuous encouragement.

The Water Research Commission provided the funding for the research.

The following persons contributed to the thesis through constructive discussions and support during periods of fieldwork and completion of the thesis:

- Professor Yongxin Xu — Colleague as well as promoter and supervisor of the research
- Mr. Shafick Adams — Colleague and fellow PhD candidate
- Mr. Kevin Pietersen — Staff member of the Water Research Commission

I would also like to acknowledge the following persons and individuals:

- The Community members and farmers in the Namaqualand region for allowing me access to their boreholes
- The staff of the Earth Science Department, University of the Western Cape
- The Post-Graduate students (2001-2002), Groundwater Group, UWC
- Mr. Des Visser (Toens & Partners)
- Mr. Julian Conrad (GEOSS)

The staff at the following laboratories that performed the chemical and isotopic analyses:

- Bemlab – Somerset
- ARC - Infruitec (Stellenbosch)
- Analytical Services - CSIR (Stellenbosch)
- Stable Isotope Laboratory - University of Cape Town

Brian Lawrence (UWC) for the tremendous logistical support given during this study.

# Table of Contents

# List of Figures

# List of Tables

# Chapter 1

# Background

## 1.1: Introduction

In 1994, the then government of National Unity started the implementation of the Reconstruction and Development Programme (RDP). Within this programme, a high priority was given to the delivery of water supply and sanitation services. This was because approximately 12 million people did not have access to a basic water supply. It became a major goal to supply every South African with at least 25 liters of water per day.

A five-year project was started in 1996 to develop a groundwater supply and strategy for sustainable delivery of water services in the arid regions of the Western Karoo, Namaqualand and Bushmanland. The research presented in this thesis, focusing primarily on the basement aquifer system in Namaqualand, formed part of the larger project. Through this process, lessons could be learnt for groundwater development and management in basement aquifers, with emphasis on arid zones in sub-Saharan Africa.

The Namaqualand area is one of the driest regions of the country. Effective management of the region's water resources is essential to meet the water requirements in a sustainable manner. The study area is particularly dependent on groundwater due to the virtual absence of surface water.



## 1.2: Problem statement

This research aims to investigate the following hypotheses:

- The groundwater chemistry is a result of the preferential dissolution and leaching of evaporated surface water in addition to water-rock interaction reactions that involves the more soluble carbonate minerals as well as the thermodynamically unstable silicate minerals.
- The groundwater chemistry is also influenced by hydrochemical processes (i.e. cation exchange, common ion effect, etc) other than near-surface processes (i.e. evaporation, dissolution and leaching processes of evaporitic salts, etc.) or water-rock interaction reactions.
- The spatial variability in the groundwater chemistry can be related to dynamic/active groundwater flow systems or non-active groundwater flow systems (i.e. the point of sampling within either an active or relatively non-active flow system) and/or a complex, fractured aquifer system (i.e. basement rocks) with significant variation in the water chemistry among closely spaced/located fractures (i.e. compartmentalised flow).
- The general relation between the chemical composition of the groundwater and the various rock types and/or lithological units.

In the absence of surface water, the only water supply option to rural communities is groundwater, predominantly developed in the basement aquifer system. Previous studies in the study area clearly indicated significant water quantity and quality problems. A number of consultancy reports on water supply to rural towns and villages in the region have been produced by Toens *et al.* (1991, 1993, 1994, 1995 & 1996). Similar reports were produced by Esterhuyse (1987, 1990 and 1991). Regional perspectives on groundwater quality, including the Richtersveld and the north-western parts of the Namaqualand region, are given in Toens *et al.* (1993 and 1996).

The completion of this study will contribute to the existing literature on basement aquifers in arid zones. In particular, the study will focus on the hydro(geo)chemical processes that result in the relatively poor groundwater quality for basement aquifers in the semi-arid to arid Namaqualand region. Comparisons will be drawn between the findings of this study and the results of similar studies from literature (see Chapter 2). This regional study on basement aquifers, with its focus on the groundwater chemistry, is one of the first such studies for Namaqualand.

### 1.3: Research objectives

The overall aim of the research was to contribute to the sustainable development and management of groundwater resources in the semi-arid north-western part of South Africa.

The primary objectives of the study were:

- To provide a quantitative understanding of the region's resources in terms of quality, and
- To investigate the cause(s) that result in the relatively 'poor' groundwater quality characteristic of the region.



The specific objectives of this study are:

- To develop a database of the physio-chemical parameters (pH, EC and temperature), aggregate determinants (eg. alkalinity), concentrations of major ions (both cations and anions) and certain trace elements.
- To describe the geologic and geomorphic framework for the development of the aquifer systems in Namaqualand.
- To describe the characteristics of as well as the hydro(geo)chemical processes influencing the groundwater chemistry.
- To relate the groundwater chemistry to rock types and/or major lithological units.
- To conceptualise groundwater flow patterns at both local and regional scales.
- To describe the sustainability of the groundwater resources with reference to groundwater quality as a limiting factor (or with reference to the hydrochemical development of the groundwater).

Due to the vastness of the region, the study area (Figure 1.1) was limited to the Buffelsriver catchment (i.e. secondary drainage catchment F30).

A number of towns (i.e. Springbok, Komaggas, Kharkams and Garies) as well as mining towns (i.e. Kleinzee and Nababeep) are situated in this catchment. Many of the rural communities (i.e. Buffelsrivier, Tweerivier, Leliefontein, Nourivier, Kamassies, etc.), the agricultural communities as well as the towns of Komaggas, Kharkams and Garies depend on the groundwater resources. In order to understand the groundwater system in the catchment, information from the adjoining catchment was also utilized.

### 1.4: Research framework (meeting the objectives)

In order to achieve the objectives the following outcomes were required:

- Analysis of the physical conditions of the region.
- An evaluation and validation of hydrogeological data pertaining to the study area and prioritization of areas for which a paucity of data exists.
- Field surveys and data capturing that will enhance the existing national base regarding borehole population distribution, water quality and usage.
- Defining of aquifer geometry and characteristics.
- Conceptualization of the groundwater flow regime(s)
- Prioritization of the processes that influence the groundwater chemistry.
- Define the 'available' water (i.e. groundwater) resources in terms of its quality.

#### 1.4.1: Inception period activities

The first phase of the study consisted primarily of a desktop study involving:



- Data retrieval from the Department of Water Affairs and Forestry (DWAF) and other organisations:
  - Obtaining DWAF reports on groundwater projects in the Northern Cape.
  - Acquiring relevant reports from consultants.
  - Accessing existing physical information (borehole data, climate data) from various sources e.g. National Groundwater Database (NGDB).
  - Acquiring relevant data from the Department of Environment Affairs and Tourism (DEAT).
- Review of previous work of relevance to the study area and the collation and analysis of all relevant data pertaining to groundwater resources in basement aquifer systems:
  - Geological and geomorphological literature on the study area.
  - Geohydrological reports and literature on the characteristics of basement aquifers.
  - Establishment of a database containing all the relevant information.
  - Review of groundwater monitoring networks.

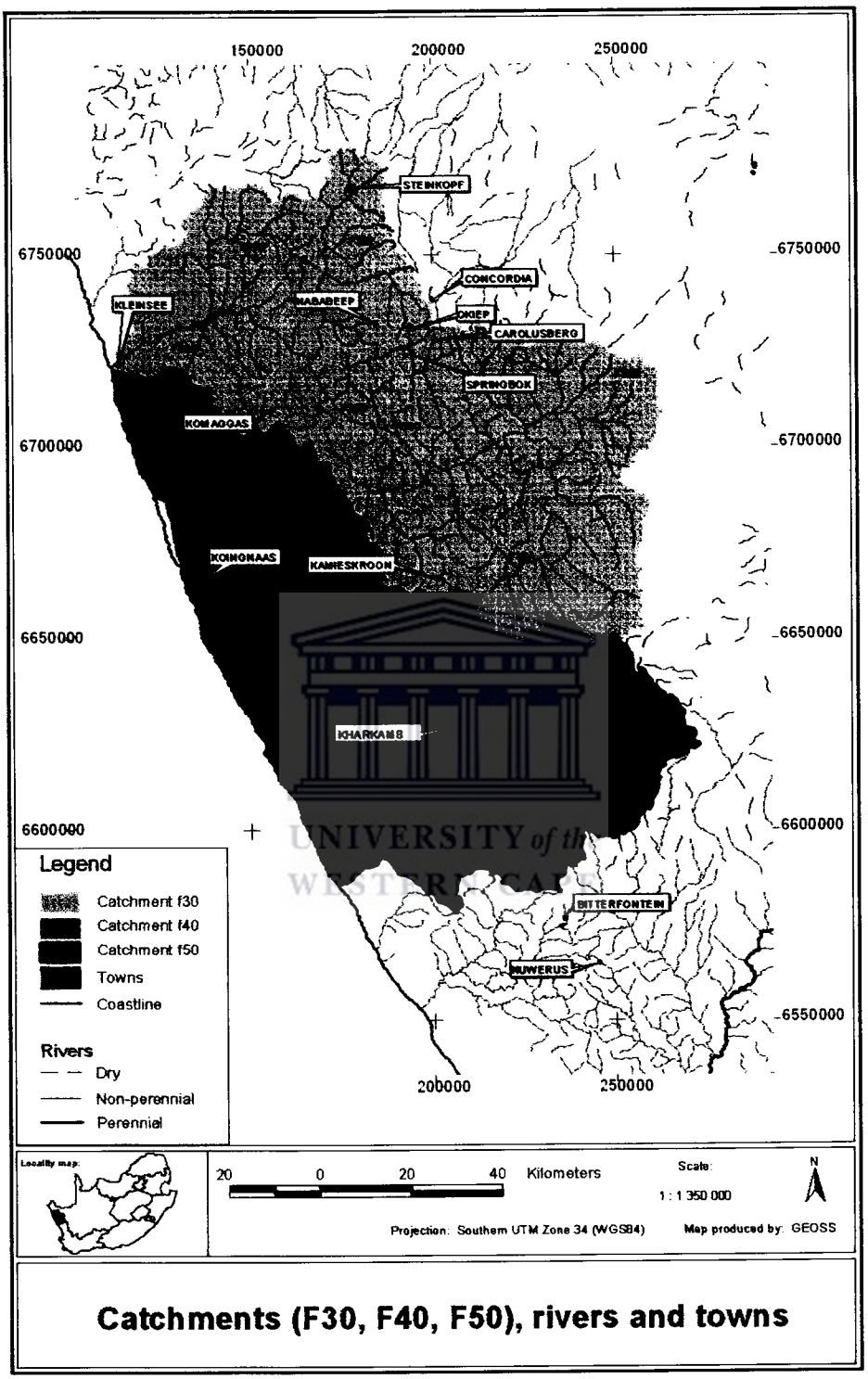


Figure 1-1: The study area comprising of secondary drainage catchments F30, F40 and F50.

- Determination of a field investigation programme for the study area:
    - Liaising with DWAF on where the study can fit in with DWAF programme objectives.
    - Identifying target areas to achieve a regional coverage of the secondary drainage catchment F30 (Figure 1.1).
    - Collection of the necessary topographical maps (in printed and digital format), geological maps and DEM coverage.
    - Obtaining the necessary satellite images from the USGS.
    - Numerous field visitations.

The inception phase resulted in an understanding of the geological (including the tectonic) background, the geomorphological evolution and the historical climatic changes for the region. It was observed that the resource for community water supply in the Northern Cape region is (a) of poor quality (b) insufficient quantity and (c) unreliable. To alleviate water problems will require knowledge of not only the resource, but also the impact of the resource on the end user. The latter statement, i.e. the impact of the resource on the end user, will not be addressed in this research.

### 1.4.2: Water (i.e. groundwater) resource assessment

The activities associated with the second phase can be summarized as:

- Hydrogeological and hydrochemical data collection, analysis and interpretation (see Chapters 6, 7 and 8), and
- The presentation of detailed conceptual models on the groundwater resources of the study area (see Chapters 7 and 8).



Essentially the second phase focused on the implementation of a field programme that included groundwater mapping as well as the analyses and comprehensive interpretation of the field data. This contributed to an improved understanding and an initial representation of the basement aquifer systems for Namaqualand, especially with regard to the physical and chemical nature of the groundwater systems. Such groundwater systems are located primarily in the weathered and fractured bedrock, while water (i.e. groundwater) is also abstracted from alluvial systems for at least three rural towns.

## 1.5: Structure of the thesis

This thesis presents the current status and knowledge of the occurrence and attributes of basement aquifer systems in the Namaqualand region (see Chapters 2 to 8).

Introductory information is given in Chapter 1. The purpose of this research is discussed with reference to a larger five-year research program. The hypotheses, primary objectives and specific objectives of this study are defined. A detailed research framework is presented.

A general overview of research conducted on basement aquifers internationally and within South Africa is presented in Chapter 2. This literature review provides an insight into the development and characteristics of basement aquifer systems. The review guided the research

conducted in Namaqualand and provided an opportunity to compare the results obtained to similar studies on basement aquifers that developed under different climatic conditions.

A locality description is presented in Chapter 3. This includes information on the location, climate (including precipitation, potential evapotranspiration and temperature) and vegetation of the study area.

Chapter 4 is a review of the lithological and intrusive relations of the aquifer medium (i.e. basement rocks) and its Proterozoic deformation history. The effects (if any) of the Pan African Gariep orogeny were not recorded for the basement rocks of the Namaqua Province. There is also a dearth of published information on neotectonic activity for the region. In conclusion, the younger cover sequences of late Proterozoic and Phanerozoic ages are briefly discussed. Four Precambrian deformation phases were recognized and described by various authors (Van der Merwe, 1995; Visser, 1989; Van Aswegen et al., 1987; Hartnady et al., 1985; Albat, 1984; Blignault et al., 1983; Tankard et al., 1982; Lipson, 1978; Moore, 1977; Joubert, 1971).

A description on the geomorphology of the Namaqualand region is included as Chapter 5 of this thesis. This chapter describes the macro-scale geomorphology of the Namaqualand region including the development of the extensive erosional surfaces, the most prominent geomorphic features (i.e. bornhardts) within this escarpment zone, as well as the drainage patterns.

Chapter 6 describes the methodology employed with regard to fieldwork and subsequent analyses. The data is presented in various graphical formats and described through utilizing statistical analyses. In addition, the environmental isotope data are described and conclusions drawn.



Chapter 7 focuses on the characteristics of the soil profile for the Escarpment zone and on carbonate and silicate incongruent mineral weathering reactions. Processes in the soil zone influence the character of the infiltrating water, while certain clay minerals that result from incongruent weathering reactions are documented to occur within the soil zone. The development of deep, kaolinised weathered mantles is associated with the warm and humid tropical climate of the Cretaceous period (see Chapter 5). A weathered profile for the Namaqualand region is presented at the end of this chapter.

Various hydrogeochemical processes are described in Chapter 8, and conceptual models presented, to explain the origin of the groundwater composition. This chapter focuses on the processes that resulted in the dominant NaCl character of the groundwater. In addition, emphasis is placed on a mineral-dissolution approach based on the reaction between primary minerals and $CO_2$-charged water to produce the measured dissolved constituents. As a result, the effects of both carbonate and silicate weathering processes (see also Chapter 7) are discussed to explain concurrent changes in the groundwater composition. Local and intermediate flow systems are described for the near surface environment that is based on the hydrogeochemical models presented.

A summary of the main findings, addressing the objectives of the research, is presented in Chapter 9.

# Chapter 2

# The challenges of basement aquifers

## 2.1: Introduction

This chapter provides a general overview of relevant research conducted on basement aquifers internationally and within South Africa. This literature review specifically provided an insight into the development and characteristics of basement aquifer systems, guided the research conducted in Namaqualand and provided an opportunity to compare the results obtained for the study area to similar studies on basement aquifers that developed under different climatic conditions. Very limited research has been conducted on the basement aquifers in Namaqualand. Previous studies have focused mainly either on development type projects for water supply to various rural communities throughout the Buffels River catchment (i.e. secondary drainage catchment F30) or on very comprehensive and detailed studies limited to the selected site(s) for nuclear waste disposal.

Basement aquifers (i.e. usually fractured, Precambrian crystalline rocks) are found extensively in sub-Saharan Africa. The only viable water supply to many communities is, more often than not, located in these systems. A number of important constraints are recognized in development of these resources (Wright, 1992). These are:

- The frequent high failure rate of boreholes commonly in the range of 10 - 40%, with the higher rates in drier regions or where the weathered overburden is thin;
- The shallow occurrence and fissure permeability of the bedrock aquifer component which makes it susceptible to surface pollutants;
- The low storativity of basement aquifers, which may therefore deplete significantly during sustained drought periods. Recharge is also sensitive to certain land-use changes, notably those associated with desertification.

Basement aquifers are developed within the weathered overburden and fractured bedrock of crystalline rocks of intrusive and/or metamorphic origin that are mainly of Precambrian age (Wright, 1992). The properties of basement aquifers are largely controlled by structural features, such as faults and shear zones. The following are concluded about basement aquifers (Lloyd, 1999):

- They are poor aquifer materials
- Their primary aquifer characteristics are negligible
- Lithology is not notably significant in influencing aquifer characteristics
- Fracturing is the most important aspect of aquifer potential but is inconsistent both laterally and in depth
- Weathering does not appear to generally enhance fractured hard rock aquifer potential

- They should be assessed in conjunction with any juxtaposed potential aquifer material.

## 2.2: General overview of studies on basement aquifers internationally

Studies on basement aquifers around the world have predominantly focused on the development of groundwater resources in thick regolith (i.e. weathered overburden) with dominant intergranular flow in tropical to sub-tropical regions (i.e. Western and Southern Africa, South America, Norway and Sweden) compared to dominant fissure flow in temperate and higher latitude regions. The weathered overburden is usually the main groundwater storage compartment, although boreholes may be developed in the underlying fractured bedrock. The development of basement aquifers is notoriously complex, especially where a thinner weathered overburden is present (Lloyd, 1999; Chilton and Foster, 1995; Gustafson and Krásný, 1994; Rebouças, 1993; Olofsson, 1993; Wright and Burgess, 1992; Commonwealth Science Council (CSC) Technical Paper (TP) 273, 1990; and Acworth, 1987).

A summary of the characteristics of basement aquifers, based on a number of research projects, was produced by Lloyd (1999) and Wright and Burgess (1992). Chilton and Foster (1995) reviewed the hydrogeological character and water supply potential of basement aquifers in the more humid regions with comparisons to the more arid regions of tropical Africa (i.e. Malawi, Zimbabwe, Botswana and Nigeria). Gustafson and Krásný (1994) gave an account of the occurrence, properties and importance of basement aquifers in particularly Third World countries. These authors suggest that the term 'hydraulic conductor', to describe the storage and flow of groundwater in fractured crystalline rocks, should replace the term 'aquifer'. Basement aquifers, and their associated hydraulic conductors, being predominantly exposed in shield areas (i.e. Canadian, Guianan and Amazonian, Baltic, African, Indian, Australian, Angaran/Siberian and Antarctic shields) are composed of magmatic and metamorphic rocks of the Precambrian age. Less extensive, but locally important, basement rock exposures can be found outside shield areas (e.g. Armorican Massif, Bohemian Massif, etc). Rebouças (1993) reviewed the groundwater bearing properties of Precambrian basement rocks in both South America and Western Africa. Most of the Precambrian crystalline rocks in South America (i.e. 90%) are located within the humid to sub-humid tropical regions of Brazil with an average, annual rainfall of between 1000mm and 3000mm, resulting in densely developed drainage systems. The Precambrian rocks of Western Africa are subjected to dry, tropical climatic conditions with less than 40% of the total surface area of Western Africa receiving an average annual rainfall varying between 500mm and 2000mm. Olofsson (1993) reviewed the flow of groundwater from soil to crystalline bedrock. The infiltration of water from soil to crystalline rock only occurs at specific sites where a combination of suitable geological features (such as fracture zones) and hydrological variables (i.e. thickness of overburden) occur.

The characteristics of basement aquifers and their associated groundwater resources are, according to Acworth (1987), greatly influenced by the dominant conditions within the

study area. The hydrogeological characteristics in particular, are dependant upon the quantity of recharge to the weathering zone and the geomorphological conditions under which the weathering is occurring. As a result, a general framework for the investigation of basement aquifers is not possible due to the diversity of weathering environments.

The hydrogeological characteristics of the weathered crystalline rock derive from and are related to long-term, tectonically controlled geomorphic processes (Taylor and Howard, 2000). However, rainfall continues to drive the geomorphic processes, in particular deep weathering and stripping, acting on deeply weathered basement rocks.

### 2.2.1: The nature of basement aquifer systems

Crystalline material (igneous and metamorphic rocks) is generally comprised, according to Lloyd (1999), of an unweathered and intact matrix with planes of discontinuity, including both faults and joint planes, and often precipitates from late phase fluids (i.e. vein infill). The matrix of crystalline rocks generally does not have a significant primary porosity due to its mode of formation. Furthermore, crystalline formations are usually characterized by the intrusion of late phase fluids that further reduces any initial intergranular porosity. Gustafson and Krásný (1994) refer to crystalline rock aquifers as hard rock aquifers that are predominantly comprised of fractured igneous and metamorphic rocks with negligible matrix porosity and matrix permeability.

Crystalline basement rocks (usually of Precambrian age) have generally been subjected to multiple tectonic events under varying stress conditions which result in complex patterns of ductile folding and brittle fracturing in the near-surface regions of the Earth's crust (Lloyd, 1999). Near-surface fractures, to depths of 100m and even deeper, are considered to be in a state of tension with enhanced groundwater movement.

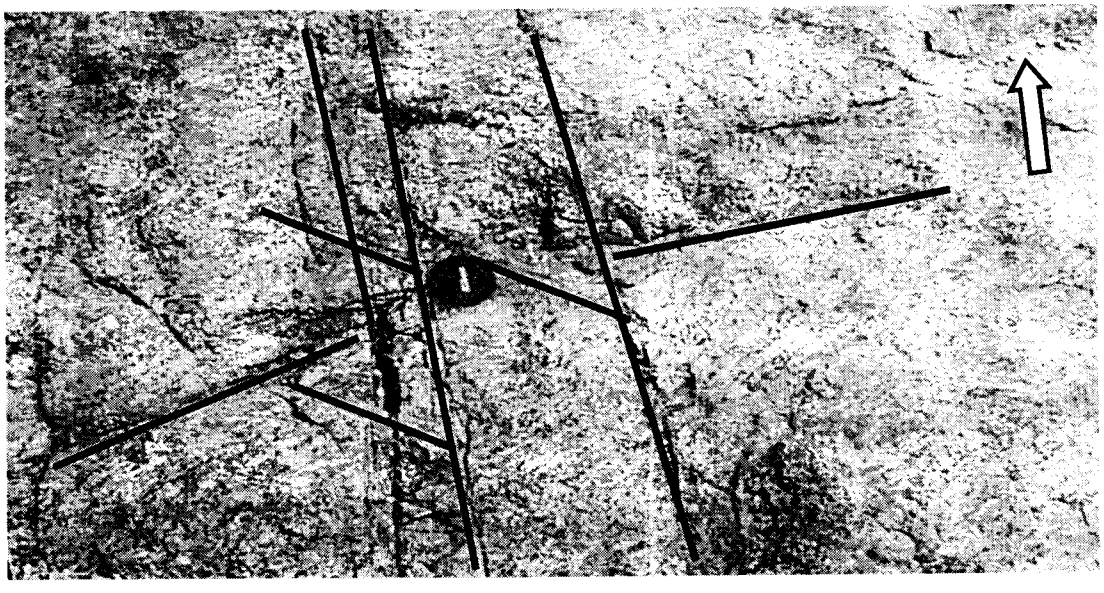

Figure 2-1: NNW-SSE, ENE-WSW and NW-SE orientated fractures in the Gladkop Suite south of Springbok. The Namaquan-aged fabric (i.e. foliation) of the rock is approximately east to west.

As an example, the fractured crystalline rocks of Namaqualand were subjected to varying stress conditions, as illustrated in Figure 2.1. The fracture orientations were identified based on the interpretation of regional satellite images and regional geophysical data. The vertical to sub-vertical lineament of the fracture systems represents a predominantly brittle deformation phase, in the upper 5km to 8km of the crust, that can also be associated with the break-up of Gondwana (± 180 Ma to 30 Ma). The north-northwest to south-southeast (NNW-SSE) fractures systems parallels the present-day stress field and probably represents the most 'open' structures.

### 2.2.2: The weathered overburden

Past weathering and erosion processes have resulted in the formation of a regolith, a zone of alteration products, normally more than 10m thick and overlain by residual soil (Taylor and Howard, 2000; Chilton and Foster, 1995; Gustafson and Krásný, 1994; and Acworth, 1987). Aggressive weathering and differential leaching has, through the downward movement of infiltrating waters, resulted in deep regolith profiles (Figure 2.2). The residual soil is generally characterized by kaolinite, quartz and oxidized iron (Fe) minerals. The soils are underlain by laterite beds or stone-lines and have a relatively high infiltration capacity as well as pathways for preferential flow in low permeability soils (Chilton and Foster, 1995).

The regolith is a result of the infiltrating and acidic rainfall reacting with the host minerals, followed by leaching of the more soluble and mobile elements (or compounds) with contemporary as well as subsequent re-precipitation of the less mobile elements or compounds (i.e. the formation of Al/Fe oxides and kaolinite as examples). The saprolite (Figure 2.2) is characterized by massive accumulations of secondary clay minerals (especially kaolinite) with both primary minerals as well as intermediate weathering products. The hydrogeologic properties of the regolith, including the rate and depth of weathering, are influenced by bedrock type, by the presence of Fe-Mg minerals and by the density of structural features such as fracture zones and dykes. Fracture permeability, characteristic of the saprock and fresh bedrock, is dependant on aperture and connectivity as well as frequency (Chilton and Foster, 1995). The deposition of secondary clay minerals, associated with certain lithological types, may also reduce the fracture permeability of the weathered bedrock.

According to Rebouças (1993), crystalline rocks with deeply weathered overburden (from 10 to 100m thick) comprise 70% to 90% of the Precambrian basement regions in both South America and Western Africa (Figure 2.3). The weathered overburden in certain parts of Brazil may, however, be more than 200m thick in regions subjected to neotectonic uplift and an annual rainfall varying between 2000mm and 3000mm.The average thickness is estimated at approximately 42m. The thickness of the weathered mantle for Western Africa (i.e. Senegal., Ivory Coast, Ghana, Niger and Zaire) varies from10m to 175m, with an average thickness of 30m. Chemistry, mineralogy, petrology, structure, the age of the land surfaces and particularly long-term climatic conditions

influences the weathering process and thus the development of the weathered overburden (Rebouças, 1993; Gustafson and Krásný, 1994).

The weathered overburden is considered to have low to moderate transmissivity but high storativity, while the fractured bedrock is characterized by high transmissivity and low storativity (Rebouças, 1993). Taylor and Howard (2000) disagrees and describes a more transmissive and porous weathered mantle (T = 5 to 20 $m^2/d$) providing storage to the underlying bedrock fractures (T = 1 $m^2/d$). Gustafson and Krásný (1994) described this composite or 'near surface' aquifer as approximately uniform, characterized regionally by its mean transmissivity rather than the sporadic fault or fault zones although these are more permeable and extend to great depths.

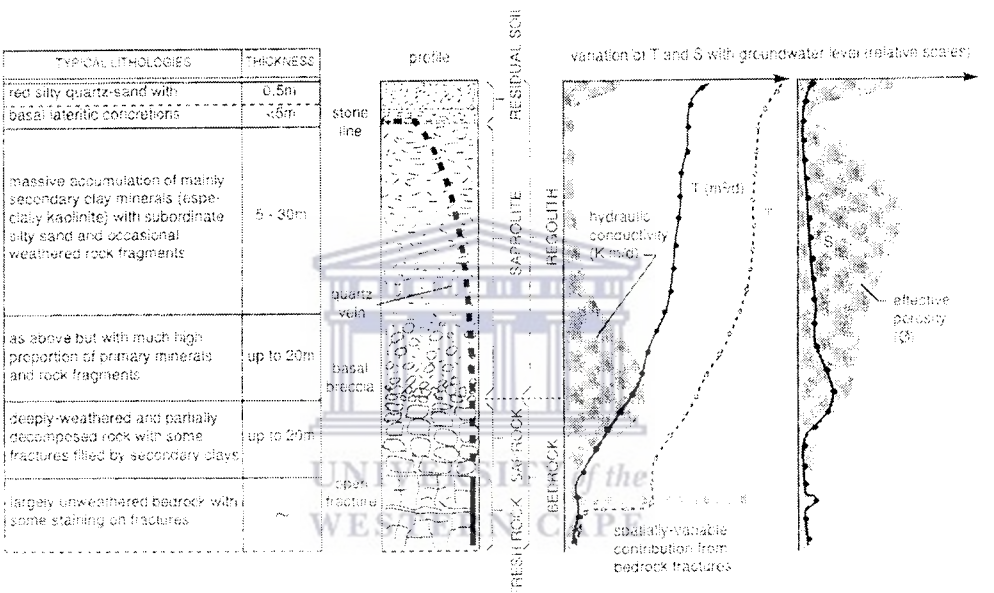


Figure 2-2: Typical weathered profile for Precambrian basement rocks (from Chilton and Foster, 1995 and see also Taylor and Howard, 2000).

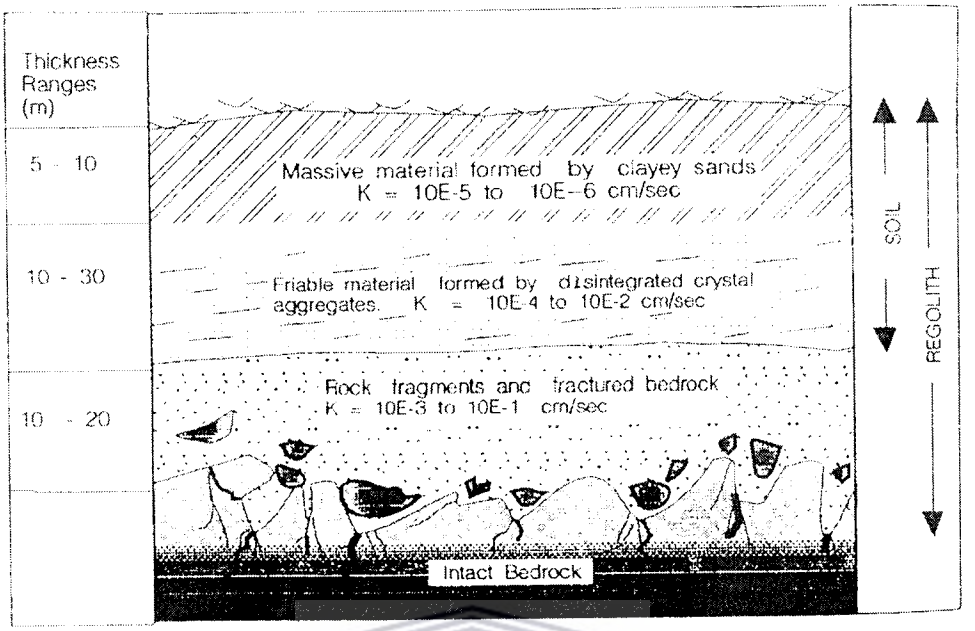


Figure 2-3: Typical weathered profile for Precambrian basement rocks (from Reboucas, 1993).

The upper interfaces between the weathering zones are mostly planar since they are related to the presence of the water table (Acworth, 1987). The lower interfaces are more irregular and are influenced by the prevailing fracture systems and changes in mineralogy of the parent rock. In fact, the interface between the fresh bedrock and the overlying weathered zone (i.e. fresh rock to saprock change) is characterized by isolated fresh rock or corestones.

The in-situ weathered products can be observed around relatively fresh core blocks within road cuts in Namaqualand (Figure 2.4). The weathering front on these predominantly ellipsoidal core blocks is easily observed. The shape of the weathering front may be related to the tectonic history of the region resulting in orthogonal fracture sets. Weathering can also be seen along fracture zones internal to these relatively fresh core blocks. The weathered overburden is assumed to be much thicker (i.e. deeper) in the structurally controlled, open valleys characteristic of Namaqualand.

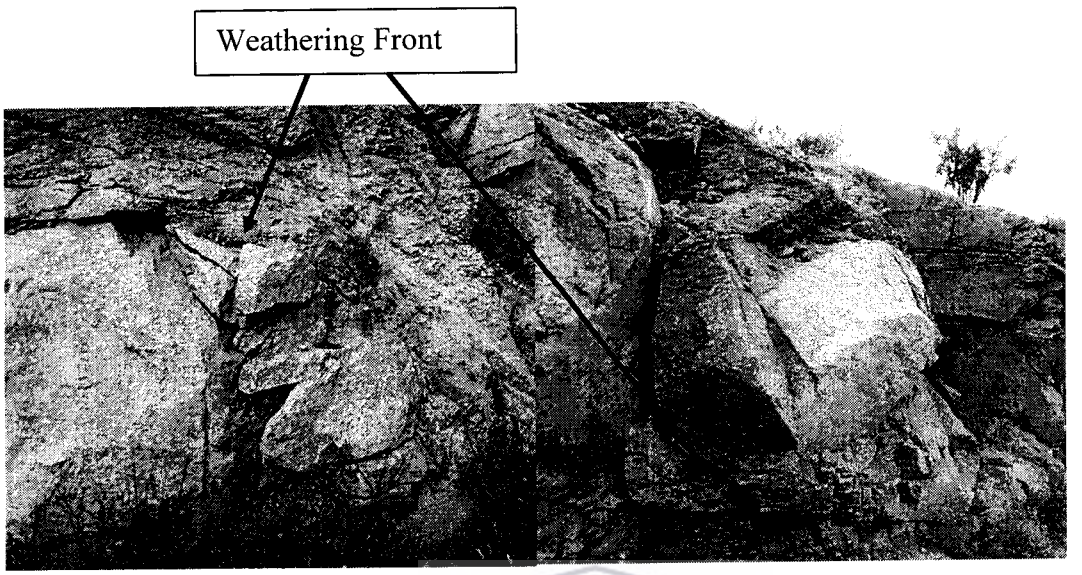


Figure 2-4: The weathering front and the resultant in-situ clayey products exposed in a road cut. Visible weathering around an ellipsoidal core block, and a 3D view parallel to the long-axis of an ellipsoidal core block, bounded by a vertical fracture to the left and a shear at the bottom of an ellipsoidal core block (left photograph).



### 2.2.3: Groundwater storage and flow

The basal part of the regolith, which is the approximate base of the saprolite and the top of the weathered saprock (i.e. the weathered bedrock), has sufficient permeability to support successful boreholes for small-scale village water supply (Chilton and Foster, 1995). Rebouças (1993) supported the latter statement and referred to the most productive zone for groundwater development corresponding to the lowest zone of the weathered profile and top of the fractured bedrock. Rebouças (1993) stated that the optimum zone for groundwater development is from 20m to 50m. Furthermore, a thick saturated regolith is essential (especially in humid regions) for adequate aquifer storage and available drawdown (Taylor and Howard, 2000; Chilton and Foster, 1995; and Acworth, 1987). The average yield from a production borehole in weathered basement aquifers is normally less than 1 l/s (Chilton and Foster, 1995). The average yield for wells and boreholes located in fractured and/or weathered rocks is $16m^3/h$ for Brazil compared to an average yield of $3m^3/h$ for certain countries in Western Africa (Rebouças, 1993). The groundwater usually has a low total dissolved solid load (TDS) of less than 100 mg/l. Groundwater, within the lowermost unweathered basement rocks, is stored in interconnected systems of fractures, joints and fissures associated with regional tectonism (Rebouças, 1993). The yield from these unweathered basement aquifers, located in humid

and sub-humid tropical climatic sub-regions, vary between $1m^3/h$ and $20m^3/h$ with a TDS of less than 100mg/l (Rebouças, 1993).

More intensive development of the groundwater resources is possible at locations where favorable lithology, structural features and weathering coincide to form zones of higher transmissivity (Chilton and Foster, 1995). Fractures (i.e. faults, joints, veins, etc.), dykes and zones of weathering and/or overburden deposits are targets for the exploitation of groundwater in Precambrian crystalline rocks (Rebouças, 1993). The infiltration of water from soil to rock is strongly heterogeneous and requires permeable soils, or permeable horizons (i.e. 'infiltration routes'), as well as 'open' and interconnected fracture systems in the bedrock (Olofsson, 1993). Hydraulic continuity must exist between groundwater reservoir(s) in the overlying soil horizons (or weathered overburden) and the underlying bedrock. The fracture zones act as conduits for deeper flows from groundwater reservoirs located in upper permeable soils or the weathered overburden. Olofsson (1993) reported on a number of studies that indicate a direct correlation between the tectonic conditions (i.e. the nature of fracturing) in the superficial or upper bedrock, and drainage of the overburden. He also noted that the capacities of wells drilled into bedrock increased rapidly with the increasing thickness of the weathered overburden that represents large, highly conductive groundwater reservoirs. Sorted and conductive material usually occurs in minor depressions in the bedrock topography. These depressions result from enhanced weathering on fracture zones and are associated with the infiltration of water from soil to rock (Taylor and Howard, 2000; and Olofsson, 1993). Groundwater flow in crystalline rocks occurs, according to Olofsson (1993), predominantly in the upper parts of the underlying bedrock (i.e. superficial bedrock) through gentle dipping and interconnected fracture zones and systems. Flow can, however, occur very rapidly from the soil to depths of several hundreds of meters along conductive fracture zones (Olofsson, 1993).



Groundwater levels, in higher rainfall regions, are found within the regolith while the regolith may be above the piezometric surface in drier regions (Chilton and Foster, 1995). The groundwater levels generally reflect the surface topography that implies aquifer recharge in topographic highs and discharge in topographic lows. Chilton and Foster (1995) recognized both a shallow flow system (i.e. interflow) within the residual material as well as a deeper and slower flow system through the saprolite/saprock zone(s). These flow systems are characterized by weak and strong mineralisation processes respectively.

Infiltration for the fractured crystalline rocks in Namaqualand occurs along the vertical to sub-vertical fractures, with lateral flow predominantly along horizontal to sub-horizontal fractures (Figure 2.5).

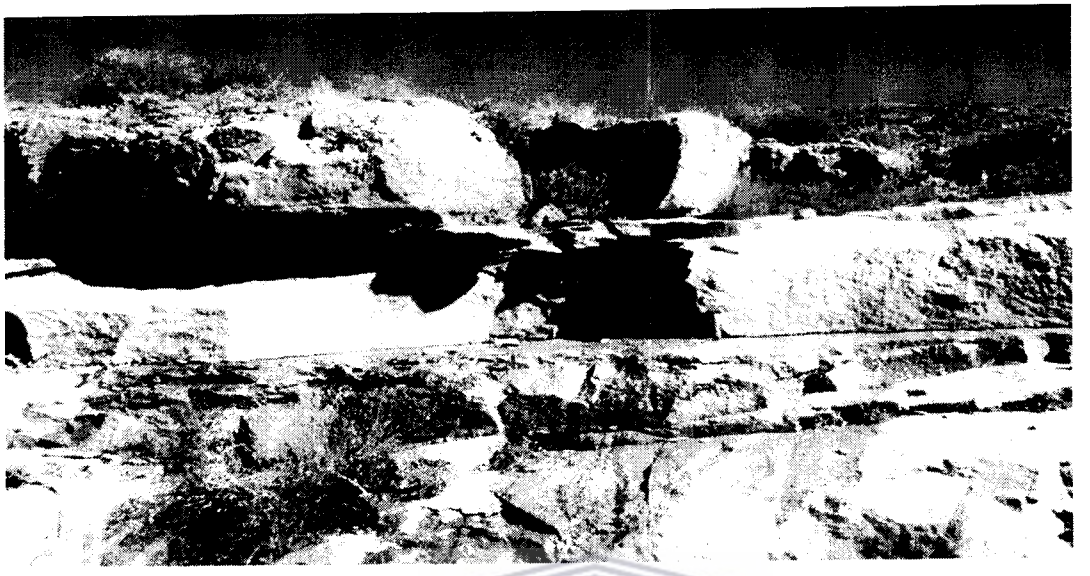

Figure 2-5: Water flowing from regularly spaced horizontal joint planes. The surface planes of the vertical joints are clearly visible.



2.2.4: The hydraulic properties of basement aquifers

Basement aquifers have very low transmissivity (T) values (i.e. geometric mean) ranging generally from 1 to 5$m^2$/day with an order of magnitude lower and/or higher than these values, calculated in relation to a saturated thickness of the regolith varying from 12m to 22m (Chilton and Foster, 1995). Basement aquifers are further characterized by poor connectivity of bedrock fractures and regions of low permeability resulting in significant local variations in yield and response to abstraction (Taylor and Howard, 2000; Chilton and Foster, 1995). The weathering (i.e. dissolution of minerals) and leaching processes tend to increase the porosity, permeability and specific yield, while the deposition of clay minerals (as products of the weathering processes) can cause a reduction in these hydrogeologic properties (Chilton and Foster, 1995; and Acworth, 1987). Acworth (1987) noted that the most successful boreholes were located in a shallow weathered aquifer system, indicating that the processes of weathering results in substantial increases in the porosity and hydraulic conductivity of the source rocks. Solid and unweathered crystalline basement rocks are characterized by very low porosity and hydraulic conductivity values. Fractured crystalline rocks are characterized, according to Gustafson and Krásný (1994), by extreme heterogeneity in their hydraulic properties. The hydraulic conductivity can vary, within the same rock mass, by orders of magnitude and over short distances. Water is generally stored and transmitted in fractures and fissures through a relatively impermeable matrix.

Structural features such as fractures and fissures, in crystalline rock, are described as hydraulic conductors while zones of intense fracturing are described as compound conductors (Gustafson and Krásný, 1994). The fractures and fissures are a result of tectonic processes and are thus not confined to any specific formation. The structural features are also extremely variable in nature (with regard to frequency, spatial extent, interconnectedness, etc.) within the relatively impervious crystalline rock mass. Gustafson and Krásný (1994) thus referred to hydraulic conductors within fractured crystalline rocks, rather than aquifers, to describe the storage and flow of groundwater in these rocks. The term aquifer implies that the groundwater reservoir is related to the formation rather than the structures within it. A hydraulic conductor includes single fractures and fracture zones in the regolith (in tropical regions) and is defined by its ability to transmit groundwater (Gustafson and Krásný, 1994).

Hard rock aquifers generally have limited storage capacity and are rapidly depleted as they also have a limited retention capacity in areas with high hydraulic gradients (Gustafson and Krásný, 1994). The removal of large fluxes of groundwater is possible in areas with high hydraulic gradients despite the prevailing low transmissivity of these rocks. However, hard rock aquifers have a low ability to accumulate groundwater, in spite of retention periods of tens of thousands of years, which have been determined by isotopic investigations. The distribution of groundwater resources in hard rock aquifers depend particularly on the prevailing climatic conditions (i.e. controlling present recharge capabilities) and is also influenced by altitude (Gustafson and Krásný, 1994).

Fractured crystalline rocks in Namaqualand are characterized by extreme heterogeneity in their hydraulic properties with poor connectivity between fractures (Figure 2.6). Water is stored and transmitted in these fractures and fissures, which serve as hydraulic conductors, through a relatively impermeable matrix.

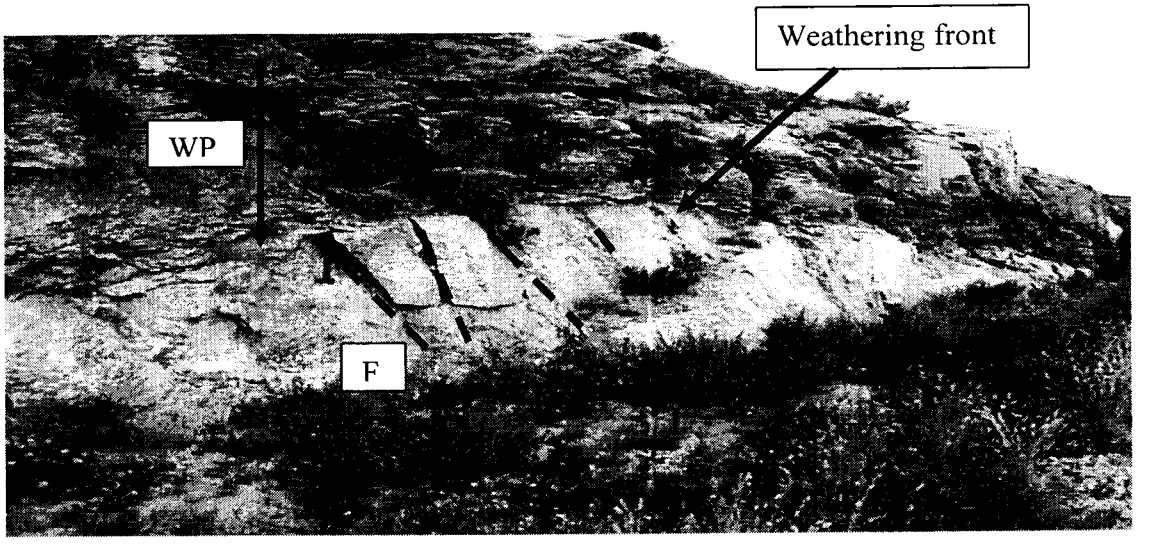


Figure 2-6: An example of either compressional or extensional "stacked" ellipsoidal core blocks, bounded by shear zones in Mesklip granites. The in-situ derived weathered products (WP) are found between the relatively fresh core blocks, with fractures (F) extending the weathering process throughout the ellipsoidal core blocks.

### 2.2.5: Groundwater chemistry

The natural chemical quality of groundwater from basement aquifers in tropical regions of Africa is considered to be of acceptable quality (Chilton and Foster, 1995). The natural groundwater chemistry, being the product of various weathering processes, will exhibit vertical differences in chemical composition due to varying mineral assemblages at different stages of weathering and leaching in the regolith (Chilton and Foster, 1995). Furthermore, the groundwater quality varies over short distances due to complex groundwater flow patterns and weathering processes. The chemical properties of the shallow, phreatic hard rock aquifers depend, on a regional scale, particularly on the prevailing climatic conditions although they are also influenced by differences in plant cover, soil types and altitude (Gustafson and Krásný, 1994). The climatic conditions control precipitation, temperature distribution as well as the character of rock weathering over the long-term. Precipitation increase and evapotranspiration decrease results in improved recharge conditions at an increased altitude. Precipitation decreases and the groundwater hydraulic gradient diminish with decreasing altitude in addition to, and influencing, a change in the nature of rock weathering from predominantly mechanical to chemical. The more important factors that influence the chemical composition of the groundwater in shallow hard rock aquifers on a local scale include:

- Surface water bodies and their chemical composition;
- Micro-climate;
- Precipitation quality;
- Anomalies in rock composition;
- Zones of discharge of deep-seated groundwater;
- Anthropogenic effects (Gustafson and Krásný, 1994).



Chemical weathering is the dominant process in the development of the weathered overburden on basement rocks (Acworth, 1987). Water is an important weathering agent in the unsaturated zone with enhanced weathering processes in the zone of water table fluctuation. Furthermore, weathering extends far below the water table in certain areas where groundwater is the principal chemical reagent. Acworth (1987) emphasized the affect that the rate of groundwater flow has on the rate of the weathering reactions.

The groundwater for igneous and metamorphic rocks within temperate climatic zones is characterized by low TDS values varying between 100mg/l to 300mg/l, by bicarbonate and calcium as the dominant ions, and by a general decrease in pH values and TDS content with increasing altitude. Trends in sulphate and nitrate concentrations are linked to anthropogenic pollution. In humid equatorial regions of Africa, groundwater of the bicarbonate type dominates and TDS values of up to 1g/l are possible. In addition, the groundwater is characterized by increased concentrations of iron and organic compounds. With increasing latitude from the equatorial zone in Africa, both southward and northward, the TDS content increases and the anion composition of the groundwater changes from bicarbonate to sulphate, and even chloride dominated groundwater with varying cation content (Gustafson and Krásný, 1994). The TDS content within desert (or

arid to semi-arid) regions, can increase up to 10g/l while the groundwater chemistry is dominated by chloride and sodium (Gustafson and Krásný, 1994). Vertical zonation in the chemical composition of groundwater as well as deep seated highly mineralized brines, within shields or massifs of crystalline rocks are evident through natural springs of mineral and thermal waters (Gustafson and Krásný, 1994).

The origin and the contribution of magmatic, volcanic and metamorphic processes to the formation of such deep-seated highly mineralized brines are still debated. Olofsson (1993) noted numerous studies that indicated a difference in the chemical composition of groundwater in soil from that of groundwater within granitic and gneissic bedrock. These studies refer to younger superficial groundwater, with higher $Ca^{2+}$, $HCO_3^-$ and $SiO_2$ contents, partly replacing the groundwater in the granitic and gneissic bedrock. Kay (1985 and 1987) found that active groundwater flow systems in weathered gneiss can exist to depths of 300m. He also found that the groundwater chemistry is controlled by near-surface processes in the overburden, such as sand and peat deposits, and that the chemical composition of the groundwater is preserved once it is stored within the fractures of the bedrock. Of particular importance, however, is a statement by Olofsson (1991c) to the effect that the water chemistry varied considerably among closely located fractures, indicating a very complex drainage pattern. Gustafson and Krásný (1994) also indicated that there is no general relation between the chemical composition of the groundwater and the various crystalline lithological units in the Czech Republic. Certain lithological units such as gabbro, amphibolite, serpentine and marble can, however, influence the chemical composition of the groundwater significantly (Gustafson and Krásný, 1994).



### 2.2.6: Groundwater development in basement aquifers

Basement aquifers in humid regions are characterized by saturated regolith thickness in excess of 10m and shallow groundwater levels (Chilton and Foster, 1995). Similar aquifers in arid regions are characterized by relatively thin saturated regolith generally present above deeper groundwater levels. The deeper groundwater levels and thin saturated regolith thickness in arid regions necessitates the drilling of deep boreholes to intercept structural features and contact zones at depth within the unweathered bedrock. In contrast to the acceptable yield and quantity for basement aquifers located in humid and sub-humid tropical climatic sub-regions, the yield and quality for basement aquifers located in wet-dry and dry tropical climatic sub regions have generally been poor (Rebouças, 1993). Groundwater in semi-arid regions has TDS values commonly exceeding 2000mg/l. The structural control on the surface drainage systems, in semi-arid regions, is evident in their alignment along fracture systems that are associated with the underlying bedrock. Recharge to the underlying fractured and unweathered bedrock, for basement aquifers located in humid and sub humid tropical climatic sub regions, is associated with the high storativity of the weathered overburden. The main source of recharge, in wet-dry and dry tropical climatic sub regions, is the drainage systems that are aligned along fracture systems. Groundwater in both humid and temperate regions is traditionally considered in terms of groundwater quality problems, such as pollution, and

for geotechnical and engineering problems, such as dewatering for mining and civil engineering purposes. In semi-arid regions, however, groundwater commonly represents the sole rural water supply and is often subjected to detailed hydrogeological investigations.

Groundwater resources are, according to Rebouças (1993), either under-appreciated and thus under-utilised or inappropriately exploited. Groundwater, developed in weathered and/or fractured basement rocks, is generally regarded as a 'local' resource for individual domestic needs, particularly in rural regions. According to Rebouças (1993), significant attention was given, over the past 25 years, to the development of groundwater resources in weathered and fractured basement rocks in South America and Western Africa. The most severe environmental and groundwater management problems in both regions include water pollution in urban areas, ill-planned development as well as public and private mismanagement (Rebouças, 1993).

### 2.3: Overview of studies on basement aquifers in South Africa

Very limited research has been conducted on basement aquifers in South Africa. As a result, this study entails a regional overview of the groundwater characteristics for the Buffels River catchment. Previous studies have predominantly focused either on projects related to water supply for various rural communities throughout the Buffels River catchment (i.e. secondary drainage catchment F30) or on very comprehensive and detailed studies related to the storage of nuclear waste. Such studies were, however, only limited to the selected site(s) for nuclear waste disposal. The relevant results of five studies (Andersen, 1986; Andreoli *et al.*, 1986; de Beer, 1986; Levin et al., 1986 and Verhagen and Levin, 1986), which were presented at the Conference on the Treatment and Conditioning of Radioactive Waste (September, 1986), are reproduced below.

Moisture transport in the unsaturated zone is slow due to the very low hydraulic conductivity and dispersivity values of the overlying clays (Levin et al., 1986). The percolation rates are thus very low, except where highly transmissive zones (e.g. fractures, cracks or other permeable zones) may permit infiltrating moisture to reach the saturated zone at lower levels. The aquifer at the nuclear disposal site is confined, with a relatively flat piezometric surface at 50m to 60m below the surface. Regional flow occurs to the northeast at a very slow rate. Storage in the fracture granitic aquifers (i.e. Norabees granites) is, according to Levin et al. (1986), limited and the joint and fracture systems are not always interconnected.

The measurement of tritium in soil moisture profiles indicated that precipitation over the past 50 years has not penetrated to depths of more than 3 m below surface (Verhagen and Levin, 1986). Measurable tritium concentrations are, however, found at greater depths in the unsaturated zone associated with fractures or root holes. The deeper clay material in the unsaturated zone acts as an aquitard for infiltrating soil water, except when fractured or cracked. Groundwater recharge is considered to be minimal under present average climatic conditions. Significant infiltration, constituting recharge to the piezometric

surface, does occur generally at certain localities, albeit during climatic conditions (i.e. periodic rainfall events), which differ from those recorded as average for the Namaqualand region. Furthermore, radiocarbon dating of groundwater suggests residence times considerably less than 10 000 years. Such lower than expected ages for the groundwater is explained by the mixing and masking of younger, active recharge by older groundwater (Verhagen and Levin, 1986).

A number of reports on water supply to rural towns and villages have been produced by Toens *et al.* (1991, 1993, 1994, 1995 and 1996). Similar reports were produced by Esterhuyse (1987, 1990 and 1991). Regional perspectives on groundwater quality are given in Toens *et al.* (1993 and 1996), including the Richtersveld and the northwestern parts of the Namaqualand region.

The aquifer systems identified in Namaqualand included the weathered overburden (i.e. regolith) and the relatively weathered and fractured underlying basement rocks (i.e. the saprock). Primary aquifers are limited to alluvial deposits, especially in the Buffels River (Toens *et al.*, 1991; Esterhuyse, 1987). Numerous small villages are dependant on water from the alluvium of the Buffels River. The water levels in these large diameter wells in the alluvium are strongly seasonal. The unconfined alluvial system is seasonally replenished, especially in the upper reaches of the Buffelsriver (i.e. at the towns of Kamassies, Nourivier and Rooifontein), while the low water levels during the dry season, and the resultant degradation of quality, are the result of inflows from the basement aquifer system. Groundwater occurs mainly in joint systems, fault, shear and thrust zones, fractured or brecciated intrusive bodies, or on the contacts with intrusive rocks. Therefore the properties of crystalline aquifers (fractured igneous and metamorphic rocks) are largely controlled by these structural features and not by matrix porosity, as is the case in primary aquifers. Fault material and the formation of secondary minerals may severely restrict the flow of groundwater in these aquifers. This results in extreme variability in the properties of the crystalline aquifers. Basement aquifers have some of the lowest hydraulic conductivity values and also the largest range of values.

Arid zones, such as the study area, are bound to have significant water quality problems. The groundwater found in the Buffels River catchment can broadly be characterised as relatively saline, commonly exploited in structurally controlled valleys, as well as the relatively lower salinity groundwater limited to the higher lying regions of the catchment. The groundwater for the northern and central parts of the Buffels River catchment is very similar in character, possessing a general sodium-chloride (Na-Cl) character. Groundwaters limited to the highest regions of the Buffels River catchment have a relatively low salt content with a similar Na-Cl character. The spatial distribution of selected parameters, especially electrical conductivity (EC), chloride (Cl), sodium (Na) and fluoride (F) illustrate the extensive poor natural water quality for the region (Figure 2.7). The good correlation that exists between the EC, Cl and Na maps indicate the dominant Na-Cl character of the groundwater and the significant and dominant contribution of the ions, Cl and Na, to the total dissolved solid load of the groundwater. The high fluoride content in the groundwater presents a serious health threat. Similarly,

nitrate concentrations (as N) in excess of 10mg/l may pose a health risk to infants if the groundwater is used for domestic purposes.

According to Esterhuyse (1991), the groundwater obtained from the Nama shale is of a better quality than that obtained from the granitic or gneissic rocks. High fluoride concentrations are typical of the granitic areas, while the Vioolsdrif granites are associated with high potassium values (Esterhuyse, 1991). Similarly, fault and joint zones in sedimentary rocks yield better quality groundwater than similar structures in granitic, metavolcanic and gneissic rocks. Furthermore, granites yield better quality groundwater than schists, leptite, and gneisses, which each yield progressively poorer quality groundwater. However, it should be noted that residence time associated with varying hydraulic and flow conditions affect groundwater quality irrespective of rock type.

Average yields for Namaqualand vary approximately between 0.2 to 2 l/s (Toens *et al.*, 1996). Boreholes with yields of 0.1 – 0.5 l/s constitute 37%, while boreholes with yields of more than 10l/s constitute only 5.5% of boreholes exploited (Toens *et al.*, 1993). In the Leliefontein Rural Reserve, blow yields varying from between 0.5 to 10l/s were measured (Esterhuyse, 1987). Boreholes in the Steinkopf region were pumped at rates varying from 0.6 to 3l/s for six hours per day (Esterhuyse, 1991). The calculated safe yields for boreholes in the Steinkopf area vary from 5.7 to 47.2$m^3$/d.

Further afield, Vegter (2001) described the groundwater resources for the Makoppa Dome in the Northern Province. The area is underlain by Swazian granite and granite-gneiss with scattered occurrences of Swazian metamorphosed metasediments and mafic intrusives. The basement rocks are covered with Cainozoic detrital deposits and calcrete. The combined saturated thickness of alluvium and weathered bedrock, along the Crocodile River, ranges between 20 m to 40 m while the average yields of the boreholes were 7.9l/s. The optimal strike depth for groundwater in these hard-rock formations ranges between 20 m to 85 m. Vegter (2001) suggested that more boreholes to the same depth will be more successful than deeper boreholes. The chemical processes, influencing the chemical character of the groundwater with resultant weathering products, are governed by the climatic and environmental conditions, the rate of water movement and the residence time. The resultant weathering products may both enhance and/or degrade the water-bearing properties of the aquifer material (Vegter, 2001).

Similar conclusions were reached for the Limpopo granulite-gneiss belt in the Northern Province (Vegter, 2001). The area is underlain by highly deformed supracrustal and intrusive rocks of Swazian age with widespread occurrences of surficial Tertiary and Quaternary deposits. Groundwater resources, in conjunction surface water resources, are exploited for household use, irrigation purposes as well as for cattle and game ranching. The drilling results for the hard-rock aquifers were poor with approximately 40% of boreholes yielding more than 0.1 l/s. The optimal strike depth, in certain localities, ranges between 50 m to 85 m below surface or between 15 m to 25 m below the water level. The depth of weathering may extend deeper than 100 m below surface in certain localities. Vegter (2001) again stressed that higher yields were not necessarily encountered at greater depths below the water level. Drilling should stop on reaching the optimal strike

depth and than continued at other localities. The water-bearing properties of the supracrustal and intrusive rocks of the Limpopo granulite-gneiss belt are the result of brittle deformation, weathering and unloading. According to Vegter (2001), the probability of striking water is the greatest where weathering extends to below the piezometric level, where the depth of weathering and of the piezometric surface do not exceed 40 m below surface and within the first 10 m below the piezometric level.

Sami (2002) reported on studies reflecting the importance of fractured basement aquifers for rural water supply. However, the groundwater exploitation potential for these aquifers systems is traditionally low due to the high frequency of low yielding boreholes and low drilling success rates. A geophysical investigation is a prominent or the main component of many groundwater exploration programmes in South Africa. The approach proved to be unsuccessful due to an inadequate understanding of the occurrence of groundwater, the factors affecting the hydraulic properties of these aquifer systems, the geologic and tectonic settings as well as the inappropriate selection of one (or more) geophysical method(s) and test pumping procedures and resultant data interpretation (Sami, 2002). Sami (2002) stressed that a multi-disciplinary approach is needed to develop the groundwater resources of complex aquifer terrains.

Groundwater quality on a regional scale depends on factors such as rainfall, evapotranspiration, topography and geology (Gustafson and Krásny, 1994). Groundwater quality varies throughout South Africa, with rainfall being an important controlling factor in determining quality (Bredenkamp *et al.*, 1991). There is generally a correlation between rainfall and groundwater quality, with poorer water quality often associated with areas receiving low average rainfall (Atomic Energy Cooperation, 1990). However, the effect that geology has on water quality should not be discounted, as well as the nature and thickness of the overburden and the types of agricultural practice (Bredenkamp *et al.*, 1991). Other important factors influencing the chemical composition of groundwater on a less extensive or even local scale include surface water bodies and their chemical composition, micro-climate, precipitation quality (which often depends on proximity to the sea), anomalies in rock composition (e.g. soluble mineral deposits such as gypsum and salts) and zones of discharge of deep-seated groundwater (Gustafson and Krásny, 1994). The more arid regions of South Africa experience the worst water quality problems, with chemical constituents frequently exceeding maximum allowable limits.

### 2.4: Summary

This review contributed to an improved conceptual understanding of fractured crystalline rocks as 'aquifer systems' with reference to:

**Hydraulic properties:** Certain authors describe the 'near-surface' regolith aquifer as approximately uniform, characterized by its regional mean transmissivity rather than the sporadic higher permeabilities of the fault zones. As a result, the weathered overburden is considered to have low to moderate transmissivity and high storativity compared to the underlying fractured bedrock with high transmissivity and low storativity.

**Storage:** Basement aquifers in humid tropical climatic sub regions are characterized by relatively thick regolith and shallow water tables. A thick saturated regolith is necessary for adequate storage and available drawdown. A direct relation exists between increasing yields and increasing thickness of the weathered overburden. However, the storage capacity for basement aquifer systems in arid regions may be limited to fracture systems and enhanced by the interconnection between such fracture systems.

**Flow:** The flow of groundwater from soil to fractured crystalline bedrock only occurs at specific sites with a combination of suitable geologic and hydrological variables. The fractures act as conduits for deeper flow of groundwater from an upper, saturated regolith. The most productive zone for groundwater development corresponds to the lowest zone of the regolith (i.e. weathered overburden) and the top of the weathered saprock (i.e. weathered and fractured bedrock). Flow in this productive zone corresponds to a deeper and slower flow system that is characterized by relatively higher total dissolved solid loads. A shallow flow system (i.e. interflow) within the residual weathered overburden is characterised by weaker mineralisation processes.

Basement aquifers are characterized by a thick regolith (i.e. weathered overburden) with dominant intergranular flow in tropical to subtropical regions compared to dominant fissure flow in temperate and higher latitude regions. Complex flow patterns probably exist within the fractured crystalline material in Namaqualand.

**Weathering process:** The regolith results from the interaction of acidic rainfall (i.e. dilute $CO_2$ enriched waters) with the thermodynamically unstable aluminosilicate minerals resulting in the leaching of the more soluble elements (i.e. releasing cations and silica) or compounds, as well as the re-precipitation of the less mobile elements or compounds. In addition, in-situ and insoluble weathering products or residues comprising of clay minerals with an increased Al/Si ratio form. Similarly, oxides of iron and manganese form.

**Groundwater chemistry:** The quality of groundwater from basement aquifers in humid and subhumid tropical climatic subregions is considered to be of acceptable quantity and quality. The groundwater, in humid and subhumid tropical climatic subregions, is characterised by low TDS values, acceptable quantity and bicarbonate and calcium as the dominant ions. The natural groundwater quality, in tropical climatic subregions, exhibits both vertical differences in chemical composition and variations over short distances spatially. Such differences result from complex groundwater flow patterns and differential weathering and leaching processes.

With increasing aridity, the TDS content increases and the anion composition of the groundwater changes to sulphate or even chloride with varying cation content. The groundwater chemistry in desert (i.e. semi-arid to arid) regions is dominated by chloride and sodium, while the yield for these aquifers is generally poor. Vertical zonation in the chemical composition of groundwater is evident through perennial natural springs of highly mineralized waters.

**Groundwater development:** Basement aquifers generally have very low transmissivity values and are characterized by both poor connectivity of bedrock fractures and regions of low permeability. These characteristics can result in significant local variations in yield and extreme variability in response to recharge and abstraction.

The most productive zone for groundwater development corresponds to the lowest zone of the regolith (i.e. weathered overburden) and the top of the weathered saprock (i.e. weathered and fractured bedrock). Flow in this productive zone corresponds to a deeper and slower flow system that is characterized by relatively higher TDS. A shallow flow system (i.e. interflow) within the residual weathered overburden is characterised by weaker mineralisation processes.

**Redefining the aquifer systems:** The aquifer system comprises predominantly of an intact and relatively unweathered matrix with a complex arrangement of interconnected fracture systems. Certain authors describe the fractured basement aquifers as 'hydraulic conductors' or 'compound conductors' with reference to the structural control on the storage and flow of groundwater.

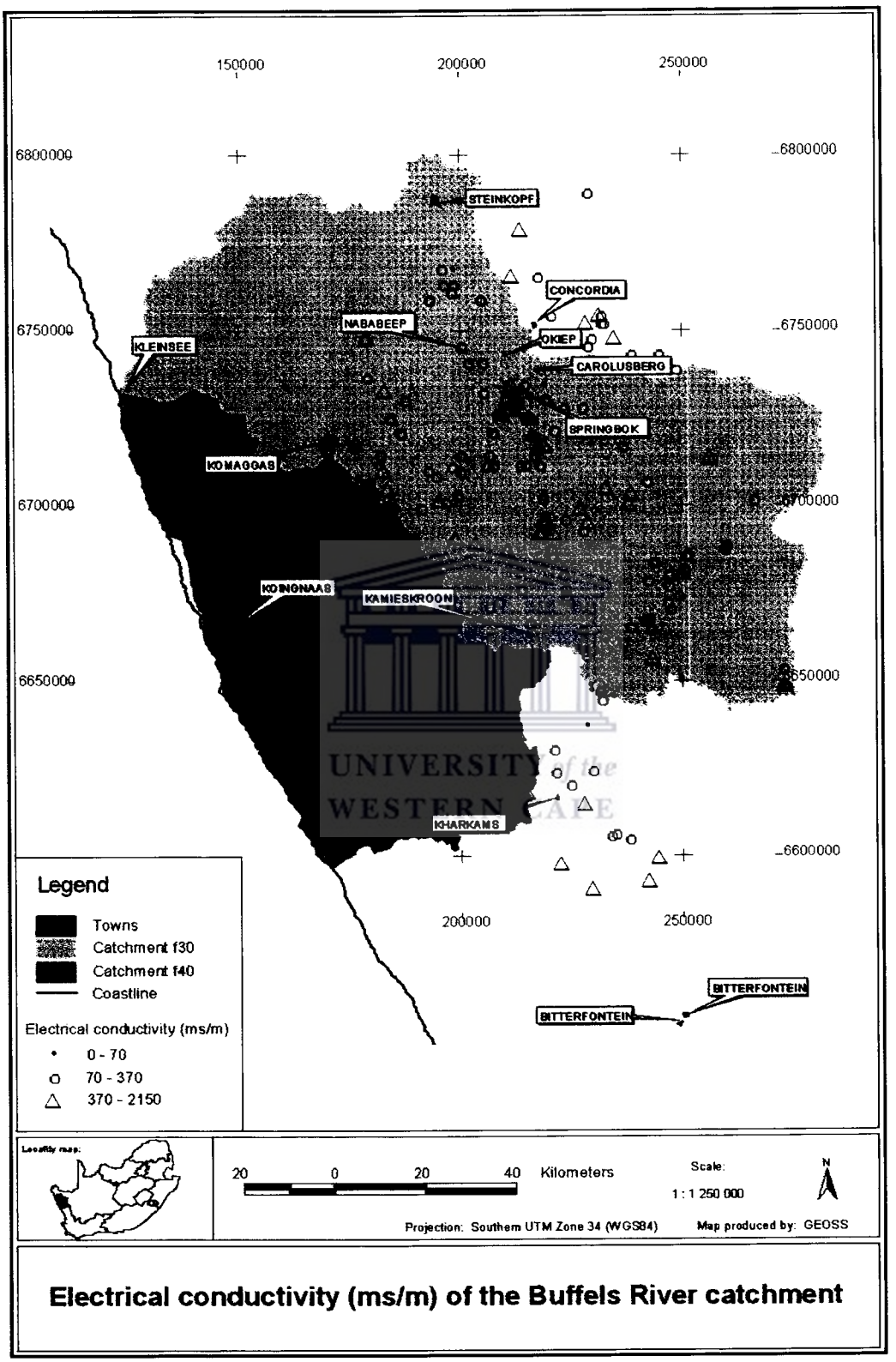


Figure 2-7: EC values (mS/m) in catchments F30, F40 and part of F50.

# Chapter 3

# Physiography of the study area

### 3.1: Location and extent of study area

Namaqualand consists of seven communal areas, namely the northern Richtersveld, southern Richtersveld, Steinkopf, Concordia, Komaggas, Pella and Leliefontein. Namakwa Water supplies surface water from the Orange River to the larger towns only, such as Springbok, Nababeep, Okiep and Kleinzee. State and privately owned farms also depend on groundwater for domestic and stock water supply.

The area is situated between latitude 17° 00' - 18°30' and longitude 29°00'- 0°30'and includes the Buffels River catchment (F30) as well as parts of catchments F40 and F50 (Figure 1.1). The Namaqualand area is classified by three physiographic regions according to topography, altitude and landforms. These regions are the higher lying Bushmanland Plateau to the east, the Namaqualand highlands (which is the escarpment zone), and the lower lying coastal area to the west (Visser, 1989). This study will focus on the Buffels River catchment (F30), although data from the adjacent catchments will be used to define clearly the boundaries between the catchments.



### 3.2: Climate

The study area falls in the arid, hot (BWh), tropical desert climatic region of South Africa, according to the Koeppen classification. The climate of the study area is determined by altitude, topography, and distance from the sea. Climatological data for the study area (i.e. precipitation, evaporation and temperature data) was received from the South African Weather Bureau, Computing Centre for Water Research (CCWR) and extracted from WR90 (Midgley *et al.*, 1994).

#### 3.2.1: Precipitation

The region can be classified as arid to semi-arid, with mountainous regions having higher rainfall than the arid lowland due to orographic effects. Rainfall occurs mostly during the winter months. Snow in the Kamiesberg Mountains is, however, not uncommon during the summer months. Climatological data (Midgley *et al.*, 1994) for the various sub-catchments are shown in Table 3.1. The quaternary catchment scale data best represent the prevailing precipitation. However, due to the strong orographic effects, precipitation at higher altitudes can be considerably higher than that determined for the quaternary

catchment scale data. Average monthly rainfall data for the three topographic zones are shown in Figure 3.1.

Table 3-1: Climatological data for the various catchments that comprise the study area (from Midgley et al ., 1994)

| **F30** | | | | |
|---|---|---|---|---|
| Catchment | Gross area ($km^2$) | MAE (mm) | MAP (mm) | MAE/MAP |
| F30A | 1954 | 2200 | 162 | 14 |
| F30B | 1462 | 2200 | 107 | 21 |
| F30C | 1655 | 2200 | 184 | 12 |
| F30D | 976 | 2200 | 162 | 14 |
| F30E | 1260 | 2200 | 153 | 14 |
| F30F | 1469 | 2200 | 112 | 19 |
| F30G | 980 | 2200 | 102 | 22 |
| F30 | 9756 | 2200 | 143 | 15 |
| **F40** | | | | |
| F40A | 984 | 1900 | 118 | 16 |
| F40B | 404 | 1900 | 130 | 15 |
| F40C | 608 | 1900 | 173 | 11 |
| F40D | 741 | 1900 | 123 | 16 |
| F40E | 1065 | 1900 | 186 | 10 |
| F40F | 682 | 1900 | 118 | 16 |
| F40G | 348 | 1900 | 168 | 11 |
| F40H | 514 | 1900 | 109 | 17 |
| F40 | 5346 | 1900 | 140 | 14 |
| **F50** | | | | |
| F50A | 1303 | 1900 | 179 | 11 |
| F50B | 603 | 1900 | 208 | 9 |
| F50C | 439 | 1900 | 159 | 12 |
| F50D | 687 | 1900 | 112 | 17 |
| F50E | 487 | 1900 | 246 | 8 |
| F50F | 575 | 1900 | 133 | 14 |
| F50G | 775 | 1900 | 96 | 20 |
| F50 | 4869 | 1900 | 159 | 12 |

The average annual rainfall generally increases from west to east until it reaches the escarpment, and decreases towards the inland. The higher lying areas within the study area receive much higher rainfall than the surrounding lower lying areas and coastal plains (see Figure 3.2). Figure 3.3 indicates how the precipitation increases from the sea to the inland areas (that is, from west to east), with the topography also changing from coastal to mountainous regions in the same direction. The rain gauge station (Dabeep) situated on the Bushmanland plateau shows a different climatic regime (Figure 3.1).

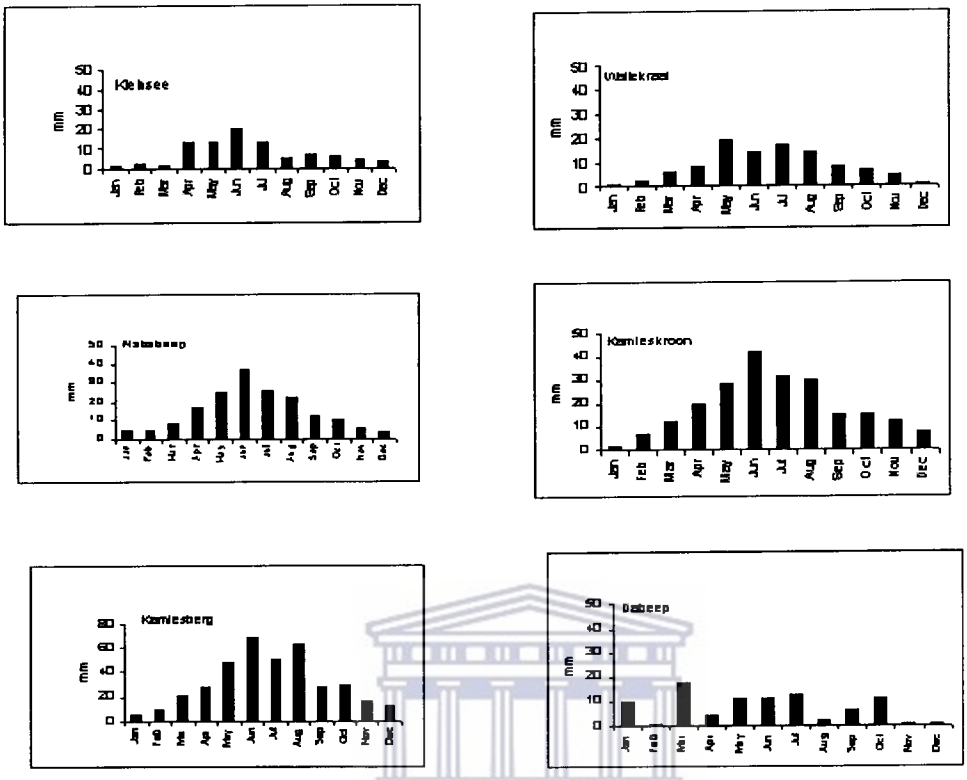




Figure 3-1: Average monthly rainfall for six rainfall stations.

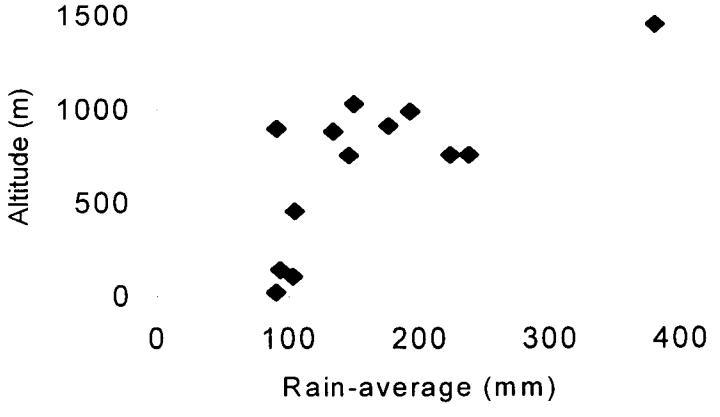


Figure 3-2: Relationship between mean annual rainfall and altitude.

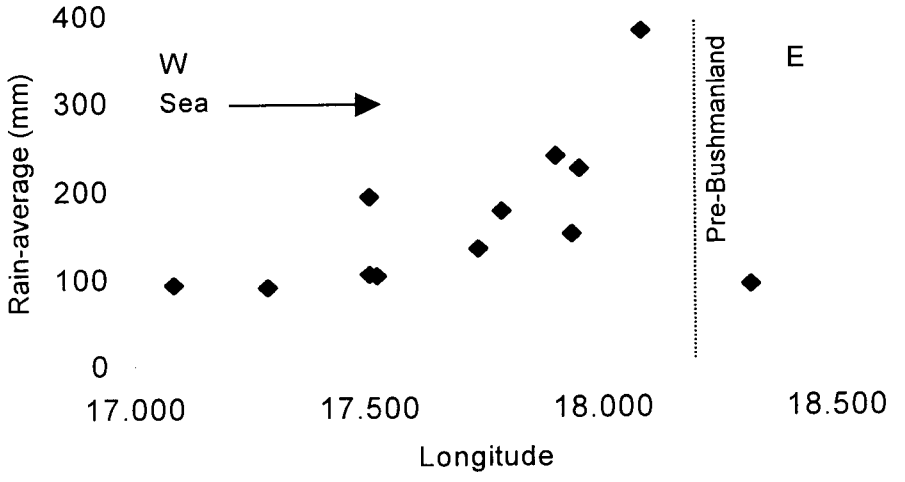


Figure 3-3: Influence of distance from sea and topography on mean annual rainfall.

3.2.2: Potential Evapotranspiration

Potential evapotranspiration can be as much as from 12 to 15 times the precipitation. In some areas, this factor is as high as 22 times the precipitation. This high evaporation to precipitation ratio means that salts will easily form on the surface, as well as in the subsurface. Campbell *et al.* (1992) found that actual evaporation occurred to a depth of 91cm in the alluvium. Van der Sommen and Geirnaert (1990) found that in areas of dense vegetation and shallow water levels, the actual evapotranspiration is much higher than in areas of sparse vegetation and where deeper water levels occur.

Three evaporation stations (Table 3.2) have S-pan and A-pan MAE (mm) data (Midgley *et al.*, 1994).

Table 3-2: Evaporation data from S-pan and A-pan experiments at selected stations in Namaqualand.

| Gauge No. | Station name | S-pan | A-pan | Years |
|---|---|---|---|---|
| F3E001 | Okiep | | 3193 | 1957-1979 |
| F3E003 | Grootmis | 1939 | 2260 | 1964-1979 |
| F4E001 | Hondeklipbaai | | 1823 | 1964-1979 |

Controversy exists over the validity of pan evaporation measurements, since wind, temperature effects and humidity can vary considerably in micro-environments and for different surface types. However, the data obtained from pan measurements can be used for baseline considerations. Evaporation is at its maximum during the summer months, and much lower during the winter months when rainfall is at its highest (Figure 3.4).

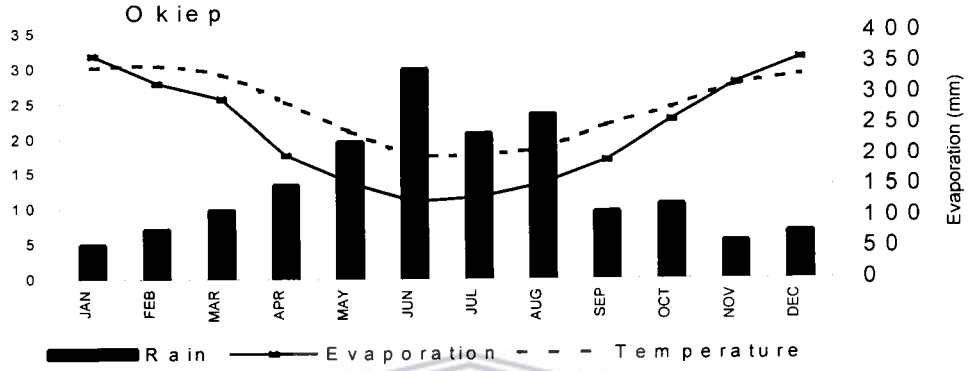


Figure 3-4: Average monthly evaporation for the Okiep area, and the relationship that exists between temperature and rainfall.



3.2.3: Temperature

Large variations between the maximum and minimum temperatures, as well as daily and seasonal temperatures exist for the region. Table 3.3 shows typical temperature variations over the three topographic regions of the study area. The average monthly temperatures for Springbok are shown in Figure 3.5.

Table 3-3: Temperature variations over the three topographic regions.

| | Summer temperature (in °C) | | Winter temperature (in °C) | |
|---|---|---|---|---|
| | Max. | Min. | Max. | Min. |
| Lowveld | 20 | 13 | 15 | 8 |
| Escarpment Zone | 30 | 17 | 16 | 8 |
| Highveld | 34 | 17 | 18 | 5 |

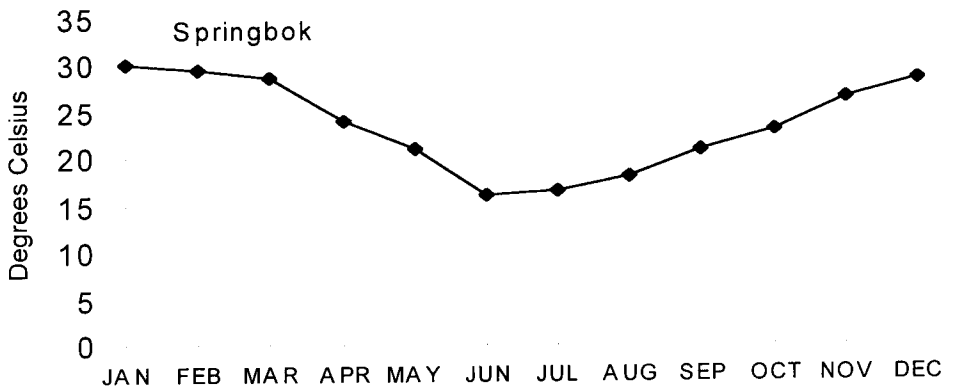


Figure 3-5: Average monthly temperatures for Springbok.



### 3.3: Vegetation

The vegetation is characterised by the Nama karoo biome, which is dominated by a mixture of grasses and low shrubs (Low and Rebelo, 1996). Most of the shrubs are classified as drought deciduous and tend to develop deep root systems.

In alluvial plains and riparian zones, vegetation is dependent on groundwater. Plant species such as *Prosopis* (moderately drought tolerant, facultative phreatophytes) form extensive thickets that indicate the availability of groundwater (Low and Rebelo, 1996). *Acacia karoo* (riparian shrubs and trees) is found in the alluvium of the Buffels River.

Acocks (1954) recognised four different vegetation types in the area:

- Succulent Karoo in the low-lying Sandveld area;
- Namaqualand Broken Veld in the lower mountain areas;
- Mountain Renosterveld in the Kamiesberg mountains;
- False succulent Karoo on the eastern Kamiesberg mountain range.

Succulents, semi-succulents and grasses are prominent in the Sandveld area (i.e. the lower lying coastal plains). The Namaqualand Broken Veld, characterised by succulents, semi-succulents and herbs, is generally found on the dome-shaped hills. The Mountain Renoster Veld is unique to the Kamiesberg Mountain range, whereas the False Succulent Karoo vegetation is found towards the east (i.e. in the Gamoep to Platbakkies area).

# Chapter 4

# Geological characteristics

## 4.1: Introduction

The geological history of southern Africa began some 3,8 billion years ago. In their synthesis, Tankard *et al.* (1982) identified a distinct sequence of crustal evolutionary stages that incorporates the geological and tectonic events that have shaped the African subcontinent. These evolutionary stages of crustal development are also summarised in Moon and Dardis (1988).

The ancient geological evolution of southern Africa can be regarded as a sequence of accretion onto a stable Kaapvaal craton during both extensional and compressional tectonic periods (Partridge and Maud, 2000). The accretion of the Namaqua-Natal mobile belt occurred between 2000 Ma and 1000 Ma and resulted in the stabilisation of the Kalahari craton around 1000 Ma. A series of orogenic belts, such as the Gariep and Malmesbury sequences, were accreted onto the Kalahari craton during the Pan-African tectonic cycle that ended approximately 600 Ma ago (Partridge and Maud, 2000). The inter-cratonic mobile belts were repeatedly uplifted during the Phanerozoic (Partridge and Maud, 2000) and are regarded as precursors of the subsequent separation of Africa and South America and India and Antarctica (Partridge, 1998).



The crystalline basement rocks of Namaqualand retained imprints of mostly Proterozoic events (Figure 4.1), although much of the present landscape appears to have developed later, following the break-up of Gondwanaland in the Cretaceous.

Surface run-off occurs over the smooth dome surfaces with infiltration along the edges and within the fault-controlled valleys adjacent to the domes. Water may, however, also infiltrate along major fracture(s) that cross the domes. Exfoliation sheets are visible with water flowing laterally along these exfoliation planes.

## 4.2: Proterozoic crustal rocks

### 4.2.1: Lithological units, Intrusives and Intrusive relations

The Northwestern Cape Region (i.e. Namaqualand) can be subdivided into three major geological provinces (Tankard *et al.*, 1982). These are the basement rocks of the Namaqua Province (further subdivided into three zones), the volcano-sedimentary rocks

of the Gariep Complex (Visser, 1989) in the northwest, and a Phanerozoic cratonic cover (Table 4.1).

Figure 4-1: Characteristic dome-shaped landscape in Namaqualand.

The Namaqua Province (Table 4.1) represents most of the crystalline basement in the northern Cape and southern Namibia (Tankard *et al.*, 1982). In Namaqualand, the margins of the Namaqua Province are largely obscured by younger cover rocks of the Gariep, Nama and Karoo sequences, as well as with Cenozoic surficial sediments to the east and west. In the west and extreme north, rocks of the Namaqua Province and its correlatives are bordered by formations of the late Proterozoic Gariep Complex and in the East abut the Kaapvaal craton with marked structural discordance in both cases. In the south, rocks of the Nama Group, the Cape Supergroup and the lowermost units of the Karoo Supergroup cover the rocks of the Namaqua Province (Albat, 1984).

Rocks of the Central Zone (Table 4.1) cover most of central Namaqualand and Bushmanland (including parts of northern and eastern Bushmanland) as well as the southwestern parts of southern Namibia (Tankard *et al.*, 1982). Joubert (1971), Jack (1980), Theart (1980) and Albat (1984) carried out detailed mapping on a 100 000 scale, of areas mostly within Namaqualand. Rocks of the Western Zone (Table 4.1) occur mostly in the north-eastern Richtersveld and northern Namaqualand regions (Tankard *et al.*, 1982; Visser, 1989; Albat, 1984). Albat (1984) referred to both the Orange River Group and the Vioolsdrif Suite as the Richtersveld Province. The Eastern Marginal Zone, just east of Upington, is a NW/SE striking transitional boundary between the gneiss terrain and the older Kaapvaal craton.

Table 4-1: Classification of major geological provinces (after Tankard *et al.*, 1982 and Visser, 1989).

| Geological Province | | Group | Age | Locality | OROGENIES & Subprovinces |
|---|---|---|---|---|---|
| Cover Rocks | | Sand, Alluvium and Calcrete<br><br>Karoo Group<br>1. Prince AlbertForm<br>2. Dwyka Formation<br><br>Nama Group<br>1. Kuibis Formation<br>2.Schwarzrand Formation | Late Phanerozoic (Cenozoic)<br><br>Early Phanerozoic (Middle/Late Paleozoic)<br><br>Late Proterozoic (Late Namibian) | Along coast. Most of WesternBushmanland<br><br>Southeastern corner of Namaqualand<br><br>Isolated strip north of Springbok | |
| | | Gariep Complex Six Formations | Late Proterozoic (Early/Middle Namibian) | Central and Western<br><br>Richtersveld | PAN-AFRICAN<br><br>Gariep Sub-province |
| Namaqua Province | Central Zone | Namaqua Metamorphic Complex, (or Province) | Middle Proterozoic (Middle Mokolian) | Most of Namaqualand and parts of Bushmanland | NAMAQUAN Bushmanland & Gordonia Subprovinces |
| | Western Zone | Vioolsdrif Intrusive Suite | Middle Proterozoic (Early Mokolian) | North-eastern and Eastern Richtersveld. Northern Namaqualand | EBURNIAN<br><br>Richtersveld Subprovince |
| | | Orange River Group | Middle Proterozoic (Early Mokolian) | North-eastern part of Richtersveld | |
| | Eastern Zone | | | Upington | |

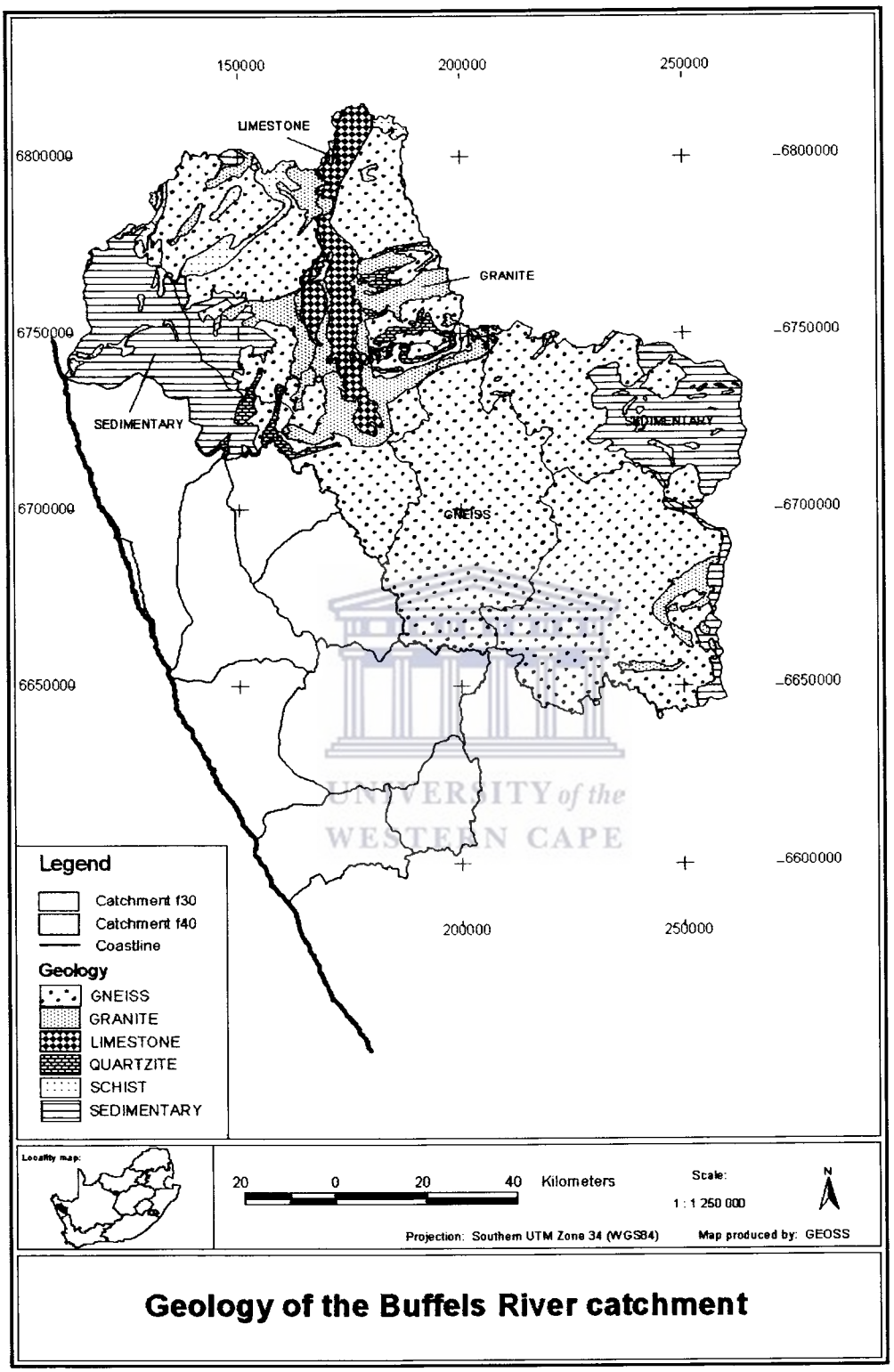


Figure 4-2: General geology (major lithological units) of the Buffels River catchment (F30).

*4.2.1.1: Richtersveld Subprovince*

The Richtersveld Subprovince (Table 4.1) is the largest zone of preserved Eburnian rocks (1900 ± 200 Ma) that have escaped reworking within the subsequent Kibaran (1400 ± 200 Ma), Namaquan (1100 ±100 Ma) and Pan-African (600 ± 100 Ma) orogens (Blignault, 1977; Reid, 1979 and 1982; Hartnady *et al.*, 1985; Thomas *et al.*, 1994 and Colliston *et al.*, 1996). The Richtersveld Subprovince comprises predominantly of the volcanic Orange River Group (Table 4.1) into which the Vioolsdrif Batholith was emplaced. Early Proterozoic low-grade supracrustal rocks of largely extrusive origin, the Orange River Group (± 2000 Ma), and an intrusive composite granitoid batholith of slightly younger age, known as the Vioolsdrif Intrusive Suite (± 1900 Ma), outcrop in the north-eastern part of the Richterveld (Tankard *et al.*, 1982; Albat, 1984 and Visser, 1989). Outcrops of the Orange River Group consist of rocks of the volcanic De Hoop Subgroup, the sedimentary Rosyntjieberg Formation, and the volcanic Haib Subgroup (Tankard *et al.*, 1982). The top of the Haib Subgroup is erosionally truncated by an angular unconformity beneath the Phanerozoic cratonic cover sequences (Tankard *et al.*, 1982). The most important occurrences of the Orange River Group (Table 4.2) are in the north-eastern part of the Richtersveld, between Vioolsdrif and Goodhouse, with possible correlatives, namely the Hom and Guadom Subgroups, which are found to the east of Goodhouse (Visser, 1989).

Table 4-2: The Orange River Group (after Visser, 1989 and * age by Reid, 1979a).

| Possible Correlatives | | | | |
|---|---|---|---|---|
| Subgroup | Group | Subgroup | Formation | Description |
| Gaudom | Oranje River Group | Haib* (1996 ±15Ma) | Nous | Meta-volcanic |
| Hom | | | Tsams | |
| | | | Windvlakte | Volcanic rocks |
| | | | Rosyntjieberg | Sedimentary (Quartzitic) |
| | | | Paradys river | Volcanic rocks |
| | | | Klipneus | Volcanic rocks |
| | | De Hoop | Kuams | Volcanic rocks |
| | | | Kook river | |
| | | | Abiekwa river | |

The Vioolsdrif Intrusive Suite, according to Tankard *et al.* (1982), is a large, pre-cratonic, composite, granitoid batholith, with the various suites suggesting an order of intrusion from basic to acid (i.e. from the older sill-like basic-ultrabasic layered suites to intrusive cross-cutting plutons of granite and alkali-feldspar granite).

The Vioolsdrif suite, found in the north-eastern and eastern parts of the Richtersveld as well as in northern Namaqualand between Vioolsdrif and Goodhouse, is intrusive into rocks of the Orange River Group (Visser, 1989). This suite is dated at between 1900 ± 30 Ma to 1731 ± 20 Ma (Reid, 1979b and Reid and Barton, 1982).

- Post-Vioolsdrif igneous activity include: Belts of en-echelon pegmatites (1000 Ma) emplaced late syntectonically (i.e. related to limited eastward translation of the area); and
- The Richtersveld and Kuboos-Bremen Intrusive suites and Gannakouriep basic dike swarm related to the Gariep orogeny (Tankard *et al.*, 1982).

The Richtersveld Suite, found in the south-eastern part of the Richtersveld, is intrusive into rocks of the Orange River Group and Vioolsdrif Suite (Visser, 1989). These rocks were dated at 920 ± 10 Ma (Allsopp *et al.*, 1979).

*4.2.1.2: Gordonia and Bushmanland Subprovinces*

The Namaquan orogen (1100 + 100Ma) is represented by the Gordonia Subprovince (Table 4.1) in southern and southwestern Namibia and the Bushmanland Subprovince (Table 4.1) in the north-western regions of South Africa. Rocks for these two subprovinces probably formed from the reworking of the older Eburnian and Kibaran domain rocks. Tectonically, the Proterozoic Namaqua Province includes the Gordonia and Bushmanland Subprovinces as well as the Eburnian Richtersveld Subprovince (Hartnady *et al.*, 1985). Tankard *et al.* (1982) describe the Namaqua Province in a similar manner. The Central Zone (Namaqua Province), a complexly deformed heterogeneous group of gneisses and intrusions of regional medium to high grade metamorphism and collectively known as Namaqua Metamorphic Complex (Tankard *et al.*, 1982) covers most of the Namaqua Province (i.e. Namaqualand and Bushmanland) as well as large parts of southern and southwestern Namibia (i.e. Gordonia). Visser (1989) describes this area as the Namaqua Metamorphic Province (rather than the Namaqualand Metamorphic Complex) consisting of an assemblage of meta-sedimentary, meta-volcanic and intrusive rocks (Tables 4.1 and 4.3). The Namaqualand region, comprising the Namaqualand highlands and the coastal plains, can, according to Tankard *et al.* (1982), be regarded as the type area for the Namaqua Metamorphic Province (Central Zone).

The Buffels River catchment, as well as the surrounding catchments, is predominantly underlain by Proterozoic crystalline basement rocks of the Namaqua Metamorphic Province (Table 4.3). Cover rocks of the Nama group overlay the basement rocks to the north of the Buffels River catchment. The margins of the Namaqua Metamorphic Province are also obscured by younger cover rocks of the Gariep Complex to the north-west as well as by Cenozoic surficial sediments to the east and west. In the south, rocks

of the Nama Group, the Cape Supergroup and the lowermost units of the Karoo Supergroup cover the rocks of the Namaqua Metamorphic Province (Albat, 1984).

Table 4-3: Namaqua Metamorphic Province (after Visser, 1989).

| | Group | Subgroup | Formations | | Descriptions |
|---|---|---|---|---|---|
| Namaqualand Metamorphic Province | Grunau | | | | Meta-sedimentary |
| | Okiep | Bitterfontein<br>Garies*<br>Khurisberg*<br>Aardvark<br>Een Riet | | | Meta-sedimentary & Meta-volcanic |
| | Bushmanland (1330 ± 170 Ma)# | Aggeneys<br>Pella | | | Meta-sedimentary |
| | | | Toeslaan | | Meta-sedimentary |
| | Korannaland sequence | | Goede Hoop<br>Rautenbach<br>se kop<br>Biesje Poort<br>Piet<br>Rooisberg | Sprigg<br>Eierdoppan<br>Jannelsepan<br>(1305 Ma) | Sedimentary & Meta-sedimentary |
| | Geelvloer | | | | Meta-sedimentary |

Note: * Rocks found in study area. # Age given by Welke (1983).



The Hoogoor suite*, and alternatively named "pink gneiss", is composed of granitic and gneissose rocks which intruded into the rocks of the Namaqua Metamorphic Province (Visser, 1989). The Gladkop Suite* of rocks are intrusive into the Een Riet and Khurisberg Subgroups of the Namaqualand Metamorphic Province. Ages for the gneisses of the Gladkop Suite in the Steinkopf area vary between 1700 to 1800 Ma (Barton *et al.*, 1981 and Reid and Barton, 1982). The Gladkop Suite consists of the members, Steinkopf Gneiss, Brandewynsbank Gneiss and the Noenoemaasberg Gneiss. The Spektakel Suite* also consists of three members; namely, the Concordia Granite, the Rietberg Granite and the Kweekfontein Granite. The Kweekfontein Granite is intrusive into all other granitic rocks in the southern part of the Copper district (Visser, 1989). The Little Namaqualand Suite* "includes all the coarse-grained, intrusive augen-gneisses" (Visser, 1989). The Little Namaqualand Suite consists of eight members, with clear intrusive relations to one another and the country rocks (Visser, 1989). Rocks of the Koperberg Suite* occur as pipes, dike-like, or irregular bodies and are intrusive into the granitic and gneissic basement rocks, especially around O'kiep. The Koperberg Suite rocks, important copper bearing rocks associated with anticlinal structures, are dated at 1100 Ma (Stumpfl *et al.*, 1976).

Researchers such as (Moore, 1989), Albat (1984), Jack (1980), Theart (1980), Moore (1977), Joubert (1971), Van Zyl, (1967), Benedict *et al.*, (1964), De-Jagar and Simpson

(1962), De Villiers and Songe (1959), Brink (1950), Rogers (1913 and 1915) classified the various rock types in terms of detailed mineralogical descriptions.

### 4.2.2: Multiphase Namaquan tectonism

An Early to Late Proterozoic (or Lower to Upper Precambrian) episode (approximately 2500 Ma to 570 Ma) of intense crustal instability can be divided on a chronologic and geographic basis into:(a) an Early to Middle Proterozoic (mainly Mokolian) tectonism resulting in the Namaqua and Natal Provinces, and (b) a long chain of Late Proterozoic (i.e. Namibian erathem) geosynclines, termed the Pan African Geosynclines, along the present southwestern coast and Namibian interior, including the Gariep Complex (Tankard *et al.*, 1982; Visser, 1989).

The Proterozoic Namaqua mobile belt, including the Richtersveld Subprovince, was subjected to the 1000 – 1200 Ma Namaquan orogeny (Blignault *et al.*, 1983; Van der Merwe, 1995). The earliest episodes of deformation of the Namaqualand, when the rocks where plastically deformed, controlled the regional distribution of the lithological units. During the succeeding stages of brittle deformation, the rocks were modified along zones of movement and resulted in the formation of a trough along the west coast where later sedimentation took place.

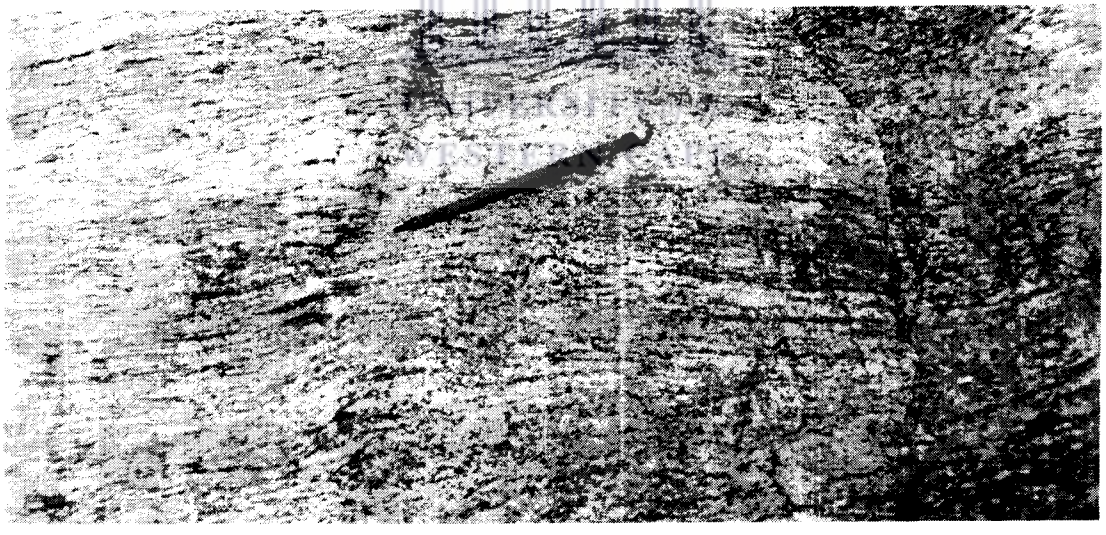

Figure 4-3: Characteristic east-west Namaquan (S2) fabric. This fabric is usually folded by subsequent deformation events.

The rocks of the Namaqualand Metamorphic Province thus underwent several phases of intensive folding (such as isoclinal folding) as well as faulting and were intruded on a large scale by syntectonic granites (Visser, 1989). Researchers such as Albat (1984), Blignault *et al.*, (1983), Lipson (1978), Moore (1977) and Joubert (1971) recognised four deformation phases within the rocks of the Namaqua Metamorphic Complex. The interpretation of both vertical and lateral stratigraphic and structural relationships, as well

as possible lateral correlatives, is extremely difficult. The high-grade metamorphism and multi-phase deformation undergone by these rocks, destroyed the normal stratigraphic criteria and produced generations of tight and isoclinal folding (Joubert, 1971; Jack, 1980). Most of the area was covered by sediments; these were later stripped off with the subsequent re-exposure of the gneisses and its varying intrusive rocks (Joubert, 1971).

The boudinage (Figure 4.4) is probably associated with a Precambrian (i.e. Namaquan) deformation phase with a roughly N/S direction of maximum compression (i.e. sigma 1). The direction of maximum extension is approximately vertical upward (view photograph from east to west). In addition, fold axes are generally orientated in an east-west direction. Where compositional layering is observed, the more pelitic layers experience more strain (including shearing) due to Namaquan deformation. Shear zones are predominantly parallel to compositional layering and thus parallel to the dominant fabric (i.e. $S_2$ fabric). Crosscutting relations were, however, also observed in the field.

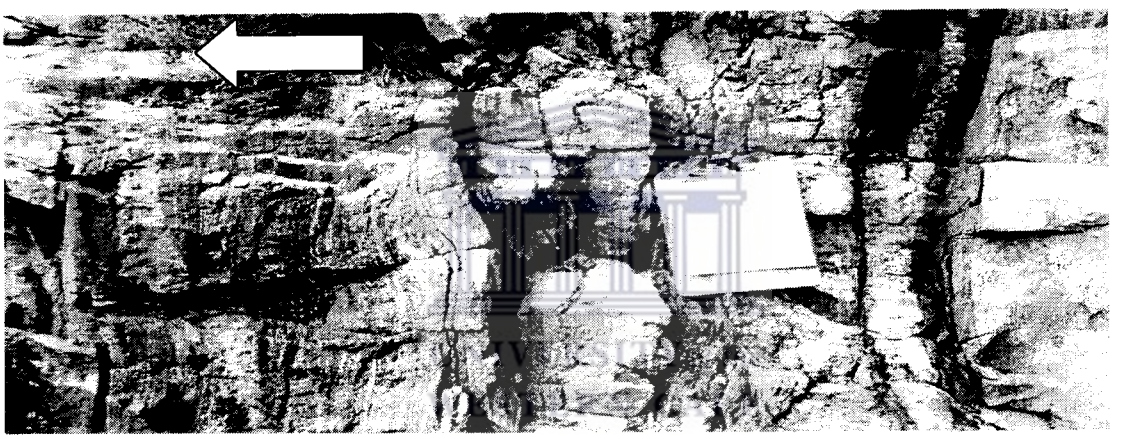

Figure 4-4: Boudinage in more resistant layers parallel to dominant fabric (i.e. S2 fabric) in Kamieskroon Gneiss.

The Namaquan deformation (1000 – 1200 Ma) is characterised by an earlier thrust event, with southwest and westward transport directions, producing the dominant regional foliation and lineation (Blignault *et al.*, 1983; Van der Merwe and Botha, 1989; Van der Merwe, 1995). The Namaqua Metamorphic Province (NMC), in particular the Bushmanland Subprovince, has thus been subdivided into various terrains (Hartnady *et al.*, 1985; Van Aswegen *et al.*, 1987) based on criteria such as metamorphic facies (Albat, 1984) and strain intensity;

- The Groothoek thrust zone, with a south-westerly transpressive transport direction (Watkeys, 1986; Van Aswegen *et al.*, 1987; Van der Merwe and Botha, 1989; Van der Merwe, 1995), forms the southern boundary of the Richtersveld domain (or Richtersveld Subprovince), while the Lower Fish River thrust and Tantalite Valley shear form its north-western boundary in southern Namibia. The domain is predominantly characterised by granitoids of the Vioolsdrif Suite (1730 – 1900

Ma) and volcanics of the Haib Subgroup (2000 Ma). The volcanics of the Haib Subgroup display upper greenschist grade metamorphism (Reid, 1977) probably related to the Eburnian orogeny, alternatively named the Orange River orogeny (Blignault *et al.*, 1983). The granitoids of the Vioolsdrif Suite become intensely foliated mylonites close to the Groothoek thrust zone. Van der Merwe (1995) described this domain as the upper crustal Richtersveld domain displaying greenschist facies and low-grade metamorphism.

A northerly-dipping penetrative foliation, containing well-developed extension lineations plunging towards the northeast, is associated with the east-west striking Groothoek thrust. This dominant and earliest fabric for the Richtersveld domain is related to the 1100 to 1200 Ma Namaquan orogenic event (Blignault *et al.*, 1983; Van der Merwe, 1995).

- The Steinkopf domain (or Steinkopf terrain) comprises medium to high-grade gneisses (Blignault *et al.*, 1983; Van Aswegen, 1983; Van der Merwe, 1995). The northern margin of this terrain is the Groothoek thrust zone and to the south the Ratelpoort shear zone bounds the terrain. The intrusive Gladkop Suite of rocks is dominant within this terrain (Van Aswegen, 1983). The mid-crustal Steinkopf domain (Van der Merwe, 1995) displays amphibolite grade metamorphism (Blignault *et al.*, 1983).

  The Ratelpoort shear zone (Figure 4.5), which is a zone of intense refoliation, originated as a thrust with subsequent rotation to a near vertical attitude and with a predominant vertical downward movement to the south. The Steinkopf domain is characterised by both pre-Namaquan and Namaquan periods of deformation, with the penetrative fabric of the Namaquan deformation phase obliterating the effects of the earlier deformation phase (Van der Merwe, 1995).

- The high grade metamorphic O'kiep Copper District granulite facies (Blignault *et al.*, 1983; Thomas *et al.*, 1994; Gibson *et al.*, 1996) comprises intrusive rocks belonging to Gladkop, Spektakel and Little Namaqualand Suites. Rocks of the Spektakel and Little Namaqualand Suites are the most abundant (Marais and Joubert, 1980a and 1980b), while the metasedimentary rocks (the. Khurisberg Subgroup) of the O'kiep Group are associated with basin and dome structures. The Koperberg suite of rocks is characterised by numerous small, irregular, dyke-like mafic bodies intruding along steep structures that are associated with tight antiforms (Clifford *et al.*, 1995; Gibson *et al.*, 1996; Watkeys, 1996; Van Zwieten *et al.*, 1996). The Ratelpoort shear zone in the north and the Buffels River shear zone in the south bound the domain.

- The Kamieskroon high-grade granulite facies is located south of the Buffels River shear zone. Further to the south, rocks of the Kamieskroon high-grade granulite terrain are thrust onto rocks of the Karkams low-grade granulite facies.

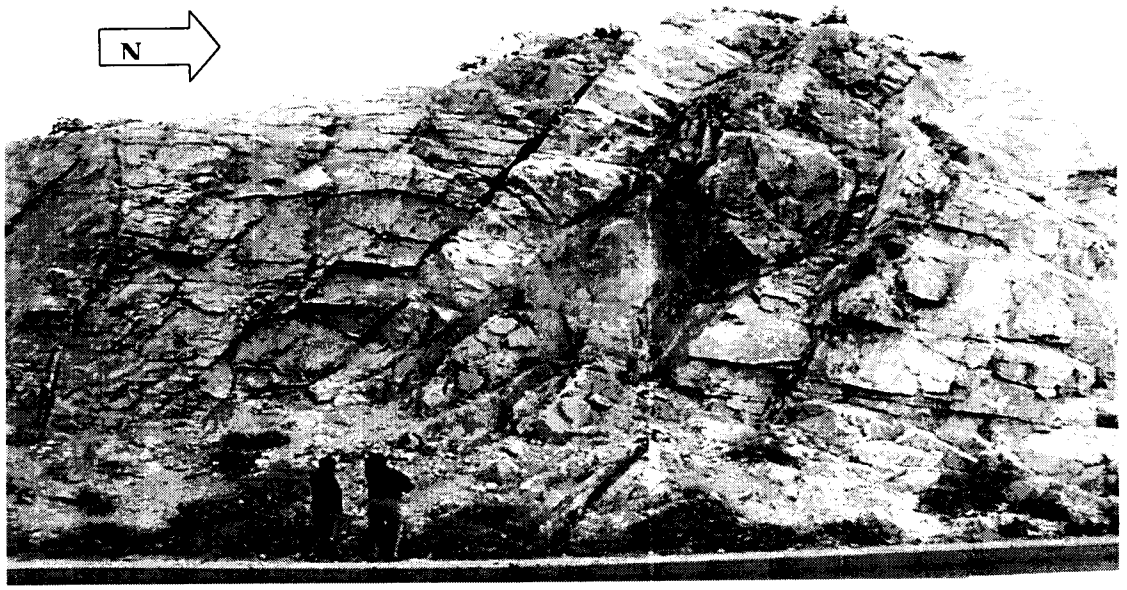


Figure 4-5: The Ratelpoort shear zone north of Springbok..

4.2.3: Neotectonic seismogenic activity

Southern Africa, according to Andreoli *et al.* (1996), is subjected to neotectonic activity occurring along the coastal regions and in the continental interior. On-shore neotectonic activity is occurring in the southwestern Cape, in Namaqualand and over a vast region extending from the Free State to the Northern Transvaal and to Natal. Neotectonic activity was initiated in the Miocene as a result of three major stress fields orientated easterly, NNE and NW to WNW (Andreoli *et al.*, 1996). Andreoli *et al.*, (1996) referred to a pervasive, predominantly north-west to west-north-westerly trending, maximum horizontal compression direction of deep seated but undetermined origin known as the Wegener Stress Anomaly (WSA). This major stress field is present throughout the southern African subcontinent. Neotectonic faults and intraplate seismicity result from an interaction between the WSA and other far field stresses (such as rifting or ridge push, for example.) acting on the African plate. Andreoli *et al.* (1996) rejected the mid-Atlantic ridge push model (Ransome and de Wit, 1992; Zoback, 1992) and the isostatic uplift models (Kooi and Beaumont, 1994; Gilchrist *et al.*, 1994) as explanations of the neotectonic activity experienced by the Atlantic seaboard of South Africa. They further reported that seismogenic Late Cenozoic tectonic activity in South Africa is more widespread than previously stated and that such seismic activity is associated with several, contrasting stress fields with poorly constrained origins.

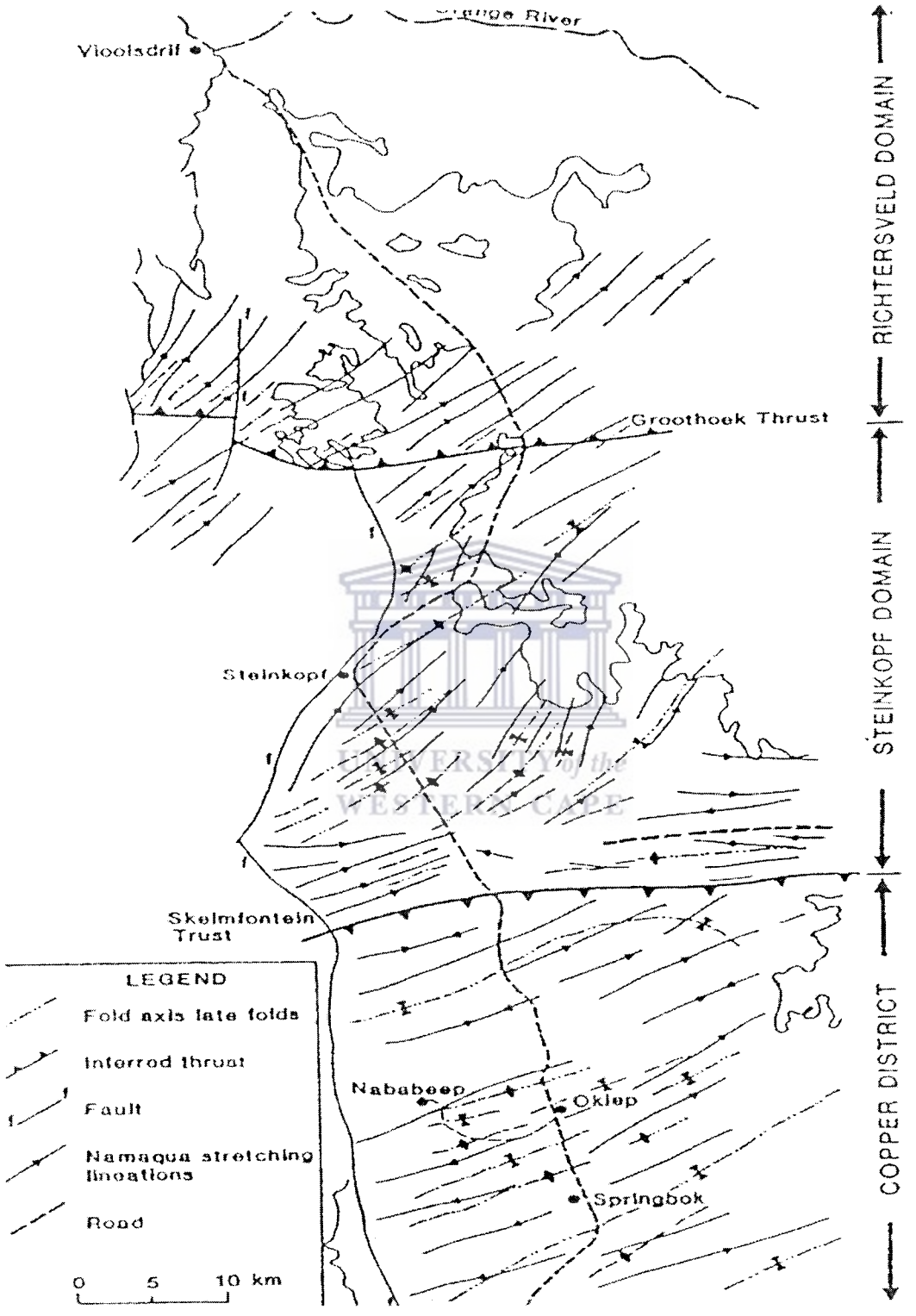


Figure 4-6: The subdivision of the Namaqua Metamorphic Province (NMC), in particular the Bushmanland subprovince, into various terrains (Hartnady *et al.*, 1985; Van Aswegen *et al.*, 1987) based on criteria such as metamorphic facies (Albat, 1984) and strain intensity.

Andreoli *et al.* (1996) discussed the characteristics of the WSA in detail and only those characteristics relevant to this study are stated below:

- The faults resulting from the NW to WNW trending, principal horizontal stress orientations are detected in Late Mesozoic to Early Tertiary oceanic crusts, in crusts affected by a Late Palaeozoic orogeny, in Mid-Proterozoic crusts (that is, the rocks of the Namaqua Province) and in an Achaean craton.
- The WNW stress orientation already existed in the Jurassic, before the break-up of Gondwana, while the NW stress orientation persisted throughout the Cretaceous and is associated with the opening of the South Atlantic.

Seismic activity in Namaqualand is limited to the Leliefontein area close to the intersection between the ENE-WSW trending Griqualand-Transvaal, and the NW-SE trending Kamiesberg Late Cenozoic uplift axes (Andreoli *et al.*, 1996). In fact, WSA-related tectonic activity in the Namaqualand domain has been linked to uplift along the Griqualand-Transvaal axis between the Miocene and Pleistocene. A principal direction of maximum horizontal compression, orientated NNW-SSE during the Mid-Late Cenozoic, controlled the development of extensional fault-bounded sedimentary basins in the Vaalputs area close to Leliefontein. NNW trending extensional faults are preserved in Late Cretaceous residual silicretes, in Early Cenozoic alluvial deposits, and even in more recent siltstones. East of Vaalputs, rare ENE trending faults and two NE orientated axes of above Pliocene age, probably represent the western extension of the Griqualand-Transvaal axis of uplift.

The development of NNW trending extensional faults (Figure 4.7) is probably related to the principal, horizontal stress direction, orientated NNW-SSE during the Mid-Late Cenozoic. These are extensional fractures with oblique strike-slip components and are intruded by dyke material (Figure 4.8).

The NW-SE trending fractures are probably related to the NW stress orientation that is related to the opening of the South Atlantic approximately 140 Ma years. The ENE-NE trending faults probably represent the western extension of the Griqualand-Transvaal axis of uplift. The ENE-WSW fractures can also represent oceanic transform faults that cut across the entire African continent in discrete zones. These vertical to sub-vertical lineament (or fracture) systems represent a predominantly brittle deformation phase, in the upper 5 km to 8 km of the crust.

### 4.3: Proterozoic cover rocks

Late Proterozoic tectonism, commonly termed the Pan African Event, affected vast parts of the west coast of Africa and the east coast of South America resulting in the formation of a 3000 km chain of geosynclines following the western and southern coast of the subcontinent. During the Pan African orogenic event (600 +- 100 Ma), rifting resulted in the break-up of the Rhodinia super continent. The Pan African orogen includes the Damara, Gariep (or the Gariep Complex) and Saldanian sub-provinces in southern

Africa. Subsequent collisional tectonics resulted in the creation of the Pangaea super-continent.

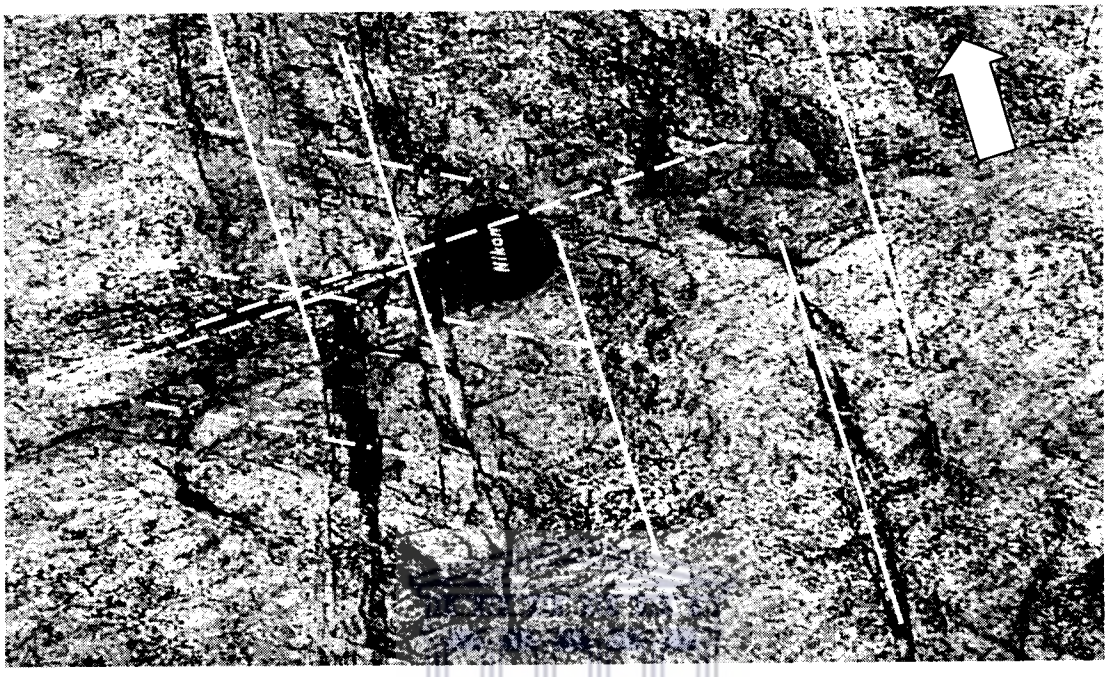

Figure 4-7: NNW-SSE, ENE-WSW and NW-SE fractures in the Gladkop Suite south of Springbok. The Namaquan fabric (i.e. foliation) of the rock is approximately east to west.



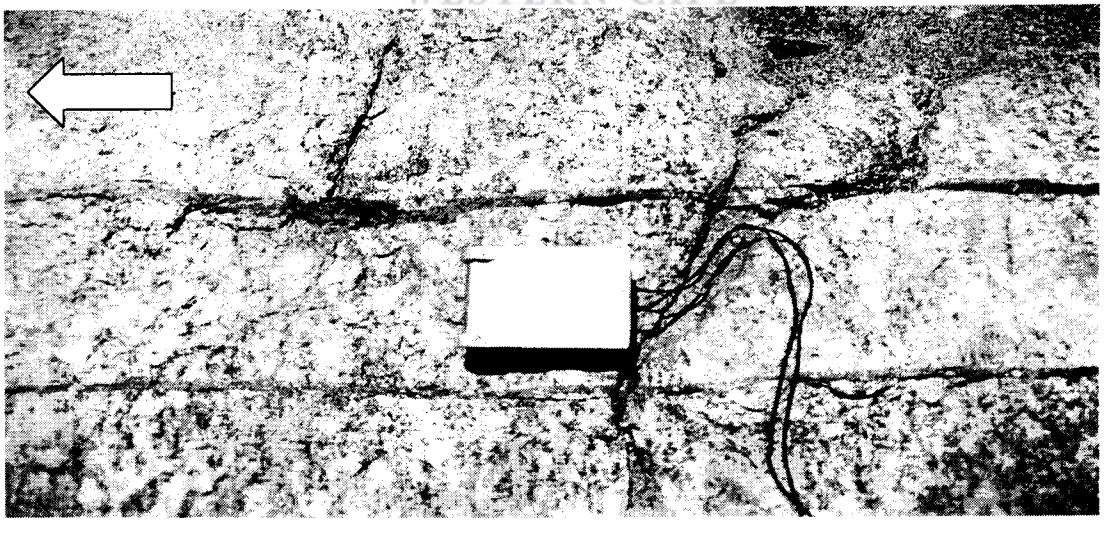

Figure 4-8: NNW trending extensional faults (Strike/Dip = 353/88°) intruded by dyke material.

Figure 4-9: NNW-SSE (Strike/dip = 355/89°) and ENE-WSW (Strike/Dip = 258/86°) fracture systems.

The rocks of the Gariep Complex were deposited in a trough formed due to the rifting of the continental crust and the subsequent opening of the proto-South Atlantic Ocean during the late Proterozoic (approximately 900 Ma). Thick syn-tectonic clastic deposits accumulated in the basin fed by detritus from the rising Namaqua massif. Subsequent plate convergence, starting some 700 Ma ago, is most frequently suggested as the cause of metamorphism and deformation in these basins (Albat, 1984).

The Gariep Complex thus consists of volcanic and sedimentary rocks, which have accumulated over a period of approximately 300 Ma (Visser, 1989). Outcrops of the Gariep Complex are found in the central and western parts of the Richtersveld, unconformably overlying rocks of the Namaqua Province (i.e. the Orange River Group and Vioolsdrif Suite as well as the intrusive Richtersveld Suite) to the east (Visser, 1989). The Gariep orogeny can be regarded as a chronologic extension of the Namaqua orogenic activity (Tankard *et al.*, 1982). Gariep sedimentation started approximately 950 Ma ago and ended 550 Ma ago.

The platform deposits of the Nama Group unconformably overlay the Proterozoic basement rocks of the Namaqua Province (Figure 4.10). The Nama Group, dated at approximately 550 Ma, is extensively preserved in southern Namibia and along the Orange River. The Group consists of over 2500 m of sandstone, mudstone and carbonate rocks. In Namaqualand, rocks of this group occur in a synclinal klippe unconformably overlying basement rocks of the Namaqua Province.

In northern Namaqualand the Nama Group forms the Steinkopf and Neint Nababeep plateaus (Visser, 1989). The Nama Group comprises of three formations, namely the Kuibis Formation (unconformably overlying the granite and gneiss of the Namaqua Province) followed conformably by the Schwarzrand Formation and in turn conformably

overlain by the Fish River Formation (Visser, 1989). Nama related rocks also occur to the north-west of Vanrhynsdorp. The Nama Group has been intruded by the Bremen pluton dated at approximately 506 +- 10 Ma (Burger and Coertze 1973).

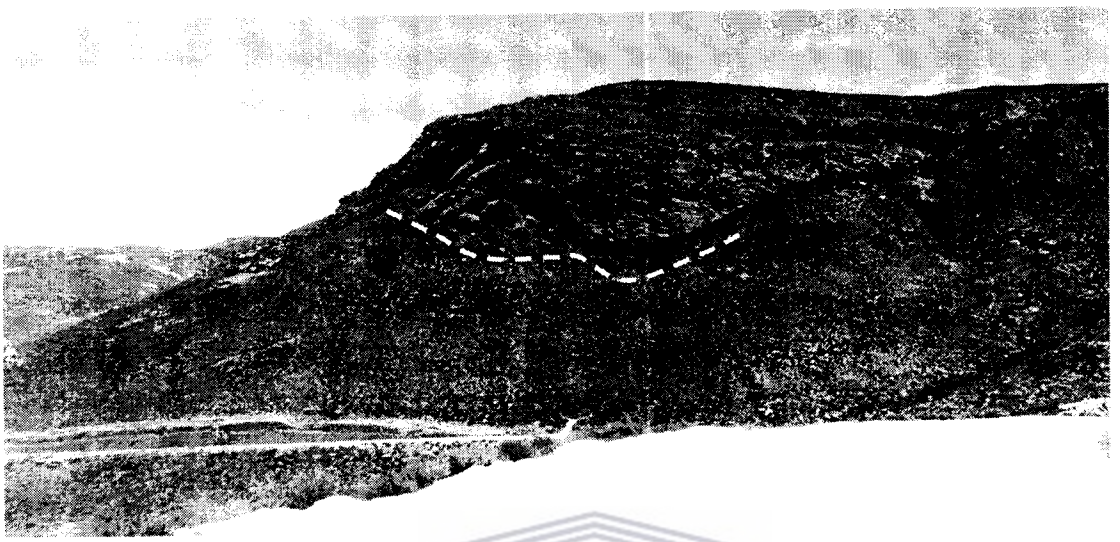

Figure 4-10: Rocks of the Nama Group unconformably overlying Proterozoic basement rocks.



### 4.4: Phanerozoic cover rocks

The Karoo sequence is unconformably overlaying the gneisses of Namaqualand Metamorphic Complex. Albat (1984) encountered these sequences at the western-most end of the Karoo basin.

- Sediments of post-Kimberlite age;
  Extensive parts of the Bushmanland plateau are covered by thin sequences of superficial sediments comprising of unconsolidated boulders and pebbles and, in restricted areas (pans), minor salt deposits.
- Intrusives of Phanerozoic age:
  I. Karoo dolerite.
  Outcrops of dolerite occur over an extensive area that is underlain by sediments of Karoo sequence. Outcrops are generally encountered along the outer margins of small circular depressions (Albat, 1984).
  II. Plugs of olivine melilitite and related volcanic rocks.
  The area between Gamoep, Platbakkies and Aggeneys contain small plugs of olivine melilitite and olivine nephelinites. Moore (1979) distinguished three different types of volcanic pipes:
  - Olivine melilitite and olivine nephelinite;
  - Pseudo-kimberlites which Moore (op.cit) considers to be hyperthermaly altered olivine melilitites;
  - Sediment filled kimberlite pipes and breccia necks.

III Kimberlite pipes.

Numerous circular features, generally in the form of depression are found in the Kliprand, Gamoep and Aggeneys areas. A large number of these are known to be underlain by kimberlite (Renning, 1931; Cornelissen and Verwoerd, 1975). The greatest concentration of these kimberlites pipes is found in the area north-west of Platbakkies. Although some of them occur on N-S faults, they appear to be concentrated along north-east lines (Joubert, 1971). Similar structures occur west of Garies. The exact age of these diatremes is still uncertain, but the fossil evidence points towards a late Cretaceous to early Tertiary age (Haughton, 1969).

# Chapter 5

# Geomorphologic framework

## 5.1: Introduction

The macro-scale geomorphological evolution of southern Africa was the result of an Archean geological history as well as changing climatic conditions, massive fluvial erosion, associated with the evolution of major drainage networks, and the formation of elevated interior plateaus during the late Mesozoic (i.e. the Cretaceous period) and Cenozoic eras (Partridge and Maud, 2000).

Three physiographic regions (Visser, 1989), viz. the western Coastal Lowveld (or Western plateau slopes), the Great Escarpment zone (or Namaqua Highlands) and the extensive Highveld (or Bushmanland Plateau), can be distinguished in the Northern Cape region (Figure 5.1).

## 5.2: Macro-scale geomorphology

### 5.2.1: Introduction



The morphology of southern Africa is to a great extent controlled by the underlying geology, predominantly consisting of granitic to gneissic bedrock and by the processes affecting it. Most of southern Africa is characterized by a mature landscape with different erosion surfaces separated by prominent geomorphic scarps. These erosion surfaces resulted from successive phases of erosion, initiated by continental uplift, at various times since the fragmentation of Gondwana. Preservation of the erosion surfaces of varying ages occurs by pediplanation, in which back wearing predominates (King, 1951). Both back-wearing and down-wearing had, according to Moon and Dardis (1988), contributed to the presence of the erosional surfaces in the present African landscape.

Extensive erosional surfaces and stepped relief have been suggested as evidence for sequences of erosional phases. Numerous erosion surfaces have been recognized on the African landscape. According to Moon and Dardis (1988) and Partridge and Maud (1987), conflicting interpretations arose due to problems associated with correlating surfaces across the Great Escarpment, the ambiguity of the results from dating the surfaces, and to the structural control (such as lithology, stratigraphy, tectonics, etc.) of the landscape development. Partridge and Maud (1987, 1998 and 2000) have re-interpreted the macro-scale denudation history of the subcontinent and provided a complete literature summary on this topic.

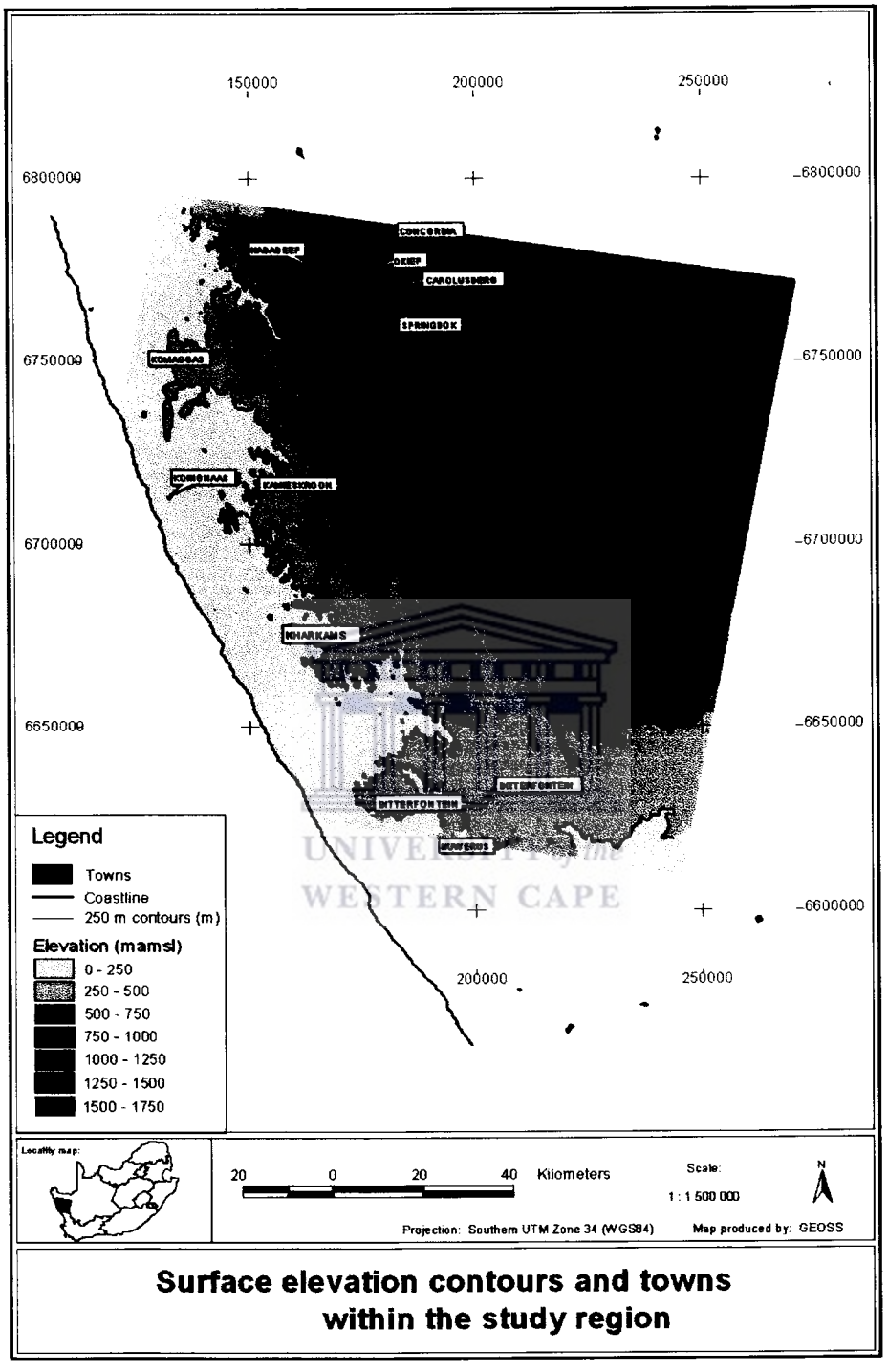


Figure 5-1: The three physiographic regions (Visser, 1989) the western Coastal Lowveld (or Western plateau slopes), the Great Escarpment zone (or Namaqua Highlands) and the extensive Highveld (or Bushmanland Plateau), in the Northern Cape region can be recognized from surface elevation contours.

The surfaces identified by Partridge and Maud (1987) conform to King's terminology (King, 1967), but do not imply agreement with King's denudation history. The oldest and most widespread is the Gondwana surface (Jurassic) and African surface (mid-Cretaceous) followed by the Post-African surface inland of the Great Escarpment. Seaward of the Great Escarpment, two surfaces of Post-African age have been recognized, referred to as Post-African I (Miocene) usually present as dissected tablelands, and a younger Post-African II (Late Tertiary) surface expressed as recent incisions of coastal gorges.

### 5.2.2: The African, Post- African I and Post- African II erosion surfaces

#### *5.2.2.1: The mid- to late –Cretaceous African erosion surface*

Rifting, separating Africa from South America and associated with pre-existing Pan-African orogenic welts, occurred between 129 Ma and 121 Ma in the west (Partridge and Maud, 2000). Rifting in the west post-dates an earlier separation of India and Antarctica in the east. Uplift along the rift shoulders resulted in a major marginal escarpment (this is the current Great Escarpment) that was driven inland by erosion during the early Cretaceous. The Cretaceous period is characterised by warm, humid tropical climatic conditions (Tyson and Partridge, 2000) resulting in accelerated weathering and fluvial erosion due to dense well-integrated drainage networks (Partridge and Maud, 2000).

Erosion and planation in southern Africa occurred simultaneously both below and above the Great Escarpment (Partridge and Maud, 2000). Vast erosional surfaces of late Cretaceous age were formed above and below the Great Escarpment (Partridge and Maud, 2000), and correctly termed much earlier as the African surface by King and King (1959). The warm and humid tropical climate of the Cretaceous period also resulted in the development of deep, koalinised weathering mantles especially on susceptible lithologies (such as crystalline rocks containing thermodynamically unstable alumino-silicate minerals). Towards the end of the Mesozoic (which belongs to the upper/late Cretaceous) kaolinised profiles of depths of 50 m or more were underlying remnants of the African surface (Partridge and Maud, 1987 and 2000; Tyson and Partridge, 2000).

The African surface, the highest and oldest erosion surface, is characterized by deep weathering kaolinised profiles beneath silicrete duricrusts (Moon and Dardis, 1988; Partridge and Maud, 1987). Late Cretaceous and early Paleocene pedocrete cappings (i.e. duricrusts) protected the African surface, and its deeply kaolinised saprolite, from erosion processes in many localities (Partridge and Maud, 2000). The pedocrete cappings, comprising predominantly of silicrete and calcrete in the western and central parts of the southern African subcontinent, formed in response to the onset of drier climates towards the end of the Cretaceous period (Partridge and Maud, 2000; Tyson and Partridge, 2000). The Cretaceous-Tertiary boundary (the K-T boundary) is characterised by significant cooling and aridification in southern Africa that is linked to major changes in atmospheric chemistry (Tyson and Partridge, 2000). The climatic changes during the early Cenozoic are associated with Decan volcanism in India and to the catastrophic

events resulting in the abrupt global extinctions at the end of the Cretaceous (Tyson and Partridge, 2000). Wetter conditions persisted in the east of the subcontinent, establishing an east-west climatic gradient across southern Africa that existed since the early Cenozoic (i.e. Paleocene).

The African erosional phase was of long duration (>100 million years) and erosion proceeded to different base levels between the interior plateau and seaward of the Great Escarpment. Planation within the African cycle, according to Partridge (1988), was complete before the end of the Cretaceous, while massive duricrust formation ended by the early Paleocene. Huge thicknesses of material were removed during this period.

The African landscape was not subjected to significant regional tectonism during the Paleogene (Partridge and Maud, 2000). In addition, arid conditions persisted into the early Eocene in the western parts of the African subcontinent while more humid conditions prevailed in the east (Tyson and Partridge, 2000). Both factors contributed to slow landscape development during the Paleogene (Partridge and Maud, 2000).

*5.2.2.2: The Miocene Post-African I erosion surface*

Moderate but asymmetrical early Miocene crustal uplift along several axes caused the westward tilting of the subcontinent and resulted in a slight steepening of the courses of westward flowing rivers (Partridge and Maud, 1987 and 2000; King and King, 1959). The early Miocene crustal uplift and subsequent erosion resulted in the mid-Miocene Post-African I erosion surface (Partridge and Maud, 1987) dated at ages ranging between 12 Ma to 19 Ma (Pickford *et al.*, 1996). Early Miocene uplift is associated with limited incision of drainage channels of up to 100 m to 200 m below the African surface (Partridge and Maud, 2000; Pickford *et al.*, 1996). The Post-African I landscape development phase involved the removal of the deeply weathered mantles underlying the African surface (Partridge and Maud, 2000). In areas (i.e. western parts of southern Africa) subjected to minimal Miocene uplift, scattered residuals or reduced thicknesses of the weathered mantles remained. The Post-African I surface dominates the southern African landscape (Partridge and Maud, 2000).

The late Oligocene and early Miocene epochs are characterised by a period of global oceanic warming regionally influencing atmospheric circulation patterns (Tyson and Partridge, 2000). As a result, rain producing weather systems penetrated the arid western (i.e. Bushmanland and Gordonia) parts of southern Africa resulting in a sub-tropical wet climate and a well-integrated drainage system (Tyson and Partridge, 2000). The wet interval of the early Miocene was brought to an end with the onset of cold upwelling in the Benguela Current system on the west coast. The global effects of cooling and drying, especially during the Eocene and mid-Miocene, have greatly impacted on the southern African environments with the onset of true coastal desert conditions (at approximately 15 Ma) along the west coast of southern Africa (Partridge and Maud, 2000; Tyson and Partridge, 2000).

The advent of warmer and more humid conditions during the early Pliocene resulted in a rejuvenation of major drainage systems in the semi-arid western interior.

Massive and significantly asymmetrical late Pliocene uplift interrupted the Post-African I erosion phase and accentuated the westward tilting of the subcontinent. The results of the late Pliocene uplift in the western parts of southern Africa include; (a) further increases in the gradients of westward-flowing rivers with renewed incision within river valleys, and (b) renewed movement along the Griqualand-Transvaal axis (Tyson and Partridge, 2000). The large-scale regional uplifts, within the south-eastern and eastern hinterland of the subcontinent, induced major influences on the regional climatic conditions. The east-west precipitation gradient is thus a result of the existence of contrasting current regimes along the east and west coasts as well as the enhanced regional uplift in the eastern parts of the African subcontinent. Late Pliocene uplift resulted, according to Partridge and Maud (2000) in a steepening of the east-west climatic gradient with the establishment or re-establishment of desert conditions in the western part of the African subcontinent. Furthermore, the initiation of the various phases of uplift coincided with the onset of an interval of global cooling at approximately 2.8 Ma (Tyson and Partridge, 2000). This resulted in the aridification of large tracts of sub-Saharan Africa with the development of extensive but discontinuous dune systems (such as the mega Kalahari) extending into the Northern Cape Province of South Africa.

*5.2.2.3: The Post-African II erosion phase*

The Post-African II phase is a result of erosional processes occurring over the last two to three million years (Partridge and Maud, 1987; Moon and Dradis, 1988). King (1967) also subdivides the Quaternary cycle into three phases, and he suggests that the initiation of each cycle is related to tectonic movement.



5.2.3: Geomorphology of the Buffels River catchment (i.e. secondary drainage catchment F30)

Three physiographic regions (Visser, 1989), viz. the western Coastal Lowveld (or Western plateau slopes), the Great Escarpment zone (or Namaqua Highlands) and the extensive Highveld (or Bushmanland), can be distinguished in the Northern Cape region. Deep valleys associated with fault zones occur throughout the area, and are prominent in the mountainous escarpment zone.

*5.2.3.1: Lowveld*

The coastal plains form the Lowveld west of the Escarpment. Partridge and Maud (1987) recognised the oldest African surface on these coastal plains. The Lowveld is a gentle seaward dipping plain covered by a thin layer (0-2 m) of unconsolidated material. In some places, the rocks are covered by ferricrete/silicrete of the African surface, which have dark red and purple succulents as typical vegetation. The vegetation is probably fed by sea fog. The ferricrete/silcrete is very resistant and cause some low relief in the area. Koppies of a maximum of 15 m high can be found on the Lowveld. Some inselbergs can

be identified, disappearing towards the coastline. Small dunes are found parallel to coast and along the Buffels River north of Komaggas area.

*5.2.3.2: Highveld*

The Highveld or "Bushmanland erosional surface" is the plateau (in other words, the African erosional surface) to the east of the Springbok High, with a constant elevation of 950 m. The Highveld slopes gently towards the Orange River with a few inselbergs of a maximum of 80 m in relief. It is taken up by the African surface, locally designated as the Bushmanland surface. McCarthy *et al.* (1985) and De Wit (1993) describe the Highveld-geomorphology of western Bushmanland. The Bushmanland plateau is correlated with the African surface that is preserved in localised occurrences of silicrete caps with thicknesses varying between 30 cm and 100 cm. This surface marks the onset of the aridity at the end of the Cretaceous. Partridge and Maud (1987) correlate the area covered by the Bushmanland calcrete with the Post-African I surface. However, Post African surfaces have been recognised at elevations of 800 m, 600 m and 450 m as sub-cycles below the Bushmanland plateau (Mabbutt, 1955).

According to De Wit (1993), a thin veneer of red sand, underlain by mature calcrete, generally covers the surface of the Highveld. The calcrete is between 20 cm and 100 cm thick and is characterised by a typical pedogenic cross-section with a cap of laminar and hardpan calcrete overlying nodular calcrete that passes into calcified bedrock. It is unlikely that this calcrete developed before the Early Pliocene because of the presence of Early Pliocene horse remains below thin calcrete approximately 65 km east of Springbok (Haughton, 1969).



*5.2.3.3: The Escarpment zone*

The Buffels River catchment is confined mainly to the Great Escarpment zone. This zone is characterised by relatively high local relief (Gilchrist *et al.*, 1994). The Great Escarpment of southern Africa is a prominent geomorphic feature along the edge of the southern part of the African continent. The Great Escarpment, which is approximately parallel to the coastline, separates the elevated interior plateau of the subcontinent from the coastal plain lowland (Moon and Dardis, 1988) and trends roughly parallel to the coast at distances between 50 km and 300 km.

At certain places, the Great Escarpment is extensively described and its formation has been the subject of ongoing debate (Ollier, 1985; Summerfield, 1985 and 1991; Partridge and Maud, 1987; Gilchrist *et al.*, 1994). The Escarpment is considered to be a result of the break-up of Gondwanaland that started about 140 Ma ago, developing geomorphologically since then. Along the southern and southeastern sections of the subcontinent, the Great Escarpment is believed to result from major doming, which followed the rifting and continental separation (Partridge and Maud, 1987). Dingle *et al.* (1983) proposes that separation along the western margin of the subcontinent started roughly 127 Ma ago. Some researchers (Dixey, 1955; de Wit, 1993), however, suggest

that the Great Escarpment must be a much older feature that may have existed since Carboniferous times.

One of the main items of current research is a focus on the processes that preserved the morphology of the Great Escarpment during the Tertiary to make it such a prominent geomorphic feature (Summerfield *et al.,* 1985 and1991; Gilchrist *et al.,* 1994; Van der Beek *et al.,* 1995; Kooi and Beaumont, 1996). To explain the present situation, the geomorphic and geologic processes that acted since the formation of the Escarpment have to be understood both qualitatively and quantitatively.

Escarpments along passive continental margins are quite common features and are recognised in several parts of the world (Ollier, 1985). The Great Escarpment of southern Africa is one of the most famous and prominent escarpments resulting from passive margin rifting (Summerfield, 1988), and associated with the break-up of Gondwanaland.

Ollier (1985) expresses a generalised morphotectonic model for continental margins where escarpments develop:

- An original continental slab is isolated from the original super continent (e.g. Gondwanaland) by crustal-scale faults and newly formed sea floor.
- Erosion and scarp retreat inwards create the coastal lowlands backed by a major escarpment.
- Then two modes of development can be envisaged:
    - The continental plate tends to sag in the middle with bulges towards the margins (i.e. rising towards the edges). The watershed does not correspond to the top of the Escarpment, but lies slightly inland, as is the case in Namaqualand.
    - The continental plate tends to sag in the middle and rise at the edges. A simple tilt block is formed, bounded by a fault scarp, and the watershed corresponds to the edge of the block. An example is the Drakensberg Mountains in Natal.

Another distinctive feature in connection with the Great Escarpment is the uplift of the Bushmanland plateau along an axis perpendicular to the coastline. Dingle *et al.* (1983) have interpreted this feature as a palaeo-high already present during Karoo sedimentation. Partridge and Maud (1987) however, suggested that the Griqualand-Transvaal axis of maximum uplift is of Miocene and Paleocene age. Regional episodes of uplift resulted in the higher structural position and elevation of the Namaqua Mountains composed predominantly of Proterozoic basement rocks.

### 5.2.4: Topography of the Buffels River catchment

The topographic cross sections (Figures 5.2, 5.3 and 5.4) through the Buffelsrivier catchment have been computed from a Digital Elevation Model (DEM) available at the USGS on the Internet. The sections are orientated N-S and W-E.

N-S cross sections (Figure 5.3):

- NS1 (Profile 4): The northern section extends into the Springbok Highlands while the higher lying areas around the town of Komaggas are clearly shown. The incision of the Buffels River is also visible on this cross-section. The southern part of this cross-section shows the gentle westward sloping of the coastal lowlands.
- NS2 (Profile 5): This cross-section is along the escarpment zone. The Springbok High and Kamiesberg High are prominent features while the incision of the Buffels River is again clearly visible.
- NS3 (Profile 6): This cross-section is along the boundary of the Escarpment zone and the Bushmanland Highveld. The plateau-like nature of the Highveld is shown with an almost constant elevation below mean sea level.

The W-E cross sections (Figure 5.4) show less variation than the N-S sections, since the Escarpment zone between the Coastal Lowveld and Bushmanland Highveld is primarily a N-S feature. These sections also show the Coastal Lowveld as a gently dipping coastal plain dissected by some river courses. In the western part of the Escarpment zone, the meta-sediments of the Nama age are prominent and resist erosion, thus forming a plateau.

- WE1 (Profile 1): This section shows the Coastal Lowlands and a prominent rise in elevation to the Springbok High. The Springbok High is bordered by the low relief; gentle sloping Bushmanland Highveld towards the east.
- WE2 (Profile 2): Similar to WE1, although the Kamiesberg High is intersected. This section crosses the Escarpment zone through the center of the catchment.
- WE3: This section shows the southern part of the secondary drainage catchment F40 (i.e. part of Coastal Lowlands) and the top of the secondary drainage catchment F50.

The above-mentioned cross-sections are compared to shed light on the characteristics of the regional drainage systems, which in turn exerts control on the extent of groundwater basins and groundwater flow regimes at a regional scale.

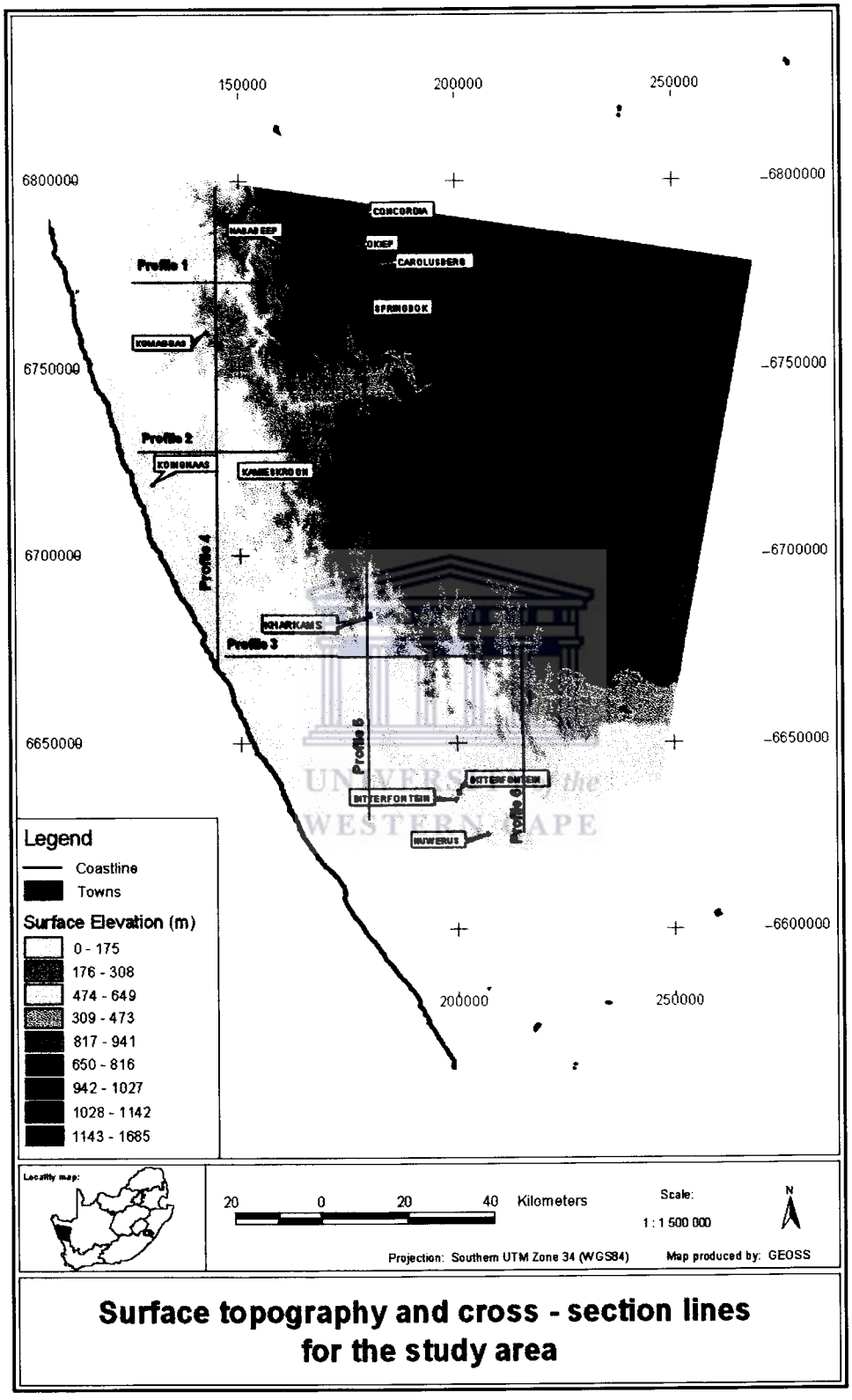


Figure 5-2: Surface topography and lines for the N-S and W-E cross-sections.

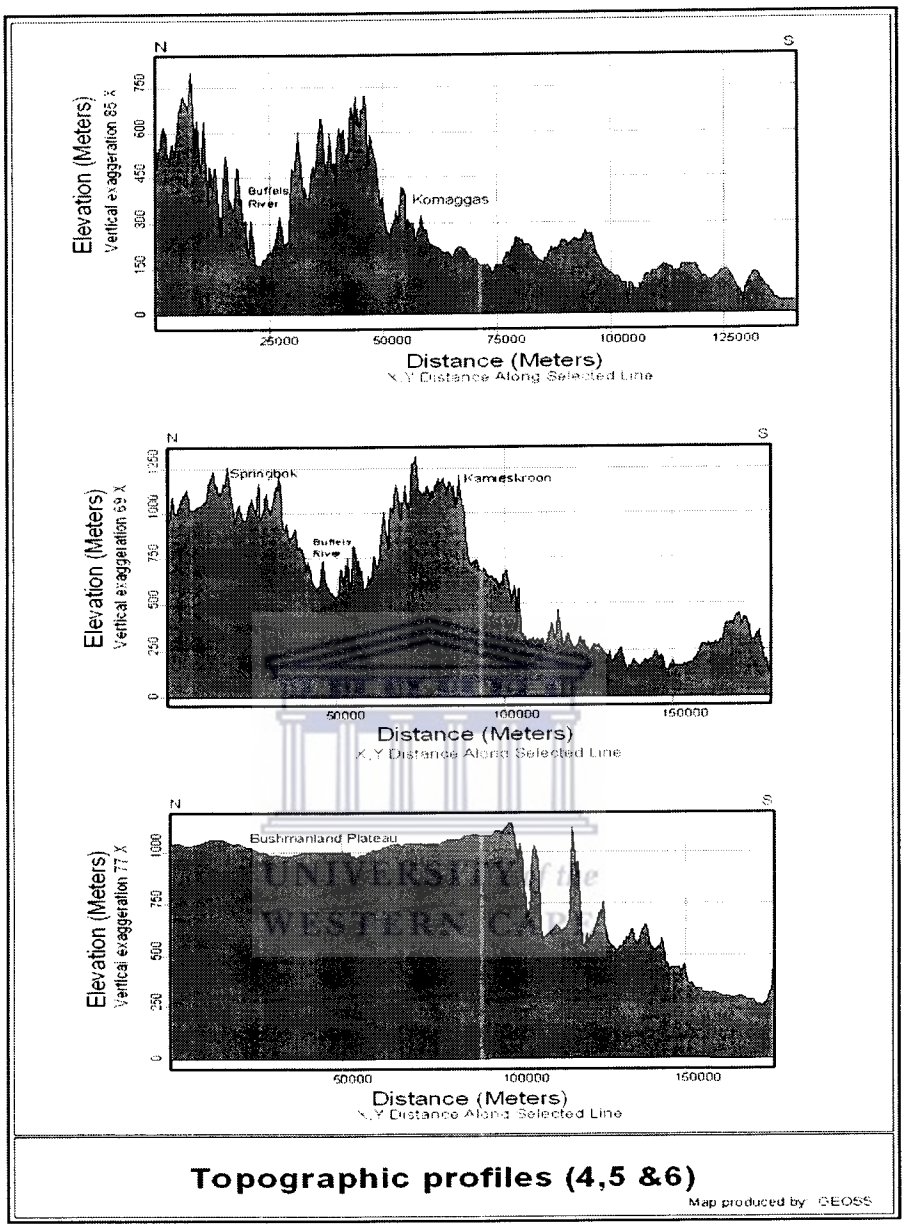


Figure 5-3: N-S cross-sections. The locations of the cross-sections are given on a topographic map prepared from a DEM.

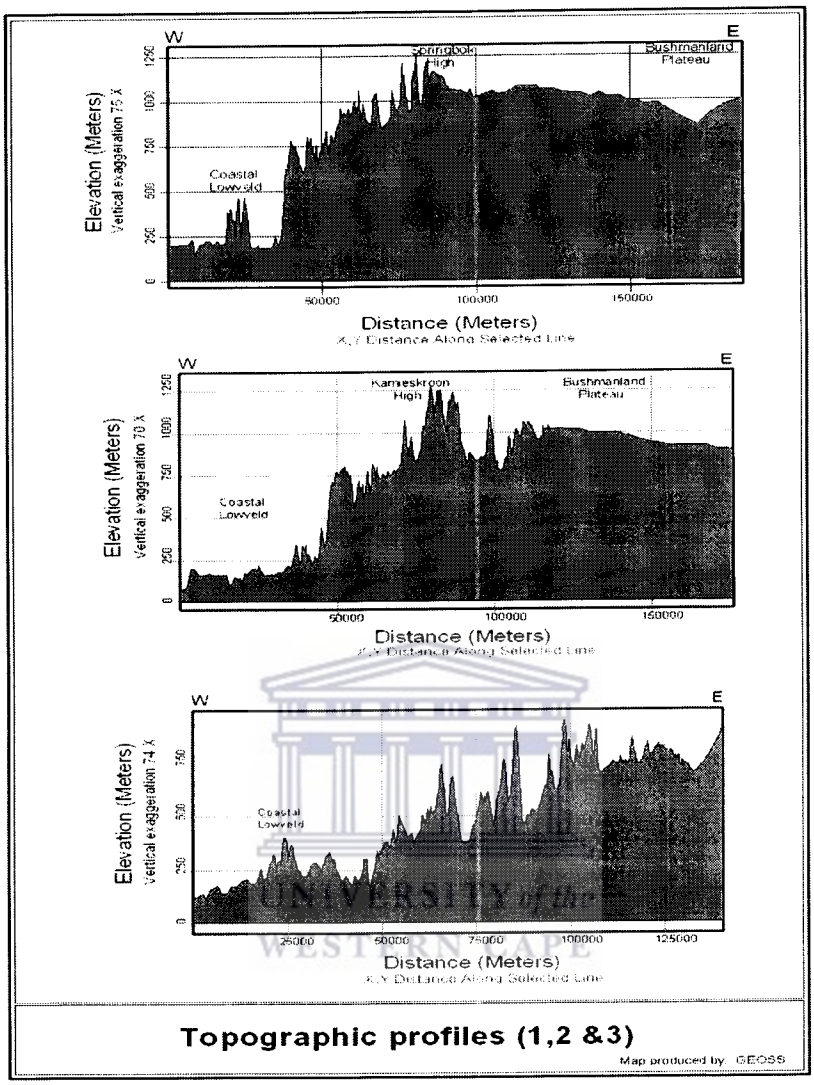


Figure 5-4: W-E cross-sections.

5.2.5: Prominent geomorphological features

Bornhardts (Twidale, 1976, 1982 and 1988; Ollier, 1984; Rice, 1988 and Bridges, 1990) are the most prominent geomorphological features of the escarpment zone. Bornhardts are inselbergs or 'Island Mountains' with rounded dome-shaped forms usually prominent in the granitic and gneissic rocks of Namaqualand. The shapes of the bornhardts are determined by the orthogonal fracture systems and by the upward-arching sheeting planes. The orthogonal fracture systems developed either during emplacement or during subsequent tectonic events affecting the crystalline rocks. Bornhardts can be massifs or juxtaposed groups of domes arranged in an ordered pattern due to the structural control on its development. The Kamiesberg mountain range is a complex massif of large,

predominantly dome-shaped bornhardts developed on major fracture systems with various orientations. The bornhardts are separated by valleys and narrow plains formed by pronounced weathering and erosion of the fracture zones. Deep subsurface weathering is essential for bornhardt development.

Several hypotheses have been proposed to explain the development of bornhardts (Twidale, 1976, 1982 and 1988; Ollier, 1984; Rice, 1988 and Bridges, 1990):

- Bornhardts probably have a tectonic origin and the scarps or bluffs are a result of faulting. Large-scale faulting cannot, however, account for the development of most bornhardts.

- There may be differences in rock type, and associated resistance to weathering processes, between the residuals and the plains. Most bornhardts are, however, composed of the same rock type as the rocks that underlie the adjacent plains.

- Bornhardts may develop due to variations in the spacing of fractures (i.e. fracture density) from hills to plains. Fractures are preferred pathways for the infiltration of water and more densely fractured materials are more prone to weathering processes than massive, dense material. The Namaqualand rocks were subjected to tectonic forces that resulted in folds, thrust and shear zones, and faults with the associated joint systems. The more transmissive and especially larger fault zones have been weathered and eroded more intensely to form the valleys that separate the massive domes. Within the most weathered sections, core stones of fresh granite are present in a matrix of weathered rock derived from in-situ weathering of the host rock. Ordered groups of bornhardts are particularly evident in the mountainous regions. The variation in fracture density is probably due to recurring stresses resulting in rhomboidal shaped fracture patterns and the propagation of secondary fractures. Such recurrent stresses resulted in bornhardts as massive, compressionally stressed core zones (such as the compressive core zones of anticlines) in a matrix of highly weathered fractured rock. On a regional scale, the massive and stressed core zones (i.e. massive domes) can be regarded as enormous core-stones within and surrounded by a matrix of weathered rock expressed as the fault-controlled valleys and narrow plains.

The hypothesis that bornhardts are composed of massive, compressional core zones accounts both for:

- The observed paucity of open fractures in bornhardt masses;
- The association of bornhardts and sheet structures. The development of sheet structures can be attributed to both erosional off-loading and compressional stresses.

The landscape for crystalline terrains can be attributed to two stages of development (Twidale, 1982):

I. Differential subsurface weathering (i.e. moisture controlled weathering) exploiting varying rock composition and texture as well as variations in the fracture density. Differential subsurface weathering results in a highly irregular weathering front (or lower limit of significant weathering). Moisture is responsible for both the chemical alteration (which occurs when there are reactions between water and rock) and physical disintegration of the crystalline rocks. Humid to subhumid paleao-climates are responsible for ancient differential subsurface weathering.

II. Subsequent erosion and exposure of the more resistant rocks (i.e. the bornhardts). The massive bornhardts are thus protrusions of the dynamic weathering front (which is the exposed parts of the lower limit of significant weathering) upward into the regolith or overlying weathered material. Fluvial erosion is primarily responsible for erosion and the exposure of the bornhardts.

### 5.2.6: Drainage

Non-perennial rivers drain the catchments. The drainage patterns are well developed and are often controlled by geologic structures. In areas where the sediment cover is sparse or absent, the fault patterns are reflected in the drainage patterns, which include the Buffels River.

Two effects are particularly important to the geomorphic development of rifted margins (Gilchrist and Summerfield, 1994). Firstly, during the first phase of formation of the passive margin, extension within the rift zone causes subsidence and the formation of sedimentary basins that lower the base level of fluvial systems draining into the rift. Secondly, extension can cause significant surface uplift immediately adjacent to and landward of the newly formed sedimentary basins, thereby generating a rift flank uplift that can deflect the existing drainage systems. The result of these mechanisms can be the re-orientation of the existing drainage system into two major fluvial systems. The exterior catchment drains directly into the rift and in the interior catchment the drainage systems are deflected away from the rift toward the continental interior. Such re-orientation would not occur if rates of fluvial incision exceed surface uplift rates. The deflected drainage patterns on young-rifted margins suggest, however, that re-orientation commonly occurs (Gilchrist and Summerfield, 1994).

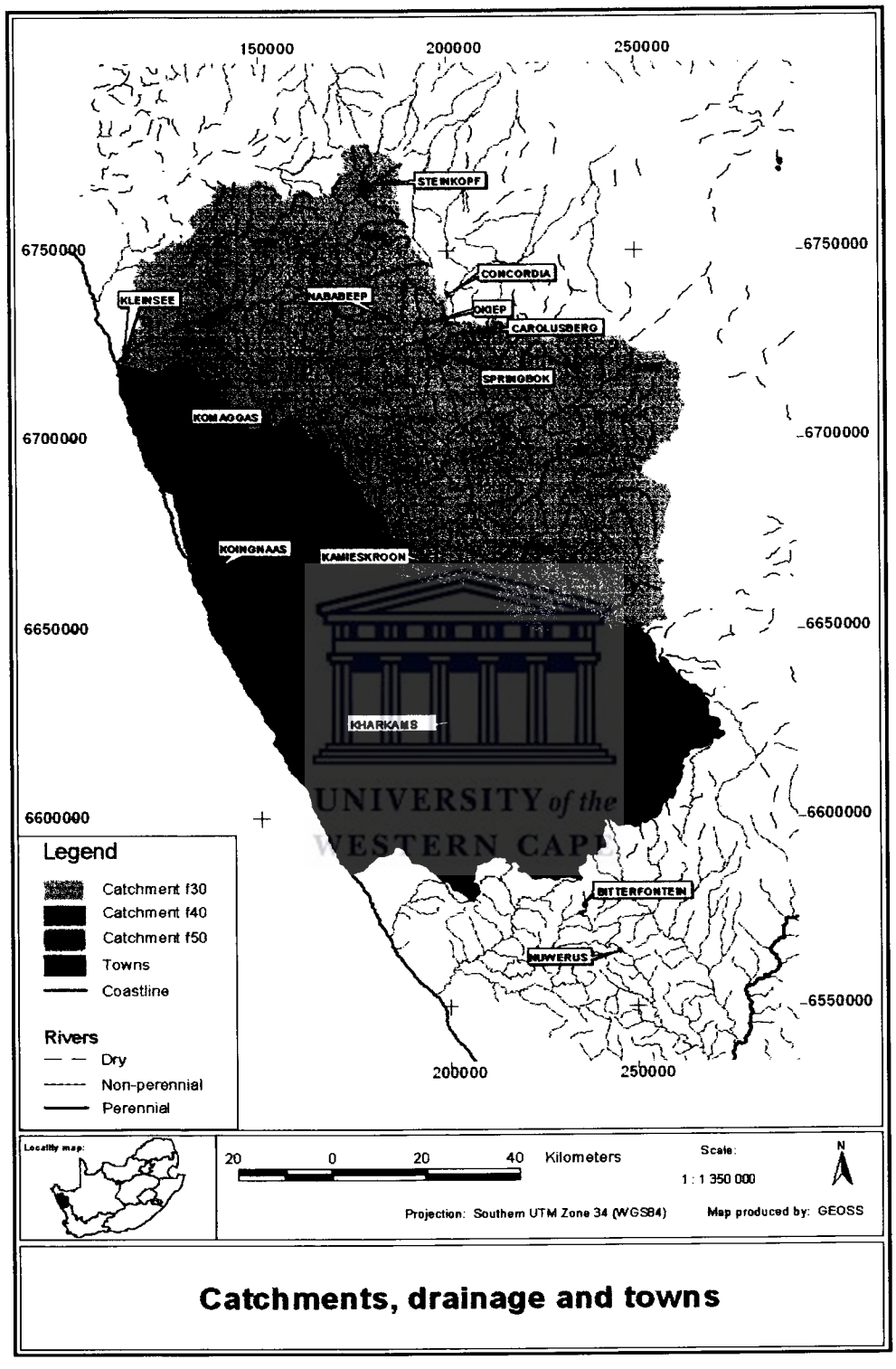


Figure 5-5: Drainage patterns for the secondary drainage catchments F30, F40 and F50.

The "synrift" drainage pattern drains the rift flanks through short, steep rivers that are aligned perpendicular to the rift. The tectonically induced fall in the base level promotes rapid incision and catchment growth by the retreat of headwaters, rejuvenating the landscape into a high relief.

As rivers incise the exterior catchment, the water divide retreats toward the continental interior. This pattern of drainage growth leads to increased competition between neighboring river systems, and the more aggressive back-wearing/incising systems capture the upland regions of adjacent catchments. Large catchments develop and grow headward most rapidly with the possibility of capturing the deflected drainage of the continental interior.

Lithology and climate exert additional controls on the evolution. The intrinsic strength of the rocks, secondary structures such as joints and faults, and the degree of weathering will determine the erodibility of back-wearing velocity.

The Buffels River has a length of about 250 km and finds its main source in the Kamiesberg Mountains, peaking 1371 m above sea level, and with an annual average precipitation of 305 mm. The catchment is further fed by the western part of the Bushmanland plateau at an elevation at 900 m, which gets an annual precipitation of 102 mm. The catchment is also fed by the Springbok highlands at an elevation of approximately 1100 m and with an average rainfall of 178 mm per year (Marais, 1975). On the average, the Buffels River flows once every three years, only for short periods and only after heavy rainstorms (estimated to be at least 60 mm of rain per day). Close to the source, near Kamieskroon, the river flows inland to the east, away from the Escarpment edge representing the water divide. Around Pedroskloof the rivers follow the directions indicated by the rectangular fault pattern. After Goraap, the river flows to the North in the direction of Rooifontein. After Tweefontein the river flows westward through the depression between the Springbok High and the Kamiesberg High where the Escarpment is transected. The depressions are probably partly lithologically controlled. Hereafter, the river continues in a north-westerly direction before it enters the Lowveld near the Spektakelpas.

The terraces of the Buffels River and the Orange River have been extensively mined for diamonds, which have been transported by these rivers away from the kimberlite intrusions in the central part of South Africa. The evolution of the drainage system has therefore been the subject of several studies. These try to reveal the source areas of the sediments in the rivers in order to predict where diamondiferous deposits might be located.

The evolution of the Buffels River catchment corresponds to a great extent to the generalised model for the drainage development of southwest Africa as presented by Gilchrist *et al.* (1994). Within the Buffels River catchment the earlier interior and exterior (sub-) catchments can still be recognised. The edge of the Escarpment is still the water divide over the largest part of the area, except where crossed by the Buffels River.

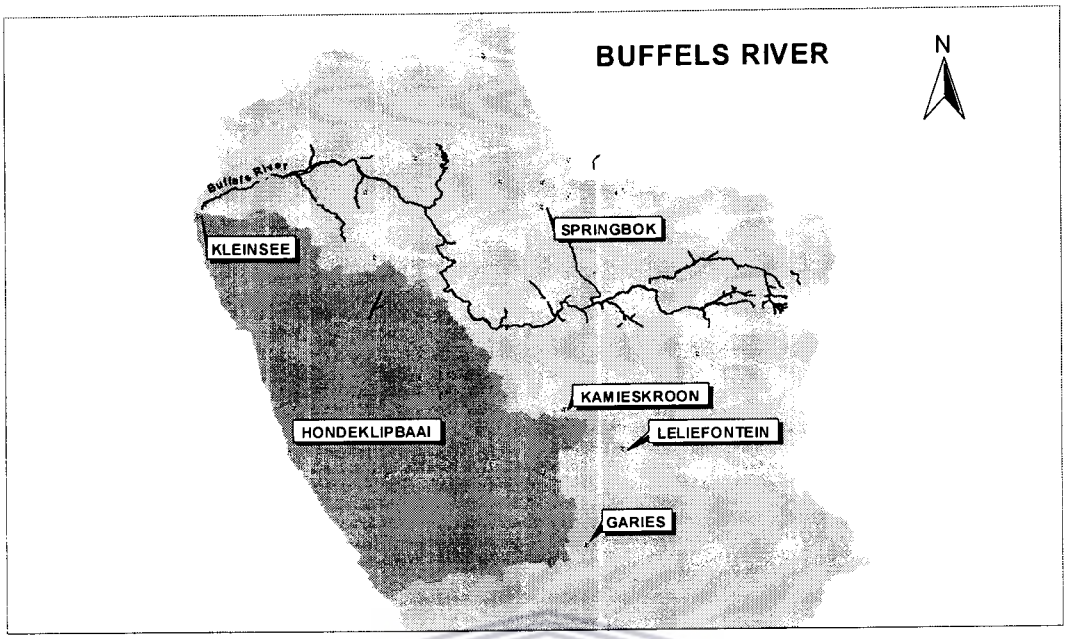


Figure 5-6: The course of the Buffels River in secondary drainage catchment F30.

The sub-catchments of the Buffels River have been split into two groups separated by the water divide that is formed by the Escarpment edge transected only by the Buffels River itself. The exterior sub-catchments are located west of the Escarpment edge while the interior sub-catchments are east of the Escarpment edge. The three most extensive sub-catchments are those of the Brak River on the interior side and of the Stry River and Schaap River on the exterior side.

The drainage system of the Buffels River catchment shows a large variation in drainage characteristics, such as the channel width and depth, the sediment thickness, the drainage density and the development of river terraces. The development of the drainage pattern can be described and the variation explained by the model proposed by Gilchrist *et al.* (1994). The influence of the underlying geology on the drainage characteristics is significant.

# Chapter 6

# Characteristics of the groundwater

## 6.1: Introduction

This chapter describes the methodology employed with regard to fieldwork and subsequent analyses. The data is presented in various graphical formats and described through utilizing statistical analyses. In addition, the environmental isotope data are described and conclusions drawn.

A total of 320 boreholes, wells and springs were sampled for chemical analyses (Table 6.1). The subsequent discussion on the groundwater conditions refers to a vertical zone of water intersections ranging between 2 m to approximately 80 m below ground surface. The shallow water strikes are likely to represent water levels in alluvium, whereas the deeper ones represent water strikes in semi-confined conditions. The coordinates of all boreholes visited were determined with the aid of a Magellan Global Positioning System (GPS) with an accuracy of ± 12 m. Figure 6.1 shows the spatial distribution of the boreholes visited during this project. Where boreholes were not equipped, grab samples were taken by means of bailing.

Table 6-1: Boreholes, wells and springs sampled for study.

| Secondary Catchment F30 | | Secondary Catchment F40 | | NGDB Data | |
|---|---|---|---|---|---|
| Sampled | Error < 10% | Sampled | Error < 10% | Extracted | Error < 10% |
| 249 | 203 | 71 | 56 | 215 | 165 |

A regional approach, at a secondary drainage catchment scale, to the study was adopted (see section 1.4). Limited data existed for the boreholes, including the depths and construction of these boreholes. An attempt was made to sample all boreholes south of the town of Springbok in the secondary drainage catchments F 30 and F40. Groundwater sampling was conducted in the coastal lowlands (i.e. F40 catchment) and predominantly in the Escarpment and pre-Bushmanland regions (i.e. F 30 catchment). The major structurally controlled valleys and the mountainous regions in the F30 catchment (i.e. Buffelsriver catchment) were targeted for groundwater sampling.

The spatial distribution of the boreholes, and the distances between them, limited the interpretation derived at to a regional scale. It was, however, possible to describe the groundwater flow patterns and the hydrochemical development of the water at a smaller scale in certain parts (i.e. larger villages) of the catchment where boreholes were numerous and less scattered. Furthermore, the groundwater sample collected represents an average water sample integrated over the depth of the borehole. It was, however, possible to distinguish between different types of water.

### 6.1.1: Sampling methods

All boreholes were pumped for a sufficient period to purge the boreholes of all stagnant water before groundwater sampling proceeded. Purging of the boreholes was essential since most of the boreholes visited were equipped with windpumps. In most cases the windpumps were in use when sampled. All samples were filtered with a hand held syringe through a 0.45 µm filter membrane in the field. Samples were collected in three new 100 ml polyethylene bottles. All water bottles were washed with de-ionised water and again twice with filtered sample water. The samples were kept cool on ice in a cooler box before being dispatched to the laboratories.

Parameters that were measured and recorded at the time of sampling were alkalinity, electrical conductivity (EC), pH, temperature and redox potential (Eh). Alkalinity was measured using a Hach® field titration kit. The EC, pH, temperature and Eh were measured using portable Orion and Cyberscan EC and pH meters. All portable meters were calibrated at the beginning of each day and properly washed with deionised water after every sampling occasion. These parameters had to be measured at the time of sampling because they may alter as a result of aeration and degassing (Parker, 1994). They also provide a preliminary overview of the water quality, which determined the extent of sample collection (Weaver *et al.*, 1996).

### 6.1.2: Major and trace element analysis

Samples were filtered in the field with a hand-held syringe using 0.45 µm membrane filters. Samples were collected in three new 250 ml polyethylene bottles. All sampling bottles were washed with de-ionised water and again with filtered sample water. Chemical analyses of the water samples were undertaken at the laboratories of Infruitec (Soil Science section). The laboratory of the Council for Scientific and Industrial Research (CSIR) in Stellenbosch was used to analyse for nitrate plus nitrite as N ($NO_x$ - N) and F, and for quality control, some duplicate samples were sent to this laboratory to corroborate analyses done by the laboratories of Infruitec. Samples were also sent to Bemlab CC, an independent laboratory, for chemical analyses. The physical and chemical determinants are shown in Table 6.2.

Infruitec and Bemlab CC laboratories performed major and minor ion analyses using a Varian Vista ICP Atomic Emission Spectrometer, except for nitrate and fluoride which was analysed at the laboratories of the CSIR, using the cadmium reduction column method for nitrate and a specific ion electrode for fluoride.

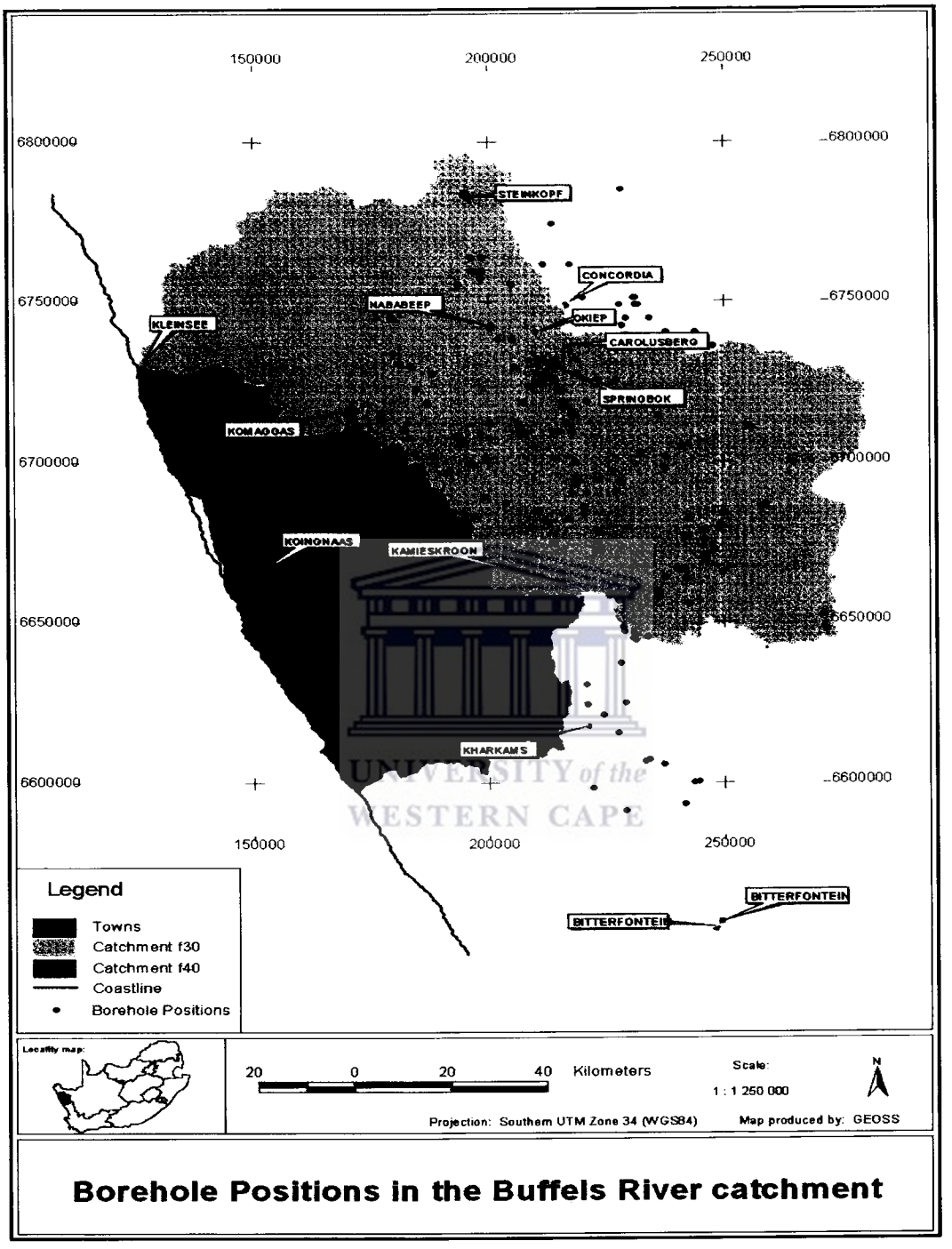


Figure 6-1: Spatial distribution of sampling points for the secondary drainage catchments F30 and F40.

Table 6-2: Physical and chemical determinants.

| Group | Determinants |
|---|---|
| Physical determinants | EC, pH, Temperature, Eh |
| Major cations | Na, Mg, Ca, K, Si |
| Major anions | Cl, $SO_4$, $NO_3$, F, $HCO_3$ |
| Trace elements | Al, Ba, Ni, P, Sr, B, U, Cu, Mn, Zn, Fe, Pb, Li and As. |
| Aggregate determinants | Alkalinity |

6.1.3: Isotopic analyses

Two unfiltered samples for each site were taken for isotope analysis in new 250 ml polyethylene bottles and properly sealed with plastic tape. A back-up sample was needed in case of leakage or contamination of one of the samples. All samples were kept cool during the period before being despatched to the laboratory.

The stable isotope analyses were performed at the Geochemistry Department of the University of Cape Town. Hydrogen isotopes were determined using the Zn-closed tube method and oxygen isotopes were determined by the $CO_2$ equilibration method using 7 ml vacutainers. All isotope ratios were measured using a Finnegan MAT252 mass spectrometer.

The standards V-SMOW and SLAP were adopted to determine the degree of compression of raw data and the equations of Coplen (1988) were used to convert to the SMOW scale (Harris *et al.*, 1999). Drifts in reference gases were corrected by analysing an internal standard (CTMP), calibrated against V-SMOW and SLAP, with each batch of samples (Harris et *al.*, 1999). The precision of the data, based on typical mean differences of duplicate analyses of standards, should be better than ± 0.15 ‰ for oxygen and ± 1 ‰ for hydrogen.

Stable isotope data are presented in "delta notation" where δ (‰) is defined as

**Eq. 6.1:** $$\delta = \left( \frac{R_{sample}}{R_{standard}} - 1 \right) 1000\ ‰$$

Where $R_{sample}$ and $R_{standard}$ = $^{18}O/^{16}O$ or $^{2}H/^{1}H$.

### 6.1.4: Quality control

To determine the accuracy of the laboratory analyses duplicate samples were sent to two laboratories using different analytical techniques. Duplicate samples were also sent to the same laboratory. Comparison of the data was considered necessary in order to ensure confidence in the results. Accuracy of the analyses of the ions can be determined from the electro-neutrality condition since the sum of the positive and negative charges in the water must balance (ions are expressed in meq/L) (Appelo and Postma, 1993). Samples that had ionic balance errors (IBE) above 10% were removed from the data set. The IBE is expressed as:

**Eq. 6.2:** $$IBE = \frac{\left(\sum cation - \sum anions\right)}{\left(\sum cation + \sum anion\right)} * 100\,\%$$

### 6.1.5: Data handling

All the data (physical and chemical) was stored in the Excel spreadsheet program (Microsoft®). The program was used to manage the data and perform elementary statistical analysis on the data. It was also used to generate graphs. The Statistca (Statsoft) computer program was used to perform the more advanced statistical analysis.

The laboratories report $NO_x$ as N, phosphate as P, silica as Si as sulphate as S. In order to convert these analyses to the oxidised species the following conversion was performed:



**Eq. 6.3:** X (mg/l) = [Y (mg/l)/Y (atomic mass)] * X (atomic mass)

Where: X = oxidised species
Y = reported species

The computer programs Rockware Utilities and Groundwater for Windows were used to generate Piper, Stiff and Schoeller diagrams.

The extent of mineral saturation of sampled water was calculated using the NETPATH software package, through a WATEQF subroutine (Plummer *et al.*, 1992). WATEQF calculates the ion activities and the state of saturation of the mineral phases in the water. The saturation index is expressed as:

**Eq 6.4:** $$SI = \frac{\log IAP}{KT}$$

Where: IAP = ion activity product
K = solubility product
T = temperature

Finally, all data was transferred to PC ArcView for the generation of maps and data storage.

## 6.2: Macro groundwater chemistry

This section presents the analyses of groundwater sampled in catchments F30 and F40 as well as a few groundwater samples collected in the northern-most sections of catchment F50. The dissolved constituents (which are major ions and trace elements) and environmental isotopic content ( $\delta$ D and $\delta$ $^{18}$O) of the groundwater are discussed for the individual catchments as well as comparisons drawn between the catchments. Over-simplified borehole logs were sourced in various consultancy reports for a few borehole sample points. However, seven lithological units (Table 6.3) were selected on the new 1:1000 000 geological map and characterised by the dissolved constituents of selected groundwater samples.

The laboratory results of the groundwater samples are described element by element and with reference to two secondary drainage catchments (F30 and F40) and selected lithological units (Table 6.3). The analyses have been divided into anions, cations and trace elements. The environmental isotopes will be presented with reference to the entire Namaqualand region.

A large dataset of groundwater samples exists for these catchments on the National Groundwater Database (NGDB) under the auspices of the Department of Water Affairs and Forestry (DWAF). This data will not be represented here, but will be referred to in subsequent chapters for the purpose of comparing the current groundwater analyses with earlier data sets.



Table 6-3: The seven lithological units identified for groundwater classification purposes.

| INTRUSIVES | | METASEDIMENTS | | |
|---|---|---|---|---|
| Suite/Group | Formation | Group | Subgroup | |
| Little Namaqualand Suite (1200 Ma years) | *Mesklip Granite (Mme)<br>*Buffels River Granite (Mbc)<br>Nababeep Gneiss (Mnp) | Bushmanland | Khurisberg (Mkh)<br>Bitterfontein (Mbt) | AGE ↓ |
| *Stalhoek Complex (Msc) | *Kamieskroon Gneiss (Mkg) | | | |

(* Not yet accepted by SACS but incorporated into the latest 1: 1000 000 geological map of South Africa)

The bicarbonate ($HCO_3$) concentrations, as a percentage of the total anion concentration, generally decrease with increasing salinity, while the chloride (Cl) concentrations, as a percentage of the total anion concentration, generally increase with increasing salinity (Figure 6.2). At very low TDS values the $\%HCO_3$ is equal to or even greater than the %Cl for a few samples. A change in the dominant dissolved anion with increasing salinity is observed that may reflect the effects of repetitive evaporation processes and the conservative nature of Cl once in solution. The cationic fields of the piper diagrams (Figure 6.2) illustrate the dominance of the sodium (Na) ions with respect to the other dissolved cations throughout the salinity range for the groundwater. Cation exchange may occur (see Section 8.2.5), although Na remains the dominant cation in solution. In addition, the Na concentrations, as a percentage of the total cation concentration, increase with increasing salinity. The piper diagrams thus reflect the dominance of a NaCl facies for the groundwater of Namaqualand (Figures 6.2, 6.3 and 6.4). There is excellent similarity between the groundwater data, in terms of ionic ratios, that were collected recently (Figure 6.2) and the data extracted from the NGDB collected over an extensive period of time (Figure 6.3). The groundwater data for secondary drainage catchment F40, in terms of ionic ratios plotted on a Piper diagram (Figure 6.4), is also remarkably similar to the groundwater data for secondary drainage catchment F30 (Figure 6.2).

The (ground-) water in the highest lying mountain ranges has a relatively low salt content covering a range of chemical compositions (Figure 6.5). The (ground-) water is probably derived from recharged rainwater, which has leached the more soluble salts, particularly sodium chloride and sodium carbonate, from the soil and rock matrix as it infiltrates. The groundwater of the lower lying regions generally has total dissolved solids loads ranging between 1000 mg/l to 10 000 mg/l and can be classed as brackish water. The groundwater is very similar in chemical character with a dominant Na-Cl signature (Figure 6.6). Strong acids dominate over weak acids, indicating that chlorides play a more important role in defining the water chemistry than carbonates and bicarbonates, while non-carbonate alkalis (i.e. primary salinity) exceed 50% (Piper, 1953). Alkalis and strong acids dominate the chemical properties of the groundwater. This chemical characteristic is shared with ocean water and brines that plot in the same field on a piper diagram.

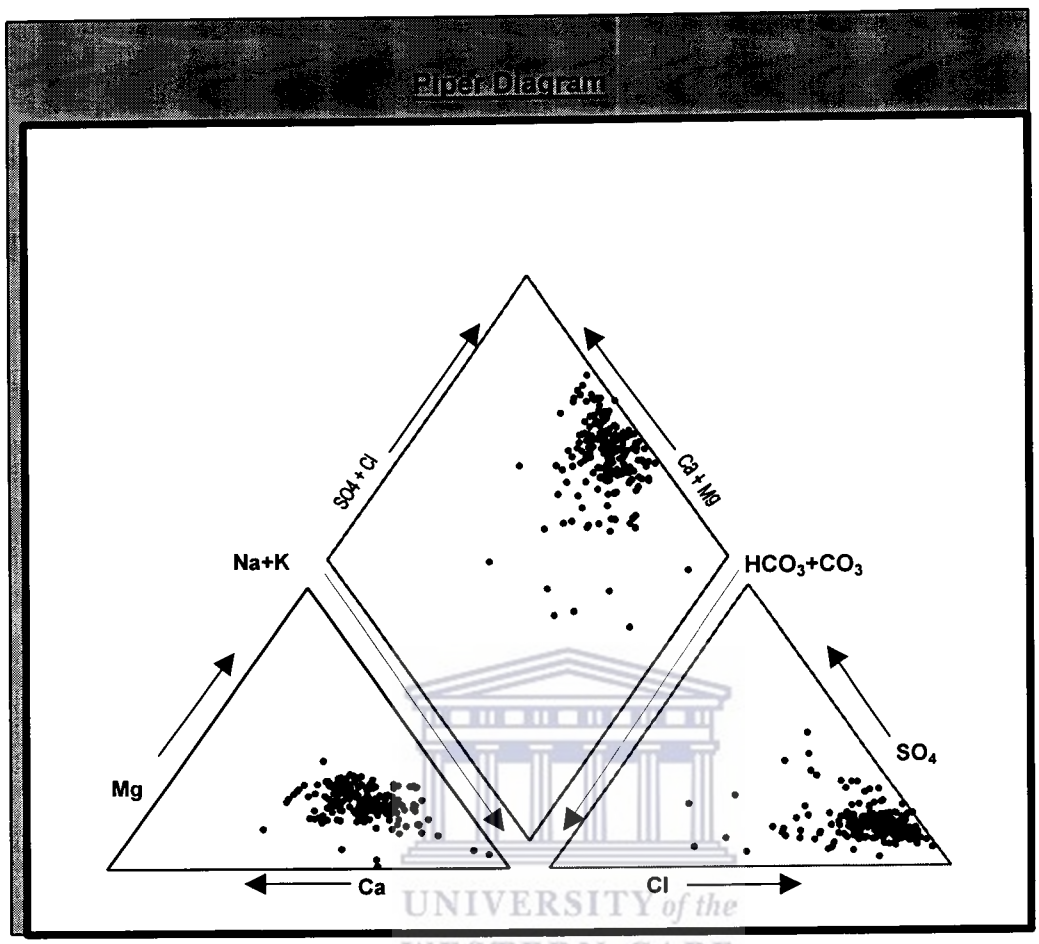




Figure 6-2: Piper diagram for the groundwater of secondary drainage catchment F30.

.

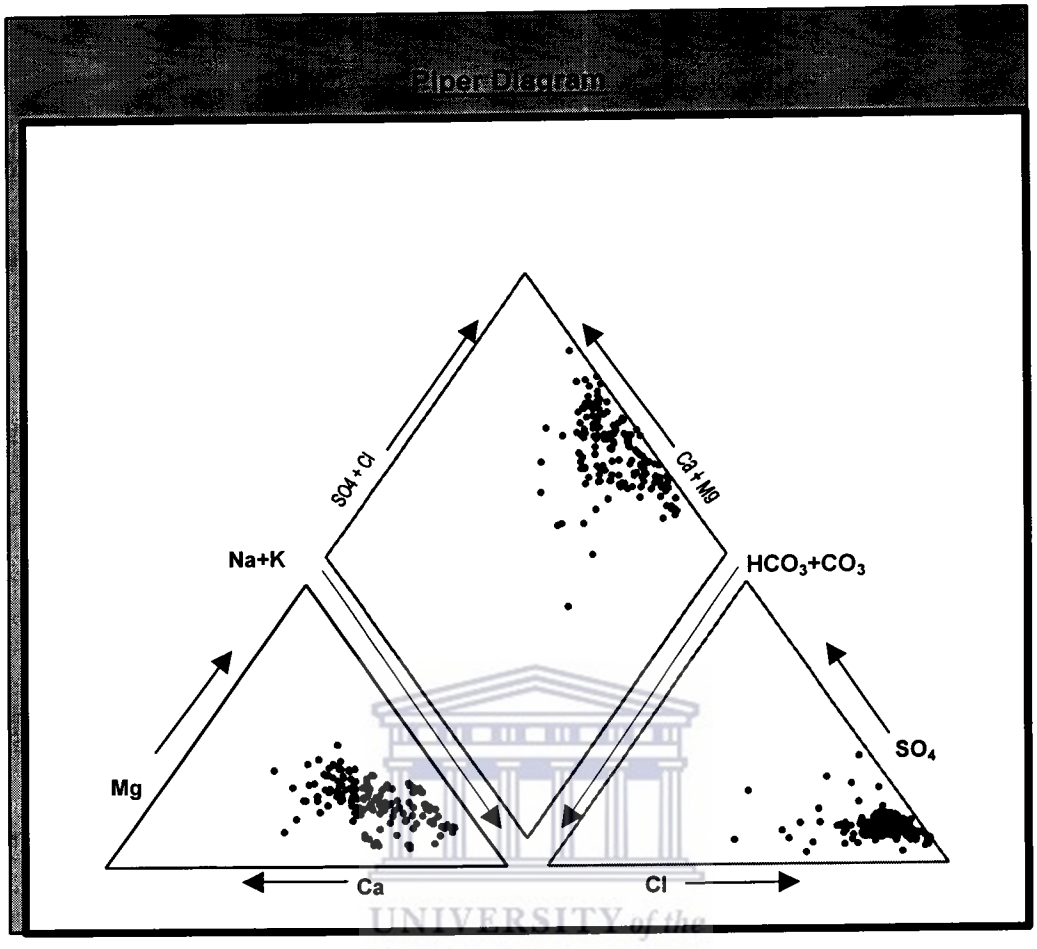




Figure 6-3: Piper diagram for the groundwater data extracted from the NGDB database for the secondary drainage catchment F30.

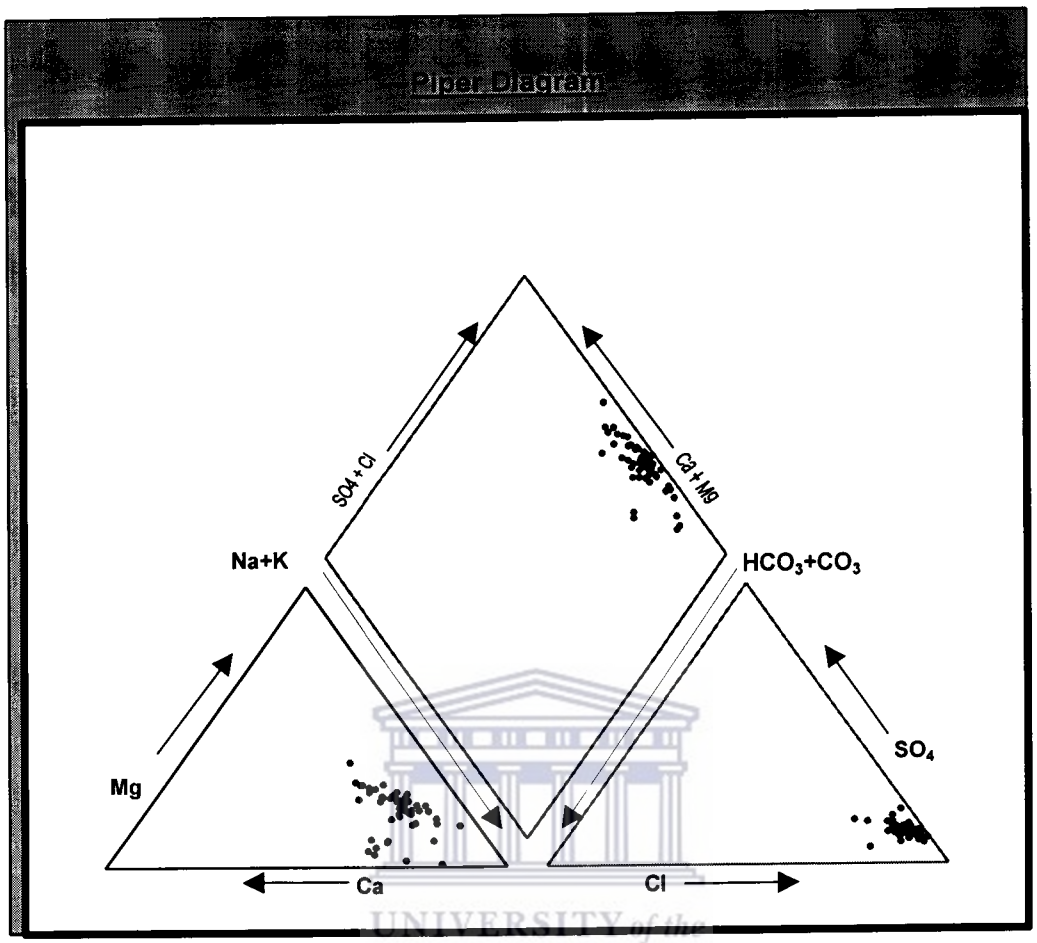




Figure 6-4: Piper diagram for the groundwater of secondary drainage catchment F40.

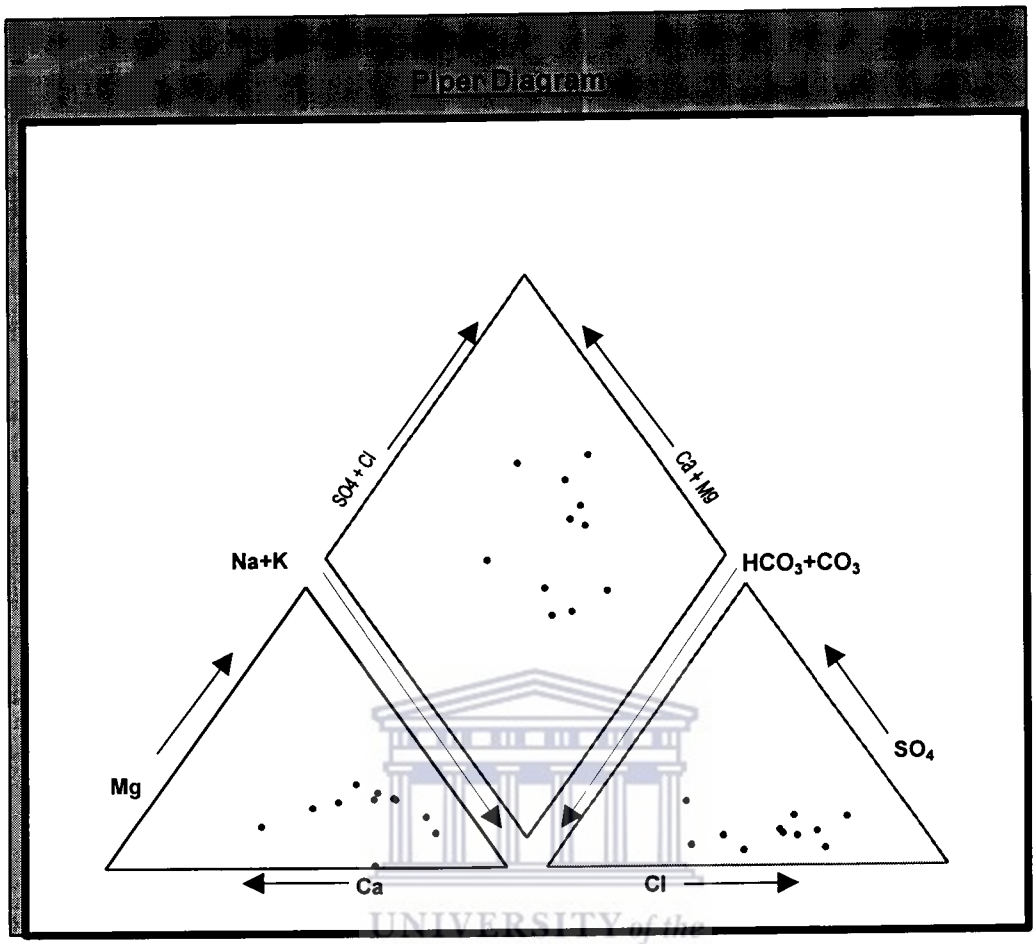




Figure 6-5: Piper diagram for groundwater of the highest (i.e. Leliefontein) lying regions of the Kamiesberg mountain range.

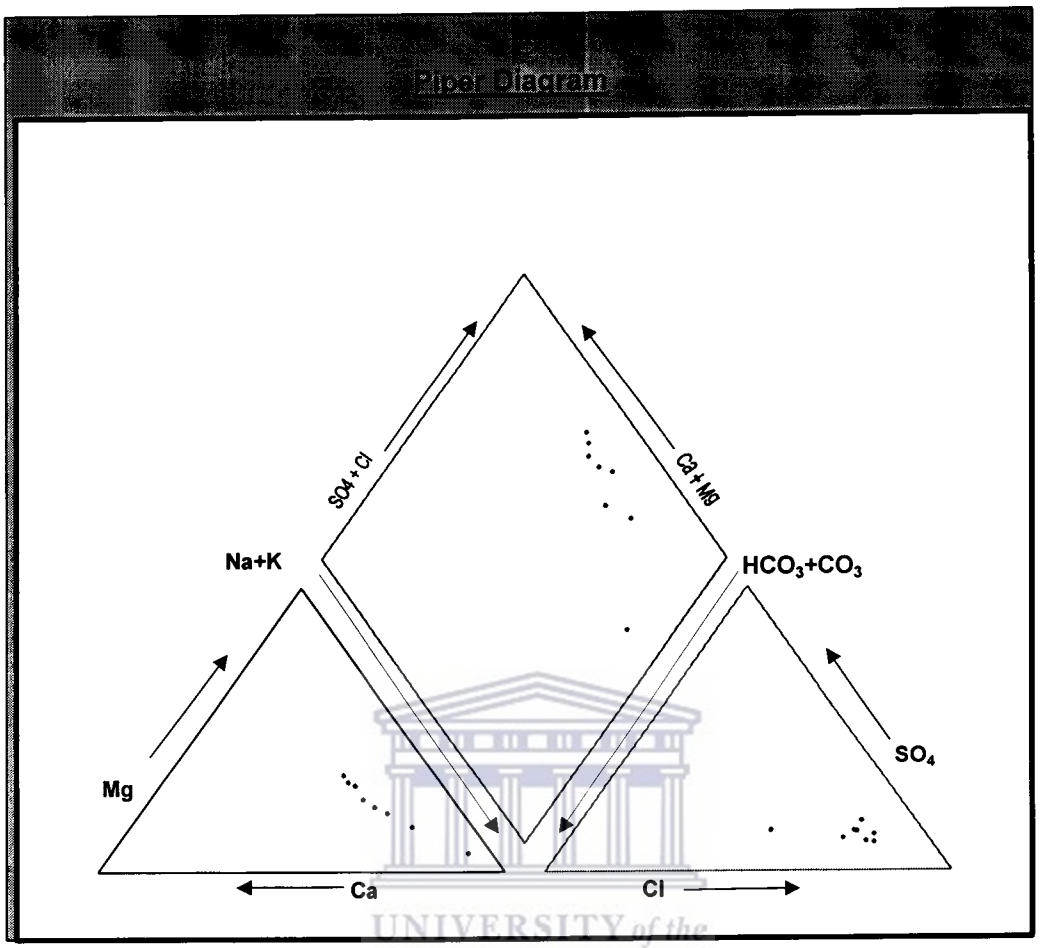


Figure 6-6: Piper for groundwater of the lowest lying (i.e. Kamassies) regions of the Kamiesberg mountain range.

Water types are classified based on the expanded Durov diagram to better reflect features of the macro groundwater chemistry. The groundwater for the secondary drainage catchments F30 and F40 plot respectively in fields 8 and 9 for catchment F30 (Figure 6.7) and predominantly field 9 for catchment F40 (Figure 6.8) on the expanded Durov diagram. Similar trends observed for the groundwater of catchment F30 extracted from the NGDB database (Figure 6.9). The explanation (Lloyd and Heathcote, 1985) for these fields is given as:

> "8. $Cl^-$ dominant and no dominant cation indicates that the groundwaters may be related to reverse ion exchange of $Na^+$-$Cl^-$ waters"; and
>
> "9. $Cl^-$ and $Na^+$ dominant frequently indicate end-point waters. The Durov diagram does not permit much distinction between $Na^+$-$Cl^-$ waters."

This rigid, mathematical approximation based on the cation and anion content of the groundwater and the associated explanation for field 8 do not seem to apply to the groundwater of Namaqualand. Similarly, the trend as indicated from field 9 to field 8 couldn't be applied to the groundwater for Namaqualand. Variations, based on the cation content, for the groundwater could not be detected at a significant level. The trends for

the major cations, except K, mirror each other. However, the $Na^+$ and $Cl^-$ dominated groundwater for Namaqualand can be described as end-point waters.

The application of statistical analyses is a common, first order approach to the manipulation of large data sets (Usunoff and Guzman-Guzman, 1989; Ashley and Lloyd, 1978; and Dawdy and Feth, 1967). Multivariate statistics were used, particularly Pearson's correlation matrices, to find any significant correlation between the various chemical parameters (i.e. variables) of the groundwater in the secondary drainage catchments F30 and F40. Correlations are a measure of the relation between two or more variables (Levinson, 1980) and correlation coefficient matrixes are used to express the variance of each variable in relation to the other variables in the data set. The degree of linear correlation is termed the correlation coefficient ( r) and the variance is a measure of the scatter of values around the mean. Correlation coefficients range from +1.00 (i.e. a perfect positive correlation) to –1.00 (i.e. a perfect negative correlation). Variables with correlation coefficients of r = | 0.7 | show strong correlations while correlations of r = | 0.5 – 0.7 | are considered moderate (Table 6.4).

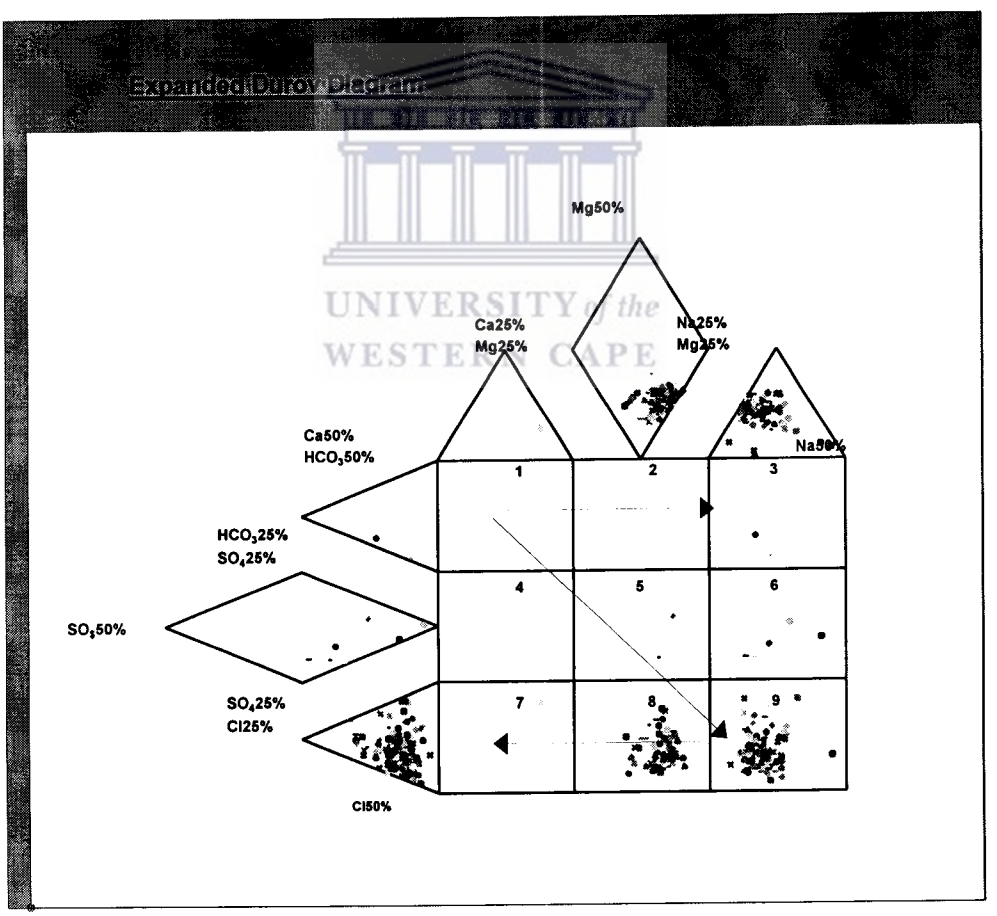


Figure 6-7: Expanded Durov diagram for groundwater of secondary drainage catchment F30.

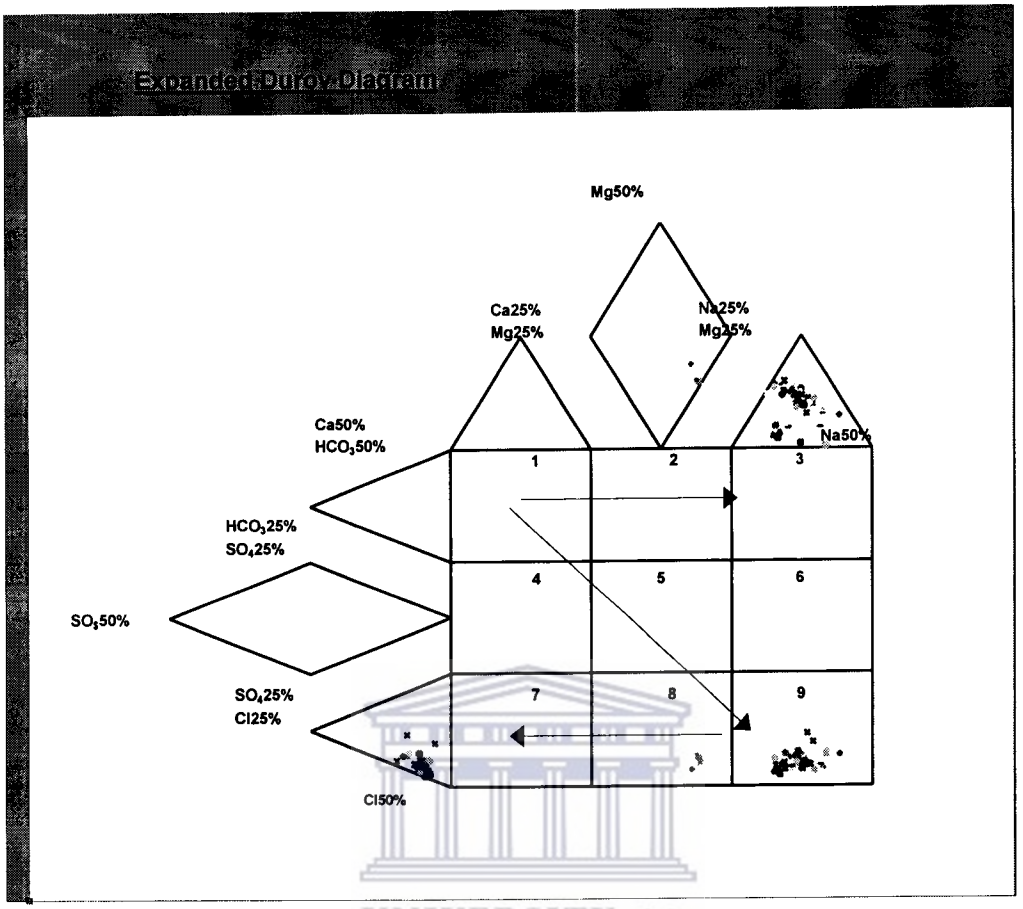




Figure 6-8: Expanded Durov diagram for groundwater of secondary drainage catchment F40.

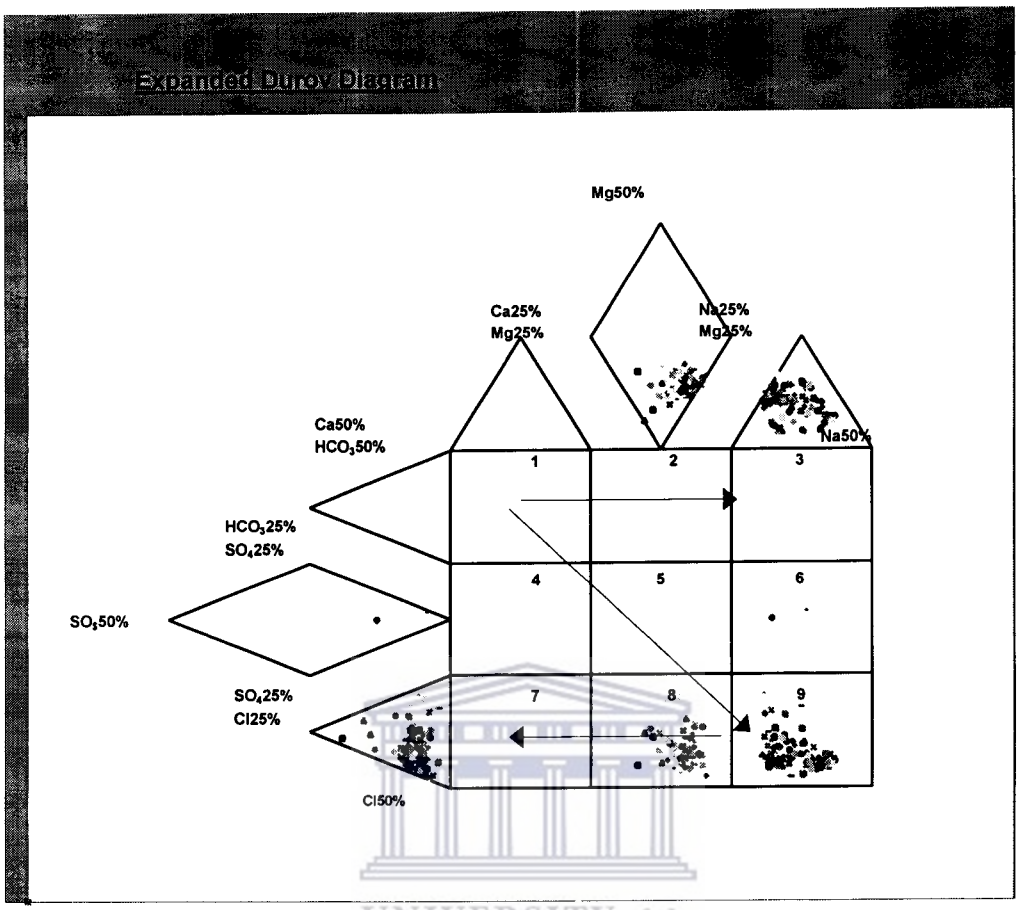




Figure 6-9: Expanded Durov diagram for groundwater data from the NGDB database for the secondary drainage catchment F30.

Table 6-4: Pearson's correlation matrices for groundwater of F30 showing moderate to strong correlations at a significance level of $p < 0.05$.

| Variables | Field EC | Field pH | Na | Cl | Ca | K | Mg | SO4 | F | Si | Sr | Deuterium | Oxygen - 18 |
|---|---|---|---|---|---|---|---|---|---|---|---|---|---|
| Field EC | 1.00 | | | | | | | | | | | | |
| Field pH | | 1.00 | | | | | | | | | | | |
| Na | 0.97 | | 1.00 | | | | | | | | | | |
| Cl | 0.99 | | 0.99 | 1.00 | | | | | | | | | |
| Ca | 0.94 | | 0.93 | 0.94 | 1.00 | | | | | | | | |
| K | 0.84 | | 0.89 | 0.88 | 0.82 | 1.00 | | | | | | | |
| Mg | 0.97 | | 0.97 | 0.98 | 0.94 | 0.87 | 1.00 | | | | | | |
| SO4 | 0.89 | | 0.87 | 0.87 | 0.93 | 0.75 | 0.86 | 1.00 | | | | | |
| F | | | | | | | | | 1.00 | | | | |
| Si | | | | | | | | | | 1.00 | | | |
| Sr | 0.95 | | 0.94 | 0.95 | 0.98 | 0.84 | 0.94 | 0.91 | | | 1.00 | | |
| Deuterium | 0.61 | | 0.64 | 0.65 | 0.48 | 0.62 | 0.67 | | | | 0.54 | 1.00 | |
| Oxygen-18 | 0.64 | | 0.70 | 0.70 | 0.54 | 0.73 | 0.70 | | | | 0.58 | 0.89 | 1.00 |

The correlation matrix (Table 6.4) indicates:

- Strong positive correlations of electrical conductivity (EC) with all major ions and some trace elements (Sr, Al, B and Ba) and moderate positive correlations with others (i.e. Li and P). Moderate positive correlations also exist between EC and the environmental isotopes (i.e. oxygen-18 and deuterium).
- A very significant positive correlation (r = – 0.99 –) exists between Cl and Na. Both ions are strongly correlated with all cations and anions, the trace elements of Sr, Al, B, and Ba as well as with oxygen-18. The latter ions are moderately correlated with the trace elements Li and P as well as with deuterium. The other cations and anions, as well as the trace elements Sr and Al, show approximately similar trends to that of Cl and Na, except that they are moderately correlated to the environmental isotopes.
- Fluoride (F) and silica (Si) show no correlation with any of the major anions and cations as well as no correlations with any of the trace elements. Only a moderate correlation of F with lithium (Li) is shown.
- All the above-mentioned elements, as well as $HCO_3$, show no significant correlation with pH.

These trends can be interpreted as follows:

- The dominant contribution of Cl to the EC of the groundwater is reflected in the significant relation it has (i.e. r = – 0.99 –) with EC. The strong correlations of Cl with all other major ions (i.e. anions and cations) probably indicate the relevance of Cl as a tracer of the groundwater salinity. The possible sources for Cl are discussed in section 8.2.2.
- The major exchangeable ions (i.e. Na, Ca, Mg, K and Sr) all correlate positively. Moderate to strong negative correlations, due to for example cation exchange processes, were not evident in using the correlation matrices. The significant contribution of the dissolution and leaching of evaporitic salts (see Chapter 8) to the salinity of the groundwater masks the effects of other processes (such as the effects of carbonate and silicate weathering and cation exchange). The weathering of carbonate and thermodynamically unstable aluminosilicate minerals also contribute cations (including Si in the case of the aluminosilicate minerals) and influence the $HCO_3$ content and thus the pH of the solution. The probable sources for the cations are varied and are discussed in sections 8.2.4 and 8.2.5. The correlation between F and Li may, for example, refer to lithium-containing mica minerals as a significant source of F in groundwater.
- The positive correlations of EC with the environmental isotopes show that the higher salinity groundwater is generally characterized by enriched stable isotopic values. Higher salinity groundwater is generally associated with the lower rainfall, lower lying regions of Namaqualand. The relation indicates that the salinity of the groundwater is more than likely derived from the infiltration of previously evaporated surface waters and/or the solution and flushing of evaporative salts in the subsurface. In addition, considerable evaporation occurs within large diameter wells depending on the relative humidity within the wells. Groundwater sampled

in mountainous regions is characterized by depleted stable isotopic concentrations (see Section 6.3.5).

## 6.3: Characteristics of the groundwater constituents

An overview of the descriptive statistics of the physio-chemical parameters (i.e. EC and pH), various dissolved major (i.e. both anions and cations) and trace elements, and the environmental isotopes are presented in this section.

### 6.3.1: Physio-chemical parameters

The following discussion illustrates that informed hydrogeological decisions are crucial to identify probable target areas for groundwater development in order to supply communities with groundwater of adequate quantity and quality.

*Electrical Conductivity (EC) and Total Dissolved Solids (TDS)*

There is a good correlation (Figure 6.10) between the field electrical conductivity (EC $_{field}$) mean values and the laboratory determined electrical conductivity (EC $_{lab}$) mean values as well as the laboratory determined electrical conductivity (EC $_{lab1}$) mean values compared to 'foreign' laboratory determined electrical conductivity (EC $_{lab2}$) mean values for groundwater of catchment F30. The EC $_{field}$ value for groundwater of catchment F40 is lower than the EC values determined in the laboratories.

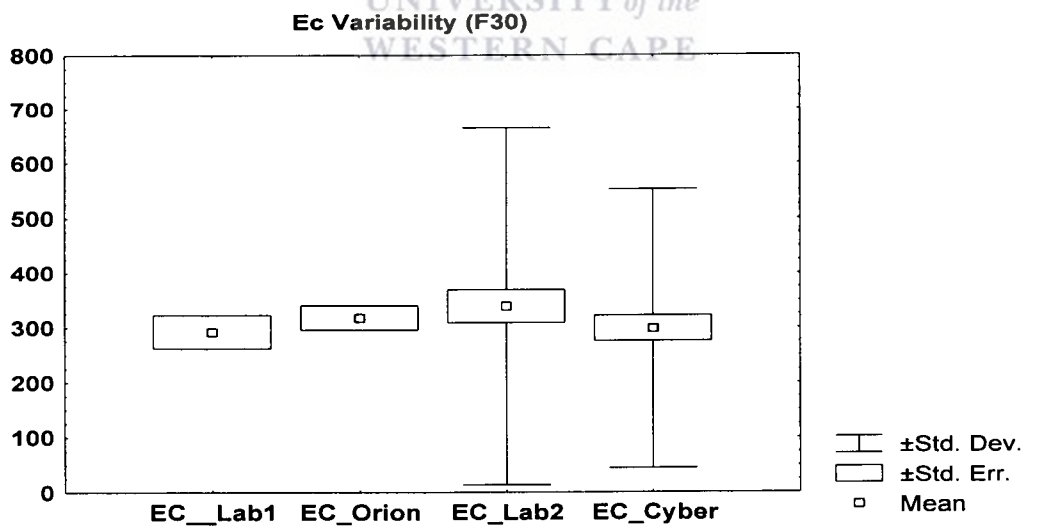


Figure 6-10: EC field (i.e. field electrical conductivity mean values) versus EC lab (i.e. laboratory determined electrical conductivity mean values). Including, EC lab1 (i.e. laboratory determined electrical conductivity mean values) compared to EC lab2 (i.e. 'foreign' laboratory determined electrical conductivity mean values).

The variability in the EC values (Figure 6.10) recorded in the field and determined at two different laboratories, for the groundwater of catchment F30, seems to be insignificant. The variability in the EC values recorded in the field and compared to those determined at two different laboratories, for the groundwater of catchment F40, seem to be considerable. Furthermore, the mean EC values for groundwater in catchment F40 are much higher than similar values for groundwater in catchment F30.

A histogram (Figure 6.11) shows a highly skewed $EC_{field}$ population towards higher EC values for groundwater in catchment F 30. Most EC values, associated with groundwater of F30, are concentrated over an interval up to an EC value of 250 mS/m. The latter may indicate that most of the boreholes may be strategically placed, through trial and error, to intercept groundwater of the 'best' or adequate quality for the region. Boreholes for this study were, however, targeted to provide an even distribution especially at a regional scale (i.e. secondary drainage catchment scale). The EC population for groundwater of catchment F40 displays a normal distribution centered on a range between 600 mS/m to 800 mS/m.

The highest mean EC (Figure 6.12) values are associated with the intrusive Stalhoek Complex (Msc) and the intrusive Buffels River granites (Mbc). The lowest mean EC value is associated with the Khurisberg subgroup (Mkh). Groundwater from the intrusive granitic and gneissic rocks (i.e. Little Namaqualand Suite, Kamieskroon gneiss (Mkg) and Stalhoek Complex (Msc) generally has higher mean EC values than the metasedimentary rocks (i.e. the Bitterfontein (Mbt) and Khurisberg subgroups (Mkh). This phenomenon can be ascribed to the thermodynamically unstable nature of minerals contained within the granitic and gneissic rocks associated with the emplacement of these rocks at or near the Earth's surface and its exposure to low temperature weathering reactions.



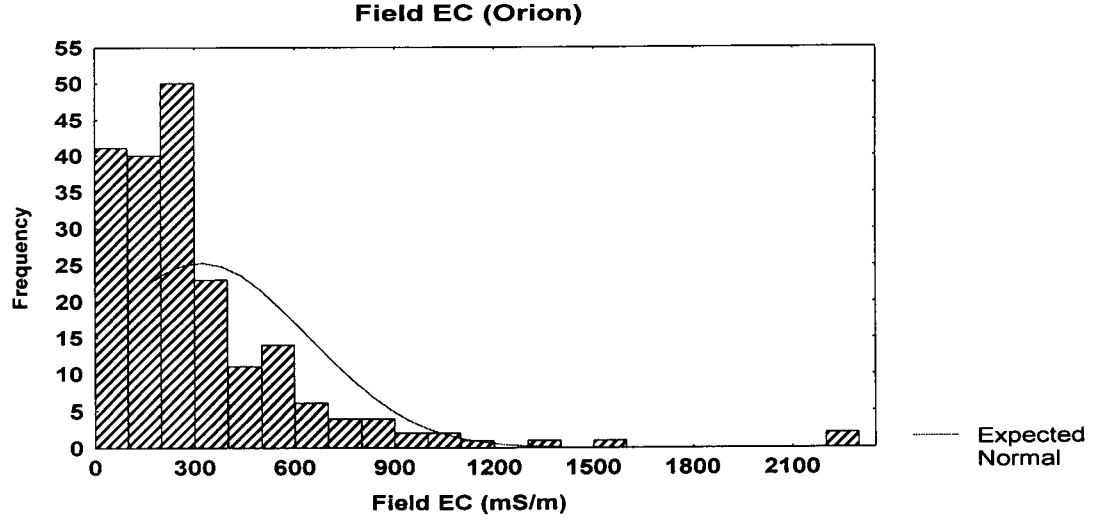


Figure 6-11: EC field population for groundwater in catchment F 30.

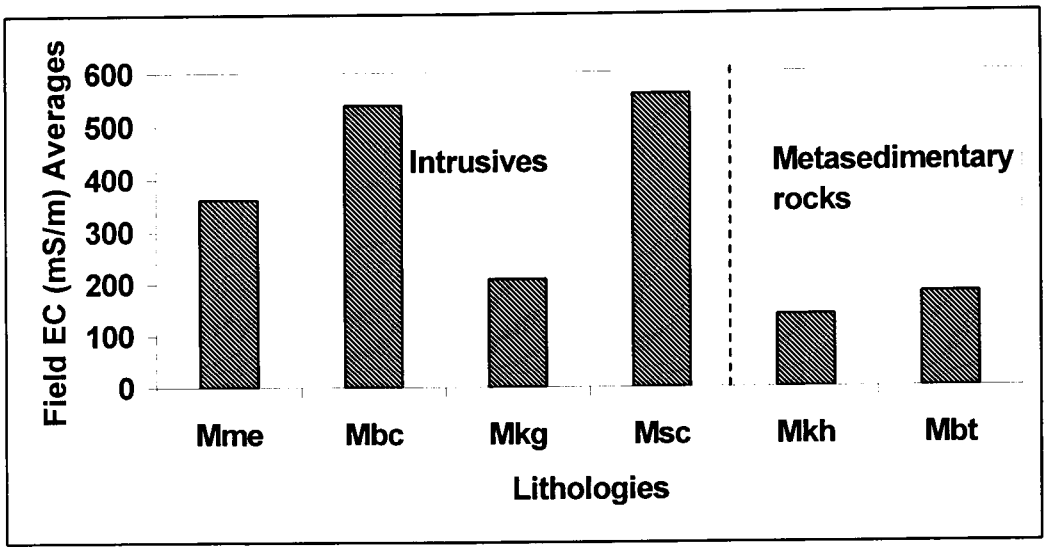


Figure 6-12: The variation in field EC values for the intrusive and metasedimentary rocks.

*pH*

The pH values for groundwater of catchment F30 display an almost perfect normal distribution centered on a value of 7 (Figure 6.13), as opposed to an irregular distribution of the pH values for groundwater of catchment F40. There is a good correlation in the spread of pH values recorded in the field and those determined in the laboratory for the groundwater of catchment F30. A similar comparison is observed for the pH values of catchment F40. The pH value determined in the laboratory is always slightly higher than the field value (more for catchment F40), perhaps due to carbon dioxide ($CO_2$) loss/emission to the atmosphere or a loss to the unfilled top portion of the sampling bottle (Figure 6.14). The sampling bottles were, however, filled to the top and sealed properly.

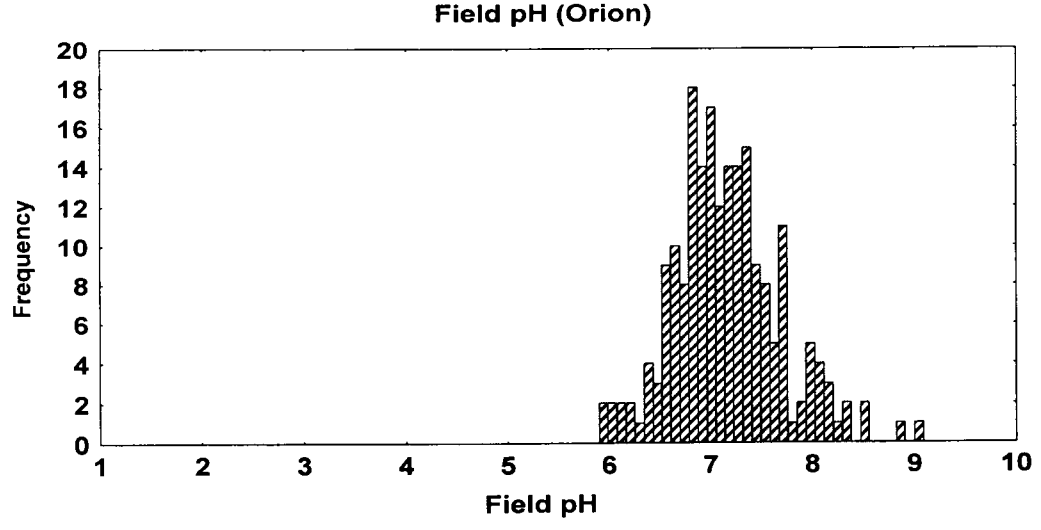


Figure 6-13: The pH values for groundwater of catchment F30.

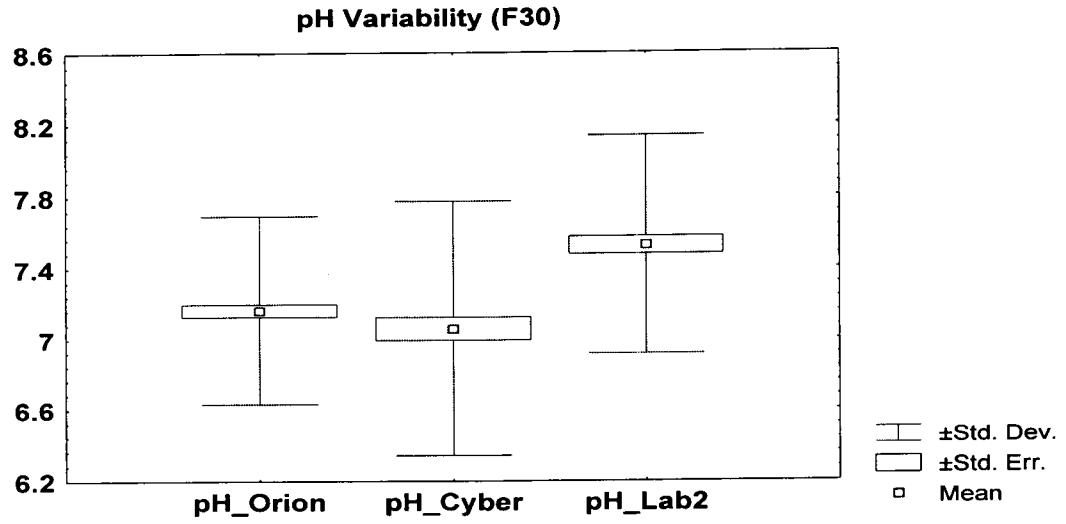


Figure 6-14: The pH values, and pH variability, for groundwater of catchment F30.

Groundwater in the Buffels River granites (i.e. Little Namaqualand Suite) has the highest mean pH value, while groundwater in the Khurisberg subgroup (i.e. Bushmanland Group) have the lowest mean pH value (Figure 6.15). The Khurisberg subgroup is composed primarily of 'unreactive' quartzite that is normally less prone to chemical weathering processes and a limited buffering capacity.



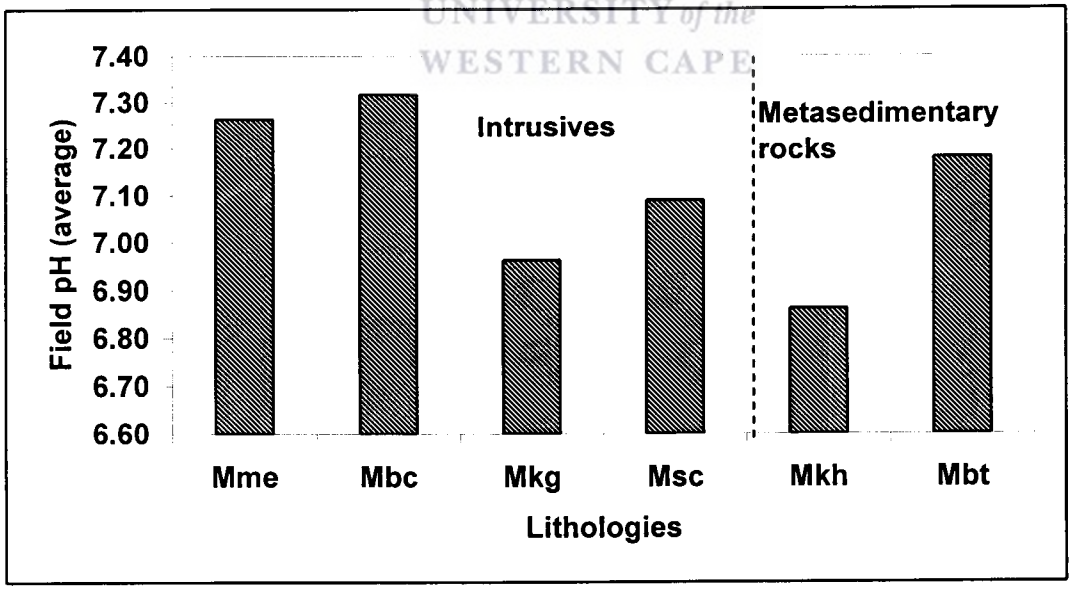


Figure 6-15: The variation in field pH values for the intrusive and metasedimentary rocks.

6.3.2: Major elements – Anions

Chloride (Cl) is by far the dominant dissolved anion in the groundwater of both catchments F30 and F40. A histogram (Figure 6.16) shows a highly skewed Cl population towards higher Cl values for groundwater in catchment F 30. Most Cl values, associated with groundwater of F30, are recorded over an interval up to a value of 1000 mg/l. Similar trends are observed for groundwater of catchment F40. However, the mean value of Cl for groundwater of catchment F40 is far greater than a similar mean value for groundwater of catchment F30.

Bicarbonate ($HCO_3$) and sulphate ($SO_4$) are the second-most dominant dissolved anions in both catchment F30 and F40 (Figure 6.17). The bicarbonate ($HCO_3$) population for the groundwater of catchment F30 display an asymmetrical and erratic normal distribution centered on a range of values from 130 to 140 mg/l. The distribution of bicarbonate ($HCO_3$) concentrations for groundwater of F40 is highly irregular. The sulphate ($SO_4$) population, for groundwater of catchment F30, is highly skewed towards the higher $SO_4$ concentrations with most values being recorded below 500 mg/l. The sulphate ($SO_4$) population for groundwater of catchment F40 displays a lesser skewness to the right. The distribution of fluoride (F) concentrations, for groundwater in both catchments, is also highly irregular with most values being recorded over an interval up to a value of approximately 3.5 mg/l (Figure 6.18). The mean concentrations for $HCO_3$, $SO_4$ and F are higher for catchment F40 compared to catchment F30.



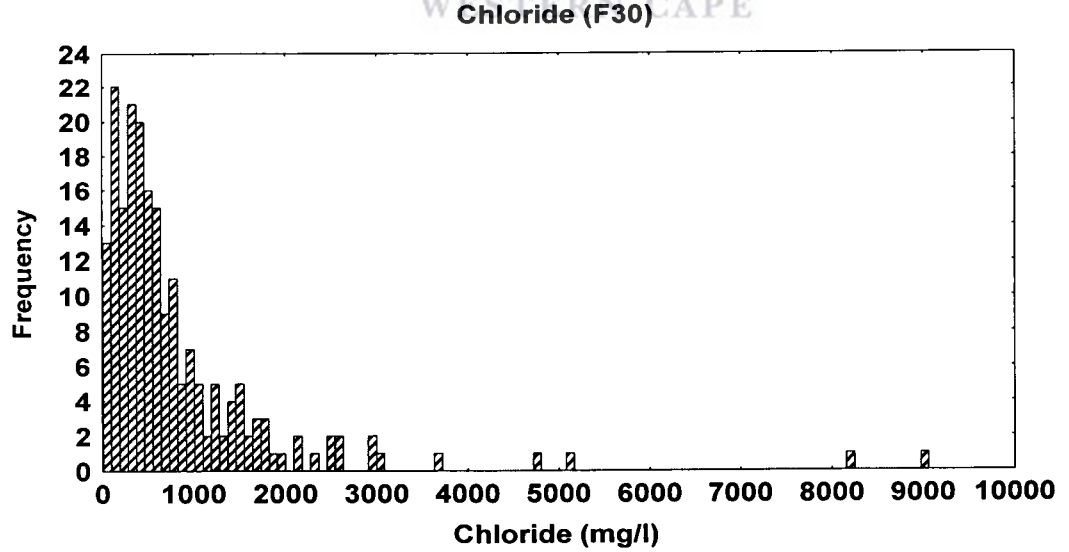


Figure 6-16: Chloride (Cl) population for groundwater in catchment F 30.

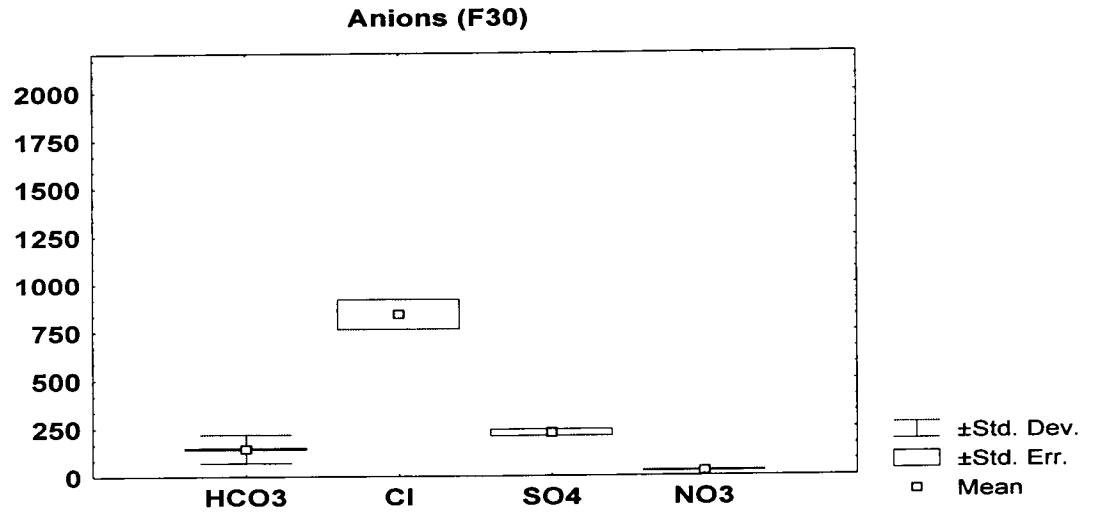


Figure 6-17: A comparison of dissolved anion constituents for catchment F30.

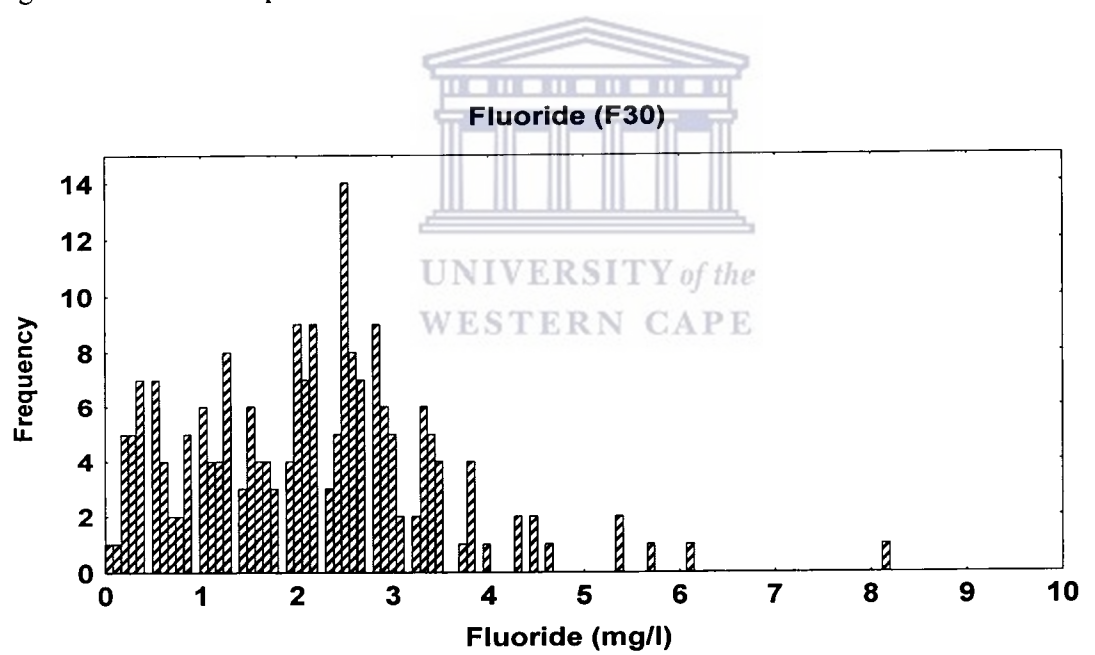




Figure 6-18: Fluoride (F) population for groundwater in catchment F 30.

The mean concentrations of the anions Cl, $SO_4$ and F, in groundwater are higher for the intrusive rocks than those for the meta-sedimentary rocks (Figures 6.19 and 6.20). No distinct trends could be observed in the mean concentrations of $HCO_3$ and $NO_3$ in groundwater for the intrusive rocks compared to the meta-sedimentary rocks. The highest mean $SO_4$ concentrations were recorded in the Buffelsriver granite (Mbc), Stalhoek Complex (Msc) and Kamieskroon gneiss (Mkg), with lesser mean values in the Mesklip granite (Mme) and Nababeep gneiss (Mnp).

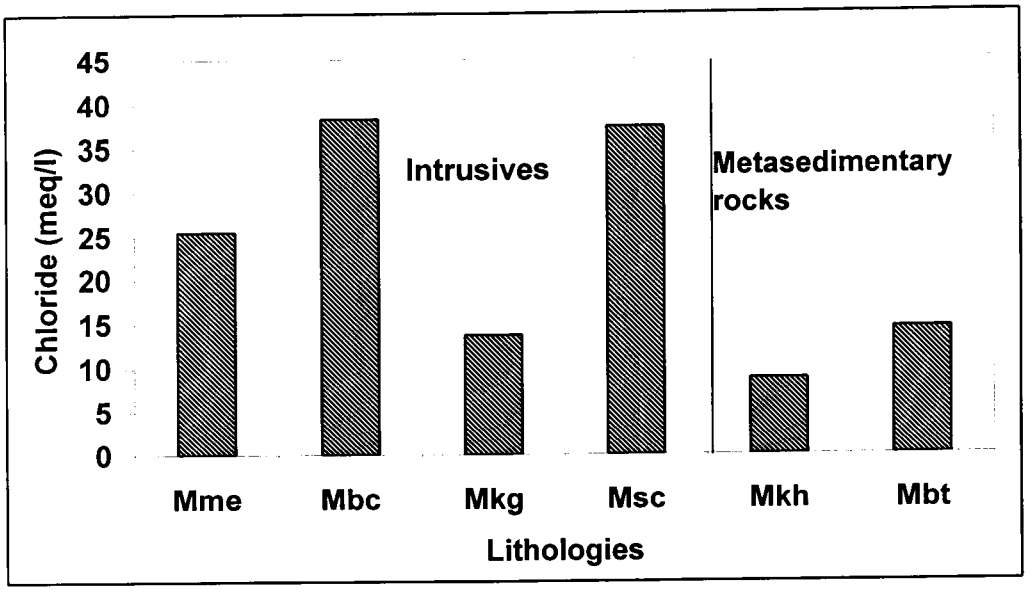


Figure 6-19: Chloride (in meq/l) concentrations for various lithologies.

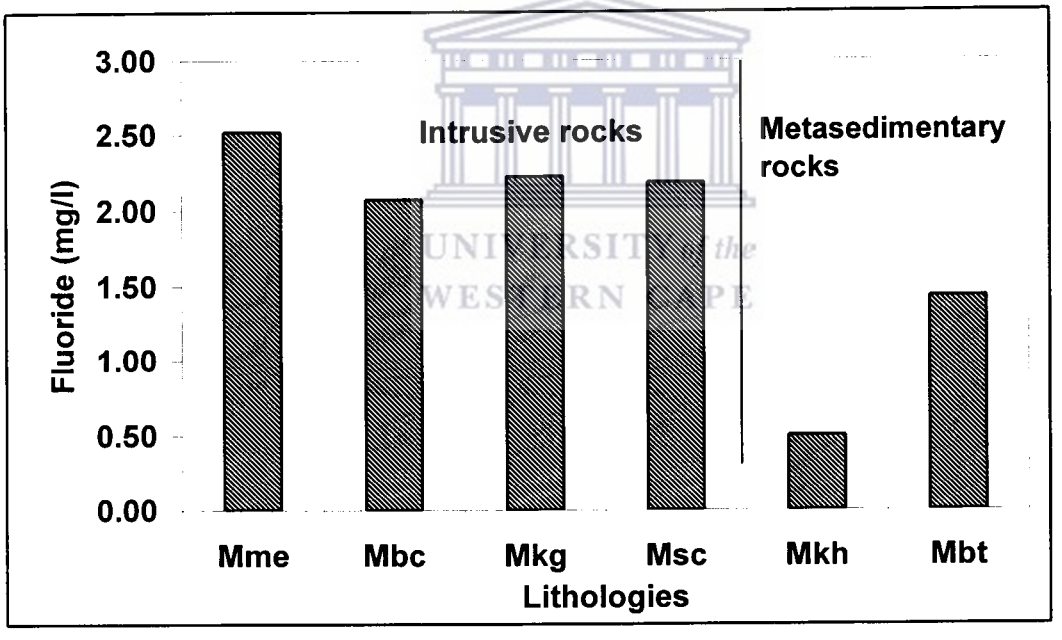


Figure 6-20: Fluoride (in mg/l) concentrations for various lithologies.

The hydrogeological controls on the concentrations of the dissolved anions will be discussed in subsequent chapters. The nitrate concentrations can be linked to anthropogenic activities since most boreholes and wells are stock watering points that are not properly managed. The $SO_4$ and F concentrations in the groundwater are probably also related to the presence and weathering of the sulphide and fluoride-bearing minerals (predominantly mica-group minerals) within the intrusive granitic and gneissic rocks.

6.3.3: Major Elements – Cations

Sodium (Na) is by far the dominant dissolved cation in the groundwater of both catchments F30 and F40. A histogram (Figure 6.21) shows a highly skewed Na population towards higher Na values for groundwater in catchment F30. Most Na values, associated with groundwater of F30, are recorded over an interval up to a value of approximately 600 mg/l. A highly irregular distribution of Na values is observed for groundwater of catchment F40. However, the mean value of sodium for groundwater of catchment F40 is far greater than a similar mean value for groundwater of catchment F30.

Calcium (Ca) and magnesium (Mg) are the second-most dominant dissolved cations in both catchment F30 and F40 (Figure 6.22). The Ca population, for groundwater of catchment F30, displays skewness to higher Ca concentrations. Most Ca values were recorded below concentrations of approximately 150 mg/l, although groundwater samples with Ca concentrations of 200 to 220 mg/l were sampled quite frequently. The distribution of the calcium (Ca) concentrations for groundwater of F40 is fairly similar, although Ca concentrations between 100 mg/l to 300 mg/l were recorded frequently. The magnesium (Mg) population, for groundwater of catchment F30, is highly skewed towards the higher Mg concentrations with most Mg values being recorded below 120 mg/l. The distribution of the Mg concentrations, for groundwater of catchment F40, is highly irregular. The silica (Si) concentrations, for groundwater of catchment F30, display a fairly normal distribution centered on values ranging between 14 to 16 mg/l (Figure 6.23). An irregular distribution pattern, for Si concentrations, is observed for groundwater of catchment F40. The mean concentrations of Ca and Mg are higher for groundwater of catchment F40 compared to catchment F30. The mean concentrations for Si are similar for the groundwater of both catchments F30 and F40.



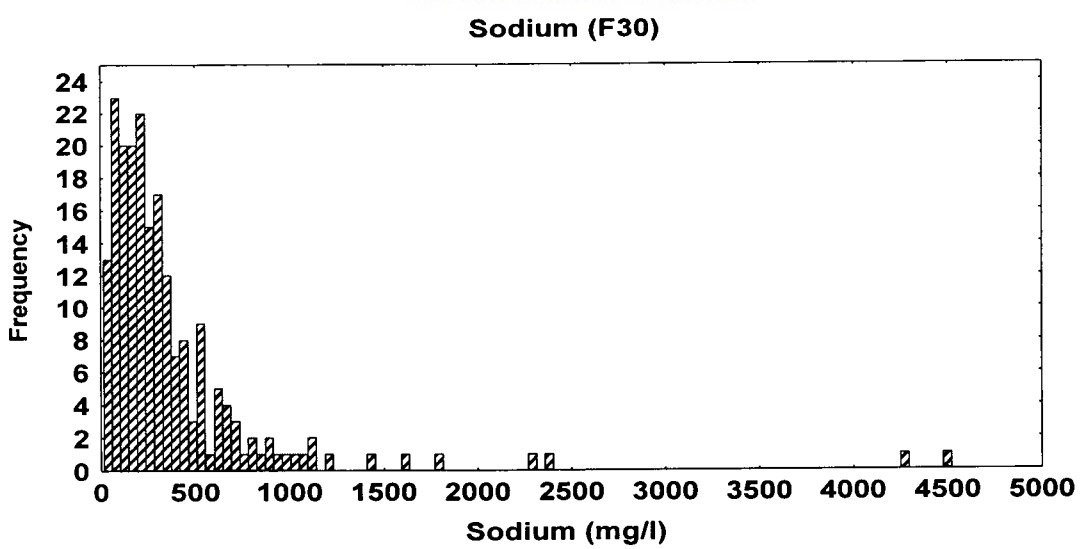


Figure 6-21: Sodium (Na) population for groundwater in catchment F 30.

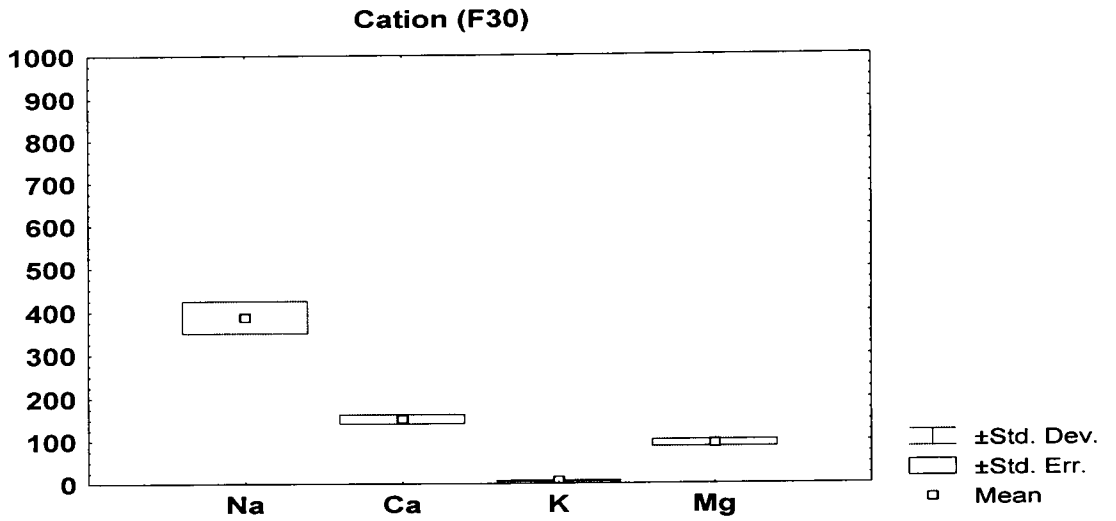


Figure 6-22: A comparison of dissolved cation constituents for catchments F30 and F40.

The mean concentrations of the cations Na, Ca, Mg and Si, in groundwater are higher for the intrusive rocks compared to the meta-sedimentary rocks (Figure 6.24). An anomalously high, mean Si concentration was recorded for groundwater samples (i.e. Mkh) of the Khurisberg subgroup (Figure 6.25). The boreholes are, however, drilled either on or close to the contact between the schists and meta-quartzites of the Khurisberg subgroup and the augen gneisses of the Nababeep formation (i.e. Little Namaqualand Suite).



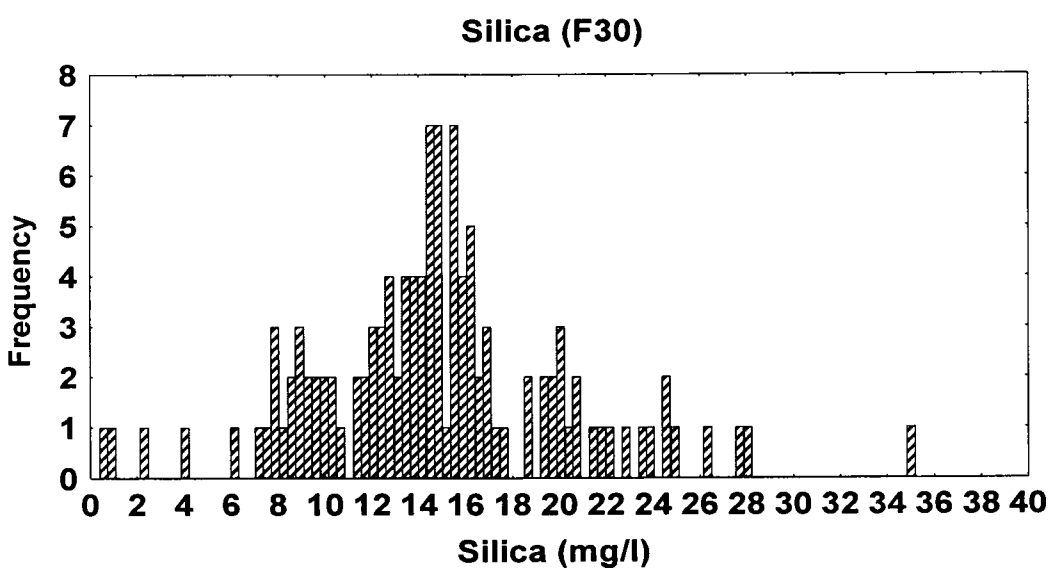


Figure 6-23: Silica (Si) population for groundwater in catchment F 30.

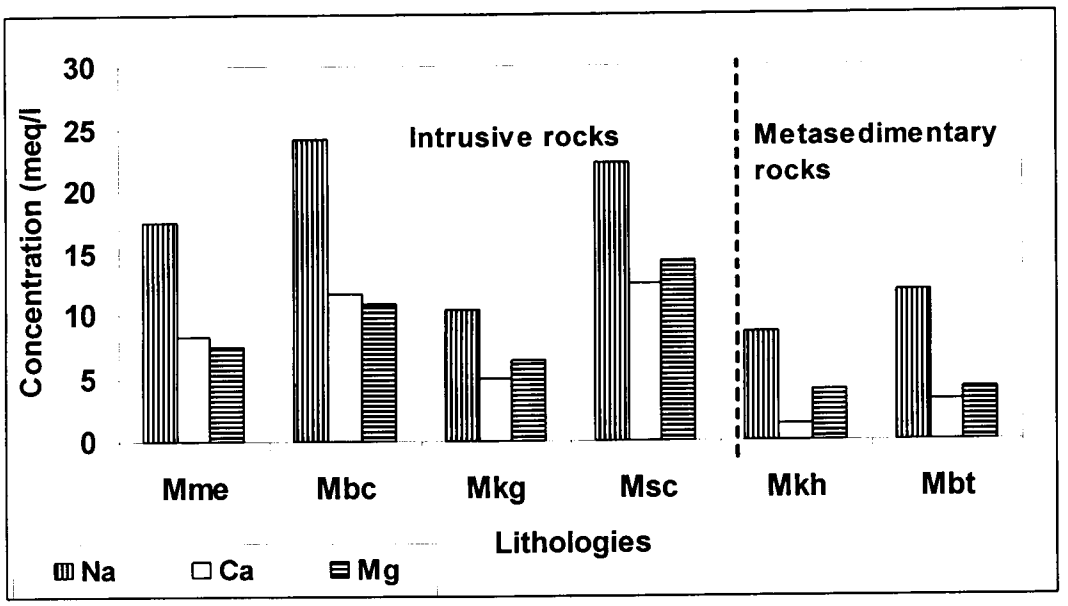


Figure 6-24: The sodium (Na), calcium (Ca), and magnesium (Mg) concentrations for the intrusive rocks compared to the meta-sedimentary rocks.

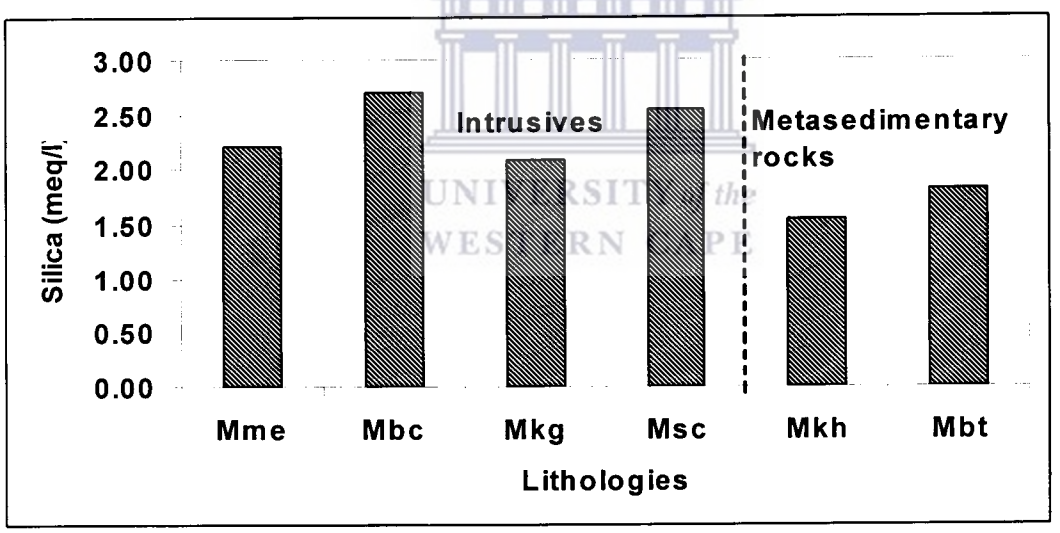


Figure 6-25: The silica (Si) concentrations for the intrusive rocks compared to the meta-sedimentary rocks.

The hydrogeological controls on the concentrations of the dissolved cations will be discussed in subsequent chapters although probably related to dissolution and weathering processes involving rock salts, carbonate minerals as well as the weathering of thermodynamically unstable alumino-silicate minerals predominantly present within the intrusive granitic and gneissic rocks.

6.3.4: Trace Elements

The groundwater samples were analysed for a number of trace elements. The mean concentrations of strontium (Sr), for groundwater from both catchments, are compared. The mean concentrations of other selected trace elements are compared with reference to intrusive and meta-sedimentary rocks. Lead was not sampled for at all sites and is thus omitted from this discussion.

A histogram (Figure 6.26) shows a highly skewed strontium (Sr) population towards higher Sr values for groundwater in catchment F30. Most Sr values, associated with groundwater of F30, are recorded over an interval up to a value of approximately 1.5 mg/l. A highly irregular distribution of Sr values is observed for groundwater of catchment F40. However, the mean value of Sr for groundwater of catchment F40 is far greater than a similar mean value for groundwater of catchment F30. The mean concentration of strontium in groundwater is relatively higher for the intrusive rocks compared to the meta-sedimentary rocks (Figure 6.27). This is expected since rocks of different composition and age differ in their $^{87}Sr/^{86}Sr$ ratios. Groundwater, through water-rock interaction, will in time acquire the Sr isotopic signature of the rocks.

A good linear correlation exists between increasing chloride concentrations and increasing Sr concentrations (Figure 6.28). The increasing Cl concentration is an excellent tracer of the increasing salinity of the groundwater. The Sr ion thus behaves in a similar manner when compared to the major cations. Caution must thus be exercised if strontium isotope ratios (i.e. $^{87}Sr/^{86}Sr$) are used to determine groundwater pathways through varying geological environments.



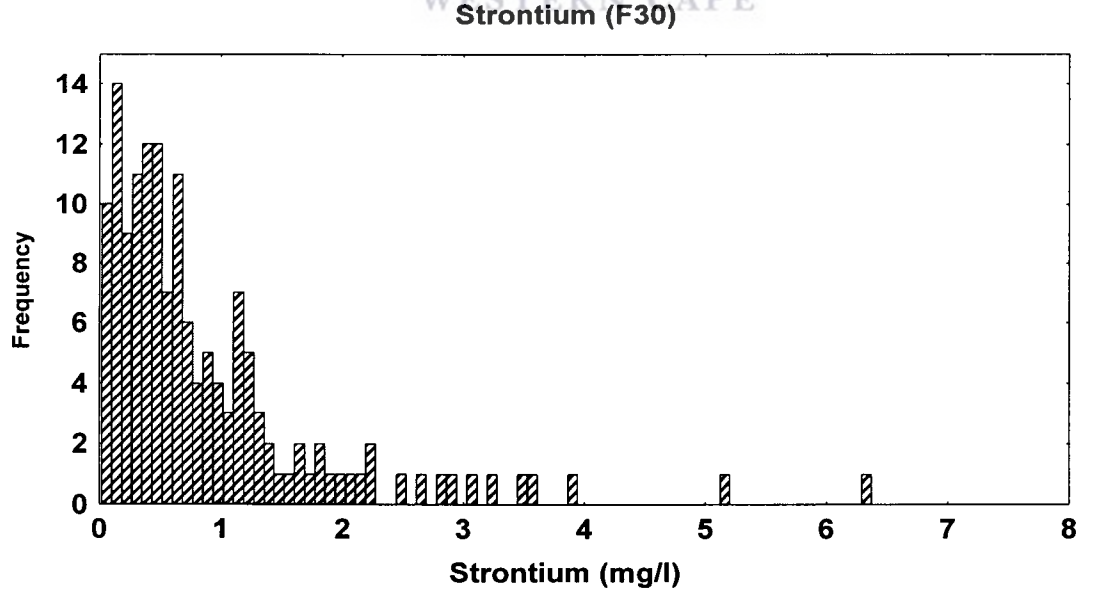


Figure 6-26: Strontium (Sr) population for groundwater in catchment F 30.

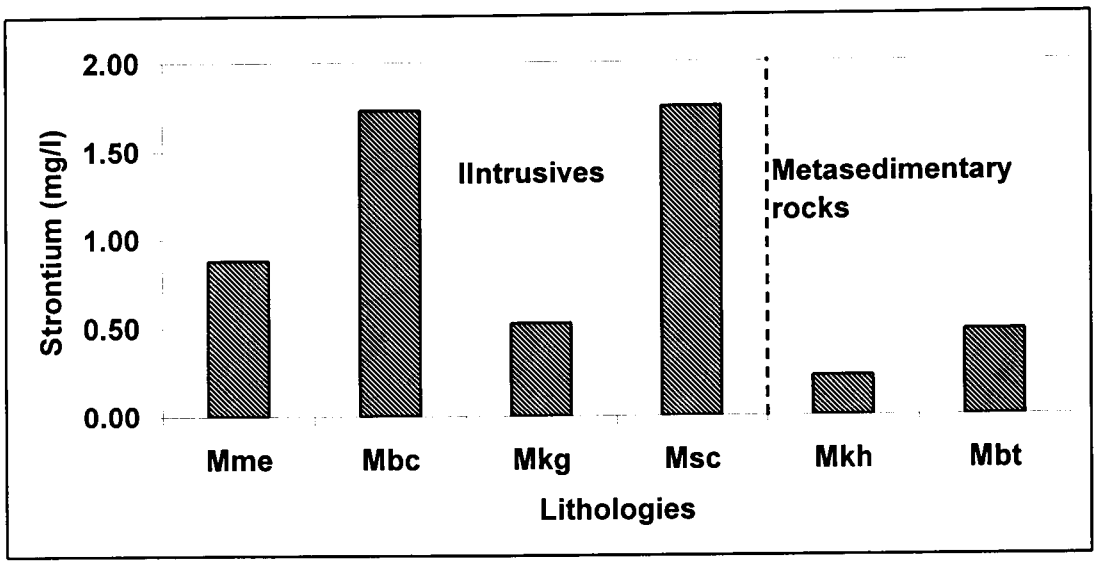


Figure 6-27: The mean strontium (Sr) concentrations for the intrusive rocks compared to the meta-sedimentary rocks.

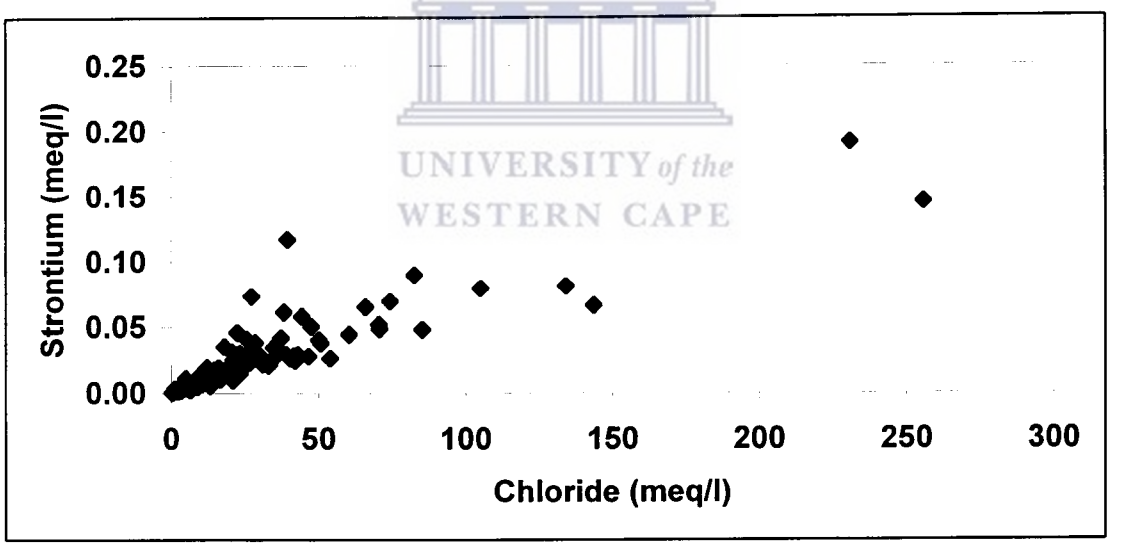




Figure 6-28: Bivariate plot for strontium and chloride.

An assumption is made in subsequent discussions that all aluminium (Al) is preserved within the in-situ weathering products (see Section 7.2.2). Indeed, analytical diagrams such as silicate stability (i.e. activity-activity) diagrams assume that all aluminum (Al) is preserved in the weathering product (Appelo, 1993). However, aluminium (Al) enriched residues may be transported as colloids due to its insoluble nature at normal pH levels of groundwater. Studies (Xu pers comm., 2000) have indicated that the concentrations of aluminium (Al) measured in an unfiltered sample (i.e. colloidal phase) can be

approximately two orders of magnitude higher than the aluminium (Al) concentrations measured in a similar filtered sampled. The low concentrations of dissolved aluminium (Al), within the neutral pH range for groundwaters, render accurate detection difficult. A plot of aluminium (Al) concentrations against pH for groundwater of catchments F30 confirms the low solubility of aluminium (Al) at common pH ranges and shows that no trend exists (Figure 6.29). Similar observations hold for the groundwater of F40.

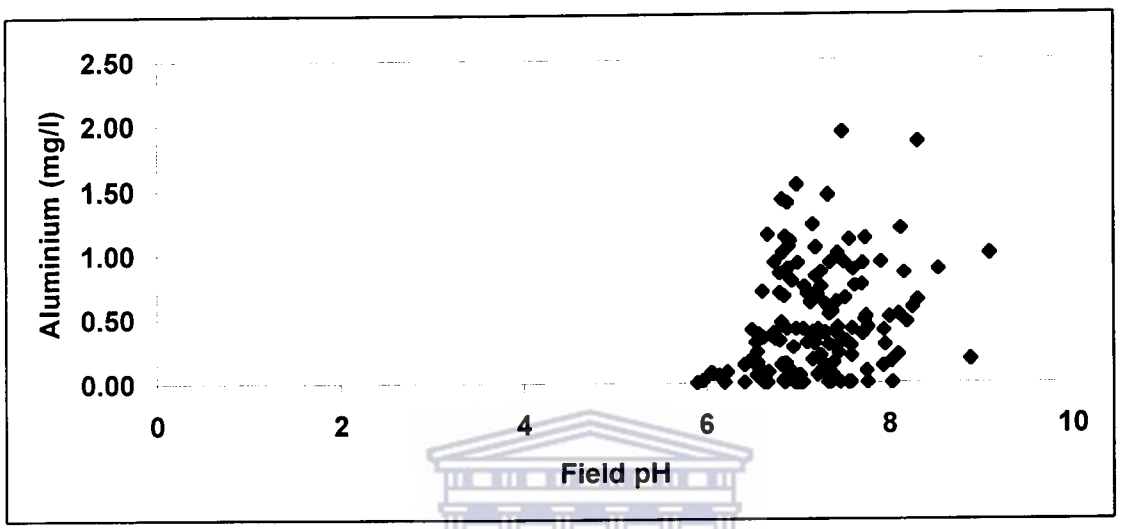


Figure 6-29: Aluminium concentration plotted against pH for groundwater of catchments F30.

The mean concentrations of aluminium (Al) and boron (B) for groundwater of catchment F40 are greater than similar mean values for groundwater of catchment F30. An opposite trend is observed for zinc. The mean concentrations of aluminium (Al), boron (B) and zinc (Zn) in groundwater are higher for the intrusive rocks compared to the meta-sedimentary rocks (Figure 6.30).

Most trace elements (i.e. barium, lithium, manganese, phosphate, arsenic and nickel) do not show broad trends when groundwater from intrusive rocks is compared to groundwater from predominantly meta-sedimentary rocks. Anomalously high mean concentrations for these trace elements were, however, recorded for individual lithological units, especially for the intrusive rocks. The mean concentrations of copper are relatively higher for groundwater from the intrusive rocks when compared to groundwater from meta-sedimentary rocks, while an opposite trend is observed for iron.

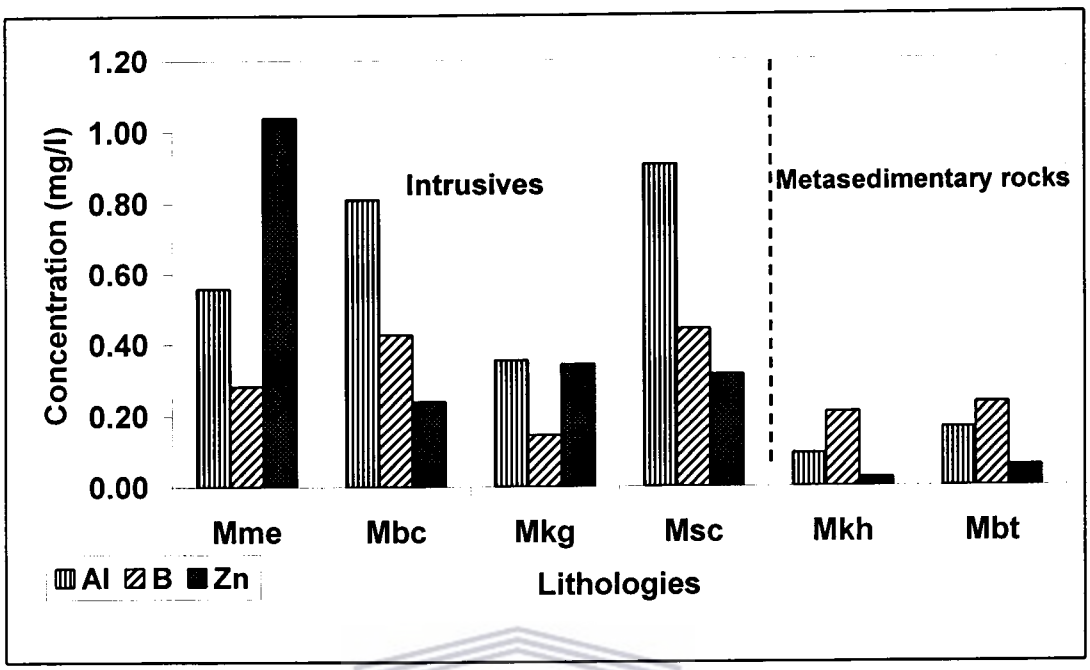


Figure 6-30: The mean concentrations of aluminium (Al), boron (B) and zinc (Zn) in groundwater for the intrusive rocks compared to the meta-sedimentary rocks.



6.3.5: Environmental Isotopes

Oxygen-18 and deuterium in groundwater give an indication of the processes occurring at, and prior to, the infiltration of rainwater. Oxygen-18 and deuterium are chemically conservative in the liquid phase below temperatures of 60 –80$^0$C (Issar and Gat, 1981). The stable isotopes $^2H/^1H$ and $^{18}O/^{16}O$, which are constituents of the water molecules, are regarded as perfect tracers unaffected by reactions such as exchange and absorption (Mook, 1994).

The isotopic variations (i.e. $O^{18}$ and $H^2$ concentrations) in precipitation are temperature dependant, becoming isotopically depleted with increasing latitude and altitude (Mook, 1994 and Dansgaard, 1964). Mook (1994) reported $O^{18}$ and $H^2$ variations with altitude of approximately –0.1 to –0.6%/100 m and –1%/100 m to –4%/100 m respectively. Annual variations in average $^{18}O$ values is small (1%) for temperate regions and to a large extent controlled by varying average annual temperatures (Mook, 1994). Larger variations are evident for semi-arid regions with a "less regular rain distribution in time" creating difficulties with respect to the interpretation of $^{18}O$ in groundwaters. The isotopic variations (i.e. $O^{18}$ and $H^2$ concentrations) in precipitation can also be due to varying $O^{18}$ and $H^2$ concentrations for summer and winter precipitation (i.e. seasonal effect), depleting $O^{18}$ concentrations in precipitation with distance from the oceans (i.e. continental effect) depending on the direction of movement of the air masses, and due to

isotopic depletion associated with high intensity rainfall events (i.e. amount effect) through the rainout of heavy isotopes (Mook, 1994 and Dansgaard, 1964). Graig (1961) developed a globally relevant relation, $^{2}H = 8^{18}O + d$, for precipitation that has not been subjected to significant evaporation. The deuterium excess (d) has a value of 10 (Graig, 1961) but can vary locally due to local atmospheric humidity conditions (Mook, 1994 and Merlivat and Jouzel, 1979).

The $^{18}O$ content of groundwater in moderate climatic regions tends to reflect the $^{18}O$ content of the average annual rainfall (Mook, 1994). More specifically, the $^{18}O$ content of groundwater approximates the $^{18}O$ content of precipitation during periods of significant infiltration. The correlation between the $^{18}O$ content of groundwater and that of precipitation for semi-arid regions is more complex, with large variations in the $^{18}O$ content of precipitation compared to small variations in the $^{18}O$ content of groundwater (Mook, 1994). Light rain, in semi-arid regions, completely evaporates before infiltration while ground recharge only occurs during periods of high intensity rainfall events. The $\delta^{18}O$ and $\delta^{2}H$ relation can, according to Mook (1994), demonstrate whether a groundwater sample originated from direct infiltration of meteoric water, mixing with seawater or through evaporation prior to infiltration.

Evaporative processes affect the above-mentioned $O^{18}$ and $H^{2}$ relations in precipitation (Sami, 1992). The concentrations of $^{18}O$ and $H^{2}$ in groundwater depend on factors such as the conditions of condensation during precipitation, evaporation before infiltration, and recharge selectivity". If recharge is subjected to evaporation before infiltration the $O^{18}$ and $H^{2}$ values of the recharging waters will have a more positive isotopic signal and will deviate from the world meteoric water line (Mook, 1994). The deviation results from an enrichment in the stable isotopic values ($O^{18}$ and $H^{2}$ ratios) in the residual liquid due to isotopic fractionation between liquid and gaseous phases. The effects of evaporation (or the leaching of previously evaporated salts) can be recognized by a deviation, with slopes of 4 to 6, depending on the relative humidity and degree of evaporation, from the world meteoric water line (Kay, 1985 and Gieske, 1992). This deviation from the world meteoric water line can, however, be due to both evaporation from open surface water and exchange with the aquifer material (Domenico and Schwartz, 1990).

The stable isotope ratios of $O^{18}$ and $H^{2}$ were measured for a number of groundwater samples in Namaqualand (Figure 6.31). The isotopic ratios for groundwater of the higher lying regions (i.e. Leliefontein and Wildeperdehoek) plot fairly close to the World Meteoric Water Line (WMWL) indicating the dominance of direct rainfall recharge in these areas with little evaporation other than water-rock interaction (i.e. dissolution). However, the groundwater for the higher lying Leliefontein region has more depleted isotopic concentrations compared to the groundwater for the Wildeperdehoek region. Stable isotope ratios (the $O^{18}$ and $H^{2}$ concentrations) are temperature dependant becoming isotopically depleted with increasing altitude. Most of the 'other' data has been subjected to evaporative processes prior to infiltration (Figure 6.31). The 'other' data also includes large diameter wells, usually located in alluvium, with an evaporative signal related to the relative humidity within such a well. The mountainous regions of Leliefontein (i.e Kamiesberg mountain range) and Wildeperdehoek have been identified as regional

recharge zones, at different elevations, on the boundaries between the secondary drainage catchments F30 and F50 as well as F30 and F40 respectively (Figure 6.32). The environmental isotopes as well as the variation and trends in groundwater chemistry (see Chapters 8 and 9) have shown that the latter regions can be regarded as no-flow boundaries between the respective secondary drainage catchments limited to the depths of the groundwater sampled (i.e. approximately 80 m below surface). Intermediate to regional groundwater flow systems may exist with high salinity artesian springs as expressions of such intermediate flow systems that originate in the mountainous regions.

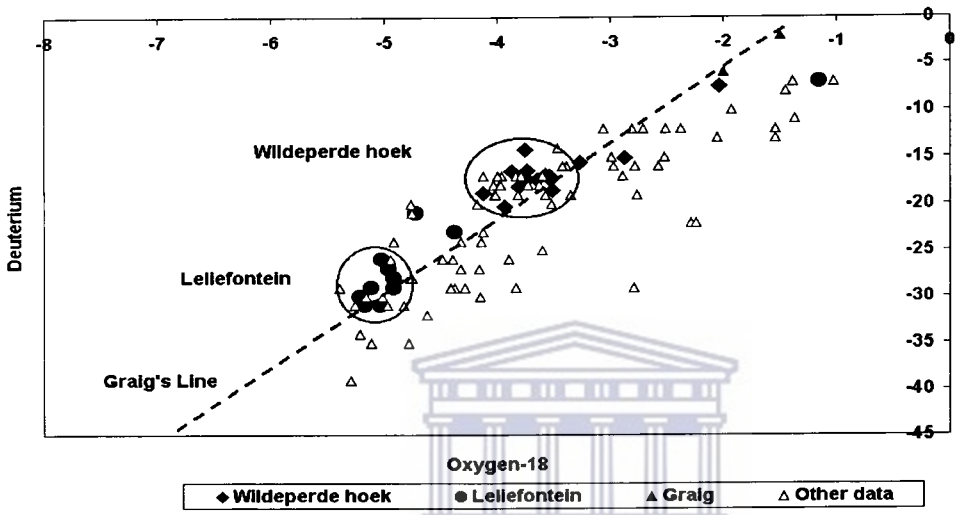


Figure 6-31: Stable isotopic composition of groundwater for the Leliefontein and Wildeperdehoek ranges as well as the lower lying regions in Namaqualand.

The stable isotopic data for Namaqualand indicates the following:

Salinisation of groundwater in the higher lying regions, where direct rainfall recharge dominates, results predominantly from the dissolution of aquifer material. Both direct rainfall recharge as well as an increasing altitude result in depleted environmental isotopic signatures. The positive correlations of EC with the environmental isotopes show that the higher salinity groundwater is generally characterized by enriched stable isotopic values. This relation may be due to the infiltration of previously evaporated surface waters and/or the solution and flushing of evaporative salts into the subsurface. With decreasing altitude, associated with lower rainfall, the periodic leaching and contribution of evaporated recharge water to groundwater salinity become more significant. These processes will result in enriched environmental isotopic signatures. Localised evaporation of groundwater discharge in large diameter wells may show a deviation, although with a lesser slope, from the Global Local Meteoric Water Line (GMWL). The slope of this deviation, that approximates an evaporation line, is influenced by the relative humidity in these large diameter wells.

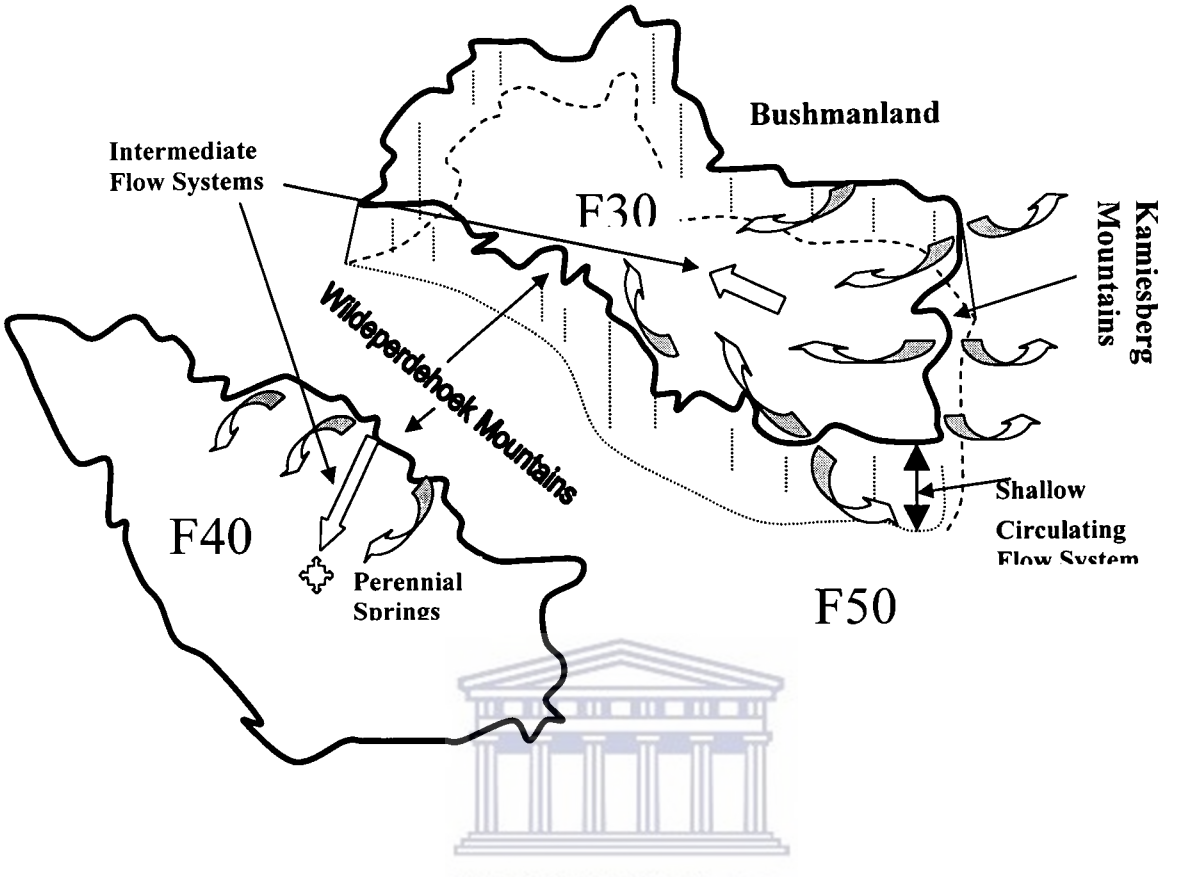




Figure 6-32: Regional recharge zones or no-flow boundaries (solid black lines) between the secondary drainage catchments F30, F40 and F50 for a near surface groundwater flow system.

# Chapter 7

# Soil characteristics and weathering processes

## 7.1: Introduction

This chapter focuses on the characteristic soil profile for the Escarpment zone (Namaqualand region) and on carbonate and silicate mineral weathering processes. Processes in the soil zone influence the character of the infiltrating water, while the products of incongruent weathering reactions are documented to occur within the soil zone. Section 7.1 provides, in the absence of detailed textural and mineralogical studies, an overview of the primary and secondary mineral phases present in the soil profile. The development of deep, kaolinised weathered mantles is associated with the warm and humid tropical climate of the Cretaceous period (see Section 5.2.2). In conclusion, a weathered profile for the Namaqualand region is presented at the end of this chapter.

The physical and chemical characteristics of the complex soil zone for the Namaqualand region influence the chemical character of the recharging waters.

Ellis (1988) distinguished two broad physiographic regions, located between the lower lying coastal zone in the west and the higher lying Bushmanland Plateau to the east. He described a mountainous physiographic region (i.e. the Escarpment zone) of predominantly high relief and a soil zone dominated by rock fragments. The Escarpment zone incorporates the secondary drainage catchment F30 that constitutes the study area.

Lithosols, comprising of imperfectly weathered rock or rock fragments (van der Walt and van Rooyen, 1990; Driessen and Dudal, 1991; and Soil Classification Working Group, 1991), with high lime content (as $CaCO_3$ and $Ca(OH)_2$) dominate (Ellis, 1988). Calcrete horizons (i.e. calcareous crusts), cemented by calcium carbonate and/or calcium-magnesium carbonates, occur generally within the region. As a result, the influence of carbonate mineral dissolution on the groundwater compositions is discussed in sections 7.2.1 and 8.2.7.

Soil horizons, comprising A-, B- and E-horizons (van der Walt and van Rooyen, 1990; Driessen and Dudal, 1991; and Soil Classification Working Group, 1991), are usually shallow but differ over short distances due to the complex geomorphology of the region and the spatial differences in rainfall intensity (Ellis, 1988). $A_{ca}$ as well as A, E and $B_2$ soil horisons were described for the schists and phyllites of the Gariep sub-group and granitic sequences respectively.

A-horisons are described as mineral horizons with a darker colour due to the accumulation of humified organic matter which is associated with the mineral fraction (van der Walt and van Rooyen, 1990; Driessen and Dudal, 1991; and Soil Classification Working Group, 1991). Ellis (1988) referred to orthic A-horisons, predominantly with

sandy textures. An orthic A-horison does not show an organic or humic character (van der Walt and van Rooyen, 1990; Driessen and Dudal, 1991; and Soil Classification Working Group, 1991) and these A-horisons are usually well drained topsoil horizons.

In the higher rainfall areas, lime is absent with E-horisons present (Ellis, 1988). An E-horison is a structureless mineral horison characterised by resistant minerals (eg. quartz) due to the removal of colloidal matter in the form of iron oxides, silicate clay and organic matter (van der Walt and van Rooyen, 1990; Driessen and Dudal, 1991; and Soil Classification Working Group, 1991). Redox reactions can also result in the removal of iron oxides and organic matter from this horizon.

Ellis (1988) furthermore described lithocutanic B2- mineral horizons. The lithocutanic B-subsoil horizons are described as heterogeneous zones comprising soil material (without traces of parent rock) interspersed with parent rock (or saprolite) in differing stages of weathering (van der Walt and van Rooyen, 1990; Driessen and Dudal, 1991; and Soil Classification Working Group, 1991). In addition, the B-horison is characterised by silicate clay, oxides of iron, aluminium and manganese, organic matter as well as lime (Acworth, 1987; van der Walt and van Rooyen, 1990; Driessen and Dudal, 1991; and Soil Classification Working Group, 1991). The silicate clay, oxides of iron, aluminium and manganese, organic matter as well as lime can concentrate in a specific horizon through the processes of illuviation (i.e. removal in solution or in suspension and subsequent deposition), residual accumulation (i.e. in-situ disintegration) and alteration (i.e. total obliteration of parent material). The products of the weathering processes involving aluminosilicate minerals are evident in the B2-horison.



### 7.2: Weathering Processes

This section focuses on the theoretical principles regarding carbonate and silicate weathering processes. Relevant data for the groundwater of Namaqualand is presented distinguishing between open and closed carbonate dissolution systems and silicate weathering processes. As a result, a weathered profile for Namaqualand is proposed.

The weathering process starts when water enters both the sub-horisontal and sub-vertical fractures that are often spatially extensive (Acworth, 1987). Chemical weathering is the dominant process in the development of a weathered mantle on crystalline rocks assisted by fracturing that exposes fresh surfaces to the effects of chemical weathering. Groundwater is the principal chemical reagent in the saturated zone and the rate of groundwater flow determines the reaction rate of the weathering processes (Acworth, 1987).

7.2.1: Carbonate Weathering

*7.2.1.1: Introduction*

Groundwater compositions are often influenced by carbonate reactions. Carbonate solution, associated with predominantly low permeability carbonate rocks, can also alter the flow systems through the development of solution channels and karst landscapes (Appelo and Postma, 1993). Carbonate minerals may also occur widely in various lithologies and soils as accessory minerals or as cementing agents and will, due to their relatively higher solubility, have a greater effect on the groundwater compositions compared to the weathering of unstable aluminosilicate minerals (Appelo and Postma, 1993). Groundwater is likely to be in contact with carbonate minerals for part of its flow path with the most important carbonate minerals being calcite ($CaCO_3$) and dolomite [$CaMg(CO_3)_2$] (Freeze and Cherry, 1979).

*7.2.1.2: Dissolution of $CO_2(g)$*

*$CO_2$ species in (ground-) water:* The solution of gaseous $CO_{2(g)}$ into rainwater produces aqueous $CO_2$ (Appelo and Postma, 1993). The sources of $CO_{2(aq)}$ are varied and include:

- atmospheric $CO_2$ with seasonal fluctuations;
- root respiration (i.e. aerobic respiration in upper soil) as a function of vegetation type and with seasonal fluctuations;
- aerobic and anaerobic (i.e. possibly deeper origin of $CO_2$ in saturated conditions) degradation of organic matter.

The groundwater usually becomes charged with $CO_2$ during infiltration through the soil zone.



Stumm and Morgan (1981) defined four equilibrium relationships ($K_w$, $K_H$, $K_1$ & $K_2$) as well as equations describing a concentration and an electroneutrality condition. The four equilibrium relations are described in table 7.1 (Appelo and Postma, 1993).

Table 7-1: Equilibrium constants for dissolved $CO_2$ species at 25°C (from Appelo and Postma, 1993 and after Langmuir, 1997).

| | | |
|---|---|---|
| $H_2O \leftrightarrow H^+ + OH^-$ | $K_w = [H^+][OH^-]$ | $K_w = 10^{-14.0}$ |
| $CO_{2(g)} + H_2O \leftrightarrow H_2CO^*_3$ | $K_H = [H_2CO^*_3]/P_{CO_2}$ | $K_H = 10^{-1.5}$ |
| $H_2CO_3^- \leftrightarrow H^+ + HCO_3^-$ | $K_1 = [H^+][HCO_3^-]/[H_2CO_3^*]$ | $K_1 = 10^{-6.3}$ |
| $HCO_3^- \leftrightarrow H^+ + CO_3^{2-}$ | $K_2 = [H^+][CO_3^{2-}]/[HCO_3^-]$ | $K_2 = 10^{-10.3}$ |

$CO_{2(g)}$ dissolves in water and forms aqueous $CO_{2(aq)}$ (Table 7.1). Aqueous $CO_{2(aq)}$ associates with $H_2O$ molecules to form carbonic acid ($H_2CO_3$) although $CO_{2(aq)}$, at $25^0C$, is exceedingly more abundant than $H_2CO_3$ (Appelo and Postma, 1993). Carbonic acid ($H_2CO_3^*$) dissociates in two steps to form bicarbonate ($HCO_3^-$) and carbonate ($CO_3^{2-}$), releasing a proton ($H^+$) in each step (Appelo and Postma, 1993). The total dissolved carbonate (or TIC) is the sum of the activities of the species carbonic acid ($H_2CO_3^*$), bicarbonate ($HCO_3^-$) and carbonate ($CO_3^{2-}$).

**Eq. 7.1**: $CO_{2(aq)} + H_2O \Rightarrow H_2CO_3^*$, where $H_2CO_3^* \Rightarrow CO_{2(aq)} + H_2CO_3$

When $CO_2$ dissolves in water, the dissolved carbonate species carbonic acid ($H_2CO_3^*$), bicarbonate ($HCO_3^-$) and carbonate ($CO_3^{2-}$) has to be considered in addition to $H^+$ and $OH^-$ (Appelo and Postma, 1993). The electrical neutrality condition (as a function of pH) for a 'pure' system is thus defined as:

**Eq. 7.2**: $m_{H+} = m_{HCO3-} + 2m_{CO32-} + m_{OH-}$

*Open system dissolution*: Open-system dissolution (Figure 7.1) processes occur where abundant $CO_2$ is present (Freeze and Cherry, 1979). The $CO_{2(g)}$ pressure in open carbonate systems is assumed to be firstly constant and secondly, unaffected by changes in the gaseous-aqueous $CO_2$ exchange rates or by the differential consumption or production of $CO_2$ by reactions in groundwater (Langmuir, 1997). In an open system, in which gaseous $CO_2$ is supplied at a constant partial pressure (i.e. $P_{CO2}$ is fixed), the activities of both $HCO_3$ and $CO_3^{2-}$ can be calculated as a function of $H_2CO_3^*$ and pH (Langmuir, 1997; Appelo and Postma, 1993). The activity of $H_2CO_3^*$, which is constant and independent of pH, can be calculated since the $P_{CO2}$ is fixed (Appelo and Postma, 1993). A continuous supply of gaseous $CO_2$ means that the total dissolved carbonate (or TIC) is not constant but changes, along with $HCO_3^-$ and $CO_3^{2-}$, as a function of $H_2CO_3^*$ (or $P_{CO2}$) and pH.

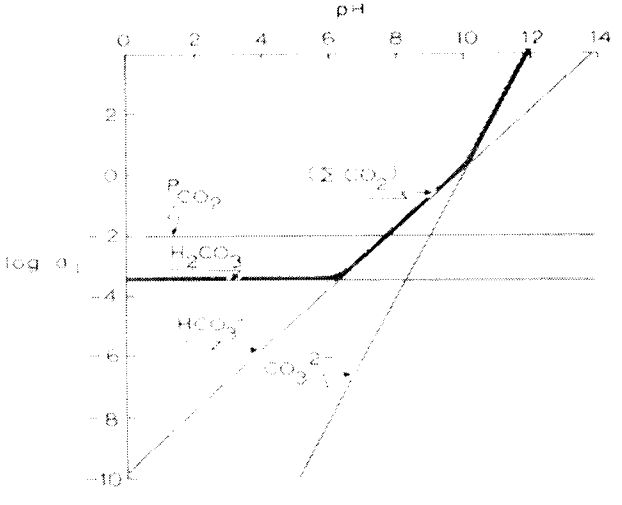


Figure 7-1: The activity of $CO_2$ species, as a function of pH, with a constant $CO_2$ pressure of 0.01 atm (from Appelo and Postma, 1993).

Equilibrium conditions are difficult to maintain for open system dissolution conditions. This is due to a continuous replacement of $CO_2$ (i.e. fixed $CO_2$ pressure and $[H_2CO_3^*]$) and resulting in a system in which mass is not conserved (i.e. $C_T$ is not constant). Such conditions may characterise dynamic groundwater flow systems associated with high hydraulic gradients in the mountainous regions of Namaqualand with relatively higher rainfall.

*Closed system dissolution*: Closed-system dissolution conditions occur, when the zones of $CO_2$ dissolution (or $H_2CO_3$ and $CO_{2(aq)}$ production) and carbonate dissolution is physically distinct (Appelo and Postma, 1993). Closed-system dissolution for carbonate minerals occurs predominantly in the saturated zone. As carbonate dissolution continuous, $H_2CO_3^*$ (or $CO_{2(aq)}$) is converted to $HCO_3^-$ and both the $H_2CO_3^*$ content and $P_{CO2}$ will decline (Freeze and Cherry, 1979). In a closed carbonate system, the $CO_2$ is consumed in carbonate mineral dissolution processes occurring either at greater depths within the soil zone or below the water table (Langmuir, 1997).

The relative distribution of the carbonate ($CO_2$) species, as a function of pH, can be calculated when the total dissolved carbonate (or TIC) is kept constant. This represents a closed system in which the TIC is independent of pH and the partial pressure of $CO_2$ ($P_{CO2}$) decreases above a pH of 6.3. Mass is conserved within a closed system and only the relative activities change as a function of pH. The dominance of a particular $CO_2$ species, as a function of pH, can be calculated based on the activity ratios (i.e. equilibrium reactions) among species and mass action constants (i.e. equilibrium constants). The relative distribution of the carbonate ($CO_2$) species for groundwater in Namaqualand, as a function of pH, represents close-system dissolution (Figure 7.2).



Equilibrium conditions are real for closed system dissolution conditions. Such systems are closed to $CO_{2(g)}$ (i.e. $CO_2$ pressure and $[H_2CO_3^*]$ decrease with progressing carbonate dissolution) and mass is conserved with $C_T$ constant. These conditions (Figure 7.2) may be more representative of sluggish flow groundwater systems. Most boreholes in Namaqualand are located in major fault-controlled valleys with relatively lower hydraulic gradients assumed over the depth of water samples collected.

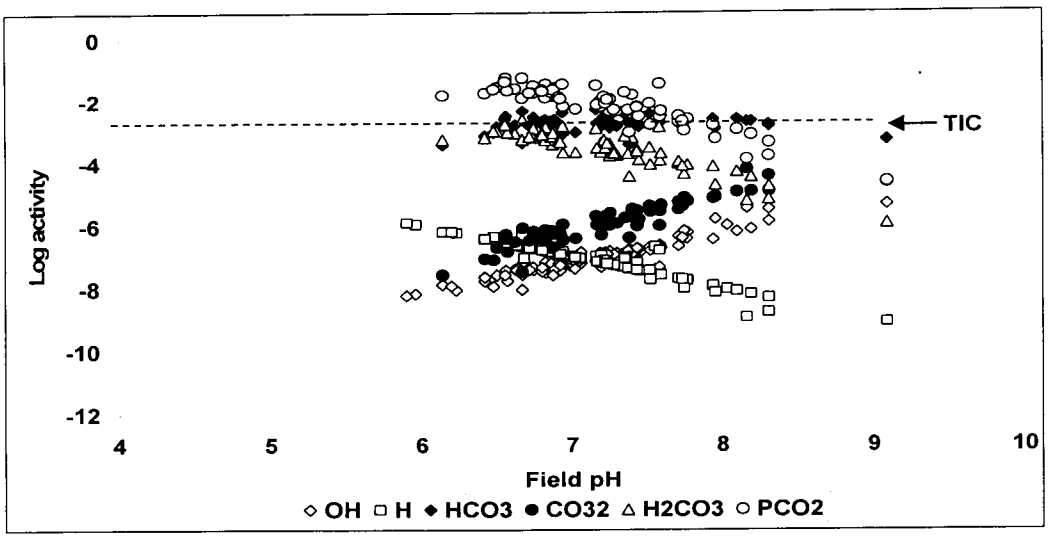


Figure 7-2: The dominant $CO_2$ species for the groundwater in Namaqualand (as a function of pH values that varies between 6 and 8.5) is $HCO_3^-$. The initial activity of $H_2CO_3$ is estimated at $10^{-3.0}$ mol/l at pH = 4. The estimated TIC activity is indicated. The temperatures for the groundwaters generally range below 25°C (after Appelo and Postma, 1993 and Langmuir, 1997).

*7.1.2.3: Dissolution of carbonate minerals*

*Open system dissolution of calcite*: Equilibrium reactions describing the solubility of carbonate minerals in water are commonly written in terms of $CO_2$ or $H^+$. When for example calcite dissolves in water, $Ca^{2+}$ is added to the solution. The equations (Langmuir, 1997, Appelo and Postma, 1993) describing the dissolution of calcite is given as:

**Eq. 7.3**: $CaCO_3$ (calcite) + $H_2CO_3^o = Ca^{2+} + 2HCO_3^-$,

and in terms of calcite and $CO_2$ (or $CO_2$ pressure) as:

**Eq. 7.4**: $CaCO_3$ (calcite) + $CO_2$ (g) + $H_2O = Ca^{2+} + 2HCO_3^-$ with $K = 10^{-5.8}$

or in terms of $H^+$:

**Eq. 7.5**: $CaCO_3$ (calcite) + $H^+ = Ca^{2+} + HCO_3^-$

The electroneutrality equation (that is pH dependant) for the above reactions (i.e. calcite dissolution) can be written as;

**Eq. 7.6**: $2m_{Ca2+} + m_{H+} = m_{HCO3-} + m_{OH-} + 2m_{CO32-}$

For pH < 10 (natural water) and that $m_{H+} << m_{Ca2+}$, than the electroneutrality equation (for calcite dissolution under open system conditions) reduces to:

**Eq. 7.7**: $2m_{Ca2+} = m_{HCO3-}$

The mass action equation (Eq. 7.8) for Eq. 7.4 shows a simple relationship between $Ca^{2+}$ concentration and $CO_2$ pressure for calcite dissolution.

**Eq. 7.8**: $([Ca^{2+}][HCO_3^-]^2)/CO_{2(g)} = 10^{-5.8}$

Table 7-2: The calculated $CO_2$ species and $Ca^{2+}$ in soil water in contact with $CO_2$ and calcite, in an open system with values in mol/l and atm (from Appelo and Postma, 1993).

| $P_{CO_2}$ | $10^{-1.5}$ | $10^{-3.5}$ |
|---|---|---|
| $Ca^{2+}$ | $10^{-2.6}$ | $10^{-3.3}$ |
| $CO_3^{2-}$ | $10^{-5.6}$ | $10^{-5.0}$ |
| $HCO_3^-$ | $10^{-2.3}$ | $10^{-3.0}$ |
| $H^+$ | $10^{-7.0}$ | $10^{-8.3}$ |
| $OH^-$ | $10^{-7.0}$ | $10^{-5.7}$ |
| $pH$ | 7.0 | 8.3 |

Where: $P_{CO_2} = 10^{-1.5}$ atm.: maximum $CO_2$ pressure in soil, and
$P_{CO_2} = 10^{-3.5}$ atm.: $CO_2$ pressure of present-day atmosphere.



The omission of $m_{H+}$, $m_{OH-}$ and $m_{CO32-}$ from the mass balance equation (Eq. 7.7) is justified due to their small concentrations compared to $m_{Ca2+}$ and $m_{HCO3-}$ (Table 7.2). Calcite dissolution thus has a major effect on the $Ca^{2+}$ and $HCO_3^-$ concentrations of water. Decalcification, according to Appelo and Postma (1994), results in the depletion of calcite from the upper levels in soils, sediments and rocks. As a result, the zone of $CO_2$ production is physically distinct from the zone of carbonate dissolution and the $Ca^{2+}$ concentrations in water must be calculated for a closed system.

*Closed system dissolution of calcite*: $CO_2$ is consumed when carbonate minerals dissolve in both open and closed system dissolution. However, in closed system dissolution the $CO_2$ pressure drops as the carbonate minerals dissolve. The zone of carbonate dissolution must be different from the zone of $CO_2$ production for a closed system (Langmuir, 1997; Appelo and Postma, 1993). When for example calcite dissolves in water, $Ca^{2+}$ is added to the solution. A mass balance equation for closed system dissolution of calcite is written as (Appelo and Postma, 1993):

**Eq. 7.9**: $3CO_2 = (3CO_2)_{root} + m_{Ca2+}$

Where $3CO_2$ is the sum of the total dissolved carbon dioxide species in upper soil [i.e. $(3CO_2)_{root} = m_{H2CO3*} + m_{HCO3-} + m_{CO32-}$] and the amount derives from calcite dissolution (i.e. $m_{Ca2+}$).

The electroneutrality equation (for calcite dissolution under closed system conditions), is pH and $CO_2$ pressure dependant, and constrained as (ignore $H_2CO_3$* if assume pH > 8):

**Eq. 7.10**: $m_{HCO3-} + 2m_{CO32-} = 2m_{Ca2+}$

The resultant mass balance equation for closed system dissolution of calcite is (Appelo and Postma, 1993):

**Eq. 7.11**: $m_{HCO3-} + m_{CO32-} = m_{Ca2+} + (3CO_2)_{root}$

The concentrations of $H^+$ and $OH^-$ are significantly smaller than the concentrations of $HCO_3^-$, $CO_3^{2-}$ and $Ca^{2+}$ and can be omitted from the mass balance equations. For lower $CO_2$ pressures the relationships between the dissolved species change (Table 7.3).

Table 7-3: The calculated $CO_2$ species and $Ca^{2+}$ in soilwater in contact with $CO_2$ and calcite, in a closed system with values in mol/l and atm (from Appelo and Postma, 1993).

| $P_{CO_{2(initial)}}$ | $10^{-1.5}$ | $10^{-3.5}$ |
|---|---|---|
| $HCO_3^-$ | $10^{-2.7}$ | $10^{-4.6}$ |
| $Ca^{2+}$ | $10^{-3.0}$ | $10^{-4.1}$ |
| $CO_3^{2-}$ | $10^{-5.3}$ | $10^{-4.2}$ |
| $H^+$ | $10^{-7.7}$ | $10^{-10.7}$ |
| $H_2CO_3$ | $10^{-4.1}$ | $10^{-9.0}$ |
| $OH^-$ | $10^{-6.3}$ | $10^{-3.3}$ |
| $pH$ | 7.7 | 10.7 |
| $P_{CO_{2(final)}}$ | $10^{-2.6}$ | $10^{-7.5}$ |



The equations indicate that carbonate (including calcite) dissolution prefers increasing $CO_2$ pressures and a decrease in pH (Tables 7.2 and 7.3), while calcite precipitation results from a loss of $CO_2$ and an increase in pH (Langmuir, 1997).

Closed-system dissolution of carbonate minerals results in lower concentrations of $C_T$, $Ca^{2+}$, $Mg^{2+}$ and carbonate alkalinity in sub-surface waters at saturation with calcite and dolomite, in contrast to results produced by similar variables in open system dissolution processes (Langmuir, 1997). $CO_2$ is consumed in the process of dissolving carbonate minerals in both open- and closed-system dissolution processes. When the $CO_2$ is not

replenished (i.e.under closed-system conditions) fewer carbonate minerals will dissolve than those estimated for constant $CO_2$ pressure in open-system dissolution processes (Appelo and Postma, 1993).

*7.2.1.4:Natural situations*

Protons ($H^+$), derived predominantly from $H_2CO_3^*$ (or determined by $P_{CO2}$), are important for the weathering and dissolution reactions of minerals (Appelo and Postma, 1993). A relatively constant partial pressure of carbon dioxide ($P_{CO2}$) in the soil zone, in equilibrium with the soil water, is assumed (Freeze and Cherry, 1979). Subsequent dissolution to saturation levels, with respect to the carbonate minerals, occurs. The dissolution of carbonate minerals results in an increase in pH and $HCO_3^-$ activities (Freeze and Cherry, 1979). The evolution paths for carbonate minerals, as a function of pH and $HCO_3^-$ activities, vary for both open- and closed-system conditions depending on the initial $P_{CO2}$ values (Langmuir, 1997; Appelo and Postma, 1993; Freeze and Cherry, 1979). Degassing (or off-gassing) results from a change (usually a reduction) in the $P_{CO2}$ with depth in the unsaturated soil zone (Appelo and Postma, 1993; Freeze and Cherry, 1979). Degassing causes a rise in the pH of the soil water. In addition, the soil water composition will become oversaturated with respect to carbonate minerals (Freeze and Cherry, 1979). The $P_{CO2}$ at greater depths in the unsaturated soil zone is influenced by the rate of gas diffusion to greater depths and the rate at which degassing occurs.

The equilibrium pH and $HCO_3^-$ values, or these values at saturation, differ for calcite and dolomite dissolution under open- and closed-system conditions (Langmuir, 1997; Appelo and Postma, 1993; Freeze and Cherry, 1979). A pH range for carbonate terrains of between 7 and 8 indicates that open-system conditions are prevalent (Freeze and Cherry, 1979). However, the relative distribution of the carbonate ($CO_2$) species for groundwater in Namaqualand, as a function of pH, clearly approximates closed-system dissolution (Figure 7.2). The effects of silicate weathering on the pH and $HCO_3$ content of the groundwater must be considered (see section 7.2.2). The chemical evolution of a water body may be influenced by a number (or combinations thereof) of factors, including the combination of open- and closed-system conditions between the points of recharge and discharge.

Calcite and dolomite often occur together and dissolve either sequentially or simultaneously resulting in incongruence relations (Langmuir, 1997; Appelo and Postma, 1993; Freeze and Cherry, 1979). Such relations are controlled by the differing dissolution rates for the two minerals, by temperature and by the $P_{CO2}$. The incongruence of the dolomite and calcite reactions influences the chemical evolution of the groundwater (Langmuir, 1997; Appelo and Postma, 1993; Freeze and Cherry, 1979). The $Ca^{2+}/Mg^{2+}$ molal ratio varies due to differences in the dissolution rates of the reacting carbonate minerals (Appelo and Postma, 1993; Freeze and Cherry. 1979). The $Ca^{2+}/Mg^{2+}$ molal ratio can vary considerably depending on sequential, simultaneous and/or incongruent dissolution processes, variations in $P_{CO2}$ and temperatures as well as cation exchange (Freeze and Cherry, 1979).

7.2.2: Silicate Weathering

*7.2.2.1: Introduction*

Silicate weathering reactions are acid consuming with a pH buffering effect as well as an influence on the ion chemistry (Domenico and Schwartz, 1990). Silicate weathering is thus an important buffer against the acidification of soil water and groundwater in the absence of carbonate minerals (Appelo and Postma, 1993).

Igneous and metamorphic crystalline rocks contain aluminosilicate minerals (eg. feldspars and micas) that are thermodynamically unstable due to their present position (to depths of hundreds or thousands of meters) within the Earth's crust (Acworth, 1987; Kay, 1985; and Freeze and Cherry, 1979). The weathering of the aluminosilicate minerals is due primarily to interaction with chemically aggressive waters (Kay, 1985; Freeze and Cherry, 1979). Chemically aggressive waters, characterized by low pH, can be formed by the dissolution of carbon dioxide ($CO_2$), which produces carbonic acid, or by free oxygen ($O_2$) in the unsaturated zone that acts as an oxidizing agent. The weathering capacity of the water in the unsaturated zone results from the interaction of $CO_2$- and $O_2$–rich waters with mineral phases (Kay, 1985). Goldich (1938) designed an empirical weathering sequence illustrating that olivine and Ca-plagioclase are the most easily weathered minerals, while quartz is the most resistant to weathering (Appelo and Postma, 1993).



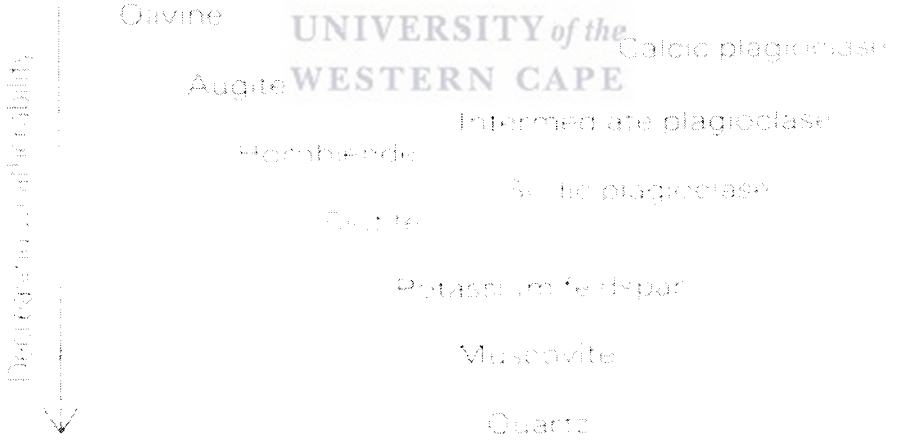


Figure 7-3: Empirical weathering sequence by Goldich (1938).

The interaction between dilute $CO_2$ enriched waters and aluminosilicate minerals results in the leaching of cations (e.g. $Na^+$, $K^+$, $Mg^{2+}$ and $Ca^{2+}$) and silica (Appelo and Postma, 1993; Acworth, 1987; Kay, 1985; and Freeze and Cherry, 1979). In addition residues, usually clay minerals (eg. kaolinite, illite and montmorillonite), with an increased Al/Si

ratio and Fe-oxides form as a result of the weathering of aluminosilicate minerals (Appelo and Postma, 1993; Kay, 1985; Freeze and Cherry, 1979). Due to the insolubility of Al-compounds, the clay minerals and Fe-oxides are insoluble residues which form during incongruent dissolution of silicate minerals (Appelo and Postma, 1993). Gibbsite can also be a weathering product of silicates. Iron present in silicate minerals may form Fe-oxides as an insoluble weathering product (Appelo and Postma, 1993). The alteration of aluminosilicate minerals (i.e. feldspars and micas) to kaolinite is a dominant process in groundwater flow systems in igneous rocks (Freeze and Cherry, 1979). The weathering reactions result in a rise in the pH and bicarbonate content of the waters (Appelo and Postma, 1993; Kay, 1985; Freeze and Cherry, 1979).

| | |
|---|---|
| Albite-kaolinite | $\underline{NaAlSi_3O_8} + H^+ + 9/2H_20 = \underline{1/2Al_2Si_2O_5(OH)_4} + Na^+ + 2Si(OH)_4$ |
| Albite-Na-montmorillonite | $NaAlSi_3O_8 + 6/7H^+ + 20/7H_2O = \underline{3/7Na_{0.33}Al_{2.33}Si_{3.67}O_{10}(OH)_2} + 6/7Na^+ + 10/7Si(OH)_4$ |
| Microcline-kaolinite | $\underline{KAlSi_3O_8} + H^+ + 9/2H_2O = \underline{1/2Al_2Si_2O_5(OH)_4} + K^+ + 2Si(OH)_4$ |
| Anorthite-kaolinite | $\underline{CaAl_2Si_2O_8} + 2H^+ + H2O = \underline{Al_2Si_2O_5(OH)_4} + Ca^{2+}$ |
| Andesine-kaolinite | $\underline{Na_{0.5}Ca_{0.5}Al_{1.5}Si_{2.5}O_8} + 3/2H^+ + 11/4H_2O = \underline{3/4Al_2Si_2O_5(OH)_4} + 1/2Na^+ + 1/2Ca^{2+} + Si(OH)_4$ |

**Reactions for the incongruent dissolution of selected aluminosilicate minerals (from Langmuir, 1997; Appelo and Postma, 1993; Freeze and Cherry, 1979). * Solid phases are underlined.**



In addition to the primary minerals (i.e. feldspars and micas), the weathering processes of the secondary clay minerals become more important as weathering proceeds (Kay, 1985). The weathering products that form on mineral surfaces as a result of incongruent dissolution processes have significant cation exchange capacities capable of changing the ion ratios in groundwater (Langmuir, 1997; Appelo and Postma, 1993; Freeze and Cherry, 1979).

| | |
|---|---|
| Na-montmorillonite - kaolinite | $\underline{Na_{0.33}Al_{2.33}Si_{3.67}O_{10}(OH)_2} + 1/3H^+ + 23/6H_2O = \underline{7/6Al_2Si_2O_5(OH)_4} + 1/3Na^+ + 4/3Si(OH)_4$ |
| Ca-montmorillonite- kaolinite | $\underline{Ca_{0.33}Al_{4.67}Si_{7.33}O_{20}(OH)_4} + 2/3H^+ + 23/2H_2O = \underline{7/3Al_2SiO_2O_5(OH)_4} + 1/3Ca^{2+} + 8/3Si(OH)_4$ |
| Illite – kaolinite | $\underline{K_{0.6}Mg_{0.25}Al_{2.30}Si_{3.5}O_{10}(OH)_2} + 11/10H^+ + 63/60H_2O = \underline{23/20Al_2Si_2O_5(OH)_4} + 3/5K^+ + 1/4Mg^{2+} + 6/5Si(OH)_4$ |
| Biotite - kaolinite | $\underline{KMg_3AlSi_3O_{10}(OH)_2} + 7H^+ + 1/2H_2O = \underline{1/2Al_2Si_2O_5(OH)_4} + K^+ + 3Mg^{2+} + 2Si(OH)_4$ |

**Reactions for the incongruent dissolution of selected aluminosilicate (i.e. secondary clay minerals) minerals (from Langmuir, 1997; Appelo and Postma, 1993; Freeze and Cherry, 1979). * Solid phases are underlined.**

*7.2.2.2: Solubility of silica*

According to Appelo and Postma (1993) as well as Freeze and Cherry (1979), an amorphous or noncrystalline form of $SiO_2$ controls the solubility of $SiO_2$ in water. A major percentage, according to Langmuir (1997), of the silica released on weathering of silicate and aluminosilicate minerals remain in solution as silicic acid ($H_4SiO_4^o$). Quartz dissolution and precipitation is extremely slow at low temperatures with equilibrium concentrations of dissolved silica [as $SiO_{2(aq)}$] equaling approximately 6 ppm in pure water systems at 25°C (Langmuir, 1997). Quartz is the most thermodynamically stable and least soluble form of $SiO_2$.The solubility of quartz is 6mg/l at 25°C, while the solubility of amorphous silica is 115 to 140 mg/l at 25°C (Appelo and Postma, 1993; Freeze and Cherry, 1979).

The dissolution of quartz below a pH of 7.8 is given as (Langmuir, 1997):

**Eq. 7.12**: $SiO_{2(quartz)} + H_2O = H_4SiO_4^o$

or:

**Eq. 7.13**: $SiO_{2(quartz)} = SiO_{2(aq)}$ with $[SiO_{2(aq)}] = [H_4SiO_4^o]$.

The least stable and most soluble form of $SiO_2$ is amorphous [$SiO_{2(am)}$] silica (Langmuir, 1997). The dissolution (i.e. equilibrium reaction) of $SiO_{2(am)}$ in water is given as:



**Eq. 7.14**: $SiO_{2(am)} + 2H_2O = H_4SiO_4^o$

or:

**Eq. 7.15**: $SiO_{2(am)} = SiO_{2(aq)}$ with $[SiO_{2(aq)}] = [H_4SiO_4^o]$.

Langmuir (1997) reported $SiO_{2(am)}$ (= $SiO_{2(aq)}$) solubilities of 117 ppm at 25°C and 363 ppm at 100°C. These concentrations of $SiO_{2(aq)}$ (=$SiO_{2(am)}$) are common in hot springs and in groundwater with temperatures exceeding 50°C. The solubility of $SiO_{2(aq)}$ (and $SiO_{2(am)}$) is thus strongly influenced by temperature.

Silica in soils occurs as both crystalline and amorphous or non-crystalline forms (Langmuir, 1997). Other crystalline polymorphs of $SiO_2$, eg. cristobalite and tridymite, both have solubilities greater than quartz but less than that of amorphous silica (Langmuir, 1997). Cristobalite and tridymite are the only crystalline non-quartz silica polymorphs found in significant amounts at low temperatures.

Silicic acid ($H_4SiO_4^o$), formed from the dissolution of $SiO_2$ (quartz), its polymorphs and $SiO_{2(am)}$, dissociates in two steps according to the following reactions at 25°C (Langmuir, 1997);

**Eq. 7.16**: $H_4SiO_4^o = H^+ + H_3SiO_4^-$ $\quad K_1 = 10^{-9.82}$,
**Eq. 7.17**: $H_3SiO_4^- = H^+ + H_2SiO_4^{2-}$ $\quad K_2 = 10^{-13.10}$

The $H_4SiO_4^o$ concentration exceeds that of the other anionic species (i.e. $H_3SiO_4^-$ and $H_2SiO_4^{2-}$) up to a pH value of approximately 9.82 (Langmuir, 1997). Furthermore, the dissolved anionic species (i.e. $H_3SiO_4^-$ and $H_2SiO_4^{2-}$) are < 1% of the total dissolved silica and can thus be ignored for pH values = or < 7.8. The solubilities of quartz, its polymorphs and amorphous silica are constant and pH-independent (Figure 7.4) for most natural waters (i.e. for pH values ranging between 6 and 9). However, the dissociation of silicic acid ($H_4SiO_4^o$) at pH values between 9 and 10 (i.e. alkaline pH ranges) results in accelerated increases in the solubility of quartz, its polymorphs and amorphous silica (Figure 7.4).

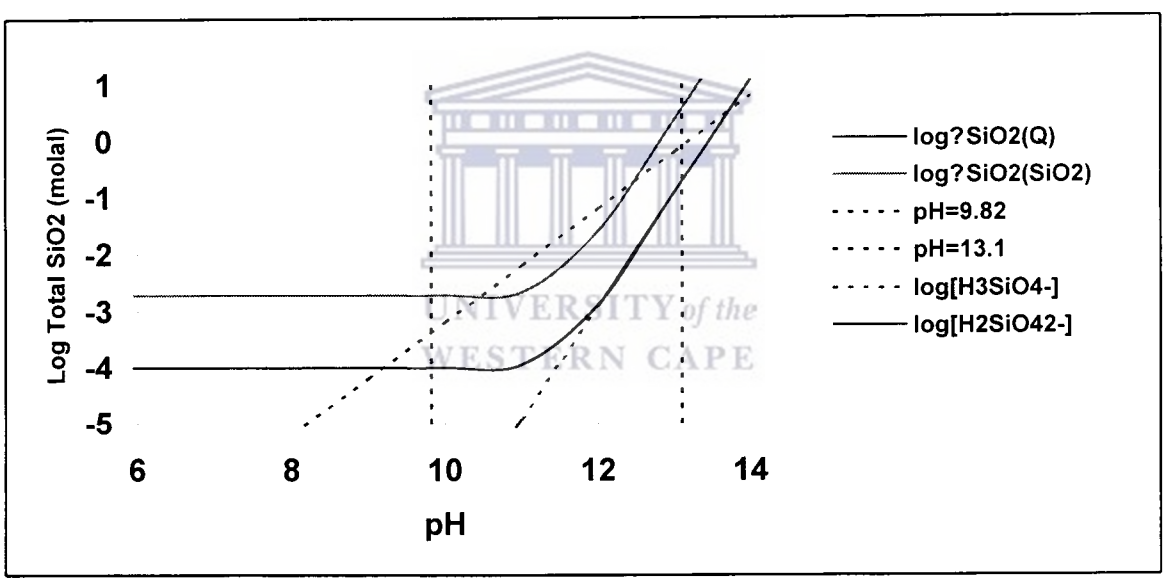


Figure 7-4: The solubility of quartz and amorphous silica as a function of pH (from Langmuir, 1997). The solubility lines for quartz and amorphous silica are shown as well as the fields of dominance of $H_4SiO_4^o$, $H_3SiO_4^-$ and $H_2SiO_4^{2-}$ as a function of pH.

The groundwater is generally oversaturated with regard to quartz and undersaturated with respect to amorphous silica (see Chapter 8.2.7). As a result, quartz and amorphous silica do not exert an important influence on the level of silica in groundwater (Appelo and Postma, 1993; Freeze and Cherry, 1979). The level of dissolved silica, as silicic acid ($H_4SiO_4^0$), in groundwater is controlled by the weathering of aluminosilicate minerals, with a high silica content indicating active degradation of silicate minerals (Figure 7.5).

Silica concentrations in groundwater are uniform (approximately 17 ppm) for most aquifer systems and are a function of the rock type (Langmuir, 1997). The highest silica concentrations are derived from high-temperature mafic minerals (eg. olivines and pyroxenes) as well as high-temperature plagioclase feldspars (eg. Ca-type feldspars). The lowest silica concentrations are found in rocks that mainly contain quartz and minor quantities of clays. In addition, clay mineral equilibria occur over years as low temperature mineral reactions within the shallow subsurface (Langmuir, 1997).

The comparison of the fresh rock and its weathered soil (Table 7.5) show the disappearances of plagioclase feldspars, biotite and hornblend (Langmuir, 1997). This comparison further shows the formation of kaolinite from the Al derived from the plagioclase and K-feldspars as well as from biotite. This process involved the addition of large amounts of water that is present as water of hydration in kaolinite clays (Langmuir, 1997). Furthermore, silica resulted mainly from the weathering of plagioclase feldspars, biotite and hornblend while quartz remained unaffected by weathering processes. The weathering process results in a weight loss of the affected rock through the release of cations and silica to the solution.

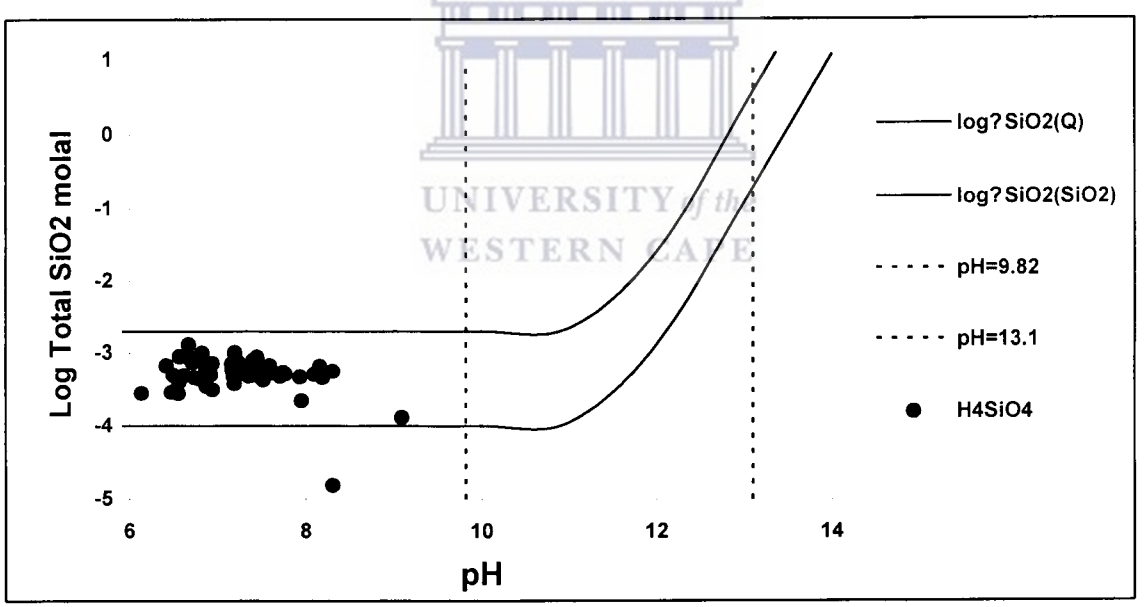


Figure 7-5: The silica activity, as silicic acid ($H_4SiO_4^0$), as a function of pH for groundwater in Namaqualand. The solubility lines for quartz and amorphous silica are shown as well as the fields of dominance of $H_4SiO_4^o$, $H_3SiO_4^-$ and $H_2SiO_4^{2-}$ as a function of pH.

Table 7-4: Log dissolution rates and theoretical mean lifetimes of a 1mm diameter cube of selected silicate and aluminosilicate minerals at pH = 5 and 25°C (from Langmuir, 1997).

| Mineral | -log rate ($mol/m^2/s$) | Lifetime (y) | Mineral | -log rate ($mol/m^2/s$) | Lifetime (y) |
|---|---|---|---|---|---|
| Wollastonite | 8.00 | $7.9\times10^{1}$ | Tremolite | 11.7 | $5.8\times10^{4}$ |
| Anorthite | 8.55 | $1.12\times10^{2}$ | Sanidine | 12.00 | $2.91\times10^{5}$ |
| Nepheline | 8.55 | $2.11\times10^{2}$ | Albite | 12.26 | $5.75\times10^{5}$ |
| Fosterite | 9.5 | $2.3\times10^{3}$ | Microcline | 12.50 | $9.21\times10^{5}$ |
| Diopside | 10.15 | $6.8\times10^{3}$ | Muscovite | 13.07 | $2.6\times10^{6}$ |
| Enstatite | 10.00 | $1.01\times10^{4}$ | Kaolinite | 13.28 | $6.0\times10^{6}$ |
| Biotite | 11.25 | $3.8\times10^{4}$ | Quartz | 13.39 | $2.4\times10^{7}$ |
| Gibbsite | 11.45 | $2.76\times10^{5}$ | | | |

Table 7-5: The composition of a granitic-type rock and of its weathering products (from Langmuir, 1997).

| Approximate Mineral Composition (Volume %) | Fresh rock | Weathered material |
|---|---|---|
| Quartz | 30 | 43 |
| K-feldspar | 19 | 13 |
| Plagioclase feldspar | 40 | 1 |
| Biotite (+ chlorite) | 7 | trace |
| Hornblende | 1 | none |
| Magnetite, ilmenite, other secondary oxides | 1.5 | 2 |
| Kaolinite | none | 40 |



*7.2.2.3:Saturation Indices (SI) and silicate stability phase diagrams*

The Saturation Indices (SI) was calculated with the NETPATH computer programme (Plummer et al., 1992) through a WATEQF subroutine. The saturation states of groundwater compositions, as a function of salinity (EC) for various mineral phases, are better illustrated with a log IAP/KT range of –10 to +10 (Appelo and Postma, 1993). These calculations indicate that the saturation states of the groundwater compositions in Namaqualand are controlled by the following mineral groups (see Section 8.2.7); framework silicates (i.e. feldspar and silicate minerals), sheet silicate minerals (i.e. micas and clay minerals including chlorite and talc) and the non-silicate minerals such as certain carbonate, sulphate and halide minerals as well as gibbsite (a hydroxide).

There are two drawbacks regarding silicate stability diagrams (see also Section 8.2.6). Firstly, the variation in the composition of plagioclase, clay and mica minerals results in uncertainties regarding the stability and dissolution (and precipitation) characteristics of these phases/minerals and, secondly, the slow reaction kinetics of silicate minerals (including clay minerals) result in uncertainties about whether true equilibrium is attained between the water composition and the mineral phase (Langmuir, 1997 and Appelo and Postma, 1993). The saturation state of a groundwater composition for a specific mineral phase is a function of the chemistry of the rock type and the leaching history that is related to rainfall intensity (Langmuir, 1997 and Appelo and Postma, 1993).

*7.2.2.4: Aluminium (Al) and clay minerals*

Silicate stability (i.e. activity-activity) phase diagrams assume that all aluminium is preserved in the weathering product (Langmuir, 1997 and Appelo and Postma, 1993). However, the aluminium (Al) enriched residues may be transported as colloids due to their insoluble nature (see Section 6.3.4).

Aluminum is considered to be insoluble, during weathering processes, at pH values ranging between 6 and 7 (Langmuir, 1997). In contrast, aluminum oxides and hydroxides are more soluble for both acidic (i.e. pH values < 5) and alkaline (i.e. pH values > 9) conditions. Solids such as aluminum oxyhydroxides (eg. gibbsite) and kaolinite dissolve to form cationic aluminum species at low pH (i.e. $Al^{3+}$, $AlOH^{2+}$ and $Al(OH)_2^{+}$) and anionic species at high pH (eg. $Al(OH)_4^{-}$). The total dissolved aluminum consists of both complexed and uncomplexed species;



**Eq. 7.18:** $\Sigma Al = m_{Al3+} + m_{AlOH2+} + m_{Al(OH)2+} + m_{Al(OH)4-}$

The cationic and anionic Al species, plotted for the groundwater of Namaqualand, define the solubility of total dissolved aluminum (Figure 7.6). The solubility of aluminum is at its lowest within the neutral pH ranges for groundwater (Figure 7.6). It seems likely that the dissolved aluminum is controlled by equilibrium with an amorphous $Al(OH)_3$ phase (or gibbsite) rather than kaolinite that is an order of magnitude less soluble than gibbsite. However, it is difficult to precisely determine which weathering product is in equilibrium with the groundwater since the stability of the Al-hydroxy complexes is highly variable (Appelo and Postma, 1993). However, the equilibrium reactions (i.e. precipitation and dissolution reactions) of the weathering products with the groundwater control the low aluminum concentrations within the neutral pH ranges of groundwater.

The alteration (i.e. weathering) of feldspars, clays and micas (i.e. aluminosilicate minerals) to kaolinite and Na-montmorillonite as weathering products seem to be an important process for the predominantly silicate rocks of Namaqualand (see Section 8.2.6). The presence of clay minerals thus influences the chemistry of natural waters (Langmuir, 1997), including the control on the dissolved aluminum concentrations. True equilibrium conditions may not be attained between the clay minerals and contacting water in low-temperature near surface environments. Secondly, clays exhibit relatively high cation exchange capacity due to their ability to adsorp cations.

Kaolinite is found in humid climates with well-leached acid soils characterized by low silica and cations concentrations (Langmuir, 1997). The more complex clay minerals of variable composition (i.e. smectites, vermiculate and illite) are abundant in arid climates with poorly leached soils. The soil moisture in arid climates is alkaline and usually contains high silica and cation concentrations. Kaolinite weathers to gibbsite in conditions characterized by high rainfall and good drainage. Kaolinite, however, is generally an order of magnitude (in terms of log Σ Al(aq)) less soluble than gibbsite.

Thermodynamic equilibrium (i.e. reversible equilibrium) between the contacting waters and the less complex clay minerals (i.e. kaolinite) in low temperature groundwater systems can be attained (Langmuir, 1997). However, complex aluminosilicates of variable composition (i.e. smectites and illites) may only attain metastable thermodynamic equilibrium with contacting waters in low temperature systems. Many mineral phases do not reach true thermodynamic equilibrium in near-surface environments.

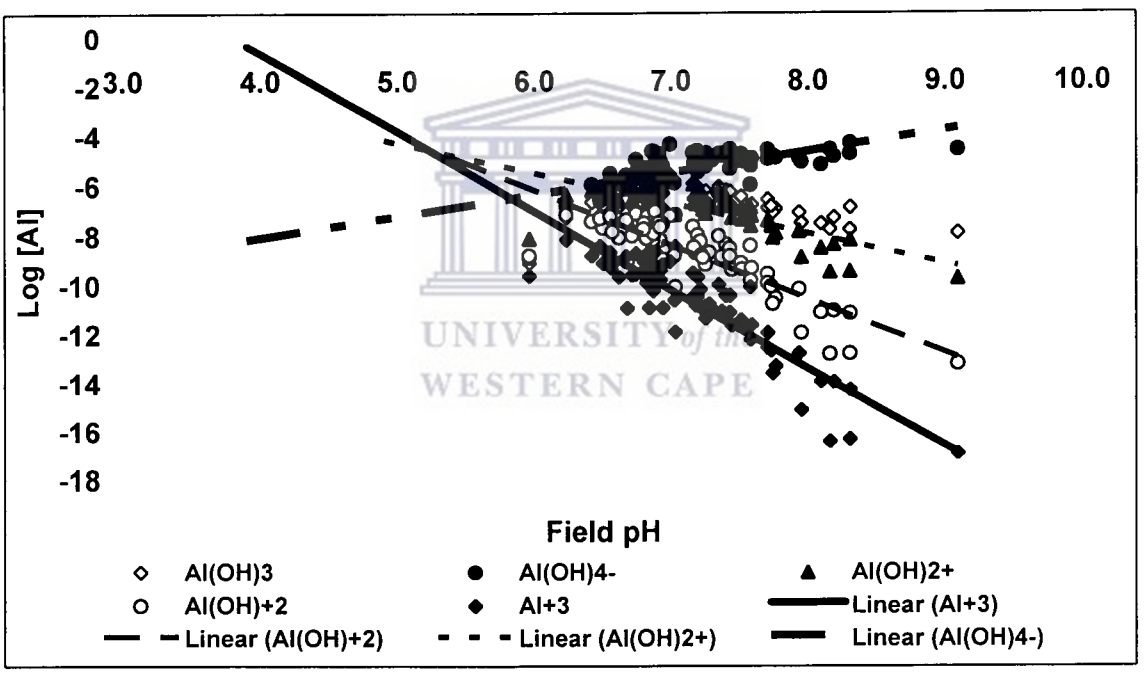


Figure 7-6: Log Σ Al(aq) and pH plot for the groundwater of Namaqualand. Log Σ Al(aq) represents the sum of the concentrations of all the Al-OH complex species as well as free $Al^{3+}$ (after Langmuir, 1997). The figure illustrates the solubility constraints on total dissolved aluminium due to weathering products such as amorphous $Al(OH)_3$ or kaolinite.

### 7.3: The weathered overburden

A general weathered profile (Figure 7.7) for crystalline basement rocks in Southern Africa is based on studies conducted by McFarlane (1987). Detailed studies have been conducted on the textural and mineralogical content as well as the hydrologic properties (the permeability and porosity) of the various zones within the weathered profile. Their studies concluded that the regolith is the main aquifer system and can attain a thickness of more than 80m. Furthermore, local groundwater flow systems dominate with the water level seldom exceeding the depth of 15m below surface. However, the basement aquifer for the Namaqualand region corresponds more favorably with the fresh rock to saprock transition zone.

An initial attempt to characterise the weathering profiles, based on data limited to the Komaggas reserve, was made for the crystalline aquifers in Namaqualand. Detailed studies on the textural and mineralogical content as well as the hydrologic properties of the weathered overburden in Namaqualand are required. The data represented is based on information gained from borehole logs (Figures 7-10, 7-11 and 7-12):

- The depth of weathering (to different scales) in the Komaggas Rural Reserve is present to depths of 54m to 60m below surface for both the metasediments of the Subgroup Khurisberg and for the granitic/gneissic rocks. In a few cases the depth of weathering, especially for the metasediments of the Subgroup Khurisberg, can extend to depths of 70m to 80m below surface or even deeper.
- Intense weathering of in-situ material can occur to depths of 40m to 49m below surface for both the metasediments of the Subgroup Khurisberg as well as for the granitic/gneissic rocks. In a few localities, associated with the metasediments of the Subgroup Khurisberg, intensely weathered, in-situ material can occur to depths greater than 80m below the surface.
- Degrees of weathering for different, as well as similar, rock types occur together with localised weathering on fracture systems, especially on the joint systems. Combinations of differential weathering of rock types together with localised weathering on fracture systems also occur. Fracture systems (eg. joint systems, fault zones and fracturing associated with vein quartz) seem to be conduits for preferred flow, especially for the granitic/gneissic rocks (Figures 7.8 and 7.9).
- A scree cover or talus, with approximate thicknesses varying between 1m to 16m, occurs in valleys. The talus comprises both clay and coarse-grained quartzitic material. The quartzitic material probably remained after leaching by groundwater.
- Where inter-layering of especially schist and quartzite layers or pseudo-layering based on degrees of weathering of the Subgroup Khurisberg occurs, groundwater is intersected over vertical zones in boreholes. Exceptions to the above do occur, where inter-layering between schist and quartzite layers, or pseudo-layering, generate single groundwater strikes. Single groundwater strikes are common in granitic/gneissic rocks. Furthermore, fractures (especially joints) with an iron-oxide coating on the fracture walls occur frequently in both the schist and quartzite. According to Toens *et. al.* (1995), groundwater strikes are usually

associated with small, isolated brecciated zones both in the schist and quartzites as well as with brecciated vein quartz.

- Secondary, semi- confined aquifer systems dominate.

Three profiles for boreholes targeting structurally controlled valleys are also presented (Figures 7.10, 7.11 and 7.12).

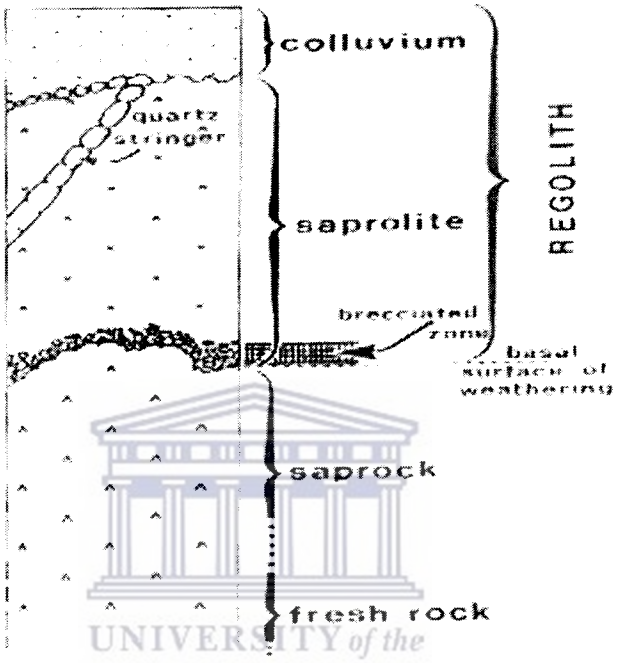




Figure 7-7: A generalised weathered profile for crystalline basement rocks, Southern Africa (McFarlane, 1987).

Figure 7-8: Weathered material, with weathering on the joint planes, over lying fresh core block of the Nababeep gneiss.

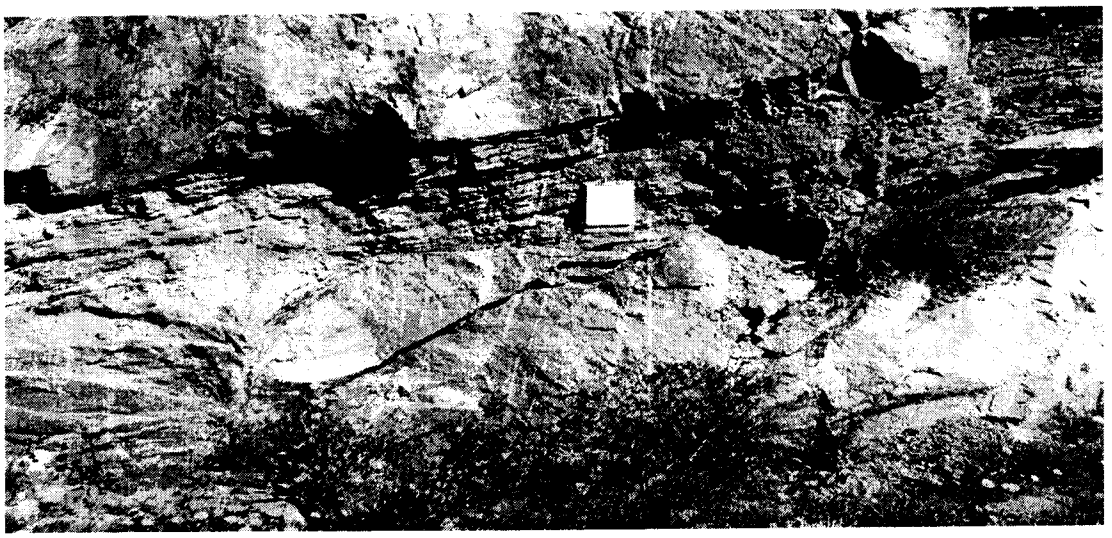

Figure 7-9: Degrees of weathering for different, as well as similar rocks types occur together with localised weathering on fracture systems. The photo depicts a thrust fault between the underlying and relatively fresh Mesklip granite (Little Namaqualand Suite) and the overlying Khurisberg metasediments.

| | | | | | |
|---|---|---|---|---|---|
| **BOREHOLE** | G37980 & G37964 | **LOCATION** | Talus bedekte Vallei<br>Komaggas Dorp | **Depth (m)** | 90 |
| **GEOLOGY** | Khurisberg Subgroep<br>Grope O=Kiep | **TARGETS** | Kwartsitiese gruise<br>Geroeste Nate en krake | **WL (m)** | 15.5 |
| **GROUNDWATER STRIKES (m)** | 10m to 16m | **Blow Yields (l/s)** | 10 | **EC (mS/m)** | 70 |
| | 29m to 57m | | 11.8 | | 70 |

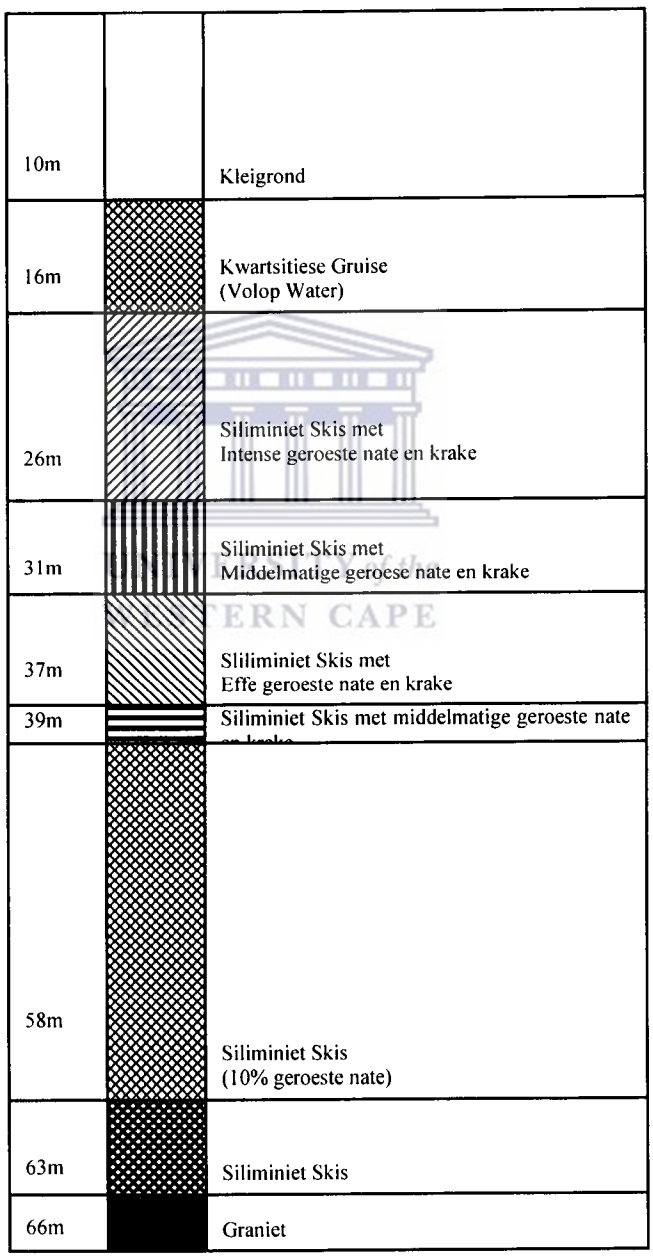


Figure 7-10: A profile for a borehole drilled in a valley close to the town of Komaggas (Geology: Rocks of the Subgroup Khurisberg).

| BOREHOLE | G37977 | LOCATION | Sesvlei Noord | Depth (m) | 102 |
|---|---|---|---|---|---|
| GEOLOGY | Khurisberg Subgroep | TARGETS | Little available information. Not within Komaggas river. Deeper waterlevel than G37975 and ∀15m from G379775 | WL (m) | 16.4 |
| GROUNDWATER STRIKES (m) | 40 | Blow Yields (l/s) | 0.02 | EC (mS/m) | |
| | 60 | | 0.12 | | |
| | 100 | | 0.48 | | |

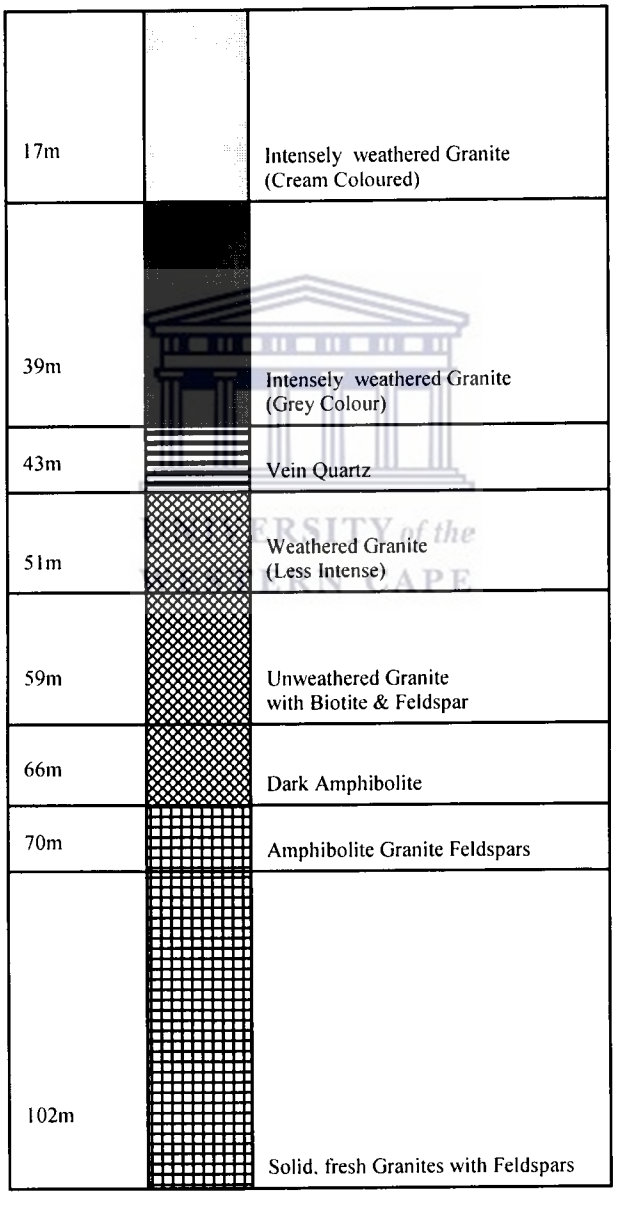


Figure 7-11: A profile for a borehole drilled in a valley close to the town of Komaggas (Geology: Rocks of the Subgroup Khurisberg).

| BOREHOLE | G37989 | LOCATION | Kamkambees | Depth (m) | 90 |
|---|---|---|---|---|---|
| GEOLOGY | Spektakel Suite | TARGETS | Major N-S fault zone comprising of intensely faulted zone filled with vein quartz that is the target at depth. | WL (m) | 15.5 |
| GROUNDWATER STRIKES (m) | 17 | Blow Yields (l/s) | 1.0 | EC (mS/m) | 230 |
| | 23 | | 0.1 | | 230 |

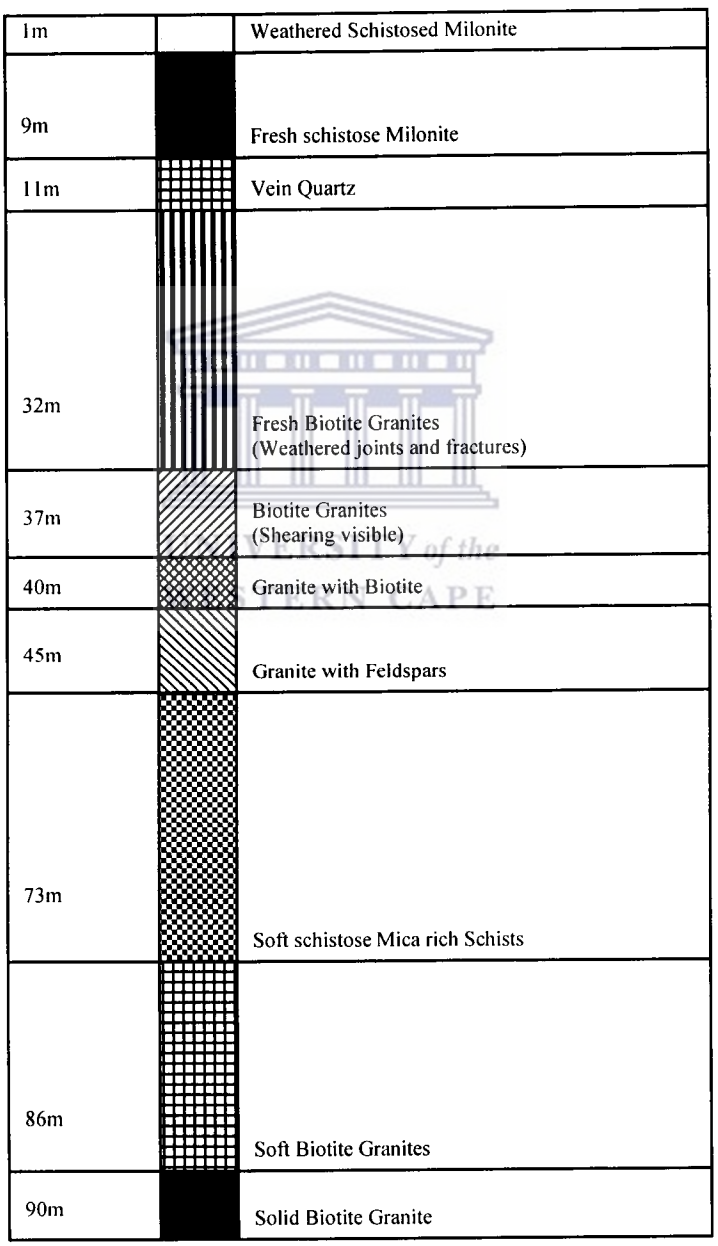


Figure 7-12: A profile for a borehole drilled on a N-S striking fault zone filled with vein quartz (Geology: Rocks of the Spektakel Suite).

# Chapter 8

# Assessment of the groundwater chemistry

## 8.1: Introduction

This chapter focuses on the processes that resulted in the dominant NaCl character of the groundwater. In addition, emphasis will be placed on a mineral-dissolution approach based on the reaction between primary minerals and $CO_2$-charged water to produce the measured dissolved constituents. As a result, the effects of both carbonate and silicate weathering processes (see also Chapter 7) are discussed to explain concurrent changes in the groundwater composition. An alternative approach (Freeze and Cherry, 1979), that is termed the mineral-reconstitution approach, involves the calculation of reaction sequences to account for the measured concentrations of the dissolved elements. In conclusion, local and intermediate flow systems are described for the near surface environment that is based on the hydro(-geo)chemical models presented. Chloride as a tracer and its effectiveness as a reference ion to explain changes in the groundwater composition with increasing salinity have been addressed in Chapter 6. The environmental isotopes were discussed in chapter 6.

Kay (1985) described a general variation of water type, in tropical crystalline basement and regolith aquifers, with increasing salinity at depth as: $Ca^{2+}/HCO_3^-$ to $Na^+/HCO_3^-$ or $Na^+/Cl^-/HCO_3^-$ to $Cl^-/Na^+/Ca^{2+}/SO_4^{2-}$. Alternatively, Johnston (1982) indicated that the groundwater chemistry in crystalline rocks is dependant on the position of the sampling point within an active or inactive (relatively stagnant) flow system rather than the rock type. Granitic rocks generally have well-developed fracture networks with active groundwater flow systems (Kay, 1985). Kay (1985) furthermore identified evaporation and transpiration, dissolution of evaporates, dissolution of host-rock, hyperfiltration, radiolysis and mixing as possible mechanisms to account for the origin of groundwater salinity in tropical and weathered basement aquifers.

## 8.2: Groundwater salinity in the Buffelsriver Catchment (Secondary Catchment F30)

Ninety-six groundwater samples were selected to represent the groundwater composition (in terms of mineral saturation indices calculations) for the Buffelsriver catchment. Sensitivity analyses, in terms of varying the relevant input parameters (i.e. field pH vs. laboratory pH, etc.), must be performed to test the robustness of the thermodynamically calculated mineral saturation indices for a specific groundwater composition. The groundwater chemistry data, upon which the conceptual models are based, was collected over the period 1997 to 1999. The boreholes were not optimally positioned, while the depth and construction of boreholes were generally unknown. Furthermore, the groundwater samples collected represent a mixed sample volume due to different inflows emanating from possibly numerous water strikes in a particular borehole.

In addition, information on the mineralogical make-up of the aquifer system as well as a reasonable understanding of the hydrogeochemical controls (including weathering processes) on the activities of the ions in solution is essential to constrain the interpretation based on mineral saturation indices. For example, pyrite minerals were frequently observed in rock samples, and the groundwater had a characteristic 'rotten egg' smell, in the vicinity of the town of Garies. The following minerals seem to have a major influence on the groundwater composition for this catchment (Table 8.1). The numerous lithological units (see Section 4.2.1) and associated variety of mineral phases within the study area prevented any further reduction or prioritization of the mineral phases that may influence the groundwater composition (see Section 8.2.4).

Table 8-1: The minerals that have a major influence on the groundwater composition for this catchment, as derived from mineral saturation indices calculated using the WATEQF chemical speciation model of Plummer *et al.*, (1992).

| SUPERGROUP | GROUP | MIINERALS |
|---|---|---|
| **Framework Silicates** | 1. Feldspar group<br>1.1 Plagioclase subgroup<br>1.2. Alkali subgroup<br><br>2. Silica group | <br>Albite to Anorthite<br>K-feldspar (i.e. Microcline)<br><br>Quartz & Chalcedony |
| **Sheet Silicates** | Mica group<br><br>Clay mineral group<br><br>Chlorite<br><br>Talc | Kmica (eg. Biotite, Muscovite, Phlogopite, etc.)<br><br>Kaolinite, Illite & Ca-montmorillonite |
| **Non-Silicates** | Carbonate minerals | Calcite, Aragonite, Rhodochrosite, Dolomite Strontianite & Witherite |
| | Sulphate minerals | Gypsum, Anhydrite, Barite & Celestine |
| | Halides | Fluorite |
| | Hydroxides | Gibbsite |

8.2.1: pH range and selected redox conditions

The pH range for most groundwater samples lies between 6 and 8 (Figure 8.1). This pH range indicates that open-system conditions, with regard to carbonate dissolution processes, may dominate (Freeze and Cherry, 1979). The dissolved inorganic carbon (DIC) is dominated by the $HCO_3^-$ species (see Chapter 6).

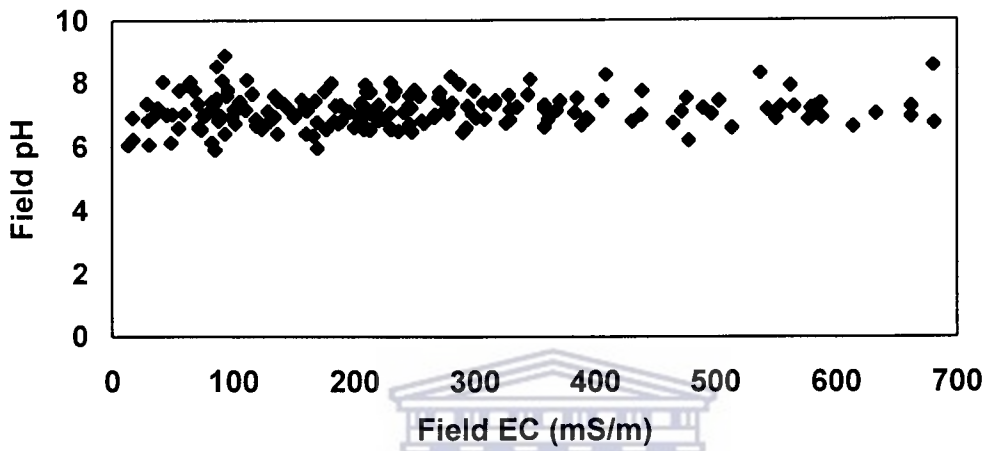


Figure 8-1: The pH values with increasing EC.

The redox state of an element determines the chemical and biological behaviour of the element as well as its mobility in a specific environment (Langmuir, 1997, Appelo and Postma, 1993 and Freeze and Cherry, 1979). Eh (or pE) – pH diagrams are used to describe the aqueous speciation and dominant mineralogy of redox sensitive elements. The various stability fields of Eh – pH diagrams depict the region of dominance of a particular species, although the species will be present in adjacent fields at much lower concentrations.

***Iron:*** Iron and manganese staining, as well as iron and manganese precipitates, are frequently observed on rock surfaces and within fractures (i.e. both joint and fracture zones) specifically on an outcrop scale.

The primary sources of iron are the aluminosilicate minerals (i.e. olivines, pyroxenes, amphiboles and biotite) in igneous and metamorphic rocks with pyrite ($Fe_2S$) and magnetite ($Fe_3O_4$) regarded as minor source minerals (Langmuir, 1997). The mobilisation and redistribution of iron, during chemical weathering processes, occurs predominantly as dissolved Fe(II) or ferrous iron under reducing conditions and as particulate Fe(III) oxyhydroxides or ferric iron in oxic environments. Under anoxic conditions, the iron is present as Fe(III) oxyhydroxides, siderite ($FeCO_3$) and as ferrous sulphides (i.e. pyrite). In general, $Fe^{2+}$ forms weak complexes [$FeOH^+$ and $Fe(OH)_2^0$] and occurs uncomplexed in most natural waters, while $Fe^{3+}$ complexes strongly with $OH^-$, $HPO_4^{2-}$ and $F^-$. Furthermore, most complexes of iron are mobile at lower pH values.

The mass balance equation for aqueous Fe(II) hydroxyl complexes is (Langmuir, 1997):

**Eq. 8.1:** $3Fe(II)_{aq} = Fe^{2+} + FeOH^{+} + Fe(OH)_2^{0} + Fe(OH)_3^{-}$

Where, $Fe^{2+}$ is the major dissolved species below a pH value of 9 while $Fe(OH)_3^{-}$ is the major species above a pH value of 10. The two species are equal at a pH value of 9.8.

The mass balance equation for aqueous Fe(III) hydroxyl complexes is (Langmuir, 1997):

**Eq. 8.2:** $3Fe(III)_{aq} = Fe^{3+} + FeOH^{2+} + FeOH_2^{+} + Fe(OH)_3^{0} + Fe(OH)_4^{-}$

Where, $Fe(OH)_3^{0}$ is the dominant aqueous species at pH values ranging between 7 and 9. Dissolved Fe(III) as $Fe^{3+}$ is thus absent between pH values of 5 to 10. However, Fe(III) oxyhydroxides occur in suspended form at a pH range of 5 to 10 in both surface and groundwater amounting to a major percentage of the total iron present.

The iron, for the groundwater of Namaqualand, is present predominantly as dissolved Fe(II), presumably indicating pervasive anaerobic conditions (Figure 8.2). Furthermore, the iron may complex with $HCO_3$ as the dominant carbonate species for the pH range of the groundwater. The Fe-$O_2$-$CO_2$-$H_2O$ system was selected since the presence of carbonate mineral phases may exert an important influence on the groundwater chemistry (see Section 7.1).



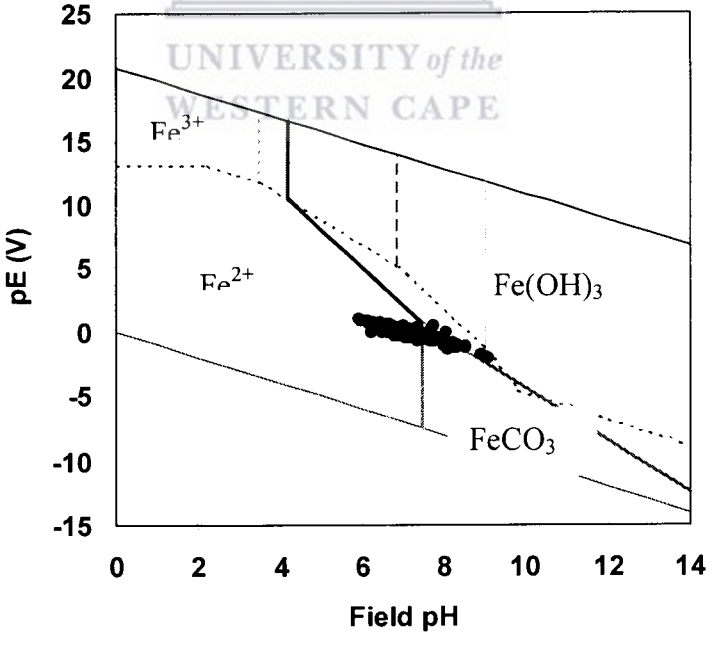


Figure 8-2: pE – pH diagram for the Fe-$O_2$-$CO_2$-$H_2O$ system at 25°C, assuming $pK_{sp}$ = 37.1 for amorphous $Fe(OH)_3$ (from Langmuir, 1997). $HCO_3$ is fixed at $10^{-2.7}$ mol/kg. Aqueous-solid boundaries and aqueous-aqueous species boundaries are shown. The field Eh (calculated as pE) and pH values for groundwater in Namaqualand are plotted for the above-mentioned system.

**Nitrogen:** A significant percentage of the water points in Namaqualand, especially the windmills and springs are used as stock watering points. The watering cribs/tanks are located in close vicinity to the windmills. In addition, spatial maps of $NO_x$ as N concentrations show an erratic point distribution rather than trends. This may indicate direct infiltration around the windmills enhanced by continuous spillages due to overflowing watering tanks and broken or insufficiently sealed pipes. However, the amount of water directly infiltrating around stock watering points is insignificant and does not influence the extremely low recharge rates calculated (Xu pers comm.., 2001) for the study area at tertiary and secondary catchment levels.

Nitrogen can exists, as a series of meta-stable nitrogen compounds, in a range of oxidation states with ammonia ($NH_3$) and nitrate ($NO_3^-$) representing the lowest and highest oxidation states respectively (Tredoux, 1993). Furthermore, nitrogen compounds are highly soluble and tend to remain in solution. Nitrate occurrence in the groundwater is probably related to anthropogenic activities such as the concentrations of livestock around watering points. Organic nitrogen in soils may also contribute to the natural accumulation of nitrate in groundwater.

The nitrogen, for the groundwater of Namaqualand, is present predominantly as dissolved $NH_4^+$, again indicating pervasive anaerobic conditions (Figure 8.3). Such conditions may exist close to the ground surface due to the layers of organic material around the windmills.



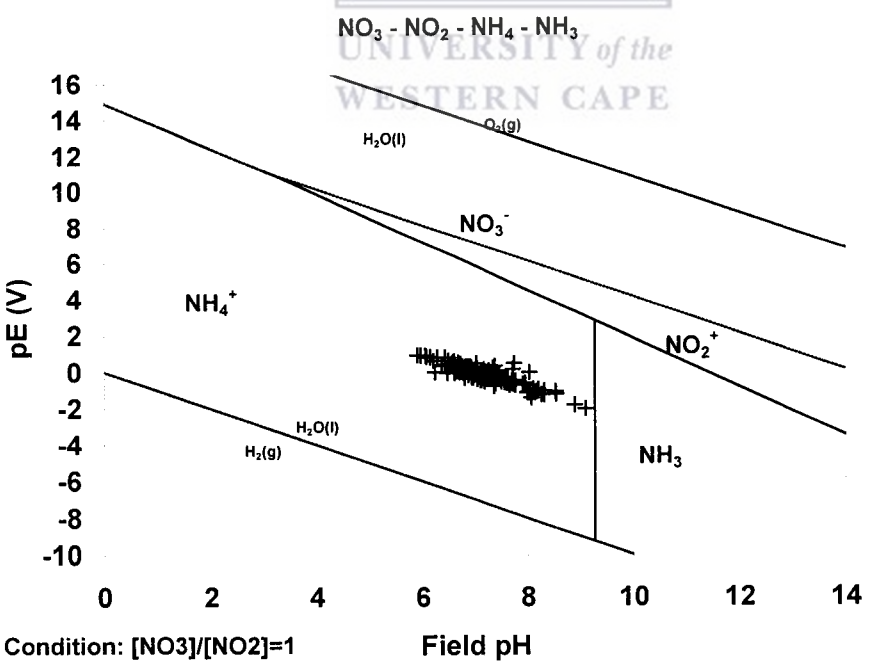


Figure 8-3: The field Eh (calculated as pE) and pH values for groundwater in Namaqualand are plotted for the above-mentioned system.

8.2.2: Dominant groundwater type

The electrical conductivity (EC) is a measure of the quality of water, which can be easily and relatively accurately measured in the field (see Sections 2.2.5 and 6.3.1). Groundwater with high EC values is generally associated with high Na and Cl values as well. The groundwater possesses a dominant Na-Cl character and has been described as slowly circulating relatively old groundwater. The limited groundwater samples with either a Ca-$HCO_3$ or Na-$HCO_3$ character may be attributed to carbonate dissolution in the soil zone coupled to selective and localised recharge processes and the associated refreshening process (see section 8.2.3). The few Na-$SO_4$ and Mg-$SO_4$ type waters are associated with mining and/or agricultural activities in the area.

The dominant NaCl character of the infiltrating waters is a result of either the direct infiltration of NaCl (or Na-K/Cl) dominated precipitation or the preferential dissolution and leaching of the more soluble evaporitic salts during the infiltration process (Table 8.3, Models 1 and 3). The water table fluctuations are assumed to be minimal for the Namaqualand region. Salt dissolution occurs as the water infiltrates through the weathered overburden. Alternatively, the direct evaporation of precipitation results in the dry deposition of salts. The dominant ions in precipitation are Na (or K) and Cl (Table 8.2). The refreshening process (Table 8.3, Model 2) is explained in section 8.2.3.

Table 8-2: Most of the precipitation in the area has NaCl or Na-K/Cl character.



| Site ID | pH | EC(mS/m) | $Ca^{2+}$ | $Mg^{2+}$ | $Na^{+}$ | $K^{+}$ | $NH_4^{+}$ | $HCO_3^{-}$ | $Cl^{-}$ | $SO_4^{2-}$ | $NO_3$-N |
|---|---|---|---|---|---|---|---|---|---|---|---|
| Spk 1 9h15 8-7-01 | 5.3 | 8.1 | 3.363 | 0.538 | 2.138 | 2.835 | 0.49 | 0.37 | 1.99 | 0.02 | 3.05 |
| Spk1 11h30 24-8-01 | 5.8 | 1.2 | 0.155 | 0.083 | 0.353 | 1.045 | 0.14 | 0.44 | 0.42 | 0.01 | 0.32 |
| Spk1 11h45 21-8-01 | 6 | 1 | 0.053 | 0.073 | 0.942 | 1.092 | 0.18 | 0.3 | 3.1 | 0.02 | 0.29 |
| Spk2 8h30 5-7-01 | 6 | 2.3 | 0.292 | 0.246 | 1.201 | 0.008 | 0.26 | 0.45 | 1.82 | 0.01 | 0.64 |
| Spk2 9h30 10-8-01 | 5.8 | 2.1 | 0.162 | 0.265 | 1.789 | 0.696 | 0.1 | 0.31 | 2.21 | 0.02 | 0.43 |
| Spk2 16H30 4-7-01 | 5.6 | 4.8 | 0.054 | 0.108 | 0.646 | 0.682 | 0.24 | 0.23 | 0.85 | 0.02 | 0.41 |
| Spk2 16H45 18-7-01 | 5.6 | 2.2 | 0.132 | 0.301 | 2.32 | 0.096 | 0.11 | 0.31 | 3.28 | 0.02 | 0.51 |
| Spk3 8H30 19-7-01 | 6 | 3.2 | 0.143 | 0.313 | 2.162 | 0.01 | 0.3 | 0.16 | 3.15 | 0.02 | 0.77 |

The initial Na/Cl character of the lower salinity groundwater in the mountainous regions is probably determined by the predominantly Na/Cl (or Na-K/Cl) character of the precipitation in areas where direct rainfall recharge is dominant (Table 8.3, see Model 1) and the preferential dissolution and leaching of highly soluble Na/Cl salts to the subsurface. Isotopic signatures confirm that direct rainfall recharge dominates in the higher lying, higher rainfall areas (see Section 6.3.5) such as the highest reaches of the Kamiesberg and Wildeperdehoek mountain ranges. The driving forces for the above-mentioned process are the dilute infiltrating waters and a reduced evaporation to rainfall ratio for the higher lying regions of Namaqualand.

The evaporation of surface water and soil moisture in the unsaturated zone results in the deposition of evaporitic salts. Above average, periodic precipitation results in the dissolution and predominantly vertical leaching of the evaporated salts to the saturated zone. Various authors attributed the NaCl character of groundwater to the preferential dissolution and leaching of the highly soluble evaporitic NaCl salts. The less soluble salts (i.e. calcite and gypsum) may only partially dissolve while any subsequent evaporation process may result in the re-precipitation of these salts. Such a process of re-precipitation will preferentially increase the concentrations of Na and Cl compared to the other major cations and anions.

The Na/Cl character of the higher salinity groundwater in the lower lying regions of Namaqualand, is predominantly related to the dissolution and periodic leaching of highly soluble salts, particularly Na/Cl salts, to the subsurface (Table 8.3, see Model 3). The isotopic signatures for these groundwaters indicate that the effects of evaporation, related either to the infiltration of evaporated surface waters or the leaching of previously evaporated salts, are dominant for the lower lying, lower rainfall areas (see Chapter 6). The driving forces for the above-mentioned process are thus the high evaporation to low rainfall ratio.

Laterally extensive, linear and structurally controlled valley system are the usual target for groundwater development within the Escarpment zone. The formation of the valleys is associated with the tectonic history and geomorphic development (i.e. bornhardt development) of the region (see Section 5.2.5). Deep and differential subsurface weathering (see Section 5.2.5) results in a highly irregular weathering front (or lower limit of significant weathering). The warm and humid tropical climate of the Cretaceous period resulted in the development of deep, koalinised weathering mantles, to depths of 50m or more, especially on crystalline rocks containing thermodynamically unstable alumino-silicate minerals (see Section 5.2.2.1). Late Cretaceous and early Paleocene pedocrete cappings (i.e. duricrusts) protected the African surface, and its deeply kaolinised saprolite, from erosion processes in many localities. Early Miocene crustal uplift and subsequent erosion, associated with limited incision of drainage channels of up to 100 m to 200 m below the African surface, resulted in the mid-Miocene Post-African I erosion surface (see Section 5.2.2.2). The Post-African I landscape development phase thus involved the removal of the deeply weathered mantles underlying the African surface (Partridge and Maud, 2000). In areas (i.e. western parts of southern Africa)

subjected to minimal Miocene uplift, scattered residuals or reduced thicknesses' of the weathered mantles remained. Visual inspection of the exposed weathered overburden (see Section 2.2.2) and a description of selected borehole logs (see Section 7.3) for the Namaqualand region showed a highly variable zone with mainly the saprock and top part of the bedrock remaining.

The aquifer system proposed (Figure 8.4) is a linear system associated with the structurally controlled valleys. The aquifer system may be laterally extensive depending on the nature of the fault systems. A microfissured model with predominantly fissure flow was adopted for the fractured, crystalline rocks of Namaqualand (see Section 2.2). Infiltration of water occurs along vertical to sub-vertical fractures with lateral flow along horizontal to sub-horizontal fracture systems (see Section 2.2.3). The water chemistry varies considerably among closely spaced fracture systems (see Section 2.2.5). The model displays a dominant vertical flow system (i.e. an infiltration phase) driven by local relief and an intermediate flow system driven by gradients along these laterally extensive valley systems.

The significant contribution attributed to the dissolution and leaching of evaporative salts to the salinity (i.e. EC) of the groundwater masks the effects of other processes, such as the carbonate and silicate weathering processes, the effects of cation exchange and oxidation-reduction reactions (see Sections 8.2.6 and 8.2.7). The dissolution and leaching of evaporative salts may also reduce the weathering capacity of the water (i.e. groundwater) with regard to other mineral phases such as carbonates and silicates due to the common ion effect.

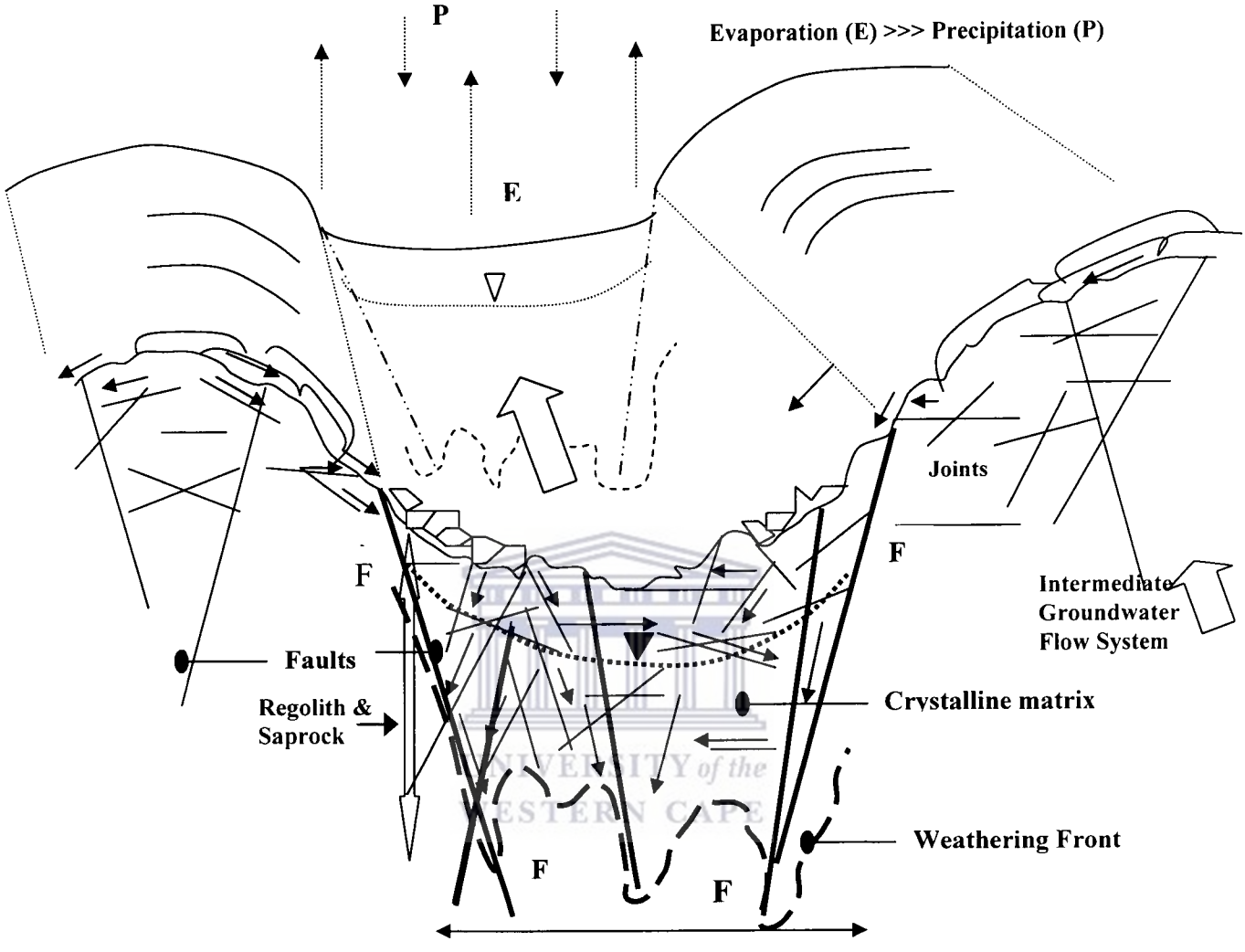


Figure 8-4: Proposed aquifer geometry and local to intermediate flow regimes for a typical structurally controlled valley within secondary drainage catchment F30.

Increasing chlorinity, in confined conditions, are also due to the conservative nature of the Cl ions in solution, the availability of chloride in the host rock and the associated rate of groundwater circulation as well as the possibility of hyperfiltration due to minute fracture apertures or fracture closure due to precipitates. The chloride content for intermediate to 'regional' groundwater flow systems, in confined conditions, can thus be attributed to a number of processes. The boreholes within the study area mostly target fracture systems in the mountainous and valley regions with prevailing semi-confined conditions.

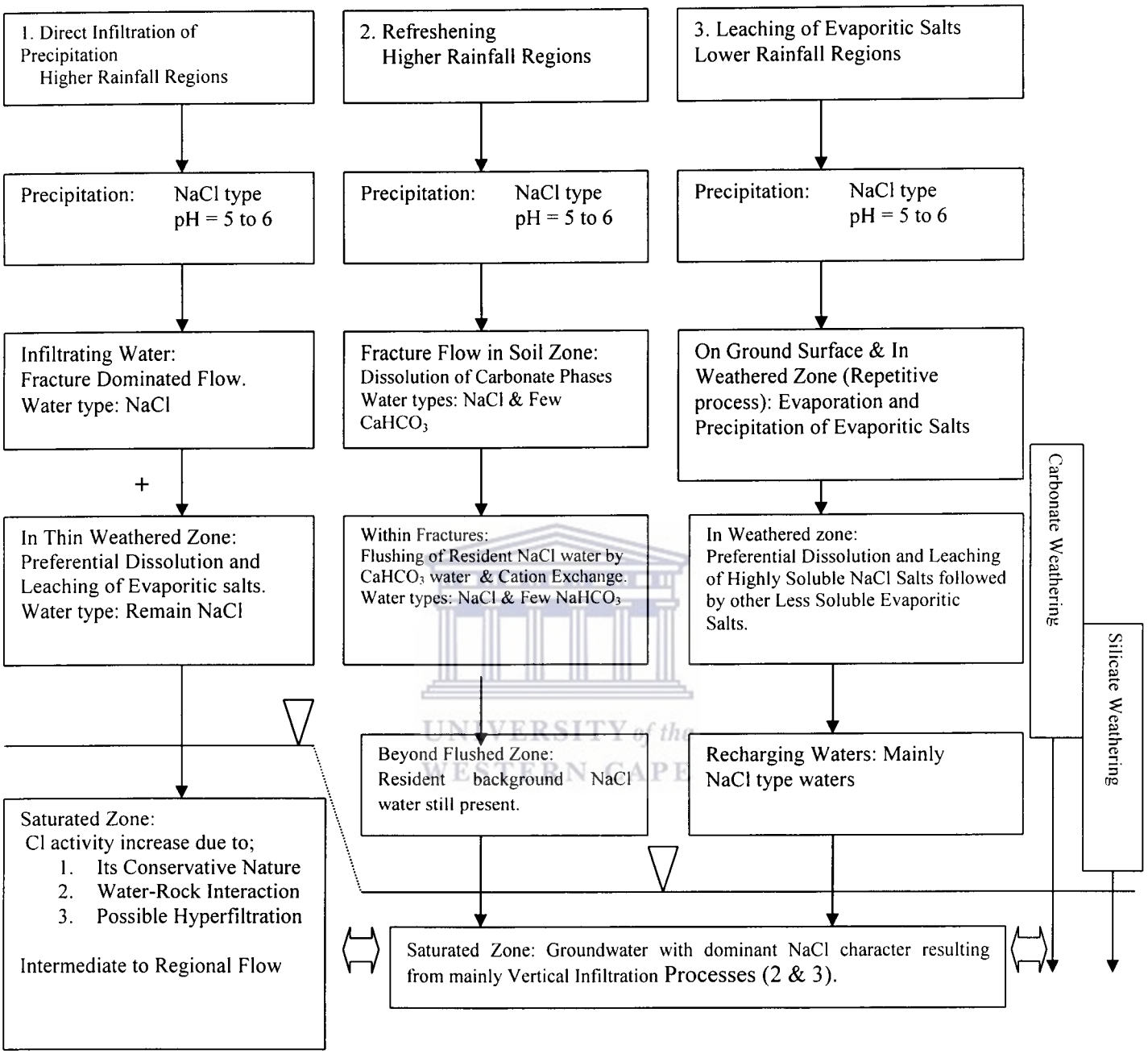


Table 8-3: Models to explain the NaCl and limited $NaHCO_3^-$ character of the infiltrating waters.

Vertical variations in the chemical composition of groundwater are evident through comparisons of perennial natural springs of both relatively fresh and highly mineralized waters. The depth of circulation of the highly mineralized springs seems to be limited due to the average surface temperatures of these waters. The distinctive characteristics for the spring systems seem to be residence time that influences the water-rock interaction

reactions and thus result in varying groundwater chemistry (Table 8.4). The highly mineralized springs may represent intermediate to 'regional' groundwater flow systems.

### 8.2.3: The refreshening process

The following equation (Jacks and Rajagopalan, 1996 and Appelo and Postma, 1993) describes the flushing of an aquifer system, dominated by NaCl type soil- and groundwater, with fresh water dominated by $Ca^{2+}$ and $HCO_3^-$ ions (i.e. refreshening):

**Eq. 8.3:** $½Ca^{2+} + Na\text{-}X = ½Ca\text{-}X_2 + Na^+$

Where, X = soil exchanger.

$Ca^{2+}$ is thus absorbed onto the substrate while $Na^+$ is released in solution. The water type changes from a $CaHCO_3$ type to a $NaHCO_3$ type water. The underlying assumption of such an approach is that a NaCl type soil and/or groundwater is present and dominant for the aquifer system.

$NaHCO_3$ type waters, due to the process of refreshening (Figure 8.5), is observed mainly in the higher lying, higher rainfall areas of Namaqualand. Similar $NaHCO_3$ type waters, in the lower lying regions of Namaqualand, is observed for relative young water intersected in highly conductive fracture zones. Such waters formed due to the initial dissolution processes, in response to slightly acidic rainfall (i.e. pH values of 5 to 6), of various carbonaceous phases in the soil zone. During the refreshening process, the infiltrating $CaHCO_3$ dominated water flushes an aquifer system characterised by NaCl type water. The effects of flushing the aquifer system and the subsequent cation exchange processes produce a flushed zone dominated by $NaHCO_3$ type water. The background NaCl water type will persist beyond the effects associated with the flushing of the aquifer system. Most water sampled for the Namaqualand region is, however, too far down an evolutionary path to reflect $NaHCO_3$ type water (Figure 8.6). The $NaHCO_3$ type waters, evident on the Kamiesberg mountain ranges, usually correspond to some of the highest values of the Na/Cl relation (Figure 8.7).

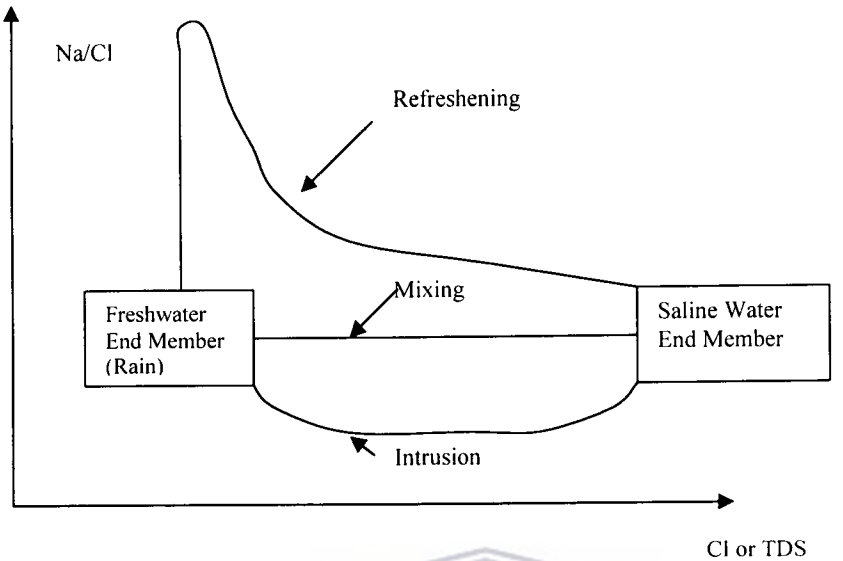


Figure 8-5: Mechanisms of salinization (after Jacks and Rajagopalan, 1996).

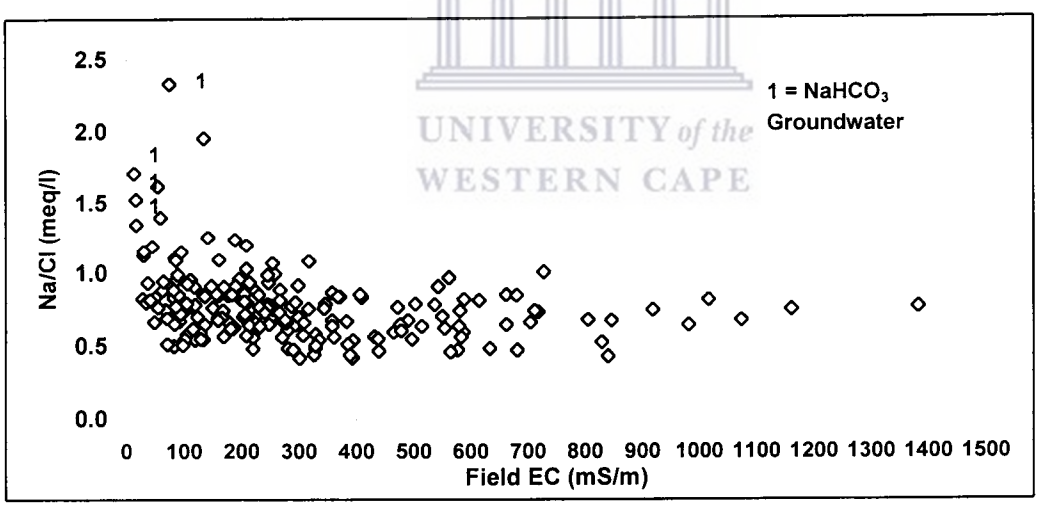


Figure 8-6: The Na/Cl – field EC relation for groundwater in Namaqualand. Some $NaHCO_3$ waters are indicated (1).

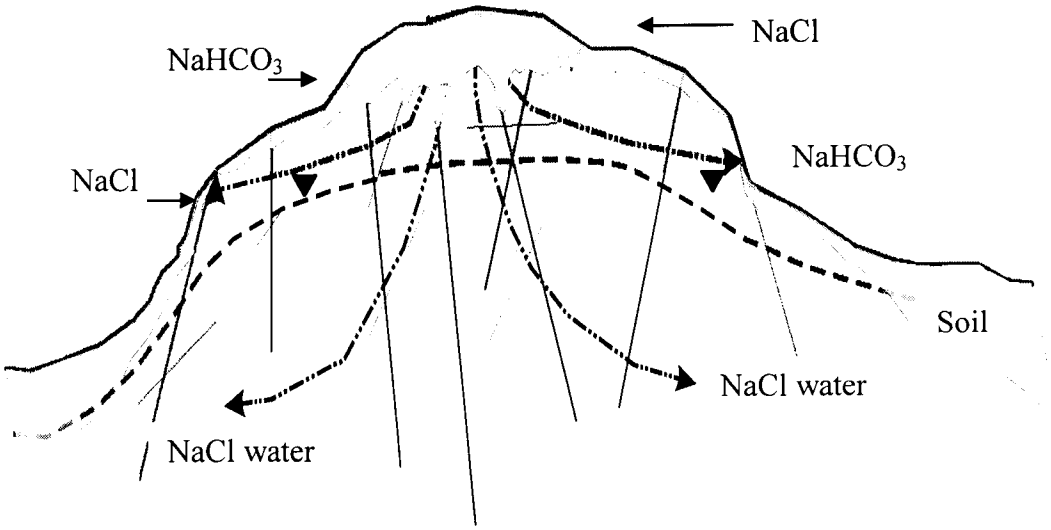


Figure 8-7: Conceptual model for flow and the process of refreshening for the Kamiesberg mountain region representing a dynamic, fracture-dominated flow system.

If the initial infiltrating water is predominantly a NaCl type water, then the process of refreshening is highly dependant on the solubility of and the processes influencing the solubility of carbonate mineral phases.

The infiltration of water is controlled by the prevailing fracture network that can vary in space and time. The process of refreshening is thus closely associated with this random infiltration process (Figure 8.7). Such observations relate to structurally controlled flow systems and varying water chemistry amongst closely spaced fracture systems. The process of refreshening occurs relatively more often in the higher lying regions due to above-average precipitation in these regions.

### 8.2.4: Ion activity trends and ratios

Various ion activity ratios are used to determine the origin of ions in solution. The dissolution of carbonate minerals (see Section 7.2.1) results in an increase in the pH and bicarbonate ($HCO_3^-$) concentrations while certain cations are leached to the groundwater (Langmuir, 1997; Appelo and Postma, 1993; Kay, 1985 and Freeze and Cherry, 1979). The weathering of aluminosilicate minerals (see Section 7.2.2) also results in the leaching of cations as well as silica with a simultaneous rise in the bicarbonate ($HCO_3^-$) concentrations and pH values. Redox reactions, in particular sulfate reduction, also produces $HCO_3^-$. An increase in the cation concentrations is generally associated with an increase in the dissolved bicarbonate concentrations, even to an extent where carbonate precipitation may result from the weathering of aluminosilicate minerals (Appelo and Postma, 1993).

The major cation ($Na^+$, $K^+$, $Mg^{2+}$ and $Ca^{2+}$) and anion ($Cl^-$, $HCO_3^-$ and $SO_4^{2-}$) concentrations increase with increasing salinity of the groundwater (Figure 8.8). The

$HCO_3^-$ concentrations increase with increasing EC for the lower salinity groundwater while remaining fairly constant for the higher salinity groundwater. Strontium (Sr) behaves in a manner similar to that of the major elements (Figure 8.9). A log scale accentuates the gradients of change in the data set for the lower salinity groundwater, while the gradients remain relatively constant for the higher salinity groundwater (Figures 8.8 and 8.9). The rates of increase (i.e. the gradients) of the dissolved ions are more significant for the lower salinity groundwater than for the higher salinity groundwater. The pH remains fairly constant with increasing salinity while no trend could be observed for the $SiO_2$ – EC relation. Values for dissolved $SiO_2$ range between 10 and 60 mg/l. The groundwater is thus generally subsaturated with regard to amorphous silica, since the weathering of aluminosilicate minerals controls the concentrations of dissolved silica in groundwater (see Section 7.2.2).

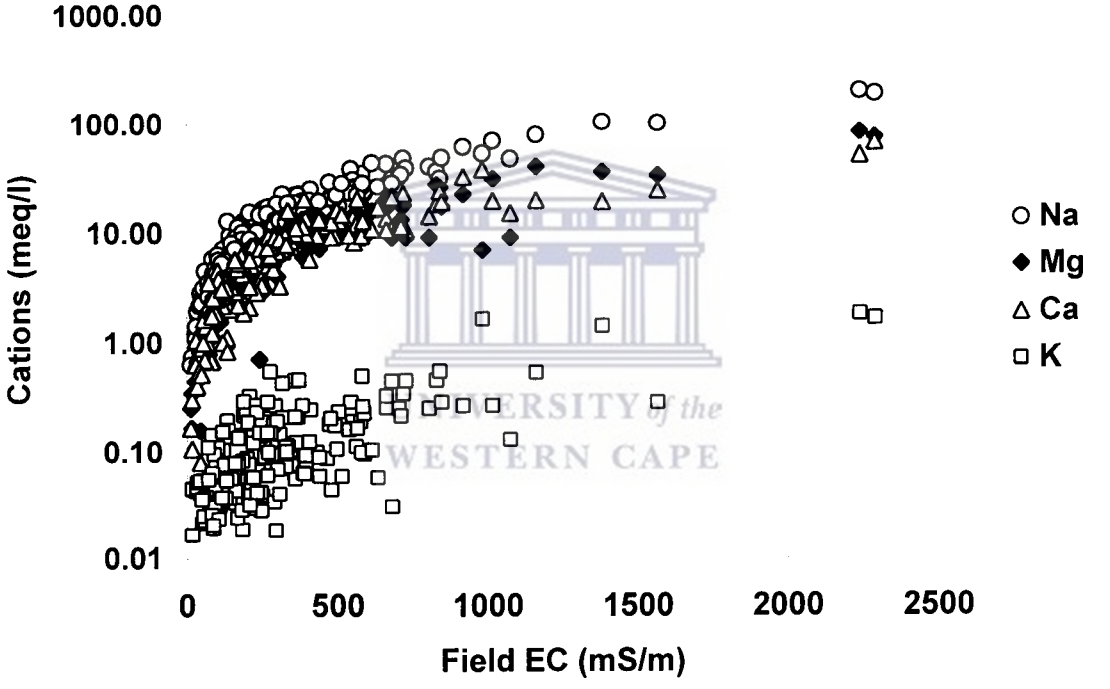


Figure 8-8: The major cation ($Na^+$, $K^+$, $Mg^{2+}$ and $Ca^{2+}$) concentrations increase with increasing salinity of the groundwater.

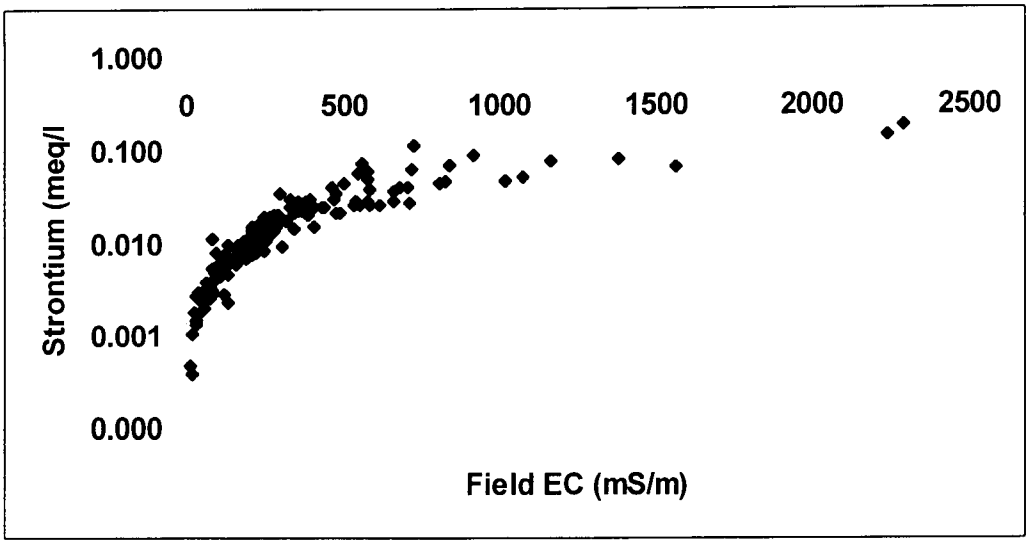


Figure 8-9: Strontium (Sr) concentrations increase with increasing salinity of the groundwater.

The activity ratios of [Na]/[H], [Ca]/[H] and [K]/[H] increase with increasing salinity, indicating active weathering of the aluminosilicate minerals (Figure 8.10). The rate of change for the latter ratios is also more pronounced for the lower salinity groundwater with EC values less than 150mS/m (Figure 8.10). The [Na]/[H], [Ca]/[H] and [K]/[H] relations remain fairly constant for the higher salinity groundwater. Kay (1985) suggested that the weathering of the secondary clay minerals become more important as weathering proceeds.

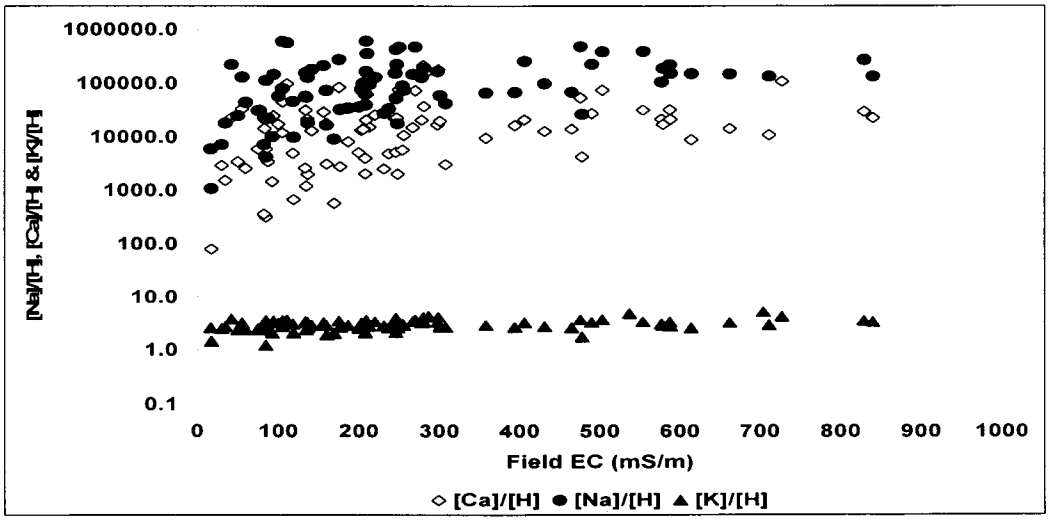


Figure 8-10: Na]/[H], [Ca]/[H] and [K]/[H] vs. field EC.

A strong relation (Figure 8.11), for the groundwater of the Buffelsriver catchment (F30), exists between %Si (as a percentage of cations), $\%HCO_3$ (as a percentage of anions), $O^{18}$ (oxygen-18) and $H^2$ (deuterium) with increasing electrical conductivity (EC).

The %Si - $\%HCO_3$ - $O^{18}$ - $H^2$ relation with increasing electrical conductivity can be used to spatially distinguish between dilute, shallow circulating and relatively young groundwater systems compared to more brackish, slower circulating and relatively older systems. The decreasing %Si and $\%HCO_3$ values suggest a reduction in the weathering capacity, with regard to the aluminosilicate and probably the carbonate minerals (see Sections 7.2.1 and 7.2.2), of the higher salinity groundwater within the lower lying valley systems. The more enriched $O^{18}$ - $H^2$ values with increasing EC are related to the effects of evaporation (see Section 6.3.5). The %Si - $\%HCO_3$ - $O^{18}$ - $H^2$ relation also suggests a continuous hydrochemical evolution between the dilute, shallow circulating and relatively young groundwater systems and the more brackish, slower circulating and relatively older systems (Figure 8.11). The two end-member groundwater systems, however, represent separate systems in a spatial context. The relatively dilute end-member is associated with dynamic, actively recharged groundwater systems with rapid through-flow rates occurring in the higher lying mountainous regions, or with infiltration through highly transmissive fracture zones within the lower lying valley systems. The more brackish end-member, associated with the valley systems or the lower lying regions, is characterized by a localized flow component (i.e. an infiltration phase) and possibly an intermediate flow component (i.e. a lateral flow phase). The infiltration phase is characterized by repetitive processes of dissolution and leaching of evaporative salts, while an inferred sluggish, lateral flow phase is driven by reduced gradients within the valleys. Stratification, representing a variation in EC with depth, in the water column was recorded in one borehole near the town of Tweerivier. The spatial illustration of the %Si - $\%HCO_3$ - $O^{18}$ - $H^2$ relation thus indicates that stacked, multiple flow systems dominate that differ in terms of flow rates and the factors influencing the groundwater flow and chemistry including the recharge rate, hydraulic gradient and hydraulic conductivity. Regional recharge areas (see Section 6.3.5), within the Buffelsriver catchment, can also be identified through this relation.

Active weathering processes, with regard to various mineral phases, are evident throughout the EC range for the lower salinity groundwater. The dilute and relatively aggressive groundwater, associated with higher lying regions, controls the weathering (eg. acid-base reactions) of the mineral phases, while the significant head differences (related to differences in elevation for these mountainous areas) result in dynamic flow systems in which equilibrium is difficult to attain while the weathering products are continuously removed. Active weathering processes thus dominate in the higher lying regions where direct rainfall recharge is dominant and contribute significantly to the dissolved load of the groundwater. Active weathering processes can also occur in lower lying areas as a result of infiltration through preferred pathways such as the weathered material at the base of gneissic domes or through highly transmissive fracture zones. Such groundwater systems are regarded as shallow circulating and relatively young.

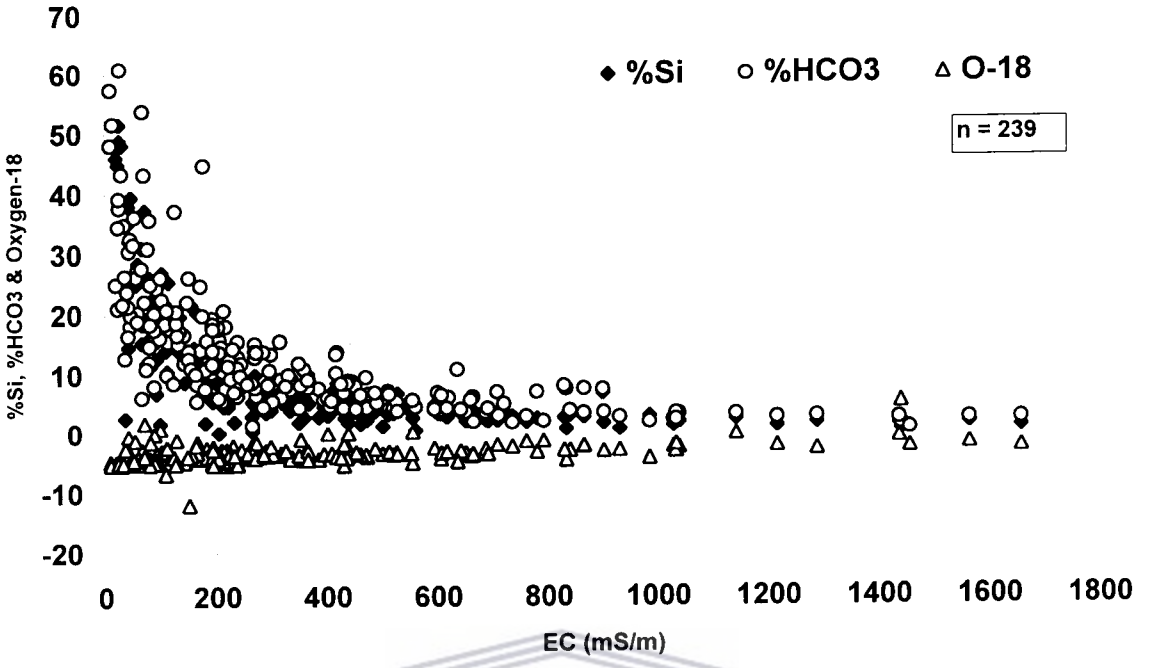


Figure 8-11: The relation of %Si (as a percentage of cations), $\%HCO_3$ (as a percentage of anions), $O^{18}$ (oxygen-18) and $H^2$ (deuterium).

A reduction in the weathering capacity, with regard to especially the carbonate and aluminosilicate minerals, is suggested for the higher salinity groundwater. The groundwater composition for the lower lying regions is a function of the infiltration of evaporated surface waters and/or the leaching of previously evaporated salts, increasing salinity related to weathering of primary mineral phases within the host rocks and/or possibly mixing with older more brackish water. Other factors that may influence the weathering capacity of the groundwater are the incongruency relations of the various mineral phases, the common ion effect, the coating of primary minerals by residual clays as well as a reduction in $CO_2$ production (related to the weathering of aluminosilicate minerals) due to anoxic conditions. Such groundwater systems are regarded as brackish, slower circulating (under reduced hydraulic gradients) and relatively older systems.

The above groundwater systems differ with respect to flow rates and the associated weathering rates as well as with regard to the various processes influencing the groundwater flow rates and chemistry. Acworth (1987) also reported that the reaction rates of the weathering process of primary mineral phases are primarily a function of the pH (or availability of hydrogen ions), the rate of supply of dissolved oxygen and the rate at which the weathering products are removed. The rate of groundwater flow thus influences the reaction rates of the weathering processes. The rate at which groundwater flows is a function of the recharge rate, the hydraulic gradient and the hydraulic conductivity of the system (Acworth, 1987). The groundwater chemistry thus seems to be dependant on the point of sampling in either a dynamic (i.e. active), evaporative or sluggish groundwater system.

8.2.5: The various sources for the dissolved ions

The relations between the cations ($Ca^{2+}$, $Na^{+}$ and $Mg^{2+}$) and $HCO_3^-$, based on the molar ratios of these ions produced during the incongruent weathering reactions for various aluminosilicate minerals, are tabulated (Table 8.4) and illustrated in figures 8.12 and 8.13. In addition, molar ratios between cations for similar weathering reactions are tabulated. The molar ratios (Figures 8.12 and 8.13) indicate that the incongruent weathering processes of various aluminosilicate minerals cannot alone account for the groundwater compositions.

Table 8-4: Expected molar ratios for the weathering reactions of some aluminosilicate minerals (after Appelo and Postma, 1993).

| Silicate Minerals | Ions | Molar Ratios |
|---|---|---|
| Albite to Kaolinite | $Na^+ : HCO_3^-$ | 1 : 1 |
| Anorthite to Kaolinite | $Ca^{2+} : HCO_3^-$ | 1 : 2 |
| Augite to Kaolinite | $Ca^{2+} : HCO_3^-$ | 1 : 3.7 |
| Augite to Kaolinite | $Mg^{2+} : HCO_3^-$ | 1 : 4.3 |
| Pyroxene to Kaolinite | $Ca^{2+} : Mg^{2+}$ | 1 : 0.7 |
| Biotite to Kaolinite | $K^+ : Mg^{2+}$ | 1 : 2 |
| Olivine (Forsterite) dissociation | $Mg^{2+} : HCO_3^-$ | 1 : 2 |



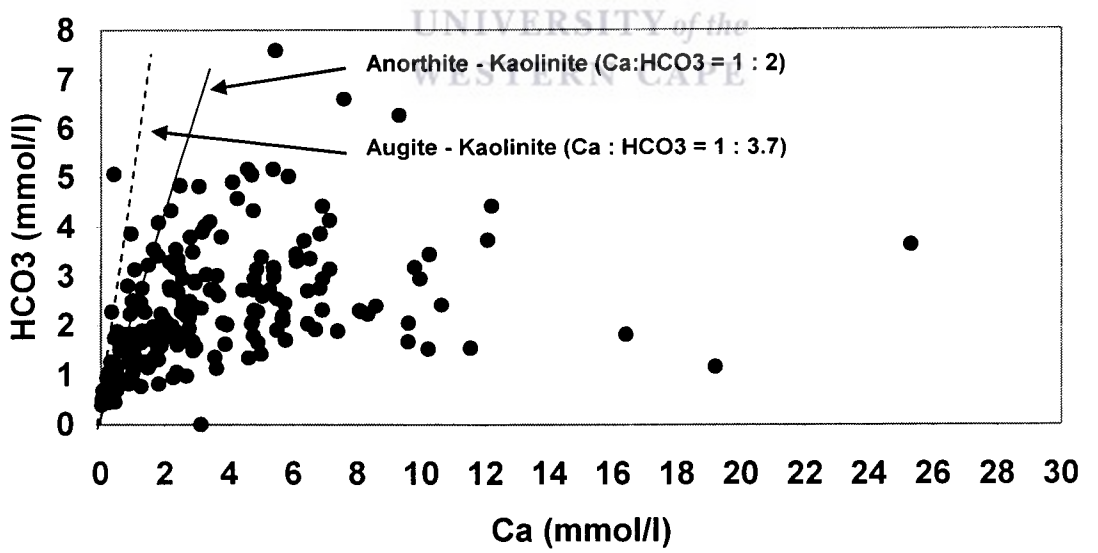


Figure 8-12: The relationships between $Ca^{2+}$ and $HCO_3^-$ in comparison to the anorthite to kaolinite as well as the augite to kaolinite weathering reaction lines (after Locsey and Cox, 2000).

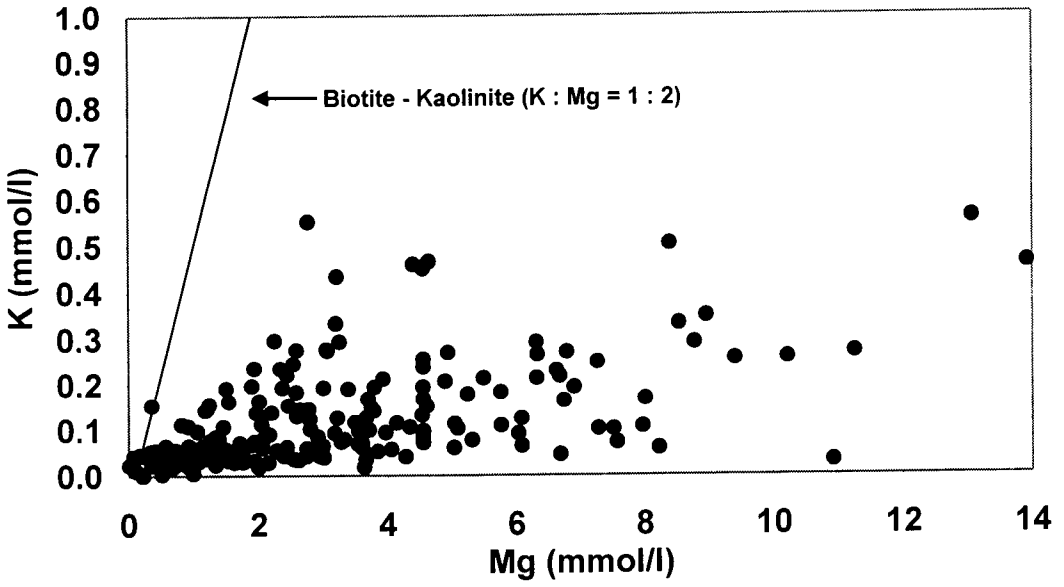


Figure 8-13: The relationships between $K^+$ and $Mg^{2+}$ in comparison to the biotite to kaolinite weathering reaction line.

Sami (1992) also used the Na/Cl ratio to distinguish between a marine/oceanic input (Na/Cl = 0.86), halite dissolution (Na/Cl = 1), aluminosilicate (i.e. albite) weathering and cation exchange processes. A $(Ca+Mg)/HCO_3$ ratio of 0.5 account for carbonate and inosilicate minerals (i.e. pyroxenes and amphiboles) as probable sources of dissolved Ca and Mg. Ratios of $(Ca+Mg)/HCO_3$ in excess of 0.5 may indicate other sources of dissolved Ca and Mg, re-dissolution and leaching of gypsum and cation exchange processes rather than $HCO_3$ depletion through the formation of carbonic acid ($H_2CO_3$) which is dependent on the pH conditions (Sami, 1992).

The Na/Cl ratio of the groundwater (Figure 8.14) decreases gradually with increasing salinity to a value lower than the equilibrium Na/Cl ratios for both oceanic water input (i.e. Na/Cl = 0.86) and halite dissolution (i.e. Na/Cl = 1). The depleting Na concentrations, relative to the Cl concentrations, may be due to the dissolution of salts other than halite (i.e. NaCl), or the result of cation exchange processes through the exchange of dissolved Na for bound Ca and Mg. There are no obvious trends in the Ca/Cl - EC and Mg/Cl – EC relations.

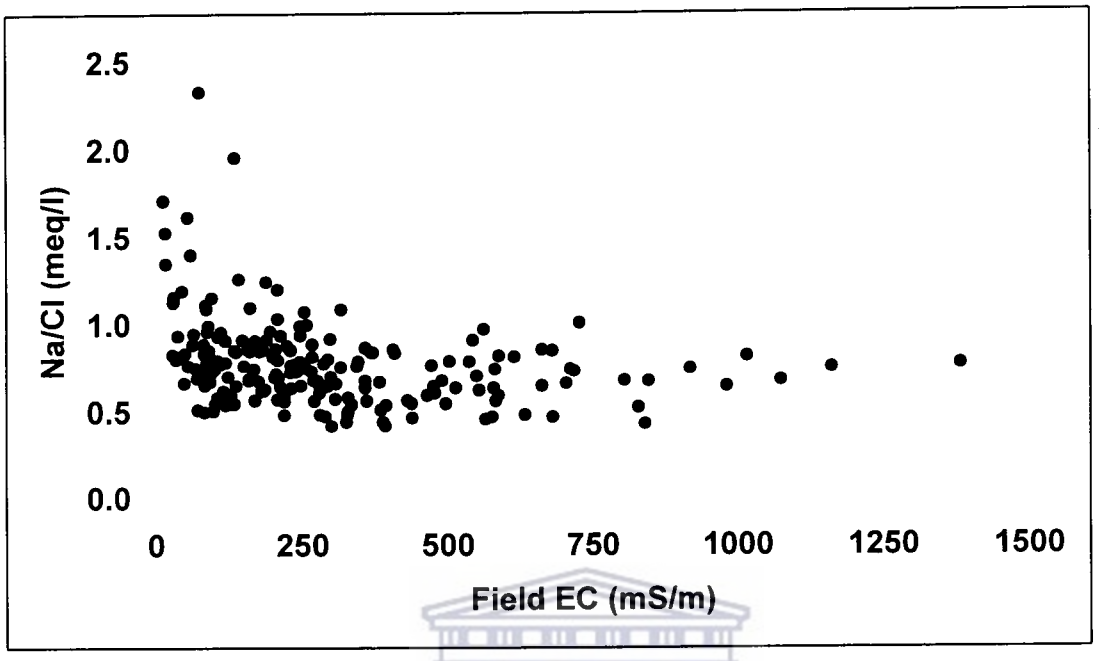


Figure 8-14: The Na/Cl – Cl ratio for groundwater in Namaqualand.

The (Ca + Mg)/$HCO_3$ ratio, in all groundwater samples, exceeds the value of 0.5 and increases with increasing salinity. An increasing trend for the (Ca + Mg)/$HCO_3$ ratio (Figure 8.15) with increasing salinity indicates that Ca and Mg are added to the groundwater at a greater rate than $HCO_3$. The increasing (Ca + Mg)/$HCO_3$ ratio also indicates that the sources of Ca and Mg are varied, in addition to carbonate dissolution and the weathering processes of inosilicate minerals. The increasing Ca and Mg concentrations in solution, relative to the $HCO_3$ concentrations, may be due to the weathering of evaporitic salts in addition to the weathering of the carbonate and aluminosilicate minerals. The increasing Ca and Mg concentrations may also be due to the remobilization of evaporitic gypsum. Cation exchange processes, through the release of bound Ca and Mg in exchange for dissolved Na, may also influence the Ca and Mg concentrations in solution.

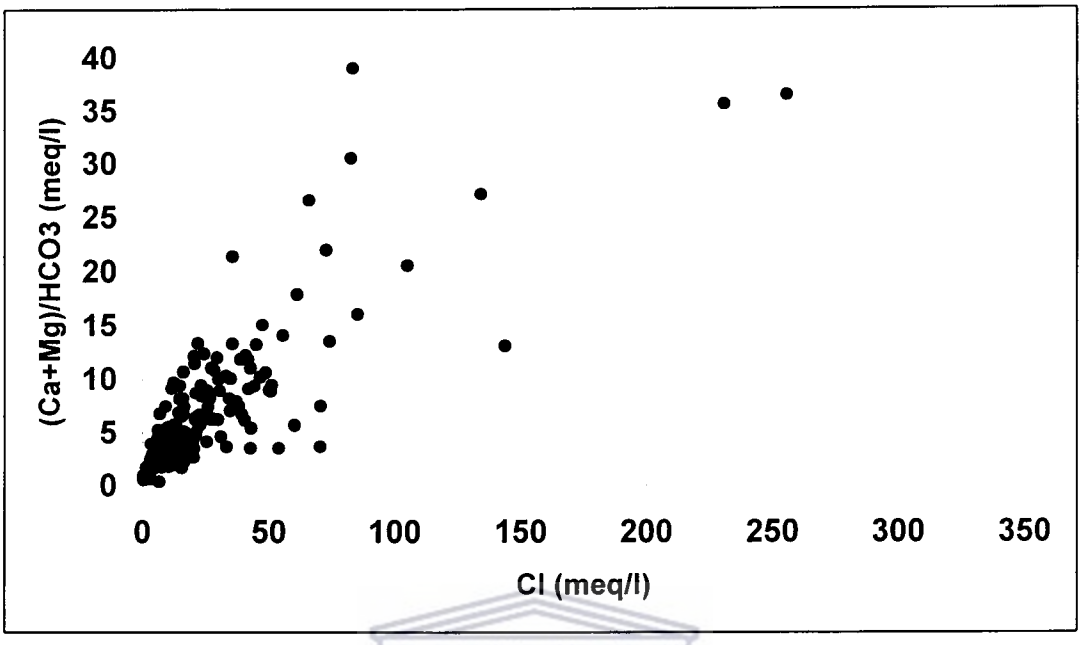


Figure 8-15: The (Ca + Mg)/$HCO_3$ – Cl relation for groundwater.

The contributions of $Na^+$, $Ca^{2+}$ and $Mg^{2+}$ to the cation load of the groundwater are thus significant, with the groundwater remaining NaCl type waters with increasing salinity (Figure 8.16). The major cation (eg. $Na^+$, $Ca^{2+}$ and $Mg^{2+}$) concentrations are predominantly balanced by the anions $Cl^-$, $SO_4^{2-}$ and $HCO_3^-$ at lower salinities, while the contribution of $HCO_3^-$, relative to the anion content, decreases with increasing salinity of the groundwater. The percentage of sodium (%Na as a percentage of the cations), increases slightly with increasing salinity while the percentages of calcium (%Ca) and magnesium (%Mg), as percentages of the cations, remain relatively constant. The percentage of silica (%Si as a percentage of the cations) decreases with increasing salinity. The cation concentrations are primarily balanced by the chloride ($Cl^-$) concentration and to a lesser extent by the $SO_4^{2-}$ concentrations, at higher salinities. According to Kay (1985), the weathering products that form on mineral surfaces as a result of incongruent dissolution processes have significant cation exchange capacities capable of changing the ion ratios in groundwater (Freeze and Cherry, 1979).

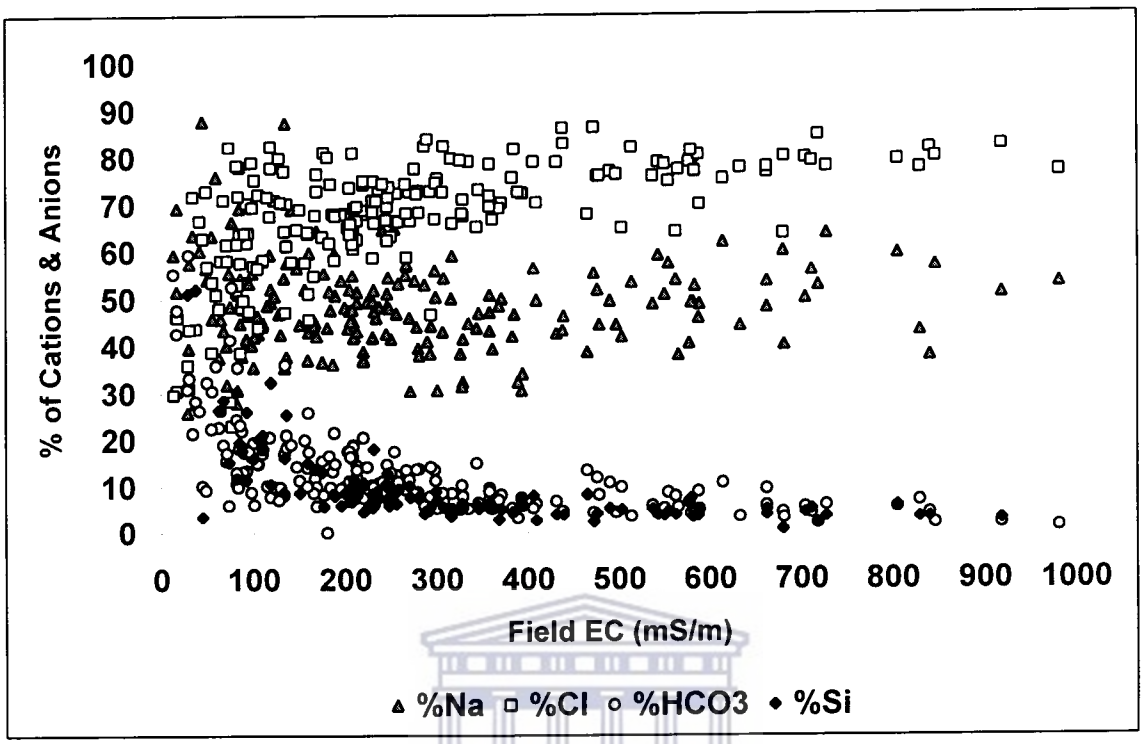


Figure 8-16: Percentages of sodium (%Na) and silica (%Si) as percentages of the cation load, as well as percentages of chloride (%Cl) and bicarbonate (%$HCO_3$) as percentages of the anion load.



8.2.6: Silicate stability diagrams

The concentrations of $Si(OH)_4$ as well as the [Na]/[H], [Ca]/[H] and [K]/[H] ratios increase with continued weathering (i.e. incongruent dissolution) of aluminosilicate minerals (see Section 7.2.2). Feldspar dissolution ceases only when the water compositions attain equilibrium with respect to a specific feldspar mineral (Freeze and Cherry, 1979). Long residence times associated with sluggish to almost stagnant flow conditions are required to attain equilibrium with respect to feldspar minerals.

The groundwater compositions, expressed in terms of log $[Ca^{2+}]/[H^+]$ and $SiO_2$ as well as log $[K^+]/[H^+]$ and $SiO_2$, generally plot in the kaolinite stability field above the solubility limit of quartz but below the solubility limit of amorphous silica. This indicates that the most likely stable alteration product formed, due to the incongruent dissolution of aluminosilicate minerals, is kaolinite. On log $[Na^+]/[H^+]$ vs. $SiO_2$ diagrams (Figures 8.17 and 8.18) the groundwater compositions plot in the Na-montmorillonite stability field indicating the probability of equilibrium or near equilibrium conditions with Na-montmorillonite as a weathering product. The alteration of feldspars and micas to

kaolinite and montmorillonite are thus important processes for groundwater in silicate terrains such as Namaqualand. Clay minerals may, however, exist as unstable amorphous precipitates or meta-stable clay mineral intermediates for extensive periods (Freeze and Cherry, 1979), therefore casting doubts on whether true equilibrium with the clay minerals is attained (see Section 7.2.2.4).

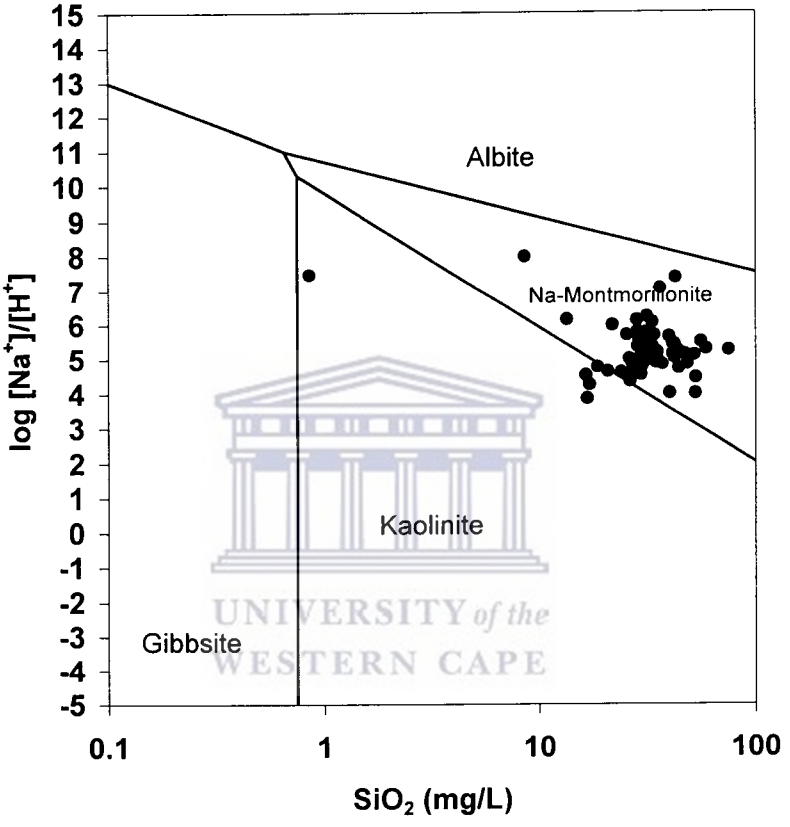


Figure 8-17: Log $[Na^+]/[H^+]$ vs. $SiO_2$ phase diagram for groundwater compositions of the Buffelsriver catchment (F30).

The higher salinity groundwater, specifically for the pre-Bushmanland Gamoep region, (Figure 8.18) plots in the Na-montmorillonite stability field. This again indicates the likelihood of equilibrium or near-equilibrium conditions with Na-montmorillonite as a weathering product.

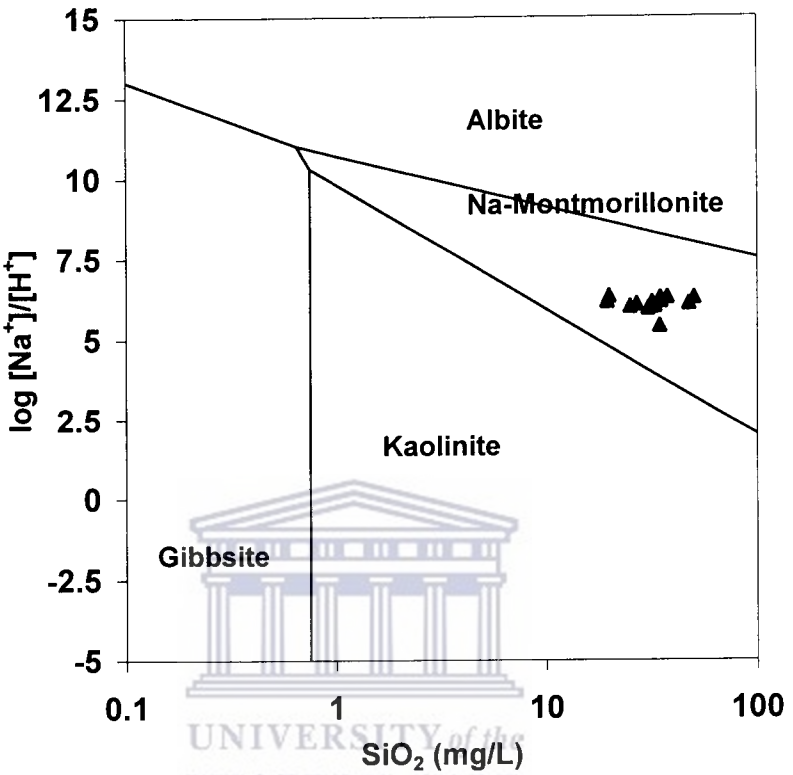



Figure 8-18: Log $[Na^+]/[H^+]$ vs. $SiO_2$ phase diagram for groundwater compositions of the Gamoep region (F30).

The distribution of the groundwater compositional data within the kaolinite and Na-montmorillonite stability fields indicate that the groundwater compositions are likely to be in equilibrium or near-equilibrium conditions with both weathering products. This may indicate that the reactions between the groundwater (or soil water) and the primary minerals are masked by reactions with the more reactive secondary clay minerals.

The composition of water that plots near the kaolinite-gibbsite boundary is influenced by dilution with fresh rainfall (and possibly runoff) and is described as water (or precipitation) dominated, dilute systems (Langmuir, 1997). Rock dominated waters are found in closed systems not affected by fresh, diluting and recharging waters. Such waters approach equilibrium with regard to silicates and aluminosilicates and are characterised by relatively higher pH, $K^+$ and silica values. Most of the groundwater samples seem to fall within the latter category. However, the relatively higher pH, $K^+$ and silica values can more confidently be ascribed to the effects of evaporation than to

weathering processes under confined flow conditions. Alternatively, the effects of evaporation masked the contribution of weathering, under confined conditions, to the salinity and composition of the groundwater.

### 8.2.7: Mineral saturation indices

The saturation states of groundwater compositions, as a function of salinity (i.e. EC) for various mineral phases, are better illustrated with a log IAP/KT range of –10 to +10 (Appelo and Postma, 1993). Variation in mineral composition for the isomorphic plagioclase range (i.e. albite to anorthite) may result in variable reaction kinetics (i.e. dissolution and precipitation) for the feldspar minerals (Appelo and Postma, 1993). The saturation state of a groundwater composition with regard to plagioclase feldspar minerals can thus vary between the saturation state of the groundwater compositions with regard to albite and anorthite (Table 8.1). Solid solution, at higher temperatures, between plagioclase feldspars and alkali feldspar further adds to the uncertainty. The variation in the saturation state of the groundwater compositions with regard to the carbonate minerals may be controlled by the minerals calcite, aragonite, rhodochrosite, dolomite, strontianite and witherite. Whether the above-mentioned minerals are present within the lithological make-up of the aquifer system must be confirmed by detailed mineralogical studies.

The degree of saturation, for a particular groundwater composition, influences the concentrations of the dissolved constituents. Subsaturation of a groundwater composition with regard to mineral phases results in further dissolution, while supersaturation results in the re-precipitation of minerals. Conditions of disequilibria (i.e. both subsaturation and/or supersaturation) can be maintained due to a number of factors. Considerable residence time is necessary for carbonate dissolution to attain equilibrium under field conditions (Freeze and Cherry, 1979). Degassing or a reduction in the $P_{CO2}$ can also result in the groundwater compositions becoming supersaturated with respect to carbonate minerals. The incongruency relations with regard to the varied carbonates, but especially with regard to the aluminosilicate minerals, also influence the chemical evolution of the groundwater. In addition, conditions of disequilibria can also be maintained due to cation exchange and the common-ion effect.

The groundwater compositions (Figure 8.19) are predominantly saturated to supersaturated with regard to the carbonates calcite, aragonite and dolomite, while being undersaturated to saturated with rhodochrosite and strontianite. The groundwater compositions become increasing saturated to supersaturated with carbonate minerals as the pH increases. The higher salinity groundwater compositions (Figure 8.20) of the pre-Bushmanland Gamoep region are saturated to supersaturated with regard to the carbonate minerals (i.e. calcite, aragonite, rhodochrosite, etc.).

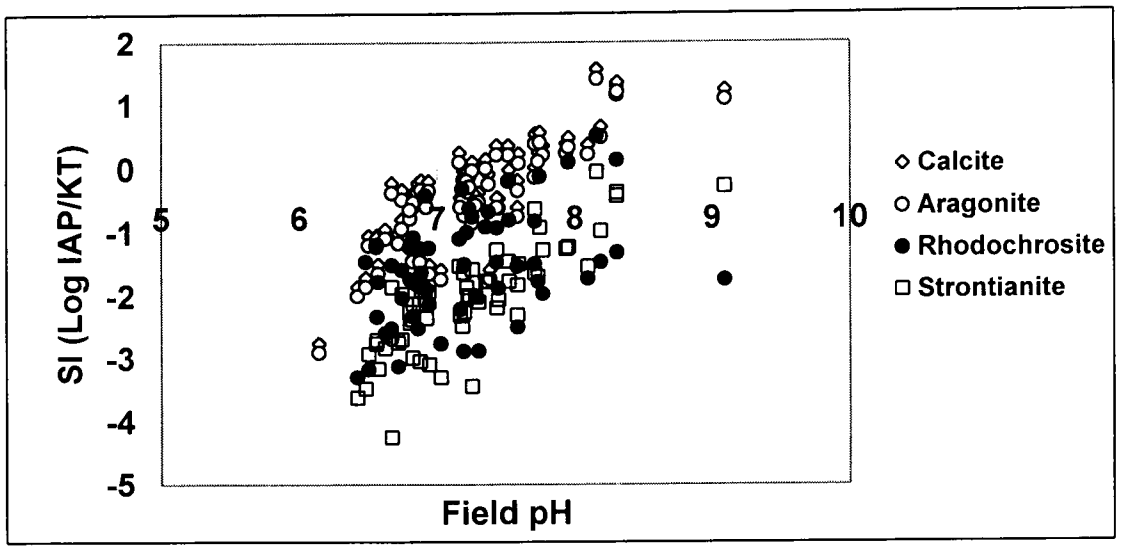


Figure 8-19: The saturation states of groundwater compositions, as a function of field pH, for various carbonate minerals.



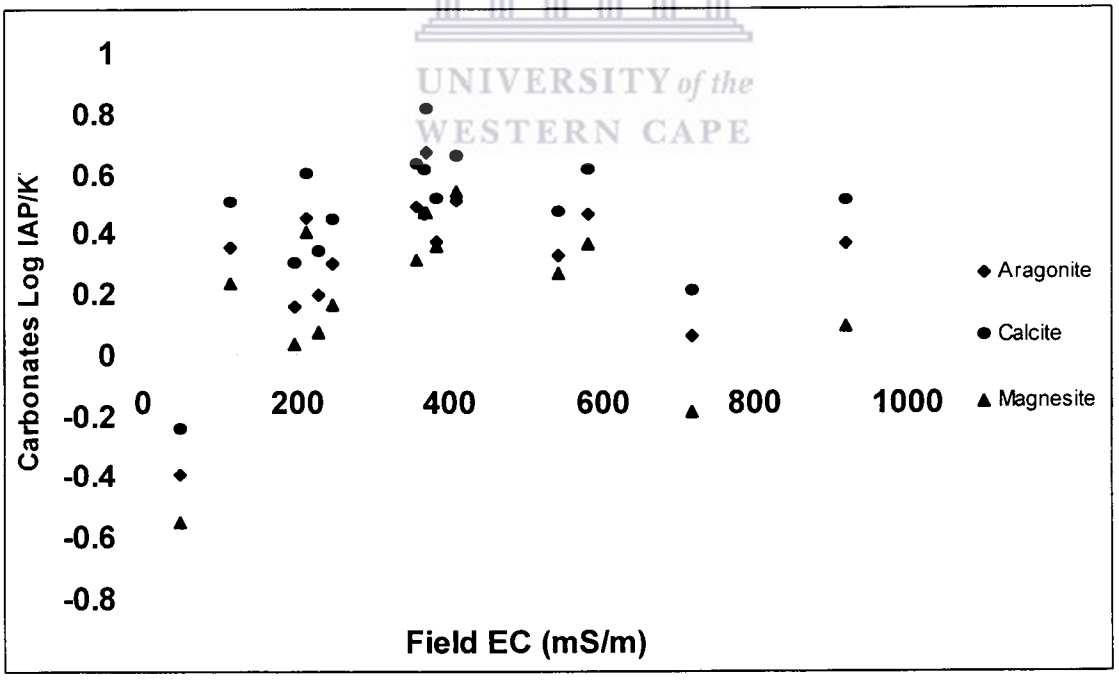


Figure 8-20: The saturation states of groundwater compositions, as a function of salinity (i.e. lab EC), for various carbonate minerals in the Gamoep region.

The groundwater compositions, above a pH value of 6.5, are generally saturated to supersaturated with regard to the feldspars albite and k-feldspar, and range from being undersaturated to super-saturated with regard to anorthite (Figure 8.21). The groundwater becomes even more supersaturated with increasing pH with regard to these feldspar minerals. Trend lines for the feldspars albite and anorthite indicate that the saturation state of a groundwater composition with regard to plagioclase feldspar minerals can vary between the saturation states of groundwater compositions with regard to the two end members of an isomorphic range (Figure 8.22). Such groundwater compositions are saturated to super-saturated with silica throughout the recorded EC ranges (Figures 8.22 and 8.23). The saturation state, with regard to the silica minerals quartz and chalcedony, of the groundwater compositions increase slightly with increasing pH (see Section 7.2.2).

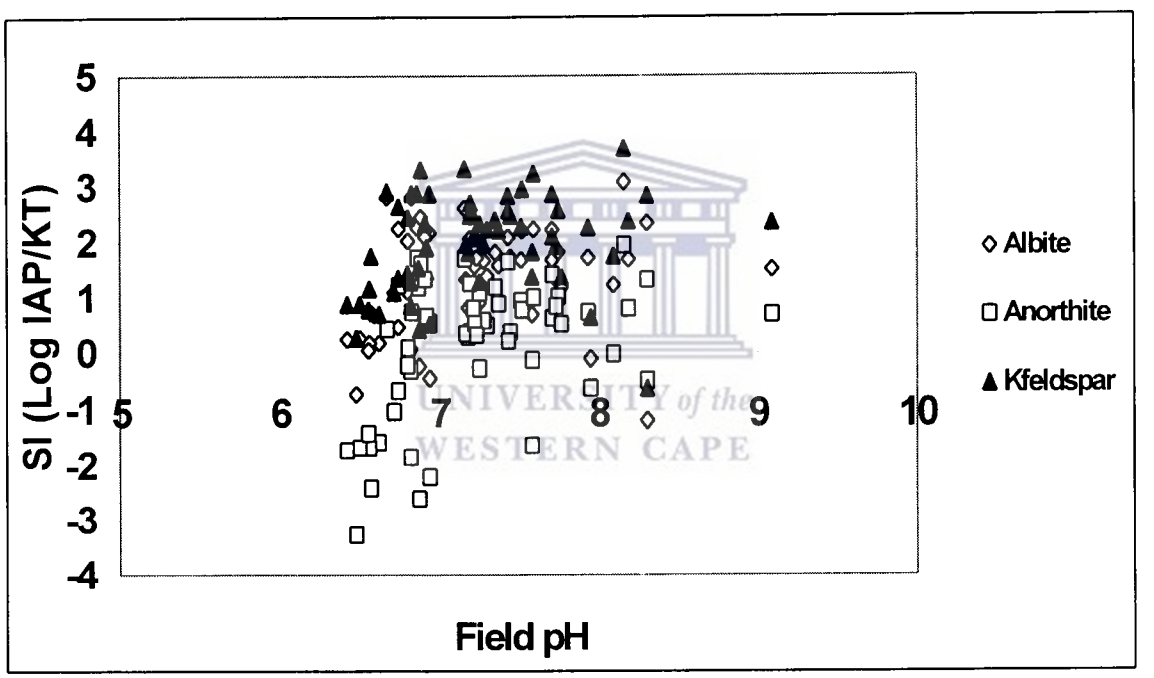


Figure 8-21: The saturation states of groundwater compositions, as a function of field pH, for plagioclase and alkali feldspar minerals.

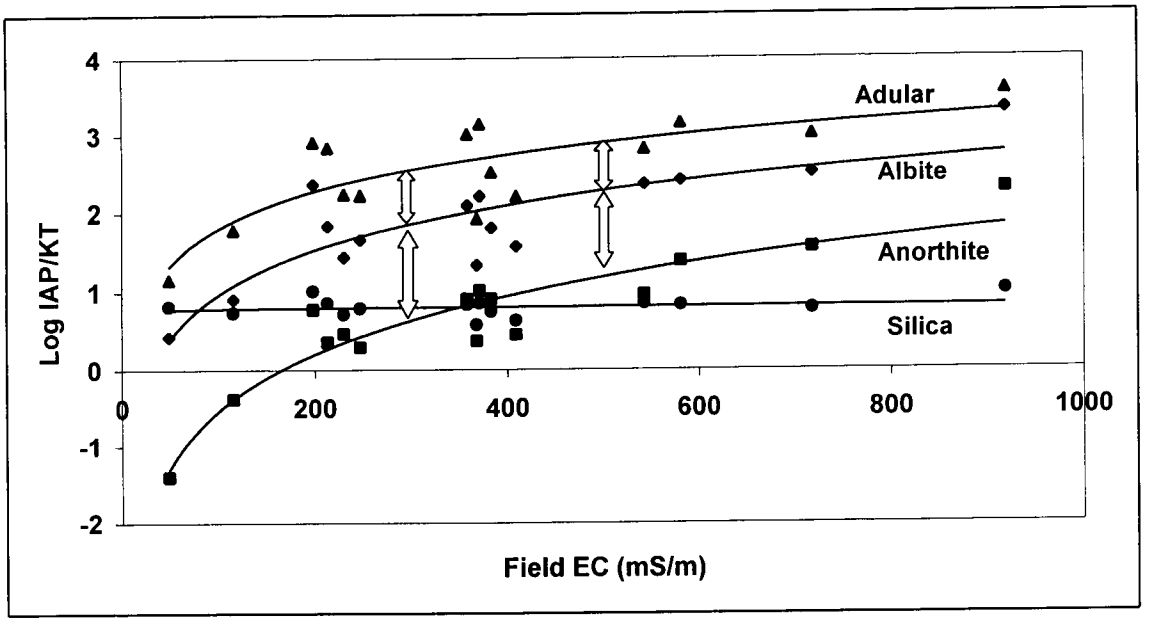


Figure 8-22 The saturation states of groundwater compositions, as a function of salinity (i.e. Field EC), for plagioclase and alkali feldspar minerals in the Gamoep region. The arrows indicate that the saturation state of a groundwater composition with regard to plagioclase feldspar minerals can vary between the saturation states of the groundwater compositions with regard to albite and anorthite.



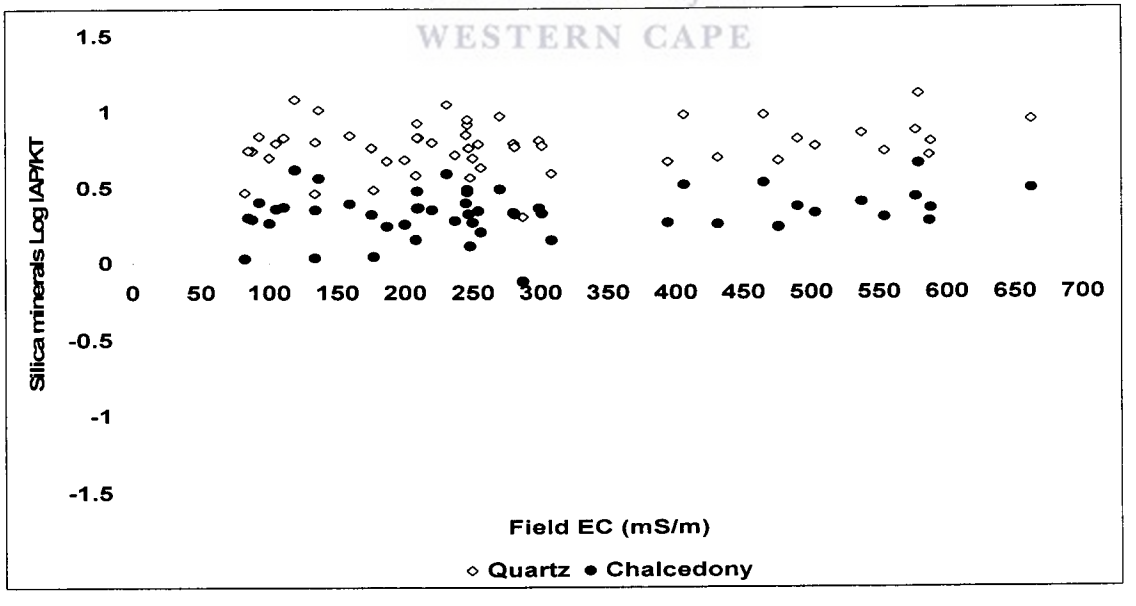


Figure 8-23: The saturation states of groundwater compositions, as a function of salinity (i.e. Field EC), for various silica mineral phases.

The groundwater compositions are undersaturated with gypsum, anhydrite and celestine while being saturated with barite (Figure 8.24). Furthermore, the groundwater compositions are subsaturated with fluorite below pH values of 7, while being in equilibrium with fluorite above pH values of 7 (Figure 8.25).

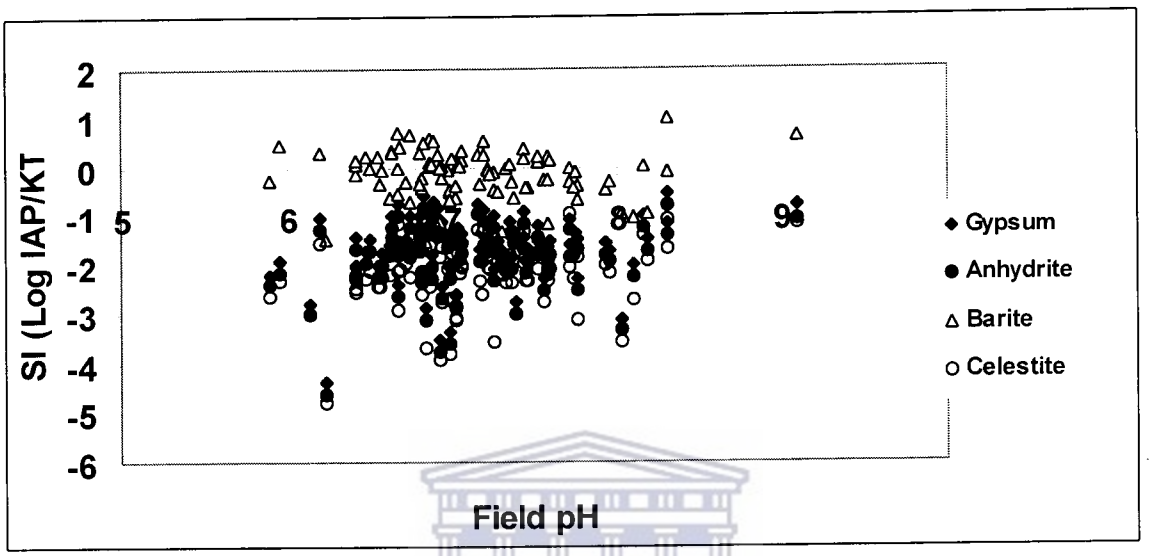


Figure 8-24: The saturation states of groundwater compositions, as a function of pH, for sulphate minerals.



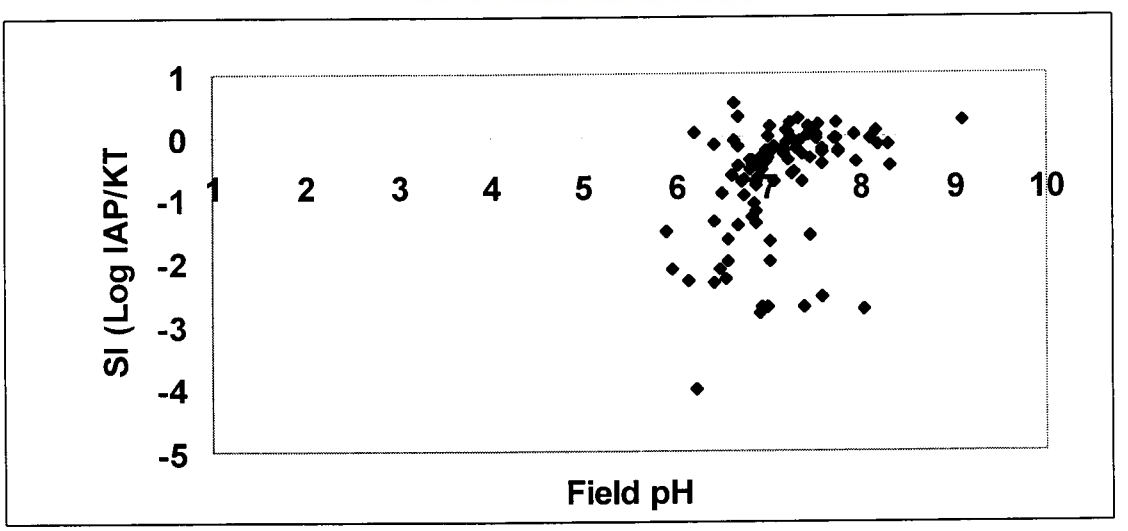


Figure 8-25: The saturation state of groundwater compositions, as a function of pH, for fluorite.

These groundwater compositions tend to be undersaturated to saturated with an amorphous aluminium hydroxide phase ($Al(OH)_3$) below a pH value of 7. The SI values of the amorphous aluminium hydroxide phase ($Al(OH)_3$) decreases below the equilibrium level (i.e. SI = 0) above a pH value of 7.2 (Figure 8.26). The groundwater compositions are also likely to be supersaturated with gibbsite and the most common potassium (K) micas such as biotite, muscovite, phlogopite, and lepidolite. A similar decrease in the SI values above a pH value of 7.2 is observed for gibbsite and potassium (K) micas.

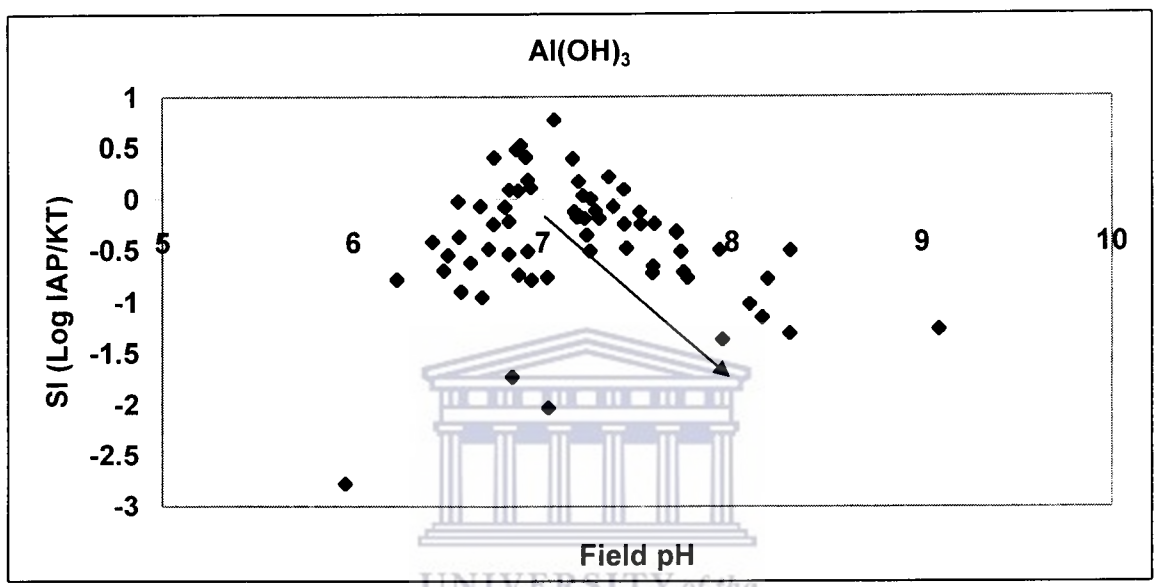


Figure 8-26: The saturation states of groundwater compositions, as a function of pH, for an amorphous aluminium hydroxide phase ($Al(OH)_3$).

The groundwater compositions tend to be supersaturated with kaolinite, Ca-montmorillonite and illite (i.e. the clay mineral group). A decrease in the SI values above a pH value of 7.2 is also observed for each of these clay mineral phases (Figure 8.27). The groundwater compositions approach equilibrium with respect to chlorite and talc below pH values of 7, while becoming increasingly supersaturated with chlorite and talc above pH values of 7.2.

Although the groundwater compositions tend to be in equilibrium with an amorphous aluminium hydroxide phase ($Al(OH)_3$), it is supersaturated with the crystallized aluminium oxide or hydroxide phases such as gibbsite, potassium (K) micas and the clay mineral group. This can be ascribed to the much higher solubility of the amorphous aluminium hydroxide phase ($Al(OH)_3$) compared to the crystallized aluminium oxide or hydroxide phases. In addition, the slow reaction kinetics of silicate minerals (including clay minerals) can result in uncertainties about the stability of the intermediate weathering products (See 7.2.2.4). The groundwater, however, tend to react with both the primary mineral phases and the weathering products (eg. the clay minerals) or at least with an intermediate, meta-stable phase.

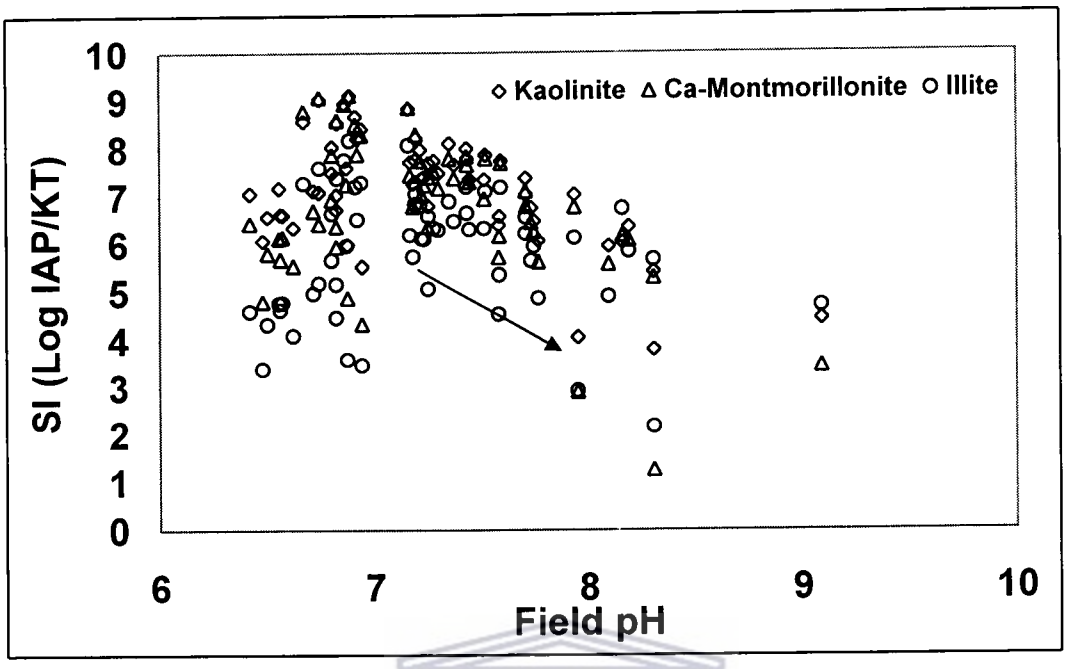


Figure 8-27: The saturation states of groundwater compositions, as a function of pH, for the clay mineral phases (i.e. kaolinite, Ca-montmorillonite and illite).



## 8.3: Construction of groundwater flow regime

Delineating exact groundwater-flow patterns is difficult to construct due to paucity of boreholes, distances between borehole positions and the spatial distribution of the boreholes. The conceptual model for groundwater flow is based on: (1) The identification of spatial and vertical variations in groundwater chemistry; (2) The numerous lineaments, at all scales, visible on a satellite (i.e. Landsat) image. These observations are supported by a wealth of data on Proterozoic deformation phases; (3) The presence, to varying intensity, of vertical to sub-vertical as well as horizontal joint planes in all lithologies; and (4) The structural control on both major and minor drainage systems. The broad range of orientations for these fracture systems may indicate that complex groundwater flow paths and groundwater systems exist (see Sections 2.2.3 and 2.2.4). Infiltration pathways also exist along the foothills of barren gneissic domes. However, the connectivity, degree of openness and depth of penetration of these fracture systems remain unsolved.

Groundwater flow in Namaqualand is a function of complex geomorphological and hydrogeological environments with more than one flow system present. Local relief is associated with prominent ridges (i.e. domes) and structurally controlled valleys. As a result, localised, shallow circulating groundwater flow systems may dominate near

surface environments, while intermediate slower circulating flow systems may follow the gradients within the valleys. Both groundwater flow systems approximate the surface drainage flow pattern. The hydraulic contrasts, for fractured crystalline rocks, between highly transmissive fracture zones and the micro-fractured crystalline matrix, or between different scales of fracture systems may influence groundwater flow patterns on an outcrop scale. The groundwater divides for the shallow circulating system thus coincide with surface water divides (i.e. ridges and valleys). The identification of discharge areas depends on the flow systems, with structurally controlled valleys being the discharge zone for local and shallow circulating groundwater flow systems. The initiation of flow paths for intermediate flow systems may coincide with distinct, although limited, recharge zones interior to the Buffelsriver catchment (i.e. a secondary drainage catchment, F30). However, such deeper confined flow conditions can only be inferred due to: (1) the shallow depths of boreholes in recharge zones intersecting predominantly near-surface flow, and the fact that (2) valleys, that represents discharge zones with relatively shallow water levels, are the traditional targets for groundwater development. The discharge zones for intermediate flow systems may coincide with that of localised flow systems and may also follow the hydraulic gradients within these valleys. In addition, structurally controlled, highly mineralized groundwater is discharging as perennial, artesian springs, especially in drainage catchment F40.

Regional flow patterns may, however, also exist for the Namaqualand region. Highly saline groundwater discharges at the mouth of the Buffelsriver near the town of Kleinzee. These regional systems may be driven by the major topographic differences between the Bushmanland Plateau and the western-most lower lying coastal zones. Numerous deeply incised, submerged canyons are documented for the west coast.



Hydraulic head differences, as a function of elevation differences, thus seem to be the major influence of groundwater flow patterns, at all scales, for the Namaqualand region (Figure 8.28).

Springs, in Namaqualand, are a function of topographic and structural control. Most springs of Namaqualand are perennial with more or less constant annual, notwithstanding low yields. Perennial springs probably drain extensive permeable sections of the crystalline aquifer systems. The salinity of spring discharges seems to be related to residence times in terms of length of flow paths. Springs are an expression of local and intermediate groundwater flow systems and can occur in both recharge and discharge areas depending on the flow system. A low rate of recharge can account for the normally low yields of springs.

Shallow circulating and relatively young (i.e. active) flow systems (i.e. predominantly interflow) were recognised together with slower circulating (i.e. non-active) and relatively older groundwater systems (Figure 8.28). The shallow circulating and relatively young flow systems (i.e. predominantly interflow) occur in the higher lying, higher rainfall regions and represent dynamic, actively recharged groundwater systems with rapid through-flow rates. Groundwater flow within topographic highs occurs along major fractures as a function of the naturally high vertical hydraulic gradients in these regions.

Perennial springs, usually located in mountainous regions, with low yields and low total dissolved solids are expressions of such shallow flow systems. Infiltration, through highly transmissive fracture systems along the foothills of the massive gneissic domes, also gives rise to shallow circulating flow systems.

The slower circulating (i.e. non-active) and relatively older groundwater systems (Figure 8.28) are associated with the lower lying, lower rainfall regions. Such groundwater systems include: (1) an infiltration phase associated with repetitive processes of dissolution and leaching of evaporative salts and (2) an inferred sluggish, lateral flow phase driven by reduced gradients within the valleys. The lateral flow phase may approximate an intermediate flow system. These groundwater flow systems, both the vertical and lateral phases, are predominantly confined to the top of the saprock (i.e. weathered and fractured bedrock) zone. Groundwater circulating deeper and slower are associated with a reduction of hydraulic gradients and hydraulic conductivity with depth.

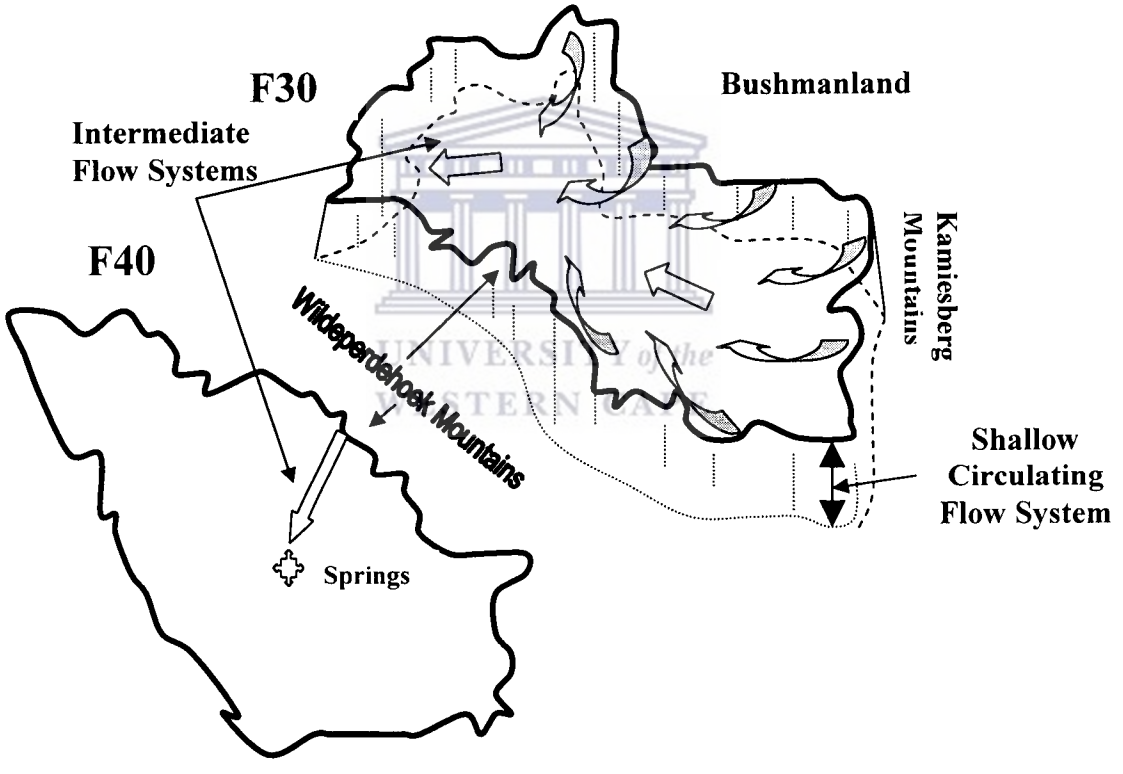


Figure 8-28: Various flow regimes for the secondary drainage catchments F30 and F40.

# Chapter 9

# Conclusions and Recommendations

## 9.1: Introduction

At the onset of this research project it became apparent that there is a dearth of research studies focusing on the groundwater resources of the region. As a result, a conceptual representation of the hydrogeological system (the specific aquifer systems, the groundwater flow regime, etc.) for the perceived problematic aquifer systems in the Namaqualand region did not exist. Data on aquifer properties (i.e. transmissivity and storativity data) were reported for individual boreholes with no reference to the geological and hydrogeological system investigated. The primary objectives are:

- To provide a quantitative understanding of the region's resources in terms of quantity, and
- To investigate the cause(s) that result in the relatively 'poor' groundwater quality characteristic of the region.

The primary objectives were addressed in the following way:

- A regional context for the study was adopted;
- Boreholes were selected, and sampled for chemical analyses, that cover the entire research study area;
- Emphasis was placed on characterizing the groundwater resources in terms of its hydrochemical evolution;

The research project contributes significantly to a quantitative understanding of the regions' groundwater resources in terms of its quality, including groundwater flow systems, but lacks sufficient detail to propose management options for the groundwater quantity at this stage.

In meeting these primary objectives, specific objectives set in Chapter 1 are addressed below.

## 9.2: Addressing the Objectives

### Aquifer development and geometry

A database of the physio-chemical parameters (pH, EC and temperature), aggregate determinants (eg. alkalinity), concentrations of major ions (both cations and anions) and certain trace elements is included as appendix I. The data will also be added to the National Groundwater Database of DWAF.

The Proterozoic Namaqua mobile belt was subjected to the 1000 – 1200 Ma Namaquan orogeny. The rocks of the Namaqualand Metamorphic Province thus underwent several phases of intensive folding (such as isoclinal folding) as well as faulting and were intruded on a large scale by syntectonic granites. The interpretation of both vertical and lateral stratigraphic and structural relationships, as well as possible lateral correlatives, is extremely difficult. The high-grade metamorphism and multi-phase deformation undergone by these rocks, destroyed the normal stratigraphic criteria and produced generations of tight and isoclinal folding.

The basement rocks of Namaqualand retained imprints of mostly these Proterozoic tectonic events, although much of the present landscape appears to have developed in the Cretaceous, following the break-up of Gondwanaland.

The morphology of southern Africa is to a great extent controlled by the underlying geology. Bornhardts, rounded dome-shaped forms usually prominent in the granitic and gneissic rocks of Namaqualand, are the most prominent geomorphological features of the escarpment zone. Bornhardts (eg. the Kamiesberg mountain range) can be massifs or juxtaposed groups of domes arranged in an ordered pattern due to the structural control on its development.

Deep subsurface weathering is essential for bornhardt development. A variation in fracture density is probably the most likely explanation for the development of bornhardts. Fractures are preferred pathways for the infiltration of water and more densely fractured materials are more prone to weathering processes than massive, dense material. The more transmissive and especially larger fault zones have been weathered and eroded more intensely to form the valleys that separate the massive domes. Bornhardts are composed of massive, compressional core zones surrounded by a matrix of weathered rock expressed as the fault-controlled valleys and narrow plains.

Most of southern Africa is characterized by a mature landscape with different erosion surfaces separated by prominent geomorphic scarps. The warm and humid tropical climate of the Cretaceous period resulted in the development of deep, koalinised weathering mantles especially on susceptible lithologies. Towards the end of the Mesozoic (i.e. upper/late Cretaceous) kaolinised profiles of depths of 50 m or more were underlying remnants of the African surface, the highest and oldest erosion surface. Late Cretaceous and early Paleocene pedocrete cappings (i.e. duricrusts), comprising

predominantly of silicrete and calcrete in the western and central parts of the southern African subcontinent, protected the African surface and its deeply kaolinised saprolite from erosion processes in many localities.

Early Miocene crustal uplift and subsequent erosion resulted in the mid-Miocene Post-African I erosion surface dated at between 12 Ma to 19 Ma. The Post-African I surface dominates the southern African landscape. The Post-African I landscape development phase, associated with limited incision of drainage channels of up to 100 m to 200 m, involved the removal of the deeply weathered mantles underlying the African surface. In areas (i.e. western parts of southern Africa) subjected to minimal Miocene uplift, scattered residuals or reduced thicknesses of the weathered mantles remained.

This sequence of events led to the development of the aquifer systems in Namaqualand. However, the aquifer systems are confined to deep valleys associated with fault zones occurring throughout the area. These fault zones are especially prominent in the mountainous escarpment zone and are the traditional targets for the development of groundwater resources.

The proposed geometry for the aquifer system can be described as laterally extensive, linear, structurally controlled valley systems. Wide, open valleys may result from the intersection of different sets of fracture systems. The saprock to saprolite transition zone constitutes the aquifer system. Infiltration of water occurs along vertical to sub-vertical fractures with lateral flow along horizontal to sub-horizontal fracture systems. The water chemistry varies considerably among closely spaced fracture systems. This model proposes a dominant vertical flow system (i.e. an infiltration phase) driven by local relief and an intermediate flow system driven by gradients along these laterally extensive valley systems.



**Groundwater chemistry and carbonate and silicate dissolution**

The groundwater for Namaqualand is generally very similar in character with a dominant NaCl signature throughout the recorded EC ranges. The $Na^+$ and $Cl^-$ dominated groundwater for Namaqualand can be described as end-point waters.

Most EC values, associated with groundwater of catchment F30, are concentrated over an interval up to an EC value of 250 mS/m. The latter may indicate that most of the boreholes may be strategically placed, through trial and error, to intercept groundwater of the 'best' or adequate quality for the region.

The pH values for groundwater of catchment F30 display an almost perfect normal distribution centered on a value of 7, as opposed to an irregular distribution of the pH values for groundwater of the coastal drainage catchment F40.

Equilibrium conditions are difficult to maintain for open system dissolution of particularly carbonate minerals due to a continuous replacement of $CO_2$. Open system

dissolution conditions probably characterise dynamic groundwater flow systems associated with high hydraulic gradients in the mountainous regions of Namaqualand. These regions are characterized by relatively higher rainfall values, while stable isotopic studies indicate the likelihood of direct rainfall recharge.

The relative distribution of the carbonate ($CO_2$) species for groundwater in Namaqualand, as a function of pH, represents close-system dissolution of carbonate minerals. Equilibrium conditions are real for closed system dissolution conditions. Such systems, that are closed to $CO_{2(g)}$, may characterise more sluggish groundwater flow systems associated with valleys in the lower lying areas of Namaqualand. Most boreholes in Namaqualand are located in these major fault-controlled valleys with relatively lower hydraulic gradients assumed over the depth of water samples collected.

A general pH range for carbonate terrains of between 7 and 8 indicates that open-system conditions are prevalent. However, the relative distribution of the carbonate ($CO_2$) species for groundwater in Namaqualand, as a function of pH, clearly approximates closed-system dissolution. The chemical evolution of a water body may be influenced by a number (or combinations thereof) of factors, including the combination of open- and closed-system conditions between the points of recharge and discharge. In addition, the effects of silicate weathering on the pH and $HCO_3$ content of the groundwater must be considered.

The groundwater is generally over-saturated with regard to quartz and under-saturated with respect to amorphous silica. As a result, quartz and amorphous silica do not exert an important influence on the level of silica in groundwater. The level of dissolved silica, as silicic acid ($H_4SiO_4^0$), for the groundwater of Namaqualand is controlled by the weathering of aluminosilicate minerals with a high silica content indicating the active degradation of silicate minerals.

The groundwater compositions are most likely to be in equilibrium or near-equilibrium with both kaolinite and Na-montmorillonite as weathering products. The even higher salinity groundwater compositions may be in equilibrium or near-equilibrium with Na-montmorillonite as a weathering product. This may again indicate longer residence periods and sluggish flow conditions for the more brackish, slower circulating and relatively older groundwater systems. However, the slow reaction kinetics of silicate minerals (including clay minerals) can result in uncertainties about the stability of the weathering products.

The groundwater thus tends to react with both the primary mineral phases and the reactive weathering products (i.e. crystallized aluminum oxide and hydroxide phases) or at least with an intermediate, meta-stable phase (i.e. amorphous aluminum oxide and hydroxide phases). Molar ratios indicate, however, that the incongruent weathering processes of various aluminosilicate minerals cannot alone account for the groundwater compositions.

**Processes Influencing Groundwater Chemistry**

The groundwater chemistry is dependant on the point of sampling in either a dynamic or an evaporative and sluggish groundwater system. Stacked, multiple flow systems dominate that differ in terms of flow rates and the factors influencing the groundwater flow and chemistry including the recharge rate, hydraulic gradient and hydraulic conductivity. The subsequent sections will clearly illustrate that the rate of groundwater flow influences the reaction rates with primary and secondary mineral phases which in turn influences the resultant groundwater chemistry. Superimposing and probably masking the latter process is the direct infiltration of NaCl dominated precipitation and the preferential dissolution and leaching of the more soluble evaporitic salts during the infiltration process.

The dominant NaCl character of the subterranean waters is a result of either the direct infiltration of NaCl dominated precipitation and the preferential dissolution and leaching of the more soluble evaporitic salts during the infiltration process. The groundwater remains NaCl type water throughout the recorded EC ranges.

- The initial NaCl character of the lower salinity groundwater in the mountainous regions is probably determined by the predominantly NaCl character of the precipitation in areas where direct rainfall recharge is dominant and to a limited extent the preferential dissolution and leaching of highly soluble Na/Cl salts to the subsurface.
- The Na/Cl character of the higher salinity groundwater in the lower lying regions of Namaqualand, is predominantly related to the preferential dissolution and periodic leaching of highly soluble salts, particularly Na/Cl salts, to the subsurface.
- Groundwater sampled in the higher rainfall, mountainous regions is characterised by depleted stable isotopic concentrations. Salinisation of groundwater in the higher lying regions, where direct rainfall recharge dominates, result predominantly from the dissolution of aquifer material and to a limited extent the preferential dissolution and leaching of highly soluble. Both direct rainfall recharge as well as an increasing altitude result in depleted environmental isotopic signatures.
- The positive correlations of EC with the environmental isotopes show that the higher salinity groundwater is generally characterised by enriched stable isotopic values. Higher salinity groundwater is generally associated with the lower rainfall, lower lying regions of Namaqualand. The relation indicates that the salinity of the groundwater in these areas is more than likely derived from the infiltration of previously evaporated surface waters and/or the solution and flushing of evaporative salts in the subsurface. The significant contribution of the dissolution and leaching of evaporitic salts to the salinity of the groundwater, especially in the lower lying regions, mask the contribution of carbonate and silicate weathering processes to the salinity of the groundwater. In addition, considerable evaporation occurs within large diameter wells depending on the relative humidity within the wells.

$NaHCO_3$ type waters, due to the process of refreshening, is observed mainly in the higher lying, higher rainfall areas of Namaqualand. Similar $NaHCO_3$ type waters, in the lower lying regions of Namaqualand, is observed for relative young water intersected in highly conductive fracture zones. Most water sampled for the Namaqualand region is, however, too far down an evolutionary path to reflect $NaHCO_3$ type water.

Active weathering processes, with regard to various mineral phases, are evident throughout the EC range for the lower salinity groundwater. The dilute and relatively aggressive groundwater, associated with higher lying regions, controls the weathering (eg. acid-base reactions) of the mineral phases, while the significant head differences (related to differences in elevation for these mountainous areas) result in dynamic flow systems in which equilibrium is difficult to attain. Weathering products are also continuously removed in such systems. It may thus be inappropriate to apply a thermodynamic approach to characterise the waters in such systems.

A reduction in the weathering capacity, with regard to especially the aluminosilicate and probably the carbonate minerals, is suggested for the relatively deeper, higher salinity groundwater in the lower lying regions of Namaqualand. The reduction in the weathering capacity of the higher salinity groundwater can be related to the infiltration of evaporated waters or the leaching of evaporated salts, the increasing concentrations of dissolved constituents with residence time (i.e. the degree of saturation of the groundwater with various mineral phases), the incongruency relations of various minerals (including carbonates and aluminosilicate minerals), a reduction in the $CO^2_{(aq)}$ (in closed systems), the effects of cation exchange, the common-ion effect or even to the coating of primary minerals by residual clay minerals. The lower lying regions of Namaqualand are characterized by intermittent, periodic recharge events, lower hydraulic gradients within the valley systems and varying hydraulic conductivity values within the saprock to saprolite aquifer zone.

**Groundwater chemistry and major lithological units.**

Groundwater from the intrusive granitic and gneissic rocks generally has higher mean EC values than the meta-sedimentary rocks. This phenomenon can be ascribed to the thermodynamically unstable nature of minerals contained within the granitic and gneissic rocks associated with the emplacement of these rocks at or near the Earth's surface and its exposure to low temperature weathering reactions.

Groundwater from the intrusive granitic and gneissic rocks generally has higher mean pH values than the meta-sedimentary rocks of the Khurisberg subgroup. The meta-sedimentary rocks of the Khurisberg subgroup are composed primarily of 'unreactive' quartzite that is normally less prone to chemical weathering processes with a limited buffering capacity.

The mean concentrations of the anions Cl, $SO_4$ and F, in groundwater are higher for the intrusive rocks than the meta-sedimentary rocks. No distinct trends could be observed in the mean concentrations of $HCO_3$ and $NO_3$ in groundwater for the intrusive rocks compared to the meta-sedimentary rocks.

The mean concentrations of the cations Na, Ca, Mg and Si, in groundwater are higher for the intrusive rocks compared to the meta-sedimentary rocks. An anomalously high, mean Si concentration was recorded for groundwater samples of the Khurisberg subgroup. The boreholes are, however, drilled either on or close to the contact between the schists and meta-quartzites of the Khurisberg subgroup and the augen gneisses of the Nababeep formation (i.e. Little Namaqualand Suite).

The Sr ion thus behaves in a similar manner when compared to the major cations. The mean concentrations of aluminium (Al), boron (B) and zinc (Zn) in groundwater are higher for the intrusive rocks compared to the meta-sedimentary rocks. Most trace elements (i.e. barium, lithium, manganese, phosphate, arsenic and nickel) do not show broad trends when groundwater from intrusive rocks is compared to groundwater from predominantly meta-sedimentary rocks. Anomalously high mean concentrations for the latter trace elements were, however, recorded for individual lithological units, especially for the intrusive rocks. The mean concentrations of copper are relatively higher for groundwater from the intrusive rocks when compared to groundwater from meta-sedimentary rocks, while an opposite trend is observed for iron.

**Groundwater flow patterns at both local and regional scales**

It is possible to spatially distinguish between dilute, shallow circulating and relatively young groundwater systems compared to more brackish, slower circulating and relatively older systems. The relatively dilute end-member is associated with dynamic, actively recharged groundwater systems with rapid through-flow rates occurring in the higher lying mountainous regions, or with infiltration through highly transmissive fracture zones within the lower lying valley systems. The more brackish end-member, associated with the valley systems or the lower lying regions, is characterized by a localized, predominantly vertical flow component (i.e. an infiltration phase associated with the repetitive processes of dissolution and leaching of evaporative salts) and possibly a lateral flow component (i.e. a lateral flow phase driven by reduced gradients within the valleys) that may approximate an intermediate flow system.

The mountainous regions of Leliefontein (i.e Kamiesberg mountain range) and Wildeperdehoek have been identified as regional recharge zones, at different elevations, on the boundaries between the secondary drainage catchments F30 and F50 as well as F30 and F40 respectively. The environmental isotopes as well as the variation and trends in groundwater chemistry have shown that the latter regions can be regarded as no-flow boundaries between the respective secondary drainage catchments limited to the depths of the groundwater sampled (i.e. approximately 80 m below surface). Intermediate to

regional groundwater flow systems may exist with high salinity artesian springs as expressions of such intermediate flow systems that originate in the mountainous regions.

### The sustainability of the groundwater resources

The medium to long-term sustainability of the groundwater resources, particularly with respect to domestic water supply, is a function of the groundwater quantity (i.e. yield) and groundwater quality associated with these fractured crystalline aquifers. The yield is dependent on the frequency and intensity of the rainfall, the rate of recharge, and in particular the physical nature (i.e. storage capacity or the extent of interconnected fracture systems and the rate of through-flow or residence time/accumulation) of these aquifer systems. The groundwater quality reflects the hydrochemical development of the groundwater resource. The exploitability of the aquifer systems for Namaqualand is based on the suggestion that yield represents an upper limiting factor, while the groundwater quality represents a lower limiting factor (Figure 9.1).

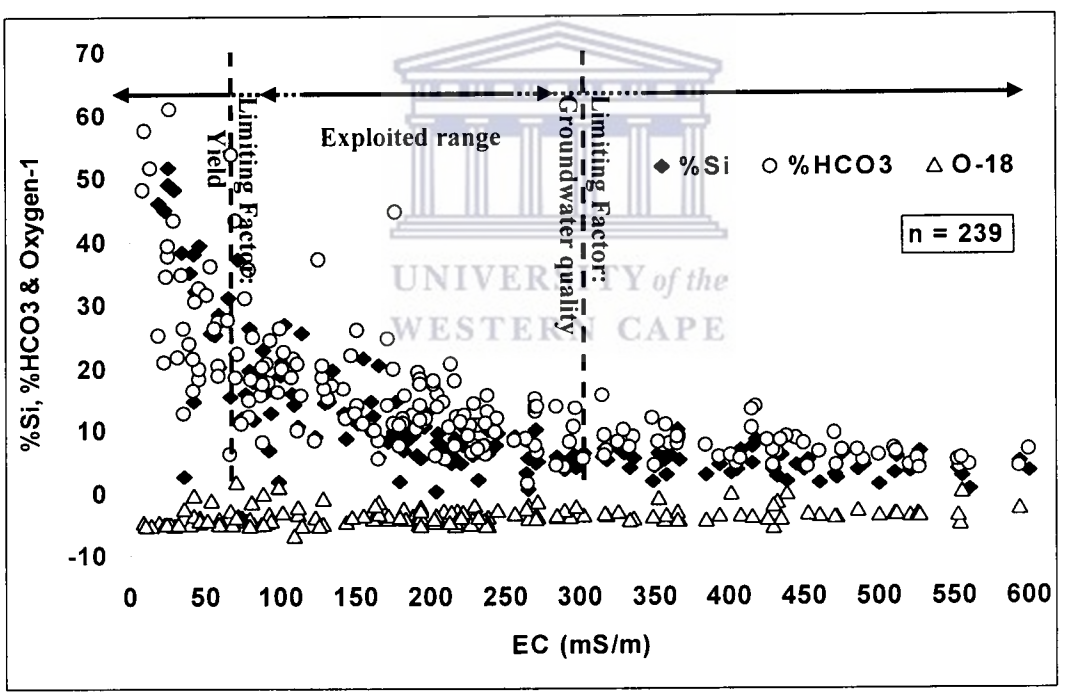


Figure 9.1: Yield and groundwater quality as upper and lower limiting factors for the exploitability of groundwater in fractured, crystalline rocks, Namaqualand.

Springs and large diameter wells commonly have low yields. Dynamic, shallow circulating and relatively young groundwater systems (i.e. predominantly interflow) occur in the higher lying mountainous areas that experience relatively higher rainfall. Such systems can, however, also occur in lower lying valleys due to rapid infiltration and through-flow in the faulted material at the base of the granitic or gneissic domes. The

groundwater compositions are generally undersaturated with regard to most mineral phases (i.e. carbonates, most feldspars and clay minerals) except for silica and albite. The low yields associated with these dynamic groundwater systems are a limiting factor, related to limited storage capacity and rapid through-flow (i.e. low residence time) along major fractures as a result of high hydraulic gradients.

The groundwater quality becomes a limiting factor at higher electrical conductivity values. Slower and deeper circulating groundwater systems dominate in the lower rainfall and lower lying regions. Such groundwater systems probably experience insignificant recharge under present climatic conditions. The groundwater compositions are generally supersaturated with respect to most mineral phases. The groundwater quality, as a limiting factor, is due to the infiltration of evaporated water or the leaching of previously evaporated salts and continuous water-rock interaction as a result of increased residence time under diffused flow conditions associated with reduced hydraulic gradients.

The current exploitable groundwater resource can be defined based on electrical conductivity values ranging mostly above the acceptable limit or target guideline range (DWA&F, 1993 and WRC/DWAF/DOH, 1998) of ≈ or ‹ 70 mS/m and the maximum acceptable limit or limit of no adverse health aspects of approximately 300 mS/m (DWA&F, 1993 and WRC/DWAF/DOH, 1998).

In conclusion, the optimal and sustainable development of the available groundwater resources for the 'problematic' basement aquifer system in the semi-arid to arid Namaqualand region is effected by:

- The 'poor' aquifer characteristics of crystalline rocks. An understanding of the development of the weathered basement aquifer systems is essential. The spatial variation in the hydrochemical development of the groundwater as well as the varying groundwater chemistry at outcrop scale due to compartmentalized flow processes. Basement aquifers are furthermore characterized by extreme heterogeneity in terms of their hydraulic properties.

- The difficulty of defining the aquifer geometry, at various scales, with an acceptable degree of certainty. This may influence the calculations for sustainable yield of the aquifer system. The granitic and gneissic rocks have been subjected to intense deformation.

- The absence of other significant aquifer systems in the region, except for alluvial systems in certain localities.

- The very low average annual recharge values for the Namaqualand region, except for the higher lying, higher rainfall mountainous regions.

- Boreholes were generally drilled to depths of 60 to 80m below surface. Deeper boreholes will increase the available saturated thickness of the fractured aquifer system.

- The lack of a regional groundwater management programme. Water levels and groundwater quality monitoring are limited to a few villages. A sustained and representative groundwater monitoring programme is essential.

### 9.3: Further research

Additional research is needed to further the aims of this project. The researchers need to:

- Conduct experiments to develop the most appropriate sampling procedures and rainfall collectors for the region. Provide a detailed account of the chemical character of the precipitation.

- Perform detailed textural and mineralogical studies for the regolith.

- Investigate the relationship between the regional groundwater flow systems and the deeper flowing artesian groundwater systems that may or may not be controlled by the same hydraulic system.

- Characterise spatially the conditions (in terms of open- or closed-system dissolution due to the available of $CO_2$) of mineral dissolution with reference to a specific flow system (under both unsaturated and saturated flow conditions).

- Define the perceived relation between groundwater storage and flow and the most dilatational (i.e. 'open') fracture orientations resulting from complex and multiple deformation phases.

- Determine the average annual recharge for the region and the spatial variations in the recharge characteristics.

### 9.4: Specific recommendations

- Conduct monitoring programmes, in terms of both groundwater quantity and quality that reflect the geohydrological system, in addition to monitoring the response of a borehole(s) to abstraction for water supply purposes.
- Provide detailed geohydrological and geological logging of newly drilled boreholes.
- The optimal positioning for monitoring boreholes, with respect to the pumping borehole.
- Conduct well managed aquifer test-pumping programmes, with due reference to those parts of a geohydrological system investigated, in order to perform applicable sustainable yield calculations.

# REFERENCES

Acocks, J.P.H., 1954. Veld types of South Africa. Third edition. Botanical Survey Memoir 57.

Acworth, R. I., 1987. The development of crystalline basement aquifers in a tropical environment. Quarterly Journal of Engineering Geology, London, Vol. 20, pp. 265 -272.

Albat, H. M. 1984. The Proterozoic granulite facies terrane around Kliprand, Namaqualand Metamorphic Complex. Ph.D. Thesis, Dept. of Geology, University of Cape Town, South Africa. In: Chamber of Mines Precambrian Research Unit. Bulletin 33.

Allsopp, H. L., Köstlin, E. O., Welke, H. J., Kröner, A. and Blignaut, H. J., 1979. Rb-Sr and U-Pb geochronology of late Precambrian- early Palaeozoic igneous activity in the Richterveld (South Africa) and southern South West Africa. Trans. Geol. Soc. S. Afr., 82, pp.185- 204.

Andersen, N. J. B., Faurie, J. N. and Fernandez, L. M., 1986. Geophysical investigations of the Vaalputs radioactive waste disposl site in the Republic of South Africa. Conference on the treatment and containmant of radioactive waste and its disposal in arid environments, In: Randwaste, Ainsle, L.C. (eds). ISBN 0-86960-832-0.

Andreoli, M. A. G.., Andersen, N. J. B., Levin, M. and Niemand, N., 1986. Geology of the Vaalputs radioactive waste disposal site in the Republic of South Africa. Explanatory notes for the geological map of the site on the scale 1: 25 000. Conference on the treatment and containmant of radioactive waste and its disposal in arid environments, In: Randwaste, Ainsle, L.C. (eds). ISBN 0-86960-832-0.

Andreoli, M. A. G., Doucouré M., van Bever Donker J., Brandt D. and Andersen N. J. B. 1996. Neotectonics of Southern Africa- a review. Africa Geoscience Review, Vol. 3, No 1. pp.1- 16.

Appelo, C. A. J. and Postma, D., 1993. Geochemistry, groundwater and pollution. Balkema, Rotterdam. 536pp.

Ashley, R. P. and Lloyd, J. W., 1978. An example of the use of factor analysis and cluster analysis in groundwater chemistry interpretation. Journal of Hydrology, 39, pp.355- 364.

Atomic Energy Corporation, 1990. Correlation between rainfall and groundwater quality throughout the Republic of South Africa. Addendum to: A report on the results of phase one of the groundwater quality of the Republic of South Africa. AEC- 89/73 (B/R).

Barton, E.S., Harmer, R.E. and Burger, A.J., 1981. Isotopic studies in the Namaqua-Natal Mobile Belt. Abstracts 19 th Congress Geol. Soc. S. Afr., 12 – 13.

Benedict, P. C., Wiid, D. De N, Cornelissen, A.K., 1964. Progress report on the geology of O'okiep Copper District. In S. H. Haughton, (ed), The geology of some ore deposits in Southern Africa, Geol. Soc. S. Afr., Vol. 2. Johannesburg.

Blignaut, H. J., 1977. Structural- metamorphic imprint on part of the Namaqua mobile belt in South West Africa. Bull. Precambrian Res. Unit, Univ. Cape Town, 23, 197 pp.



Blignaut, H.J., Van Aswegen, G.J., Van der Merwe, S. W and Colliston, W.P., 1983. The Namaqualand Geotraverse and environs: part of the Proterozoic Namaqua mobile belt. Spec. Publ. Geol. Soc. S. Afr. 10:pp.1-29.

Bredenkamp, D., Levin, M. and van Blerk, J., 1991. Countrywide characterization of groundwater quality specifically in relation to average annual rainfall distribution. Conference Proceedings: Ground Water Quality and Pollution, Midrand, August 1991.

Bridges, E.M., 1990. World geomorphology. Cambridge University Press. New York. 260 pp.

Brink, W. C., 1950. The geology, structure and petrology of the Nuwerus area, Cape Province. Univ. Stellenbosch Ann., No.26A.

Burger, and Coetzee, F. J., 1973. Radiometric age measurements on rocks from South Africa to the end of 1971. Bull. Geol. Surv. S. Afr., 58.

Campbell, E. E, Parker-Nance, T and Bate, G. C., 1992. A Compilation of the information on the magnitude, nature and importance of coastal aquifers in Southern Africa. WRC Report No 370/1/92.

Chilton, P. J. and Foster, S. S. D. 1995. Hydrogeological characterisation and water-supply potential of basement aquifers in tropical africa. Hydrologeology Journal, V. 3, No. 1 pp.36-49.

Clifford, T. N., Barton, E. S., Retief, E. A., Rex, D. C. and Fanning, C. M., 1995. A crustal progenitor for the intrusive anorthosite charnockite kindred of the cupriferous Koperberg Suite, O'Okiep district, Namaqualand, South Africa – New isotope data for the country rocks and the intrusives. Journal of Petrology, Feb. Vol. 36, No. 1.

Colliston, W. P. and Schoch, A. E., 1996. Proterozoic metavolcanic rocks and associated metasediments along the Orange River in the Pofadder terrane, Namaqua Mobile Belt. S. Afr. J. Geol., 99, pp 309 – 325.

Commonwealth Science Council (CSC), 1990. Groundwater exploration and development in crystalline basement aquifers. Proceedings of workshop, Zimbabwe, June 1987. Technical Paper (TP) 273, 1990.

Cornelissen, A. K., Verwoerd, W. J., 1975. The Bushmanland kimberlites and related rocks. In L.H. Ahrens, J. B. Dawson, A, R. Duncan, A. J. Erlank (eds.), Physics and chemistry of the earth. Oxford: Pergamon.

Craig, H., 1961. Isotopic variations in meteoric waters. Science, 133: pp.1702-1703.

Craig, H., 1961. Standard for reporting concentrations of deuterium and oxygen- 18 in natural water. Science, 133, pp.1833- 1834.

Dansgaard, W. 1964. Stable isotopes in precipitation. Tellus, 16 (4): pp.436-468.

Dawdy, D. R. and Feth, J. H., 1967. Application of factor analysis in study of chemistry of groundwater quality, Mojave River Valley, California. Water Resource Research, 3,2, pp.505- 510.

De Beer, J. H. and Blume, J., 1986. Resistivity studies on the Vaalputs radioactive waste disposal site. Conference on the treatment and containmant of radioactive waste and its disposal in arid environments, In: Randwaste, Ainsle, L.C. (eds). ISBN 0-86960-832-0.

De Jager, D. H and Simpson, N., 1962. Wollastonite near the Garies, Namaqualand. Ann. Geol. Surv. S. Afr., 1.

De Villiers, J and Songe, P. G., 1959. The geology of the Richtersveld. Geol. Surv. S. Afr., Mem. 48.

De Wit, M. C. J., 1993. Cainozoic evolution of Drainage systems in the North-Western Cape. Ph.D. Thesis, dept. of Geology. University of Cape Town. South Africa.



Department of Water Affairs and Forestry, 1993. South African Water Quality Guidelines. Domestic Water Use, 1.

Dingle, R. V., Siesser, W. G and Newton, A. R., 1983. Mesozoic and Tertiary Geology of southern Africa. A. A. Balkema. Rotterdam. 375pp.

Dixey, F., 1955. Africa, some considerations of age and origin. Transactions Geological Society of South Africa 58, pp.265-280.

Domenico P.A. and Schwartz, F.W., 1990. Physical and Chemical Hydrogeology. John Wiley and Sons. New York.

Driessen, P. M and Dudal, R,. 1991. The major soils of the world. Agricultural University Wageningen. Department of Soil Science and Geology.

Ellis, F., 1988. Die Gronde van die Karoo. PhD Thesis, University Stellenbosch, South Africa.

Esterhuyse, C. J., 1987. Grondwaterondersoek in die Leliefontein-gebied, distrik Namakwaland.Dreineringstreke F30, F40 en F50. Departement van Waterwese. Verslag No GH 3556.

Esterhuyse, C. J., 1990. Garies, Distrik Namakwaland: Evaluering van grondwaterbronne met spesifieke verwysing na kwaliteit and kwantiteit. Drieneringstreek F50. Departement van Waterwese. Verslag GH 3672.

Esterhuyse, C. J., 1990. Namakwaland-Sentraal: Ondersoek na die grondwaterbronne te Leliefontein-Wes as aanvullende bron aan Karkams. Drieneringstreek F50. Departement van Waterwese. Verslag No GH3685.

Esterhuyse, C. J., 1991.Grondwaterondersoek in die Steinkopf-Kleurlinggebied, distrik Namakwaland. Departement van Waterwese. Tegniese verslag GH 3737.

Freeze, R. and Cherry, J. A., 1979. Groundwater. Prentice-Hall Inc, New Jersey.

Gibson, R. L., Robb, L. J., Kirstes, A. F. M. and Cawthorn, R. G., 1996. Regional setting and geological evolution of the Okiep Copper Distric, Namaqualand, South Africa. S. Afr. J. Geol., 99 (2), pp.107- 120.

Gieske, A., 1992. Dynamics of groundwater recharge. A case study in semi-arid eastern Botswana. PhD thesis, Vrije Universiteit, Netherlands.

Gilchrist, A. R. and Summersfiled, M. A., 1994. Tectonic models of passive margin evolution and their implications for theories of long-term landscape development. In: Kirkby, M. J. (Ed), process models and theoretical geomorphology, John Wiley, New York, pp.58- 84.

Gilchrist, A. R., Kooi, H and Beaumont, C., 1994. Post-Gondwana geomorphic evolution of southwestern Africa: Implications for the control on landscape development from observations and numerical experiments. Journal of Geophysical Research 99, B6, : pp.12211-12228.

Goldich, S., 1938. A study in rock weathering. Journal of Geology, 46 (1), pp. 17 – 58.

Gustafson G. and Krasny J.,1994. Crystalline rock aquifers: Their occurrences, use and importance. Applied Hydrogeology. Volume 2. Issue 2, pp 64- 75.

Harris, C., Oom, B. M. and Diamond, R. E., 1999. A preliminary investigation of the oxygen and hydrogen isotope hydrlogy of the greater Cape Town area and an assessment of the potential for using stable isotopes as tracers. Water S.A., 25, 1, pp.15- 24.

Hartnady, C., Joubert, P and Stowe, C., 1985. Proterozoic Crustal Evolution in Southwestern Africa. Episodes, Vol. 8, No. 4. pp.236-244.

Haughton, S. H., 1969. Geological history of Southern Africa. Geol. Soc. S. Afr. Cape and Transvaal Printers Ltd., Cape Town.

Issar, A. and Gat, J., 1981. Environmental isotope as a tool for hydrogeological research in an arid basin. Ground Water, Vol. 19 No. 5, pp.490- 494.

Jack, A. M., 1980. The geology of Western Namaqualand. Ph. D. Thesis. Dept of Geology. University of Cape Town. South Africa. In: chamber of Mines Precambrian Research Unit, Bulletin 29.

Johnston, L. M. 1982. A review of the geochemistry of groundwater in crystalline rocks. Rept. Atomic Energy of Canada Ltd. TR-154. 99pp.

Joubert, P., 1971. The regional tectonism of gneisses of part of Namaqualand. Ph. D. Thesis. Dept of Geology. University of Cape Town. South Africa. In: chamber of Mines Precambrian Research Unit, Bulletin 29.

Kay, R. L. F., 1985. Review of applications of hydrogeochemistry to groundwater development in tropical basement and regolith. Rep. British Geological Survey WD/OS/85/4. 51 pp.

Kay, R. L. F., 1987. Groundwater exploration and development in crystalline aquifers. Technical Paper 273. Volume II, Sessions 6 to 15, pp. 69-92. Commonwealth Science Council.

Kay, R. L. F., 1987. Hydrochemistry applied to development of crystalline bedrock aquifers. Groundwater exploration and development in crysatlline basement aquifers, Vol. II, Series No. CSC(89)WMR-13, Technical paper 273.

King, L. C., 1951. South African scenery. Oliver and Boyd. Edinburgh, 699 pp.

King, L. C. and King, L. A., 1959. A reappraisal of the Natal monocline. S. Afr. Geogr. J., 41, pp.15- 30.

King, L. C. 1967. South African scenery: a textbook of geomorphology, 3rd edition (rev.), Oliver and Boyd, Edinburgh and London, 308pp.

Kooi, H. and Beaumont, C., 1994. Escarpment evolution on high-elevation rifted margins: insights derived from a surface- processed model that combines diffusion, advection and reaction. J. Geophy. Res. 99, B6, pp.12 191- 12 209.

Kooi, H and Beaumont, C., 1996. Large-scale geomorphology: Classical concepts reconciled and integrated with contemporary ideas via a surface processing model.

Langmuir D., 1997. Aqueous environmental geochemistry. Prentice Hall, New Jersey.

Levin, M., Hambleton- Jones, B. B., Raubenheimer, E. and Niemand, N., 1986. Geohydrology of the Vaalputs radioactive waste disposal facility. Conference on the treatment and containmant of radioactive waste and its disposal in arid environments, In: Randwaste, Ainsle, L.C. (eds). ISBN 0-86960-832-0.

Levinson, A. A., 1980. Introduction to exploration geochemistry. Second edition. Applied Publishing Ltd., Calgary.

Lipson, R. D., 1978. Some aspects of the geology of part of the aggeneysberge and surrounding gneisses. Namaqualand. Unpubl. M. Sc. thesis, Univ. Witwatersrand.

Lloyd, J. W. and Heathcote, J. A., 1985. Natural inorganic hydrochemistry in relation to groundwater. An introduction. Claredon Press, Oxford.

Lloyd, J. W., 1999. Water Resources of hard rock aquifers in arid and semi-arid areas. From Lloyd, J. E. (ed), 1999. Water Resources of hard rock aquifers in arid and semi-arid areas. Unesco Publishing, Studies and Reports in Hydrology. No 58, pp 13-19.

Locsey, K. L. and Cox, M. E., 2000. Chemical character of groundwater in a basalt aquifer, North Queensland, Australia. In: Groundwater – Past achievements and future challenges. Sililo et al. (Eds.). A. A. Balkema. pp. 555 – 560.

Low, A. B and Rebelo A. G., (1996). Vegetation of South Africa, Lesotho and Swaziland. Department of Environmental Affairs and Tourism. Pretoria.

Mabbutt, J. A., 1955. Erosion surfaces in Namaqualand and the ages of surface deposits in the southern-western Kalahari. Trans. Geol. Soc. S. Afr. 58, : 13-30.

Marais, J. A. H and Joubert, P., 1980a. Little Namaqualand suite, Handbook Geol. Surv. S. Afr. 8

Marais, J. A. H. and Joubert, P., 1980b. Little Namaqualand suite, Handbook Geol. Surv. S. Afr. 8.

McCarthy, T. S., Moon, B. P and Lewin, M., 1985. Geomorphology of the western Bushmanland plateau, Namaqualand, South Africa. S. Afr. Geogr. J. 67, : pp160-178.

McFarelane, M. J., 1987. Groundwater Exploration and development in crystalline basement aquifers. Technical paper 273. Volume II, Sessions 6 to 15, pp. 93-146. Commonwealth Science Council.

McFarlane, M. J., 1987. A review ot the development of tropical weathering profiles with particular reference to leaching history and with examples from Malawi and Zimbabwe. Groundwater exploration and development in crysatlline basement aquifers, Vol. II, Series No. CSC(89)WMR-13, Technical paper 273.

Merlivat, L. and Jouzel, J., 1979. Global climatic interpretation of the deuterium-oxygen-18 relationship for precipitation. J. of Geophys. Res. 84: 5029 – 5033.

Midgeley, D. C, Pitman, W. V and Middleton, B. J., 1994. Surface Water Resources of South Africa. Water Research Commission Report No. 298/1/94.



Mook, W. G., 1994. Principle of isotope hydrology: Introduction cource on isotope hydrology. Centre of Isotope Research, University of Groningen.

Moon, B.P. and Dardis, G.F. (Eds.), 1988. The geomorphology of southern Africa. Southern Book Publishers (Pty) Ltd. Pretoria. 320 pp.

Moore, J. M., 1977. The geology of Namiesberg, Northern Cape. Bull. Precambr. Res. Unit, Univ. Cape Town, 20, 69pp.

Moore, J. M., 1989. A comparative study of metamorphosed supracrustal rocks from the western Namaqualand Metamorphic Complex. . Bull. Precambr. Res. Unit, Univ. Cape Town, 37.

Ollier, C.D. 1984. Weathering. Geomorphology Text. Second edition. Longman Inc. New York. 270 pp.

Ollier, C. D., 1985. Morphotectonics of continental margins with Great Escarpments. In: Morisawa & J. T. Hack, Tectonic Geomorphology. Allen and Unwin, Boston and London, pp. pp.3-25.

Olofsson, B .O., 1991c.Groundwater conditions when tunneling in hard crystalline rocks- a study of water flow and water chemistry at Staverhult, the Bolmen tunnel, S. Sweden. Swedish Rock Engineering Research Foundation (BeFo), Research report 160:4/91.

Olofsson, B .O., 1993. Flow of groundwater from soil to crystalline rock- A review. IAH Congress. Hydrogeology of Hard Rocks, Banks S. B. and Banks D. (eds). ISBN 82-7385-093-5.

Parker, L. V., 1994. The effects of groundwater sampling devices on water quality: A literature review. Groundwater Monitoring Review, Spring 1994, pp.130- 141.

Partridge, T. C. and Maud, R. R., 1987. Geomorphic evolution of southern Africa since the Mesozoic. South African Journal of Geology, 90, pp.179-208.

Partridge T.C. and Maud R.R., 2000. Macro-scale geomorphic evolution of southern Africa. In:TL Partridge and RR Maud (eds.) The Cenozoic of southern Africa. Oxford Univ. Press, New York, pp.3- 18.

Partridge, T.C., 1998. Of diamonds, dinosaurs and diastrophism: 150 million years of landscape evolution in Southern Africa. S. Afr. J. Geol. 101 (3), pp.165- 184.

Pickford, M., Senut, B., Mein, P., Gommery, D., Morales, J., Soria, D., Nieto, M. and Ward, J., 1996. Prelimanary results of new excavations at Arrisdrift, middle Miocene of southern Namibia. C. R. Acad. Sci., Paris, 322, pp.991- 996.

Piper, A. M., 1953. A graphic procedure in the heochemical interpretation of water analyses. Groundwater notes, Geochemistry No. 12. United States Department of the Interior, Geological Survey, Washington D.C.

Plummer, L. N., Prestemon, E. C. and Parkhurst, D. L., 1992. An interview code (NETPATH) for modeling net geochemical reactions along a flow path. Water- Resources Investigation Report 91- 4078. U.S. Geological Survey.

Ransome, I. G. D. and de Wit, M. J., 1992. Prelimanary investigations into a microplate model for the South Western Cape. In: Inversion tectonics of the Cape Fold Belt, Karoo, and Cretaceous basins of southern Africa (Edited by de Wit, M.J. and Ransome, I. G. D.), 257-266pp. Balkema, Rotterdam, Holland.

Rebouças, Aldo Da C., 1993. Groundwater development in Precambrian shield of South America and West side Africa. . IAH Congress. Hydrogeology of Hard Rocks, Banks S. B. and Banks D. (eds). ISBN 82-7385-093-5.

Reid, D. L., 1977. Geochemistry of Precambrian igneous rocks in the lower Orange River region. Kroner, A. Roggers, A. W., 1904. Geological survey of the North-western part of van Rhyn's Dorp. Ann. Rept. Geol. Com. C. G. H., 9.

Reid, D.L., 1979a. Total Rock Rb-Sr and U-Th-Pd isotopic studies of precambrian metavolcanic rocks in the lower in the lower orange River region, Southern Africa. Earth Planet. Sci. Lett., 42, pp.368-378.

Reid, D. L., 1979b. Age relationships within the Mid-Proterozoic Vioolsdrif Batholith, lower Orange River region. Trans. Geol. Soc. S. Afr., 82, 305 – 311.

Reid, D. L. and Barton, E.S., 1983. Geochemical characterization of granitoids in the Namaqualand Geotraverse. Spec. Publ. Geol. Soc. S. Afr., 10 67 – 82.

Reuning, E., 1931. Contribution to the geology and palaeontology of the Bushmanland Plateau. Trans. Roy. Soc. S. Afr., 19

Rice, R.J., 1988. Fundamentals of geomorphology. Second edition. Longman Scientific & Technical and John Wiley & Sons, Inc. New York. 420 pp.

Rogers, A. W., 1913. The Nama system in the Cape Province. Trans. Geol. Comm. Cape Good Hope. 16(1911)

Rogers, A. W., 1915. Geology of part of Namaqualand. Trans. Geol. Soc. S. Afr. 60.

Sami, K., 1992. Recharge mechanisms and geochemical processes in a semi-arid sedimentary basin, Eastern Cape, South Africa. Elsevier Science Publishers; pp.26-30.

Sami, K., Neumann, I., Gqiba, D., de Kock, G. and Grantham, G., 2002. Status groundwater exploration in geologically complex and problematic terrain – Guidelines. WRC Report No. 966/1/02.

Soil Classification Working Group, 1991. Soil classification a Taxonomic system for South Africa. Soil and Irrigation Research Institute, Department of Agricultural development, Pretoria.



Stumm, W. and Morgan, J. J., 1981. Aquatic chemistry. Second edition, Wiley, New York.

Summerfield, M. A., 1985. Plate tectonics and landforms development of the African continent. In: M. Morisha and J. T. Hack (eds). Tectonic Geomorphology, Allen and Unwin, Boston, : pp.27 - 51.

Summerfield, M. A., 1988. Global tectonics and landform development. Progress in physical Geography 12, pp. 389-404.

Summerfield, M.A., 1991. Global geomorphology: An introduction to the study of landforms. Longman Scientific and Technical Publishers (Pty) Ltd. New York. 537 pp.

Tankard, A. J., Jackson, M. P. , Eriksson, K. A., Hobday, D. K., Hunter, D. R. and Minter, W. E. L., 1982. Crustal Evolution of South Africa: 3.8 Billion Years of Earth History. Springer-Verlag, New York.

Taylor, R. and Howard, K., 2000. A tectono-geomorphic model of the hydrogeology of deeply weathered crystalline rock: Evidence from Uganda. Hydrogeology Journal, 8, pp. 279 – 294.

Theart, H. F. J., 1980. The geology of the Precambrian terrane in parts of Western Namaqualand. Ph. D, Dept. Thesis. Dept of Geology, University of Cape Town, South Africa. In: chamber of Mines Precambrian Research Unit, Bulletin 30.

Toens, P. D. and Visser, D., 1991. Geohidrologiese ondersoek uitgevoer in die oostelike gedeelte van die Leliefontein Landelike gebied gedurende die tydperk Julie 1991, Verslag No 27. P D Toens and Associates.

Toens, P. D. and Visser, D., 1991. Grondwater voorkoms in die alluviale sediment van die Khiesrivier-Leliefontein Landelike Gebied, Verslag No 29. P D Toens and Associates.



Toens, P. D., Levin, M and Verhagen, B.Th. 1991. Results of pumping tests and environmental isotope analysis at Steinkopf. Toens Progress Report no. 40. Cape Town.

Toens, P. D., Visser, D., du Toit, A., Muller, A. and Otto, J., 1991. Verslag oor die geohidrologiese en geologiese ondersoek uitgevoer op die Witbank plase. P. D. Toens en Genote, Verslag Nr. 20.

Toens, P. D., Ebrahim-Trollope, Visser, D., 1993. Garies Meet Projek. P. D. Toens en Genote, Verslag Nr. 3.

Toens, P. D., Visser, D., Ebrahim-Trollope, R. and Muller, R., 1993. The loaction and management of ground water resources in the rural areas of the North West Cape. P. D. Toens and Associates c.c.

Toens, P. D., Visser, D., Ebrahim-Trollope, R. and du Toit, A., 1994. Landelike gebied Pella veesuipings- veslag oor die grondwater ondersoek an daaropvolgende boorprogram wat gedurende Oktober 1993 uitgevoer was P.D. Toens en Genote, Verslag Nr. 69.

Toens, P. D., Visser, D., Ebrahim-Trollope, R. and du Toit, A., 1995. Hidrogeologiese ondersoek van die Richtersveld Nationale Park. P.D. Toens en Genote, Verslag Nr. 78.

Toens, P. D., Esterhuyse, C. J and Visser, D., 1996. A preliminary assessment of the hydrogeology of the Northern Cape, Report No. 1. March 1996.

Toens, P. D., Visser, D. and Esterhuyse, C. J., 1996. Northern Cape community water supplies and sanitation: A prelimanary assessment of the hydrogeology of the Northern Cape. Toens & Partners, Report No. 1.

Tredoux, G., 1993. A preliminary investigation of the nitrate content of groundwater and limitation of the nitrate input. WRC Report No: 368/1/93. ISBN 1 86845 009 0.

Twidale, C.R., 1976. Analysis of landforms. John Wiley and Sons. Brisbane. 572 pp.



Twidale, C.R., 1982. Granite landforms. Elsevier Scientific Publishing Company. Amsterdam. 372 pp.

Twidale, C.R., 1988. Granite landscapes. In: Moon, B.P. and Dardis, G.F. (Eds.). The geomorphology of southern Africa. Southern Book Publishers (Pty) Ltd. Pretoria. 320 pp.

Tyson , P. D. and Partridge, T. C.,2000. Evolution of Cenozoic climates. In: TL Partridge and RR Maud (eds.) The Cenozoic of southern Africa. Oxford Univ. Press, New York.

Usunoff, E. J. and Gruzman- Gruzman, A. 1989. Estimation of natural groundwater recharge in the Karoo aquifers of South Africa. Journal of Hydrology, 121, pp.395- 419.

Van Aswegen, G., 1983. The Gladkop suite-the grey and pink gneisses of Steinkopf. In: Botha, B. J. V. (Ed), Namaqua Metamorphic Complex. Spec. Publ. Publ. Geol. Soc. Afr. 10.

Van Aswegen, G., Strydom, D., Colliston, W.P., Praekelt, H. E., Schoch, A. E., Blignaut, H. J., Botha, B. J. V. and van der Merwe, S. W., 1987. The structural- stratigraphic development of part of the Namaqua Metamorphic Complex, South Africa- An example of Proterozoic major thrust tectonics. American Geophysical Union, 207-216pp.

Van der Beek, P. and Cloetingh, S., 1995. Morphotectonic evolution of rifted continental margins: Interferences from a coupled tectonic-surface processes model and fission-track thermochronology. Tectonics 14: pp.406-421.

Van der Merwe, S. W. and Botha, B. J. V., 1989. Groothoek thrust belt in western Namaqualand; an example of a mid-crustal structure. S. Afr. J. geol., 92.

Van der Merwe, S.W., 1995. The relationship between thrusting, vertical shear and open folds in the western part of the Namaqua mobile belt. S.Afr., J.Geol. 98:pp.68-77.

Van der Sommen, J. J and Geirnaert, W., 1988. On the continuity of aquifer systems on the crystalline basement of Burkina Faso. I. Simmers (ed): Estimation of Natural Groundwater Recharge. D. Reidel Publishing Company. pp.29-45.



Van der Watt, H. v. H. and van Rooyen, T. H., 1990. A glossary of soil science. The soil science society of South Africa, Pretoria.

Van Zyl, D., 1967. The geology of the O'okiep copper mine, Namaqualand. Ann. Univ. Stellenbosch, 42.

Vegter, J. R., 2001. Hydrogeology of groundwater. Region 1: Makoppa Dome. WRC Report No. TT 135/00. ISBN No. 1 86845 643 9.

Vegter, J. R., 2001. Hydrogeology of groundwater. Region 3: Limpopo Granulite-Gneiss Belt. WRC Report No. TT 136/00. ISBN No. 1 86845 644 7.

Verhagen, B. Th. and Levin, M., 1986. Environmental isotopes assist in the site assessment of the Vaalputs radioactive waste disposal facility. Conference on the treatment and containmant of radioactive waste and its disposal in arid environments, In: Randwaste, Ainsle, L.C. (eds). ISBN 0-86960-832-0.

Visser, D. J. L. (Ed)., 1989. Explanation of the 1:1.000.000 geological map, fourth edition, 1984. Dept. Of Mineral and Energy Affairs, Government Printer. ISBN 0-621-12516-4.

Watt, H .v. H and Rooyen, T.H., 1990. A Glossary of Soil Science.The Soil Science Society of South Africa. Pretoria.

Weaver, J. M. C., Talma, A. S. and Cave`, L. C., 1996. Geochemistry and isotopes for resource evaluation in the fractured rocks aquifers of the Table Mountain Group. Report No. ENV/S- C96058. Council for Scientific and Industrial research, Stellenbosch.

WRC/DWAF/DOH, 1998. Quality of domestic water supplies. Vol. 1: Assessment Guide. WRC No: TT 101/98. ISBN No: 1 86845 416 9.

Wright, E. P. and Burgess, W. G., 1992. The hydrogeology of crystalline basement aquifers in Africa. Geological Society Special Bulletin No. 66. The Geological Society London.

Wright, E. P., 1992. The hydrogeology of crystalline basement aquifers in Africa. Wright, EP and Burgess, WG (eds.) The hydrogeology of crystalline basement aquifers in Africa. Geological Society Special Publication Number 66, pp.1-27.

Xu pers comm., 2000. Groundwater Group, Earth Science Department, University of the Western Cape.

Xu pers comm., 2001. Groundwater Group, Earth Science Department, University of the Western Cape.

Zoback M.L., 1992. First- and Second- Order Patterns of Stress in the Lithosphere: The World Stress Map Project. Journal of Geophysical Research, Vol. 97, No. B8, pp.11 703- 11 728.

# APPENDIX I

# DATABASE

| Lat | Long | Name | Field EC | Field pH | CO3 (mg/l) | HCO3 (mg/l) | Na (mg/l) |
|---|---|---|---|---|---|---|---|
| -30.1822 | 18.27417 | COU2_fontain | 2240 | 8.3 | 0.00 | 221.50 | 4521.00 |
| -30.1261 | 18.25667 | COU3_windmill | 209 | 7.2 | 0.00 | 294.90 | 261.82 |
| -30.2253 | 18.13806 | NOU1_well | 177 | 6.6 | 2.72 | 77.50 | 241.83 |
| -30.1769 | 18.18528 | 91LF88_well | 119 | 6.8 | 0.00 | 96.90 | 163.64 |
| -29.9344 | 18.04583 | NUW12_windmill | 718 | 8.1 | 21.79 | 94.20 | 1106.20 |
| -29.8911 | 18.10444 | POT1_windmill | 918 | 7.3 | 27.24 | 110.80 | 1412.97 |
| -29.925 | 18.15028 | RIETFONTEIN3_win | 581 | 7.0 | 47.03 | 135.70 | 809.65 |
| -29.8283 | 18.33194 | DAP1_windmill | 358 | 7.3 | 38.14 | 157.90 | 514.46 |
| -29.8272 | 18.32611 | DAP2_windmill | 371 | 7.4 | 54.48 | 193.90 | 527.05 |
| 0 | 0 | YBE1_windmill | 409 | 8.3 | 68.10 | 166.20 | 586.81 |
| -29.9583 | 18.01333 | YBEII_windpump | 368 | 7.1 | 68.10 | 166.20 | 514.10 |
| 0 | 0 | ROODEPOORT/372 | 431 | 6.8 | 0.00 | 180.00 | 443.21 |
| -30.2839 | 18.48389 | PLAT1_windmill | 254 | 7.6 | 13.85 | 249.20 | 382.43 |
| -30.3183 | 18.48639 | PLAT2_well | 1382 | 9.1 | 0.00 | 124.60 | 2367.13 |
| -30.3208 | 18.48944 | PLAT3_reservior | 246 | 7.6 | 10.90 | 213.20 | 299.26 |
| -29.965 | 18.06389 | NUW2_windmill | 383 | 7.1 | 46.31 | 127.40 | 454.57 |
| -29.9853 | 18.05194 | NUW3_windmill | 230 | 8.0 | 40.86 | 83.10 | 268.75 |
| -29.9158 | 18.42139 | GAM1_windmill | 213 | 7.7 | 40.86 | 193.90 | 293.98 |
| -30.0236 | 17.98389 | THD1_Elec_pump | 213 | 6.5 | 21.79 | 135.70 | 267.52 |
| -30.1094 | 18.015 | NAK1_Elec_pump | 110 | 7.2 | 40.86 | 152.30 | 150.52 |
| -30.0525 | 17.95444 | NHO1_windmill | 230 | 7.1 | 40.86 | 138.50 | 254.09 |
| -29.9128 | 17.96722 | DRO1_windmill | 105 | 7.3 | 0.00 | 110.80 | 115.85 |
| -30.1833 | 17.93833 | W/HOEK_well | 74 | 6.6 | 0.00 | 27.69 | 105.57 |
| -29.8517 | 17.71889 | SOUTKLOOF1_winc | 224 | 6.9 | 0.00 | 177.20 | 280.80 |
| -29.8436 | 17.77028 | KLI1_windmill | 100 | 7.2 | 13.62 | 119.10 | 97.58 |
| -29.8633 | 17.73583 | KLI2_windmill | 256 | 6.8 | 10.90 | 185.50 | 303.96 |
| -29.8628 | 17.73667 | KLI3_windmill | 237 | 6.5 | 0.00 | 144.00 | 286.38 |
| -29.8544 | 17.78917 | JAK1_windmill | 200 | 6.6 | 13.62 | 110.80 | 233.73 |
| -29.8547 | 17.78917 | JAK2_Elec_pump | 187 | 6.7 | 0.00 | 138.50 | 168.38 |
| -30.235 | 18.03833 | AGTER2_windmill | 68 | 7.8 | 0.00 | 69.20 | 72.73 |
| -30.2436 | 18.05472 | AGTER3_windmill | 93 | 8.9 | 0.00 | 85.85 | 84.28 |
| -30.0794 | 18.01028 | FIL1_Elec_pump | 151 | 7.0 | 13.62 | 96.90 | 170.03 |
| -30.0411 | 17.98528 | ANE1_windmill | 346 | 8.1 | 27.24 | 124.60 | 414.37 |
| -30.1258 | 18.01694 | ANE2_windmill | 329 | 6.9 | 68.10 | 166.20 | 308.14 |
| -30.1389 | 17.87139 | HAAS2_windmill | 293 | 6.6 | 27.24 | 138.50 | 312.72 |
| -29.8189 | 17.79 | NUWR1_windmill | 220 | 7.0 | 0.00 | 293.60 | 217.61 |
| -29.8111 | 17.50111 | F1_Fontain | 85 | 7.4 | 0.00 | 55.40 | 112.74 |
| -29.7808 | 17.50333 | F2_Fontain | 82 | 6.1 | 0.00 | 49.80 | 114.37 |
| -29.8039 | 17.50667 | KG93/106_windmill | 134 | 6.9 | 5.44 | 58.20 | 175.13 |
| -29.7903 | 17.50222 | KG93/107_windmill | 208 | 6.6 | 49.03 | 191.10 | 293.90 |
| -30.1489 | 17.85 | RACHEL_windmill | 258 | 6.8 | 21.79 | 163.40 | 369.61 |
| -30.2378 | 17.75861 | GBERG_windmill | 1016 | 6.8 | 81.72 | 193.90 | 1598.14 |
| -29.9592 | 17.975 | DED1_Well | 472 | 7.1 | 10.90 | 116.30 | 681.50 |
| -29.9019 | 18.15667 | RIETFONTEIN2_Buf | 543 | 7.2 | 40.86 | 132.90 | 891.95 |
| -29.7858 | 17.50528 | KG93/110_BuffelsR_ | 189 | 7.3 | 68.10 | 235.40 | 298.00 |
| -29.7386 | 17.63639 | KG93/118_BuffelsR_ | 196 | 7.1 | 40.86 | 110.80 | 285.14 |
| -30.07 | 18.27 | ROOI1_Well | 205 | 7.3 | 27.24 | 124.60 | 265.29 |
| -29.7364 | 17.63722 | BUFS1_Well | 189 | 6.8 | 27.24 | 166.20 | 260.52 |
| -29.7719 | 17.66 | BUFS5_well | 317 | 7.4 | 27.24 | 166.20 | 525.81 |
| -29.7703 | 17.65972 | BUFS3_Well | 230 | 6.6 | 10.90 | 102.50 | 301.88 |
| -29.6811 | 17.62639 | SKA1_Artesian | 550 | 6.9 | 0.00 | 180.00 | 714.37 |
| -29.6767 | 17.60222 | SKA2_Well | 2290 | 7.5 | 32.69 | 238.20 | 4255.17 |

| Lat | Long | Name | Field EC | Field pH | CO3 (mg/l) | HCO3 (mg/l) | Na (mg/l) |
|---|---|---|---|---|---|---|---|
| -30.0358 | 18.27639 | KAM1_Well | 316 | 7.3 | 0.00 | 69.20 | 379.68 |
| -30.4214 | 17.91222 | KLIPVLEI_windmill | 1161 | 7.2 | 27.24 | 180.00 | 1812.42 |
| -30.2089 | 17.70556 | BOKSKRAAL_windı | 662 | 7.3 | 68.10 | 235.40 | 993.14 |
| -29.8758 | 18.18861 | RIET4_windmill | 247 | 7.2 | 13.62 | 152.30 | 363.35 |
| -30.13 | 18.02 | Anagas | 465 | 6.7 | No data | 306.00 | 347.17 |
| -30.11 | 17.92 | Arkoep | 220 | 7.3 | No data | 114.00 | 171.57 |
| -29.71 | 17.9 | BeginWeer | 134 | 7.6 | No data | 138.00 | 106.51 |
| -29.74 | 17.93 | Biesiesfontein | 168 | 7.4 | No data | 111.00 | 178.57 |
| -29.73 | 17.88 | Bloustasie | 394 | 6.9 | No data | 101.00 | 254.70 |
| -29.72 | 17.89 | Blouputs_windmill | 210 | 7.7 | No data | 108.00 | 187.07 |
| -29.72 | 17.89 | Bloustasie_windmill | 250 | 7.8 | No data | 151.00 | 216.98 |
| -29.73 | 17.88 | Biesiesfontein_Elec | 209 | 7.9 | No data | 192.00 | 187.28 |
| -29.71 | 17.91 | Bloustasie | 280 | 8.2 | No data | 118.00 | 223.70 |
| -30.2 | 18.05 | Bovlei | 87 | 6.8 | No data | 108.00 | 85.74 |
| -29.77 | 17.94 | Deurdrif | 63 | 7.9 | No data | 91.00 | 64.34 |
| -29.77 | 17.94 | Deurdrif | 37 | 7.2 | No data | 77.00 | 41.89 |
| -29.78 | 17.95 | Deurdrif | 344 | 7.6 | No data | 279.00 | 347.73 |
| -29.78 | 17.94 | Deurdrif | 358 | 7.2 | No data | 192.00 | 354.29 |
| -29.95 | 17.97 | DeDraai | 82 | 7.4 | No data | 111.00 | 61.18 |
| -29.96 | 17.97 | DeDraai | 805 | 7.6 | No data | 252.00 | 935.75 |
| -29.74 | 17.94 | Grashoek | 328 | 7.6 | No data | 192.00 | 232.26 |
| -29.74 | 17.94 | Grashoek | 393 | 6.9 | No data | 168.00 | 254.89 |
| -29.74 | 17.94 | GoeieHoop | 271 | 7.7 | No data | 124.00 | 187.87 |
| -29.79 | 17.96 | HoudeMond | 29 | 7.3 | No data | 77.00 | 27.91 |
| -29.8 | 17.96 | HoudeMond | 439 | 7.7 | No data | 141.00 | 449.49 |
| -29.8 | 17.97 | HoudeMond | 385 | 7.5 | No data | 104.00 | 387.94 |
| -29.99 | 17.96 | Kleinfontein | 1074 | 6.7 | No data | 403.00 | 1093.00 |
| -29.99 | 17.96 | Kleinfontein | 136 | 7.4 | No data | 168.00 | 119.18 |
| -29.97 | 17.97 | Kleinfontein | 554 | 7.3 | No data | 299.00 | 609.64 |
| -30.49 | 17.87 | Klipfontein | 45 | 7.0 | No data | 24.00 | 66.55 |
| -30.49 | 17.87 | Klipfontein | 727 | 7.7 | No data | 182.00 | 908.77 |
| -30.06 | 17.91 | Komri | 577 | 6.9 | No data | 192.00 | 412.25 |
| -29.77 | 17.86 | Krymekaar | 93 | 6.4 | No data | 77.00 | 98.09 |
| -29.73 | 17.87 | Lammershoek_Elec | 281 | 7.4 | No data | 245.00 | 220.90 |
| 29.73 | 17.87 | Lammershoek | 245 | 7.3 | No data | 121.00 | 217.34 |
| -29.84 | 17.96 | Mesklip | 159 | 7.2 | No data | 111.00 | 130.99 |
| -29.84 | 17.86 | Mesklip | 175 | 7.7 | No data | 131.00 | 135.43 |
| -29.82 | 17.85 | Mesklip | 246 | 6.7 | No data | 131.00 | 270.08 |
| -29.84 | 17.85 | Mesklip | 588 | 6.9 | No data | 124.00 | 534.68 |
| -29.84 | 17.93 | OuHoek | 111 | 8.1 | No data | 101.00 | 117.18 |
| -29.84 | 17.92 | OuHoek | 301 | 6.9 | No data | 87.00 | 195.78 |
| -29.72 | 17.9 | RanchoAmigo | 680 | 8.5 | No data | 155.00 | 724.08 |
| -30.03 | 17.89 | Rotnoskop | 503 | 7.4 | No data | 205.00 | 404.86 |
| -29.82 | 17.95 | Rockoptel | 234 | 7.7 | No data | 108.00 | 214.03 |
| -29.99 | 17.99 | Ybeep | 562 | 7.9 | No data | 202.00 | 605.19 |
| -30.0133 | 17.8225 | BLOUSYFER | 704 | 8.2 | 8.29 | 210.60 | 758.54 |
| -30.045 | 17.7583 | KANARIESFONTEIN | 662 | 6.9 | 0.00 | 314.60 | 635.68 |
| -30.0014 | 17.6908 | BRANDBERG | 711 | 6.8 | 0.00 | 148.90 | 793.92 |
| -29.9086 | 17.7844 | KORINGHUIS | 248 | 6.5 | 0.00 | 84.25 | 212.17 |
| -29.9028 | 17.7825 | SANDKRAAL | 270 | 7.5 | 0.00 | 146.00 | 237.48 |
| -29.9206 | 17.7572 | WITDAM | 231 | 6.6 | 0.00 | 106.70 | 232.96 |
| -29.9172 | 17.7442 | LUISKRAAL | 490 | 7.2 | 0.00 | 264.00 | 481.56 |

| Lat | Long | Name | Field EC | Field pH | CO3 (mg/l) | HCO3 (mg/l) | Na (mg/l) |
|---|---|---|---|---|---|---|---|
| -29.9325 | 17.705 | **BUFFELSRIVER_WI** | 299 | 7.7 | 0.00 | 165.70 | 289.98 |
| -29.9244 | 17.6444 | **Wildeperdehoek_Pa** | 476 | 7.5 | 0.00 | 314.60 | 492.36 |
| -30.0056 | 17.6719 | **KEURBOS** | 1567 | 6.8 | 0.00 | 269.60 | 2286.19 |
| -30.0397 | 17.7342 | **KEURBOS** | 829 | 7.2 | 0.00 | 382.00 | 849.96 |
| -29.9994 | 17.7778 | **ARREGAS** | 840 | 6.9 | 0.00 | 227.50 | 732.16 |
| -29.8928 | 17.6328 | **OUBEEB** | 406 | 7.4 | 0.00 | 95.49 | 459.14 |
| -29.8794 | 17.5744 | **MISKRAAL** | 537 | 8.3 | 16.57 | 140.40 | 541.74 |
| -29.8364 | 17.6128 | **SANAGAS** | 308 | 6.9 | 0.00 | 106.70 | 315.43 |
| -29.8175 | 17.61721 | **SANAGAS** | 287 | 8.0 | 0.00 | 64.59 | 262.51 |
| -29.8019 | 17.5597 | **BOKKRAAL** | 119 | 6.7 | 0.00 | 42.13 | 123.33 |
| -29.8536 | 17.6233 | **SANAGAS** | 587 | 7.3 | 0.00 | 269.60 | 550.33 |
| -29.7928 | 17.5633 | **BOKKRAAL** | 579 | 7.2 | 0.00 | 126.40 | 607.16 |
| -30.2517 | 18.05778 | **Leliefontein** | 77 | 7.0 | No data | 171.40 | 79.36 |
| -30.3306 | 18.08917 | **Leliefontein** | 94 | 7.6 | No data | 97.30 | 97.74 |
| -30.3489 | 18.0925 | **Leliefontein** | 83 | 7.4 | No data | 200.70 | 56.55 |
| -30.3422 | 18.08611 | **Leliefontein** | 30 | 6.8 | No data | 114.30 | 25.42 |
| -30.315 | 18.0675 | **Leliefontein** | 50 | 7.0 | No data | 106.60 | 58.98 |
| -30.3272 | 18.06861 | **Leliefontein** | 17 | 6.2 | No data | 30.90 | 15.22 |
| -30.3361 | 18.08944 | **Leliefontein** | 17 | 6.9 | No data | 41.70 | 17.22 |
| No_value | No_value | **Leliefontein** | 13 | 6.1 | No data | 41.90 | 14.51 |
| -30.3403 | 18.11722 | **Leliefontein** | 31 | 6.1 | No data | 57.10 | 32.74 |
| 0 | 0 | **Leliefontein** | 64 | 8.0 | No data | 88.60 | 70.24 |
| 0 | 0 | **Leliefontein** | 60 | 7.0 | No data | 138.50 | 103.83 |
| -30.0797 | 18.23639 | **Rooifontein** | 208 | 6.7 | No data | 216.20 | 359.30 |
| -30.1039 | 18.23639 | **Rooifontein** | 160 | 6.4 | No data | 264.10 | 167.60 |
| -30.0764 | 18.26667 | **Rooifontein** | 614 | 6.6 | No data | 463.30 | 1007.00 |
| -30.1406 | 18.23389 | **Rooifontein** | 267 | 7.0 | No data | 237.80 | 400.60 |
| -30.0931 | 18.19361 | **Rooifontein** | 75 | 7.0 | No data | 135.90 | 81.63 |
| -30.1536 | 18.24083 | **Rooifontein** | 203 | 7.0 | No data | 231.60 | 225.00 |
| -30.0664 | 18.26944 | **Rooifontein** | 137 | 6.4 | No data | 149.80 | 181.30 |
| -30.0378 | 18.27444 | **Kamassies** | 142 | 7.3 | No data | 152.90 | 220.60 |
| -30.0406 | 18.27444 | **Kamassies** | 135 | 7.6 | No data | 308.80 | 298.10 |
| -30.0172 | 18.36278 | **Kamassies** | 205 | 6.7 | No data | 216.20 | 237.30 |
| -30.0222 | 18.35611 | **Kamassies** | 206 | 7.1 | No data | 203.80 | 221.10 |
| -30.0528 | 18.20194 | **Kamassies** | 156 | 7.5 | No data | 208.50 | 194.20 |
| -30.0358 | 18.27667 | **Kamassies** | 118 | 6.9 | No data | 146.70 | 164.30 |
| -30.0236 | 18.35556 | **Kamassies** | 213 | 7.1 | No data | 180.70 | 224.50 |
| -30.0528 | 18.20583 | **Kamassies** | 298 | 7.0 | No data | 250.20 | 427.40 |
| -30.1739 | 18.19472 | **Nourivier** | 358 | 6.6 | No data | 206.90 | 436.10 |
| -30.26 | 18.20278 | **Nourivier** | 478 | 6.2 | No data | 227.00 | 481.50 |
| -30.2219 | 18.1025 | **Nourivier** | 55 | 7.8 | No data | 111.20 | 56.20 |
| -30.1928 | 18.15417 | **Nourivier** | 85 | 5.9 | No data | 92.70 | 134.90 |
| -30.2264 | 18.13694 | **Nourivier** | 169 | 6.0 | No data | 100.40 | 263.70 |
| -30.1981 | 18.19806 | **Nourivier** | 278 | 7.1 | No data | 231.60 | 306.20 |
| -30.2453 | 18.08278 | **Nourivier** | 35 | 7.0 | No data | 44.80 | 45.29 |
| -30.2431 | 18.1425 | **Nourivier** | 42 | 8.0 | No data | 64.90 | 50.84 |
| -29.5167 | 19.93917 | **BRANDKLOOF** | 106 | 7.4 | No data | 102.00 | 105.60 |
| -29.4667 | 17.77 | **BULLETRAP** | 161 | 7.1 | No data | 197.00 | 211.60 |
| -29.45 | 17.77389 | **BULLETRAP** | 184 | 7.3 | No data | 134.00 | 235.60 |
| -29.45 | 17.77194 | **BULLETRAP** | 361 | 6.9 | No data | 130.00 | 350.70 |
| -29.4833 | 17.83444 | **BULLETRAP** | 101 | 6.7 | No data | 58.00 | 145.70 |
| -29.5667 | 18.07222 | **BULLETRAP** | 335 | 7.2 | No data | 140.00 | 434.00 |

| Lat | Long | Name | Field EC | Field pH | CO3 (mg/l) | HCO3 (mg/l) | Na (mg/l) |
|---|---|---|---|---|---|---|---|
| -29.5167 | 17.98333 | CONCORDIA | 232 | 7.6 | No data | 95.00 | 238.50 |
| -29.5833 | 17.7925 | DOOIFONTEIN | 267 | 6.9 | No data | 175.00 | 335.10 |
| -29.6833 | 17.84 | DROEDAP | 220 | 6.8 | No data | 99.00 | 177.70 |
| -29.75 | 18.04083 | EENDOORN | 183 | 6.8 | No data | 170.00 | 204.10 |
| -29.7 | 17.90944 | FONTEINTJIE | 89 | 7.0 | No data | 64.00 | 90.09 |
| -29.4167 | 17.75083 | GEMSBOK | 326 | 6.7 | No data | 109.00 | 281.50 |
| -29.7667 | 17.99083 | GOEGAB | 98 | 6.9 | No data | 47.00 | 80.49 |
| -29.7167 | 18.01194 | GOEGAB | 99 | 6.9 | No data | 89.00 | 113.30 |
| -29.6333 | 18.25472 | GROOT KAU | 241 | 7.1 | No data | 184.00 | 340.00 |
| -29.6333 | 18.20361 | GROOT KAU | 276 | 7.2 | No data | 143.00 | 331.60 |
| -29.7 | 17.97111 | GROOT KAU | 266 | 6.9 | No data | 159.00 | 349.50 |
| -29.6167 | 17.83667 | HOMEB_alluvium | 166 | 6.4 | No data | 98.00 | 162.00 |
| -29.6 | 18.21667 | KAIP | 148 | 7.1 | No data | 120.00 | 186.60 |
| -29.6167 | 17.80722 | KLIPDAM | 86 | 8.5 | No data | 74.00 | 98.96 |
| -29.4167 | 17.77389 | KLIPDAM | 55 | 6.6 | No data | 70.00 | 73.35 |
| -29.4333 | 17.90111 | KOEGAS | 633 | 7.0 | No data | 146.00 | 615.10 |
| -29.7 | 17.90472 | KOPPERBERG | 565 | 7.2 | No data | 210.00 | 513.40 |
| -29.6833 | 17.92472 | KOPPERBERG | 181 | 8.0 | No data | 0.02 | 172.20 |
| -29.6667 | 17.90028 | KOPPERBERG | 497 | 7.0 | No data | 139.00 | 511.70 |
| -29.5167 | 18.0925 | KWEEKFONTEIN | 208 | 7.0 | No data | 91.00 | 204.10 |
| -29.5333 | 18.09806 | KWEEKFONTEIN | 128 | 7.1 | No data | 50.00 | 124.10 |
| -29.5333 | 18.0925 | KWEEKFONTEIN | 91 | 8.1 | No data | 86.00 | 101.70 |
| -29.6667 | 17.92722 | KWEEKFONTEIN | 82 | 7.2 | No data | 54.00 | 85.67 |
| -29.4833 | 17.72306 | MARAS | 95 | 7.8 | No data | 95.30 | 111.40 |
| -29.55 | 19.00444 | MIDDELPOS | 294 | 7.3 | No data | 308.00 | 305.20 |
| -29.7 | 17.67083 | NARIES | 123 | 6.6 | No data | 70.00 | 131.30 |
| -29.5667 | 17.58778 | NIGRAMOEP MINE | 981 | 6.3 | No data | 71.00 | 1228.00 |
| -29.65 | 17.58833 | NIGRAMOEP MINE | 84 | 7.1 | No data | 50.00 | 88.80 |
| -29.6667 | 17.97083 | OLYNPUTS | 49 | 6.1 | No data | 27.00 | 52.99 |
| -29.5333 | 18.0925 | RATELKRAAL | 105 | 7.4 | No data | 116.00 | 131.00 |
| -29.5333 | 18.05944 | RATELKRAAL | 514 | 6.6 | No data | 115.00 | 655.30 |
| -29.5833 | 18.06444 | RATELKRAAL | 71 | 7.4 | No data | 80.00 | 82.40 |
| -29.5667 | 18.12111 | RATELKRAAL | 389 | 6.7 | No data | 93.00 | 359.70 |
| -29.6 | 18.15639 | RATELKRAAL | 71 | 6.6 | No data | 94.00 | 61.10 |
| -29.8 | 18.13861 | RIETFONTEIN | 290 | 6.5 | No data | 82.00 | 263.90 |
| -29.45 | 17.75444 | ROOIWATER | 130 | 6.8 | No data | 78.00 | 115.20 |
| -29.3333 | 17.91889 | SABIES | 583 | 7.2 | No data | 165.00 | 659.90 |
| -29.7167 | 18.05278 | SILVERFONTEIN | 86 | 7.5 | No data | 115.00 | 83.44 |
| -29.5667 | 17.58333 | SILWERFONTEIN | 169 | 6.8 | No data | 60.00 | 160.40 |
| -29.5167 | 18.08917 | SPEKTAKEL MINE | 846 | 7.4 | No data | 102.00 | 1124.00 |
| -29.7 | 17.8875 | SPRINGBOK | 307 | 7.4 | No data | 166.00 | 302.60 |
| -29.7167 | 17.92083 | SPRINGBOK | 681 | 6.7 | No data | 147.00 | 662.50 |
| -29.7 | 17.88806 | SPRINGBOK GHOLI | 438 | 7.0 | No data | 117.00 | 447.50 |
| -29.4333 | 17.95611 | SWARTPUTS | 329 | 7.2 | No data | 123.00 | 294.80 |
| -29.7 | 17.67 | TWEEDAM | 159 | 7.2 | No data | 102.00 | 165.60 |
| -29.25 | 18.06278 | VAALDAM | 115 | 7.7 | No data | 75.00 | 122.60 |

| Name | Cl (mg/l) | Ca (mg/l) | K (mg/l) | Mg (mg/l) | SO4 (mg/l) | NO3(NO2)-N | F (mg/l) |
|---|---|---|---|---|---|---|---|
| COU2_fontain | 9063.00 | 1014.10 | 71.09 | 992.08 | 878.58 | 0.33 | 1.60 |
| COU3_windmill | 585.90 | 98.87 | 2.39 | 71.25 | 177.00 | 3.90 | 4.50 |
| NOU1_well | 439.90 | 56.58 | 5.37 | 53.55 | 70.17 | 0.61 | 0.40 |
| 91LF88_well | 466.40 | 41.24 | 4.13 | 35.53 | 56.54 | <0.1 | 0.90 |
| NUW12_windmil | 2331.80 | 462.47 | 13.59 | 217.62 | 452.46 | 0.57 | 2.90 |
| POT1_windmill | 2921.40 | 657.68 | 10.55 | 273.51 | 671.36 | 9.60 | 4.30 |
| RIETFONTEIN3_ | 1680.70 | 333.60 | 19.68 | 203.86 | 346.13 | 12.00 | 1.10 |
| DAP1_windmill | 915.10 | 202.11 | 17.98 | 106.99 | 247.80 | 13.00 | 1.90 |
| DAP2_windmill | 967.90 | 215.94 | 18.21 | 112.93 | 254.53 | 15.00 | 1.90 |
| YBE1_windmill | 1082.30 | 195.52 | 9.72 | 176.57 | 369.23 | 0.32 | 2.20 |
| YBEII_windpum | 941.50 | 191.35 | 8.34 | 153.64 | 320.74 | 0.32 | 2.20 |
| ROODEPOORT/: | 1214.00 | 191.87 | 3.94 | 176.85 | 271.45 | 5.20 | 2.70 |
| PLAT1_windmill | 550.00 | 72.34 | 7.46 | 36.61 | 148.16 | 0.84 | 2.60 |
| PLAT2_well | 4752.00 | 384.72 | 55.62 | 439.84 | 673.52 | 0.35 | 3.50 |
| PLAT3_reservio | 585.20 | 115.19 | 10.78 | 63.04 | 121.91 | 10.00 | 2.20 |
| NUW2_windmill | 1047.10 | 227.87 | 10.58 | 164.97 | 237.84 | 11.00 | 1.30 |
| NUW3_windmill | 571.90 | 142.70 | 6.55 | 89.93 | 172.95 | 2.60 | 1.90 |
| GAM1_windmill | 484.00 | 93.13 | 10.84 | 74.39 | 155.84 | 3.40 | 2.70 |
| THD1_Elec_pum | 439.90 | 76.00 | 1.41 | 62.01 | 151.03 | 0.18 | 2.30 |
| NAK1_Elec_pur | 300.50 | 39.83 | 1.27 | 37.51 | 72.82 | 8.80 | 2.40 |
| NHO1_windmill | 457.60 | 101.19 | 3.66 | 96.52 | 179.23 | 23.00 | 1.50 |
| DRO1_windmill | 308.00 | 44.09 | 1.18 | 26.07 | 58.95 | 2.60 | 2.10 |
| W/HOEK_well | 219.90 | 18.40 | 2.15 | 17.57 | 35.08 | 1.90 | 0.30 |
| SOUTKLOOF1_v | 492.80 | 117.39 | 9.59 | 61.76 | 147.80 | 5.60 | 3.10 |
| KLI1_windmill | 202.40 | 77.01 | 4.19 | 22.38 | 85.09 | <0.1 | 2.40 |
| KLI2_windmill | 624.80 | 132.04 | 4.89 | 78.31 | 138.53 | 3.70 | 2.50 |
| KLI3_windmill | 572.00 | 120.94 | 5.06 | 63.06 | 137.02 | 7.90 | 1.60 |
| JAK1_windmill | 440.00 | 92.72 | 3.50 | 52.77 | 123.05 | 12.00 | 2.10 |
| JAK2_Elec_pum | 413.60 | 111.00 | 5.69 | 67.63 | 104.87 | 13.00 | 1.80 |
| AGTER2_windm | 149.60 | 20.44 | 0.13 | 12.50 | 10.82 | 4.70 | 0.40 |
| AGTER3_windm | 193.50 | 42.56 | 0.20 | 24.27 | 35.56 | 0.61 | 2.00 |
| FIL1_Elec_pump | 343.20 | 75.81 | 2.87 | 47.11 | 99.31 | <0.1 | 4.30 |
| ANE1_windmill | 809.50 | 152.63 | 3.00 | 129.09 | 244.32 | 1.40 | 4.00 |
| ANE2_windmill | 818.30 | 210.88 | 2.80 | 183.93 | 219.92 | 20.00 | 1.50 |
| HAAS2_windmil | 747.90 | 196.19 | 10.57 | 120.04 | 202.37 | 5.00 | 1.70 |
| NUWR1_windmi | 572.00 | 122.57 | 5.52 | 92.09 | 116.46 | 0.16 | 1.30 |
| F1_Fontain | 211.20 | 14.06 | 5.59 | 28.69 | 30.52 | 1.70 | 0.30 |
| F2_Fontain | 211.20 | 13.74 | 5.65 | 29.24 | 31.03 | 2.20 | 0.50 |
| KG93/106_windr | 316.80 | 22.55 | 7.69 | 46.21 | 63.45 | 2.30 | 0.30 |
| KG93/107_windr | 439.70 | 43.09 | 13.01 | 77.85 | 96.53 | 3.60 | 0.60 |
| RACHEL_windm | 571.90 | 96.65 | 3.59 | 77.41 | 183.92 | 12.00 | 2.00 |
| GBERG_windmi | 3018.20 | 392.15 | 10.56 | 381.42 | 580.44 | 1.80 | 4.50 |
| DED1_Well | 1372.70 | 220.29 | 7.13 | 139.94 | 181.67 | <0.1 | 0.90 |
| RIETFONTEIN2_ | 1513.50 | 227.57 | 11.43 | 153.53 | 353.28 | 6.30 | 1.30 |
| KG93/110_Buffe | 369.60 | 38.05 | 8.63 | 59.42 | 62.81 | <0.1 | 0.80 |
| KG93/118_Buffe | 457.60 | 86.09 | 9.19 | 56.98 | 134.96 | 0.93 | 1.00 |
| ROOI1_Well | 475.20 | 83.98 | 7.51 | 57.64 | 84.53 | 0.13 | 1.20 |
| BUFS1_Well | 440.00 | 87.06 | 11.59 | 54.74 | 108.99 | <0.1 | 0.90 |
| BUFS5_well | 747.90 | 137.30 | 16.96 | 78.17 | 289.36 | 16.00 | 1.20 |
| BUFS3_Well | 545.60 | 110.55 | 10.71 | 74.60 | 240.35 | <0.1 | 0.50 |
| SKA1_Artesian | 1566.00 | 277.15 | 7.56 | 167.78 | 426.75 | 2.60 | 2.20 |
| SKA2_Well | 8183.00 | 1316.57 | 64.62 | 888.59 | 2568.49 | 0.16 | 2.00 |

| Name | Cl (mg/l) | Ca (mg/l) | K (mg/l) | Mg (mg/l) | SO4 (mg/l) | +NO2 as N ( | F (mg/l) |
|---|---|---|---|---|---|---|---|
| KAM1_Well | 774.30 | 144.82 | 8.28 | 95.58 | 181.81 | 7.70 | 1.50 |
| KLIPVLEI_windr | 3722.10 | 399.04 | 21.01 | 493.62 | 584.16 | 2.70 | 3.80 |
| BOKSKRAAL_w | 1795.10 | 274.08 | 10.08 | 248.15 | 417.43 | 4.80 | 3.10 |
| RIET4_windmill | 598.40 | 111.57 | 5.64 | 64.22 | 150.16 | 7.10 | 2.10 |
| Anagas | 903.00 | 234.29 | 3.44 | 110.65 | 294.90 | 3.40 | 1.50 |
| Arkoep | 473.00 | 94.82 | 4.82 | 67.90 | 87.18 | <0.1 | 2.60 |
| BeginWeer | 301.00 | 55.94 | 2.76 | 41.75 | 72.06 | 1.30 | 2.70 |
| Biesiesfontein | 370.00 | 70.40 | 1.53 | 42.91 | 104.23 | 2.00 | 3.30 |
| Bloustasie | 731.00 | 196.42 | 2.78 | 110.74 | 235.83 | 26.00 | 1.40 |
| Blouputs_windn | 413.00 | 89.53 | 1.67 | 58.27 | 117.31 | 1.20 | 2.80 |
| Bloustasie_wind | 429.00 | 103.49 | 1.56 | 73.25 | 167.28 | 9.40 | 2.50 |
| Biesiesfontein_E | 362.00 | 97.27 | 2.13 | 55.48 | 122.40 | <0.1 | 2.80 |
| Bloustasie | 568.00 | 110.87 | 3.87 | 90.28 | 146.94 | 1.20 | 2.50 |
| Bovlei | 138.00 | 32.88 | 1.80 | 32.65 | 67.37 | 10.80 | 1.10 |
| Deurdrif | 112.00 | 28.79 | 1.63 | 14.85 | 49.39 | <0.1 | 2.50 |
| Deurdrif | 69.00 | 16.28 | 1.71 | 5.60 | 19.99 | 2.30 | 0.60 |
| Deurdrif | 705.00 | 170.37 | 4.13 | 105.76 | 243.61 | 0.60 | 3.00 |
| Deurdrif | 808.00 | 194.95 | 2.23 | 98.75 | 283.23 | 0.10 | 2.50 |
| DeDraai | 138.00 | 39.16 | 1.85 | 23.86 | 40.94 | 1.20 | 2.60 |
| DeDraai | 2133.00 | 285.69 | 9.99 | 110.74 | 448.76 | 81.00 | 3.30 |
| Grashoek | 740.00 | 216.34 | 2.91 | 110.65 | 274.03 | 0.90 | 2.50 |
| Grashoek | 938.00 | 273.44 | 3.70 | 110.80 | 303.02 | 5.50 | 2.20 |
| GoeieHoop | 516.00 | 188.49 | 2.69 | 86.18 | 209.81 | <0.1 | 2.70 |
| HoudeMond | 52.00 | 12.72 | 0.00 | 5.45 | 23.56 | 1.30 | 1.30 |
| HoudeMond | 1487.00 | 276.59 | 2.38 | 87.68 | 254.99 | 1.30 | 3.80 |
| HoudeMond | 1170.00 | 230.82 | 2.53 | 72.90 | 223.56 | 1.10 | 3.80 |
| Kleinfontein | 2493.00 | 303.41 | 5.13 | 110.34 | 631.23 | 69.00 | 3.00 |
| Kleinfontein | 284.00 | 52.04 | 2.59 | 29.41 | 71.37 | 1.10 | 0.60 |
| Kleinfontein | 1513.00 | 164.62 | 6.55 | 110.77 | 402.86 | 2.30 | 3.00 |
| Klipfontein | 86.00 | 1.62 | 1.62 | 1.92 | 12.40 | 0.30 | 0.10 |
| Klipfontein | 1393.00 | 216.02 | 17.75 | 110.84 | 348.40 | 1.40 | 2.80 |
| Komri | 1350.00 | 286.15 | 7.59 | 110.64 | 278.93 | 22.00 | 1.30 |
| Krymekaar | 206.00 | 35.15 | 1.83 | 19.00 | 70.90 | 2.20 | 0.40 |
| Lammershoek_E | 705.00 | 130.49 | 3.78 | 86.32 | 206.03 | 0.20 | 2.10 |
| Lammershoek | 438.00 | 89.30 | 1.67 | 71.70 | 155.20 | 4.60 | 1.70 |
| Mesklip | 293.00 | 86.45 | 2.22 | 36.52 | 92.26 | 2.80 | 2.50 |
| Mesklip | 310.00 | 110.53 | 2.31 | 30.54 | 97.20 | 0.70 | 2.60 |
| Mesklip | 421.00 | 78.45 | 1.12 | 52.46 | 197.79 | 1.40 | 2.00 |
| Mesklip | 1006.00 | 258.88 | 3.80 | 110.75 | 443.96 | <0.1 | 2.00 |
| OuHoek | 189.00 | 51.22 | 1.41 | 18.99 | 57.47 | <0.1 | 3.30 |
| OuHoek | 722.00 | 200.58 | 2.75 | 87.64 | 201.94 | 4.00 | 2.30 |
| RanchoAmigo | 1315.00 | 220.17 | 17.62 | 110.69 | 841.17 | 20.00 | 0.00 |
| Rotnoskop | 791.00 | 261.00 | 9.31 | 110.75 | 355.14 | 23.00 | 2.90 |
| Rockoptel | 439.00 | 104.57 | 2.65 | 46.32 | 114.81 | 0.70 | 2.70 |
| Ybeep | 963.00 | 244.47 | 4.46 | 100.71 | 528.51 | <0.1 | 2.60 |
| BLOUSYFER | 1773.00 | 243.95 | 9.99 | 228.45 | 409.47 | 4.20 | 2.90 |
| KANARIESFONT | 1521.00 | 215.40 | 12.95 | 207.33 | 321.02 | 4.00 | 2.40 |
| BRANDBERG | 1647.00 | 229.90 | 8.51 | 162.35 | 394.98 | 21.80 | 2.60 |
| KORINGHUIS | 504.00 | 68.05 | 7.52 | 73.12 | 124.08 | 14.70 | 0.50 |
| SANDKRAAL | 540.00 | 103.96 | 3.95 | 68.13 | 134.21 | 4.90 | 2.50 |
| WITDAM | 468.00 | 58.52 | 9.21 | 47.17 | 112.45 | 3.80 | 0.70 |
| LUISKRAAL | 1098.00 | 190.58 | 6.95 | 127.44 | 225.99 | 0.50 | 3.40 |

| Name | Cl (mg/l) | Ca (mg/l) | K (mg/l) | Mg (mg/l) | SO4 (mg/l) | +NO2 as N ( | F (mg/l) |
|---|---|---|---|---|---|---|---|
| BUFFELSRIVER | 638.90 | 141.08 | 6.35 | 49.05 | 153.62 | 0.10 | 3.40 |
| Wildeperdehoek | 1179.00 | 183.39 | 8.06 | 118.95 | 247.99 | 0.00 | 3.00 |
| KEURBOS | 5093.90 | 488.55 | 11.21 | 403.95 | 1008.70 | 1.80 | 3.50 |
| KEURBOS | 2501.00 | 372.60 | 17.97 | 338.38 | 666.96 | 2.00 | 2.80 |
| ARREGAS | 2628.00 | 483.50 | 21.77 | 317.57 | 567.84 | 13.10 | 2.10 |
| OUBEEB | 828.00 | 115.57 | 4.94 | 89.16 | 185.01 | 8.40 | 3.40 |
| MISKRAAL | 1062.00 | 191.64 | 6.38 | 163.83 | 290.89 | 6.20 | 2.40 |
| SANAGAS | 738.00 | 67.13 | 5.78 | 91.09 | 122.09 | 1.20 | 1.00 |
| SANAGAS | 522.00 | 95.27 | 7.14 | 62.84 | 94.55 | 0.00 | 2.20 |
| BOKKRAAL | 243.00 | 20.46 | 2.34 | 23.47 | 50.43 | 2.20 | 1.00 |
| SANAGAS | 1431.00 | 276.55 | 8.97 | 161.05 | 246.75 | 1.30 | 2.80 |
| BOKKRAAL | 1476.00 | 189.85 | 3.93 | 182.54 | 321.35 | 7.80 | 3.50 |
| Leliefontein | 43.60 | 33.94 | 0.88 | 0.38 | 56.77 | <0.1 | 2.50 |
| Leliefontein | 209.00 | 41.56 | 3.27 | 32.58 | 77.33 | 1.50 | 0.20 |
| Leliefontein | 174.20 | 86.61 | 2.51 | 13.93 | 48.52 | 0.10 | 1.10 |
| Leliefontein | 34.80 | 21.42 | 1.71 | 7.11 | 10.75 | 0.10 | 1.30 |
| Leliefontein | 108.90 | 18.10 | 0.84 | 15.18 | 26.20 | 0.10 | 0.50 |
| Leliefontein | 17.40 | 2.17 | 0.65 | 2.04 | 2.63 | <0.1 | 0.20 |
| Leliefontein | 17.40 | 6.14 | 1.79 | 4.24 | 7.14 | 3.70 | 0.30 |
| Leliefontein | 13.10 | 3.36 | 0.38 | 3.09 | 6.72 | 0.50 | 0.20 |
| Leliefontein | 43.60 | 7.96 | 1.85 | 7.34 | 26.14 | 1.40 | 0.20 |
| Leliefontein | 114.40 | 40.75 | 1.51 | 18.63 | 30.55 | 0.41 | 3.80 |
| Leliefontein | 114.40 | 14.08 | 0.89 | 8.55 | 37.31 | 0.28 | 0.90 |
| Rooifontein | 461.60 | 66.05 | 1.17 | 42.96 | 175.60 | 8.20 | 5.40 |
| Rooifontein | 304.90 | 87.73 | 1.32 | 63.74 | 174.80 | 1.40 | 2.90 |
| Rooifontein | 1907.50 | 218.20 | 4.13 | 193.60 | 463.70 | <0.1 | 6.10 |
| Rooifontein | 696.80 | 126.60 | 11.47 | 79.17 | 222.90 | 6.70 | 3.20 |
| Rooifontein | 54.00 | 37.17 | 1.29 | 22.84 | 67.22 | 1.00 | 3.30 |
| Rooifontein | 496.50 | 111.80 | 7.41 | 82.43 | 165.10 | 2.20 | 2.10 |
| Rooifontein | 331.00 | 50.52 | 6.32 | 37.56 | 69.21 | <0.1 | 0.80 |
| Kamassies | 270.00 | 41.42 | 1.47 | 26.59 | 100.90 | 8.70 | 5.70 |
| Kamassies | 235.20 | 16.91 | 2.11 | 11.59 | 93.05 | <0.1 | 8.20 |
| Kamassies | 452.90 | 93.75 | 2.86 | 79.74 | 144.10 | 8.10 | 2.70 |
| Kamassies | 474.70 | 96.78 | 3.06 | 80.91 | 113.50 | 15.40 | 2.40 |
| Kamassies | 348.40 | 71.96 | 2.35 | 50.14 | 107.90 | 20.00 | 2.20 |
| Kamassies | 278.70 | 44.53 | 6.07 | 30.21 | 63.64 | <0.1 | 1.00 |
| Kamassies | 540.00 | 102.60 | 2.07 | 93.57 | 143.50 | 7.70 | 2.50 |
| Kamassies | 718.60 | 136.10 | 7.57 | 92.30 | 260.70 | 4.00 | 3.50 |
| Nourivier | 1058.30 | 200.50 | 8.35 | 133.40 | 214.50 | 1.60 | 2.60 |
| Nourivier | 1228.10 | 253.90 | 1.75 | 162.50 | 290.90 | 13.20 | 2.80 |
| Nourivier | 113.20 | 33.15 | 0.98 | 14.53 | 35.98 | 0.40 | 3.20 |
| Nourivier | 187.30 | 24.66 | 0.88 | 16.35 | 70.15 | <0.1 | 0.90 |
| Nourivier | 448.60 | 45.05 | 5.36 | 47.96 | 99.73 | 1.70 | 0.40 |
| Nourivier | 714.20 | 150.20 | 5.93 | 112.10 | 183.30 | <0.1 | 1.40 |
| Nourivier | 87.10 | 8.16 | 2.05 | 8.15 | 9.33 | 0.20 | 0.40 |
| Nourivier | 95.80 | 11.24 | 2.14 | 10.20 | 12.94 | 0.10 | 0.30 |
| BRANDKLOOF | 175.00 | 68.64 | 1.34 | 24.90 | 215.20 | No data | 2.50 |
| BULLETRAP | 298.00 | 59.79 | 1.71 | 38.42 | 298.10 | No data | 5.40 |
| BULLETRAP | 586.80 | 106.10 | 3.29 | 71.00 | 137.20 | No data | 1.80 |
| BULLETRAP | 963.40 | 227.10 | 4.85 | 147.80 | 327.70 | No data | 1.00 |
| BULLETRAP | 411.60 | 91.24 | 4.37 | 49.88 | 107.50 | No data | 1.60 |
| BULLETRAP | 1235.00 | 323.10 | 4.53 | 84.93 | 323.00 | No data | 2.30 |

| Name | Cl (mg/l) | Ca (mg/l) | K (mg/l) | Mg (mg/l) | SO4 (mg/l) | +NO2 as N ( | F (mg/l) |
|---|---|---|---|---|---|---|---|
| CONCORDIA | 579.00 | 119.10 | 1.66 | 66.70 | 324.90 | No data | 1.50 |
| DOOIFONTEIN | 633.00 | 118.10 | 2.40 | 59.36 | 448.00 | No data | 2.50 |
| DROEDAP | 569.30 | 155.80 | 2.30 | 66.85 | 155.30 | No data | 1.70 |
| EENDOORN | 367.90 | 86.16 | 0.73 | 48.75 | 157.70 | No data | 3.30 |
| FONTEINTJIE | 140.10 | 40.76 | 3.77 | 25.74 | 128.60 | No data | 0.50 |
| GEMSBOK | 983.00 | 191.10 | 4.40 | 122.60 | 241.60 | No data | 1.30 |
| GOEGAB | 245.20 | 50.93 | 1.23 | 32.01 | 47.92 | No data | 1.40 |
| GOEGAB | 219.00 | 39.79 | 0.95 | 23.67 | 52.99 | No data | 2.90 |
| GROOT KAU | 718.20 | 145.00 | 6.00 | 8.65 | 175.10 | No data | 2.70 |
| GROOT KAU | 753.20 | 125.60 | 21.59 | 67.49 | 157.60 | No data | 2.50 |
| GROOT KAU | 735.70 | 147.20 | 5.97 | 59.91 | 203.10 | No data | 2.80 |
| HOMEB_alluviur | 360.00 | 96.19 | 0.95 | 48.75 | 294.00 | No data | 1.80 |
| KAIP | 315.30 | 65.99 | 2.24 | 35.14 | 108.90 | No data | 3.70 |
| KLIPDAM | 140.00 | 44.63 | 0.75 | 16.68 | 238.90 | No data | 1.00 |
| KLIPDAM | 70.00 | 20.09 | 1.45 | 9.74 | 93.73 | No data | 0.40 |
| KOEGAS | 1966.00 | 343.90 | 2.29 | 199.70 | 617.80 | No data | 2.80 |
| KOPPERBERG | 1725.00 | 410.70 | 6.55 | 194.50 | 441.40 | No data | 2.50 |
| KOPPERBERG | 429.20 | 125.70 | 1.13 | 39.68 | 136.30 | No data | 2.80 |
| KOPPERBERG | 1445.00 | 324.90 | 4.24 | 140.10 | 487.30 | No data | 2.90 |
| KWEEKFONTEIN | 551.80 | 116.00 | 1.26 | 47.25 | 90.42 | No data | 2.10 |
| KWEEKFONTEIN | 324.10 | 72.84 | 1.47 | 29.40 | 67.09 | No data | 1.50 |
| KWEEKFONTEIN | 184.00 | 40.42 | 1.21 | 21.60 | 69.01 | No data | 1.10 |
| KWEEKFONTEIN | 148.90 | 40.05 | 1.01 | 18.04 | 54.50 | No data | 1.20 |
| MARAS | 149.00 | 37.62 | 2.50 | 27.82 | 146.00 | No data | 0.70 |
| MIDDELPOS | 588.00 | 188.70 | 0.72 | 88.49 | 563.10 | No data | 4.60 |
| NARIES | 289.10 | 59.23 | 3.01 | 30.75 | 73.88 | No data | 0.40 |
| NIGRAMOEP MII | 2952.00 | 770.10 | 64.95 | 84.88 | 1144.00 | No data | 0.50 |
| NIGRAMOEP MII | 210.20 | 35.77 | 2.52 | 22.49 | 69.54 | No data | 0.50 |
| OLYNPUTS | 123.00 | 10.40 | 1.42 | 14.80 | 38.86 | No data | 0.60 |
| RATELKRAAL | 254.00 | 76.80 | 0.93 | 32.59 | 145.40 | No data | 3.40 |
| RATELKRAAL | 1594.00 | 296.10 | 2.35 | 122.30 | 361.60 | No data | 3.30 |
| RATELKRAAL | 183.90 | 72.66 | 4.37 | 19.81 | 77.19 | No data | 3.00 |
| RATELKRAAL | 1261.00 | 409.50 | 2.50 | 147.90 | 354.40 | No data | 1.60 |
| RATELKRAAL | 183.90 | 72.32 | 2.19 | 24.38 | 86.54 | No data | 2.00 |
| RIETFONTEIN | 858.30 | 184.90 | 1.36 | 89.07 | 147.10 | No data | 1.90 |
| ROOIWATER | 325.00 | 64.24 | 2.14 | 42.73 | 89.02 | No data | 1.20 |
| SABIES | 1812.00 | 258.40 | 10.36 | 153.90 | 599.00 | No data | 2.00 |
| SILVERFONTEIN | 166.40 | 52.21 | 0.81 | 22.30 | 59.70 | No data | 3.40 |
| SILWERFONTEIN | 438.00 | 107.40 | 3.13 | 50.56 | 157.90 | No data | 2.00 |
| SPEKTAKEL MII | 2575.00 | 384.10 | 11.37 | 213.20 | 794.40 | No data | 0.20 |
| SPRINGBOK | 814.60 | 177.50 | 1.61 | 104.10 | 251.20 | No data | 2.60 |
| SPRINGBOK | 2172.00 | 426.10 | 1.22 | 265.50 | 599.10 | No data | 2.00 |
| SPRINGBOK GH | 1261.00 | 268.20 | 3.54 | 146.60 | 155.30 | No data | 1.70 |
| SWARTPUTS | 904.00 | 157.80 | 4.01 | 123.70 | 396.60 | No data | 1.30 |
| TWEEDAM | 376.60 | 115.70 | 3.12 | 33.81 | 181.50 | No data | 2.20 |
| VAALDAM | 306.60 | 62.71 | 1.48 | 29.68 | 83.56 | No data | 2.20 |